AN ASSESSMENT OF THE USE OF NUCLEAR MICROPROBE TECHNIQUES IN POLLUTION STUDIES: QUANTIFICATION OF ELEMENTAL CONCENTRATIONS IN FISH SCALES

by

JF GUAMBE

A thesis submitted at the University of Cape Town for the degree of

DOCTOR OF PHILOSOPHY (PhD)

In the Faculty of Science

Department of Zoology and Freshwater Research Unit

Cape Town, South Africa

October 2013

Supervisors:

Prof. Jenny Day

Dr. Johan André Mars

List of Abbreviations, Acronyms, and Symbols

ALM	Aluminium Oxide (Al_2O_3)
APHA	American Public Health Association
ARASUL	Administração Regional de Aguas do Sul (Regional Administration of Waters of the South)
CCB	Calcium Carbonate ($CaCO_3$)
CENACARTA	Centro Nacional de Cartografia e Teledeteccão (National Center of Cartography and Teledetection)
CM	Cimentos de Moçambique (Mozambique Cement)
CMCM	Conselho Municipal de Maputo (Municipality Council of the Maputo City)
COM	Community Strategy Concerning Mercury
DAHA	Departamento de Agua e Higiene Ambiental (Department of Water and Food Hygiene)
DAS	Departamento de Aguas e Saneiamento (Department of Water and Sanitation)
DMAA	Dimethylarsinic Acid
DNA	Direcção Nacional de Aguas (National Directorate of Water)
EPUSA	Environmental Protection USA
EU	European Union
FAAS	Flame Atomic Absorption Spectrometry
FAO	Food and Agricultural Organization of the United Nations
GSH-Px	glutathione peroxidase
HAP	Hydroxy-Apatite [$Ca_5(PO_4)_3(OH)$]
IAEA	International Atomic Energy Agency
IBs	Incremental Bands
IBA	Ion Beam Analysis
IC	Ion Chromatography
ICM	Instituto de Ciencias Marinhas (Marine Institute of Science)
ICON	IC Consultants Ltd London
ICP-MS	Inductively Coupled Plasma Mass Spectrometry
IFPAC/PAT	International Forum Process Analytical Chemistry/Process Analytical Technology

IIP	Instituto de Investigação Pesqueira (National Institute of Fisheries)
INAHINA	Instituto Nacional de Hidrografia e Navegação (National Institute of Hydrographic and Navigation)
INE	Instituto Nacional de Estatistica (National Institute of Statistic)
IUCN	International Union for Conservation of Nature
KRT	Keratin
LD_{50}	Lethal Dose of a 50%
MDLs	Minimum Detection Limits
MICOA	Ministerio da Coordenação Ambiental (Ministry of Environmental Coordination)
MISAU	Ministerio da Saude (Ministry of Health)
MMAA	Monomethylarsinic Acid
MOZAL	Aluminios de Moçambique (Mozambique aluminium smelter industry)
NMP	Nuclear Microprobe
ONU	United Nation Organization
PIXE	Particle Induced X-ray Emission
QEDCs	Quantitative Elemental Distribution Concentrations
(R)BS	(Rutherford) Backscattering
SADC	Southern African Developing Countries
SEM	Scanning Electron Microscopy
UNDP	United Nations Development Programme
UNEP	United Nation Environmental Protection
UNESCO	United Nation Educational, Scientific and Cultural Organization
UNICEF	United Nations Children's Fund
US, DHHS	Department of Health and Human Services
USGS	United States Geological Survey
VCM	Vinyl-Chloride Monomer
WHO	World Health Organization

Abstract

This thesis deals with the applicability of Ion Beam Analysis (IBA) techniques for ascertaining the extent of water pollution by analyzing scales of fish that live in polluted waters. As a fish grows, ions from its immediate environment are incorporated into the matrix of the fish scale and so scales can be used as biomarkers of pollution events.

IBA techniques such as Proton-Induced X-ray Emission (PIXE) and Backscattering Spectroscopy (BS) with Electron-Induced X-ray Emission (EIXE, also called Scanning Electron Microscopy (SEM)) are useful non-destructive techniques for examining the fine-scale (micrometer) distribution of elements in a variety of materials. Analysis of the distributions of elements such as metals in biological material can assist in identifying pollutants and sometimes can even pinpoint the timing of pollution events. This thesis pilots the use of PIXE in particular and also EIXE and BS, in the analysis of fish scales. For PIXE and BS a 1.5 and 3.0 MeV proton beam was used for irradiation of the carbon-coated fish scales. The beam was obtained from a High Voltage Engineering Van der Graaff accelerator, maximum terminal voltage 6 MV, at the Materials Research Department, iThemba LABS in South Africa. For SEM a 25 keV electron beam was used for irradiation of the scales. The electron beam was obtained from a JEOL SEM, Japan.

For comparative analysis, the scales of four species of fish, *Pomadasys kaakan, Lithognathus mormyrus, Lutjanus gibbus* and *Pinjalo pinjalo*, were used. The matrices of the scales were shown to consist of calcium carbonate, hydroxylapatite and keratin. Pollutants such as Cr, Sr and Al were present. The homogeneous distribution of Al in the scale of *Pomadasys kaakan* indicates that Al contamination was relatively constant during the life of the fish. The standard deviation of Si concentration is relatively high due to heterogeneous distribution of the elements in different regions of the scale, while Sr concentrations were largely homogeneous. Comparative analysis showed that the concentrations and distribution of elements, particularly Al and S, were high in the scales of *Pomadasys kaakan,* due to the presence of these metal ions in water. In *Lutjanus gibbus* however, it was found that Fe and Cr were present in relatively higher levels than in the other specimens.

Al and S concentrations were relatively high only in the scale of *Pomadasys kaakan*. One can hypothesize that Al contamination was significant in the river where this fish was caught.

- A linear traverse analysis shows that the correlation between the concentrations of P and Ca is irregular in some regions due to dispersed distribution of the elements. Al contamination also occurs throughout fish scale. The standard deviation of Si is high due to heterogeneous distribution of the elements in different regions of the scale.

- The quantitative elemental concentration and distributions of elements such as Ca and P has the same trend in the third dimension. The elements, except Sr, are hetero-geneously distributed although the distributions of the major elements are not affected. In certain parts of the scale the distribution of these elements is sporadic and if present they are below the minimum detection limit.

From the comparative analysis of the scales of the four species, it was found that the concentrations and distributions of elements, in particular Ca, P, Al, S, Fe and Cr, were highest in the scales of *Pomadasys kaakan,* In *Lutjanus gibbus* Fe and Cr were present at higher levels.

In the scale of *Pomadasys kaakan* the concentration of Ca is approximately 1.0% and that of P is approximately 0.5%. This yields a concentration of hydroxyl apatite of 2.5%. Hence the $CaCO_3$ composition is less than 1.0%. Therefore this area predominantly consists of keratin, approximately 97%.

The concentrations of Ca and P are 5.0 % and 2.0 % respectively in the scale of *Lithognathus mormyrus*. Considering the P concentration, the concentration of hydroxyl apatite is approximately 10.0%. The excess of Ca 5.0 % and hence the $CaCO_3$ concentration is approximately 1.25 %. Therefore the concentration of keratin in this region is approximately 89.0 %.

The scale of *Lutjanus gibbus* consists of maximum 25.0% Ca and maximum 12.0% P. These concentrations translate to a maximum of 68.0% HAP and 32.0% keratin. Moreover, the Ca and P are predominantly located in the circuli of the scale, maximum 25.0% and 12.5%, and to a less extent in the annulis (maximum 5.0% and 2.5% respectively).

In the scale of *Pinjalo pinjalo*, the Ca concentration is about 16.0% and the P concentration is about 8.0%. This yields an HAP concentration of about 40.0% and keratin concentration of about 60.0%.

The Al concentration is exceptionally high only in the scale of *Pomadasys kaakan*.

The concentrations of Fe and Cr are much higher in *Lutjanus gibbus* than in the other three species.

This thesis has shown that nuclear techniques can pinpoint elemental distributions very accurately. Further work will be needed to calibrate ambient elemental concentrations with concentrations within the scales but the technique should allow us to estimate timing of pollution events and possibly even the concentrations of pollutants to which a fish is subjected throughout its life. However, due to the high cost of the instrumentation, the length of time needed for analysis, and the need for trained personnel to run the machine, these techniques are unlikely to be used for routine analyses.

PREFACE

The present research study was carried out in southern of Maputo fundamentally in Matola River, Mozambique from March 2007 and September 2009 under supervision of Prof Jenny Day and Dr. JA Mars. The work includes unpublished data obtained by the author. This study was financial support from Swedish International Development Agency SIDA/SAREC as part of project within the bilateral agreement between SIDA/SAREC and the Eduardo Mondlane University, Maputo, Mozambique. NRF-iThemba LABS center of Research/Training/Expertise and University of Cape Town, South Africa had an important role in this study, through provision of valuable scientific and logistic assistance.

DECLARATION

I declare that this thesis is my own work and that it has not been submitted before in any form for any degree to any university. Research work of other authors used in this thesis has been duly acknowledged by complete reference. Three peer reviewed paper resulting from the present work were published and is presented in the Appendix.

.....

JF Guambe

Contents

List of Figures

List of Tables

ACKNOWLEDGEMENTS

It is a great pleasure and privilege to thank my supervisors Prof. Jenny Day and Dr. J.A. Mars for their guidance and support throughout my work. Their confidence and trust in me was a positive motivation for learning and working diligently.

I humbly appreciate Prof. Rogerio J. Uthui for his sympathy attitude for have been introduced to me Dr. Wojciech J. Przybylowics and Dr. Jolanta Mesjasz-Przybylowics further more with Dr. Grzegorz Tylko we mastered the first croy chamber transfer to be connected to the Nuclear Microprobe beam. Respect goes to Prof. Craig M. Comrie who gave me an idea right way to contact Prof. Jenny Day as a potential expert in the field of freshwater. I also would like to express my satisfactory to Prof. Carlos A. Pineda for his help with the experimental set up for the nuclear apparatus.

My gratitude goes to all my colleagues in the Physics Department of the Science Faculty at Eduardo Mondlane University, Maputo-Mozambique.

These studies were made possible by financial support from Swedish International Development Cooperation Agency for Research and Education in Developing Countries (SIDA/SAREC) as part of project within the bilateral agreement between SIDA/SAREC and the Eduardo Mondlane University, Maputo, Mozambique. Without their financial support perhaps the current investigations would never have been completed.

I would like sincerely to grateful for the efficient operation of the accelerator by the technical personnel of the Material Research Department (MRD), at NRF-iThemba LABS, Somerset-West, South Africa where I developed my skills in operating the Nuclear Microprobe and the applications in materials research with the emphasis on fishscale matrices, sediments, the housefly and ants; the development of cryo-chamber stage with Dr. Grzegorz Tylko in which I contributed concept of automatic filling of the liquid nitrogen cooling system.

I also would like to thankful anonymous reviewers for their suggestions, constructive comments and critical reviews of an early draft of all my papers and the present in this Doctoral Thesis.

The author acknowledges with gratitude the SEM Unit at Physics Department, ICP-MS and IC at Geology Department, FAAS at Chemical Enginnery at University of Cape Town respectively for spatial and Chemical Analysis in water and sediments samples.

The technical assistance of INAHINA during fields work with equipment such as a boat, CTD, disk search to determine the transparence and technical people (Marine Corps, divers) is greatly appreciated. Students volunteered additional aid with the daily maintenance of the experiment.

I really would like to address special gratifications to the Marine Institute of Science (ICM (Instituto de Ciencias Marinhas, 1998)) now National Institute of Fisheries (IIP (Instituto Nacional de Investigação Pesqueira)) for an identification of different species of fishes and relevant advisories.

I thank the good and constructive environment have ever had at Ministry of Health (MISAU) special attention to the Department of Water and Food Hygiene (DAHA), Maputo –Mozambique for being provided such equipment's for water and sediments sample and for the use of pH meter for the determination of pH in the field.
I deeply appreciate the interest and advice to the current investigations provided by the National Institutions such as the Ministry of Environmental Coordination (MICOA), the Regional Administration of Waters of the South (ARASUL) and the National Directorate of Water (DNA).

I grateful the National Center of Cartography and Teledetection (CENACARTA) for higher cooperation and attention provided when become to request any relatively information related to the geographic location of the study areas.

My thanks are addressed to the Department of Water and Sanitation (DAS) at Municipality Council of the Maputo City (CMCM) for their relevant assistance and advice.

The non-governmental organization (NGO) based in Maputo city allowed me to access to their installations and providing seminars regarding the evaluation and assessment of pollutants applying ion beam techniques for water, sediments and fish scales from different group of species.

My sincerity gratitude to all staff at Zoology and Botany Department, UCT for a very good environment given during the time of the duration of my studies made me fill real home as the fish in clean water.

Here my sincere gratitude and love. I really will miss all of you and anytime you are Welcome to Mozambique!

My apologies to anyone I have omitted unintentionally. I will see you when I see you!

Finally, to the Almighty and Everlasting God for giving me the ability to complete this study.

TO MY PARENTS

&

FAMILY

DEDICATION

To my Father

Francisco Chicuendane Guambe

and my Mum

Florinda Taime Machava

For

Their love and education of their children

To my Kids

Phylo, O'hara, Nhelethy & Эурэка for their support.

and my Wife

Lisefa S. Gabriel for her love and deepest patience.

Chapter One
1 Introduction

1.1 General Introduction

There are numerous ways of estimating the quantity of elements that occur as pollutants in natural waters. Normal chemical analyses are "spot" measures applied to ascertain the extent of water pollution. However, analysis of water samples may under- or over-estimate the load of pollutants or their effects on aquatic organisms/ecosystems. The use of living organisms as monitoring tools is often a better approach and has many advantages. Organisms living in an aquatic system, including fish and invertebrates are constantly exposed to the physical, biological and chemical features of the environment and may therefore also be useful indicators of pollution. The means of assessing pollution may follow a biological or chemical approach. Biological monitoring can provide a measure of the direct adverse effects of water and sediment quality by assessing the deviation of a specific biological response from a normal value (Shugart *et al.,* 1992; Roux *et al.,* 1993; Svobodova *et al.,* 1993). It can also be used to assess pollution by examining concentrations of pollutants in the body.

1.2 Scope of investigation

The principal aim of this study is to investigate the usefulness of Ion Beam Analysis (IBA) in pinpointing pollutants in fish scales. This study therefore details:

1. The applicability of IBA techniques in identifying the spatial and temporal distribution of elements in a fish scale;

2. The application of the IBA techniques in the determination of the extent of incorporation of elements considered pollutants into the fish-scale matrix by performing:

    a. A two dimensional analysis and
    b. A three dimensional analysis of the fish scale;

3. The application of growth equations to:

a. Correlate the length of the fish to the age of the fish,
b. To correlate the growth of the scale to age of the fish,

4. comparative studies of the distribution of contaminants incorporated in the scales of different fish species.

The principal hypothesis of this thesis is presented as follows:

1. Fish scales contain elements bioaccumulated from the water in which they live.

2. Accumulated elements in fish scales are differentially distributed throughout the scale.

3. PIXE can quantify the distribution of elemental concentrations in fish scales at a sufficiently fine spatial scale to pinpoint differences in bioaccumulation over time.

4. Fine-scale distribution of elements can be used to model growth patterns in fish scales.

Pollution is caused when the concentrations of substances are high enough to be toxic to organisms living in natural waters. This is detailed in the next section of this chapter. In the following section the applicability, previous applications of IBA techniques and optimum instrumental settings are discussed. Afterwards application of growth equations and the statistical analyses are detailed.

Chapter 2 describes the methods followed in obtaining the final results. In Chapter 3 the results and discussions of the two and three dimensional (2-D and 3-D) analysis are given. Chapter 4 entails the comparative analysis of the scales of four species of fish. Chapter 5 analyses the growth patterns demonstrated by a fish scale of *Pomadasys kaakan*. Chapter 6 provides conclusions and recommendations.

Various fundamental physical, mathematical and chemical equations regarding the analytical techniques, detailed description of geographic areas, and results of water analyses are given in a series of appendices.

This study is a preliminary assessment of a value of PIXE for pollution studies and does not attempt to examine levels of pollution in the fishes' environment other than to show that trace element pollutants are present in the environment from which the fishes were collected.

1.3 Pollution

There are numerous definitions but pollution is commonly accepted to be the addition of any substance to an ecosystem in quantities that might have detrimental effects on the ecosystem (Moolenaar, 1998; Freeman, 1990; EPA, 1999; Sigman, 2000; Lemly, 2002; Burton, 2002). The elements, C, H, O, P, N, Ca, S, Na, Mg and K constitute the major part, in mass per mass percentage (m/m %)[1], of a plant or animal body. Hence, small variations at the parts per million concentration ranges of these elements, will not detrimentally affect the continued existence of a plant or an animal (Janvier *et al.*, 2007; Rauch *et al.*, 2009).

1.3.1 Metal pollution of fresh waters

Many natural water resources have, on a world-wide scale, been adversely affected by pollution caused by humans in the race to implement technologies by establishing more sophisticated industries (Meyers *et al.*, 1992; UNEP & IUCN, 1992; Boer, 1993; Ryding, 1994; Ng, Wang & Shraim, 2003; Singh, 2004; Bodansky, 2009). Most of these natural water resources, including rivers, lakes, estuaries, bays and oceans, have been contaminated, some beyond remediation (Rakocinski *et al.*, 1997; Hinrichsen, 1999; Zingde, 2005; United Nations Environment Programme, 2006; Palaniappan, Gleick *et al.*, 2011; Wolanski *et al.*, 2011). Some pollutants have directly been discharged into natural water resources by industries and municipal sewage treatment plants through sewerage systems (Leland *et al.*, 1978; Geldreich, 1978; Cloete, 1997; Field *et al.*, 1998; Koppe, 2008; Ritter *et al.*, 2002; Mason, 2002; Wang, Webber *et al.*, 2008). Others originate from polluted runoff from industries in urban and agricultural areas that are located on the periphery of natural water resources (Hammer, 1992; Chebbo, 1999; Mvungi *et al.*, 2003; Craig, 2005; Wang *et al.*, 2008; Yang, 2012).

The concentrations of the major elements in water are generally higher than those of trace elements (elements present in very small concentrations) (Maret & Skinner,

[1] In SI unit: 1% m/m=10 000 ppm= 10 000 mg/kg= 10 g/kg

2000). Elements, especially transition elements such as Fe, Cu, Mn, Zn, Ni, Sr and Cr, that are present in the environment or body in parts per million concentration ranges (ppm or $\mu g.g^{-1}$ or $mg.l^{-1}$ or $mg.kg^{-1}$) are termed trace elements (Chapman, 1992). Elements such as Cd, Hg, Pb and As, which are normally present in the parts per billion concentration ranges (ppb or $\mu g.kg^{-1}$ or $\mu g.l^{-1}$), are termed ultra-trace elements (Chapman, 1996). Trace and ultra-trace elements are usually present as ions and some might be present as dissolved gases (Schmidt & Forsten, 1977; Aiuppa *et al.*, 2000; Guo *et al.*, 2005; Craft & Pearson, 2007).

The detrimental effects of toxins are often measured as the amount of the element, termed the lethal dose, at which at least 50% of experimental animals (LD_{50}) die (Rispin *et al.*, 2002). The numerical values are usually expressed as mass per volume that is mg/L or µg/L. LD_{50} values of some elements such as Al, Cr, Fe and S (Gonzalez-Pleiter, Rodea-palomares *et al.*, 2003; Misund *et al.*, 1999; Lech, 2002; Feyerabend *et al.*, 2010) are presented in **Appendix A**.

Investigations into the pollution of resources have primarily focused on the concentrations of trace and ultra-trace elements (Calamari, 1994). Of these elements, Hg, Pb, As, Se, Cu, Cr, Cd and Al have been studied in detail because of the presence of these metals in the vast majority of industrial processes and manufactured appliances and their particularly detrimental effects on living organism, including humans.

Contamination threatens the existence of creatures in benthic sediments, exposing invertebrates such as worms, crustaceans and insects to high concentrations of toxic chemicals. The killing of benthic organisms reduces the food available to larger animals such as fish. Contaminants in the sediments are taken up by benthic organisms in a process called bioaccumulation (Weis & Weis, 1994; Weis, 1996; Streit, 1998; EPA, 1999; Bjorklund *et al.,* 2000; Neff, 2002; Van der Oost *et al.,* 2003; Cornelissen *et al.,* 2005; Monperrus *et al.,* 2005; Ruus, 2005; Simpson, Batley *et al.,* 2005; Brack, Bandow *et al.,* 2009). When larger animals feed on these contaminated organisms, the toxins are taken into their bodies, and so move up the food chain. The larger organism consumes numerous of these smaller contaminated organisms. As this result, fish and shellfish, waterfowl, and freshwater and marine mammals may accumulate hazardous concentrations of toxins (Walsh, 1990; Steffens, 1997; Shumway, Allen and Boersma, 2003; Tuzen and Soylak, 2007). This process is termed biomagnification.

Moreover, under acidic conditions, free mono and polyvalent ions of many metals may be absorbed by fish gills directly from the water. Hence, concentrations of heavy metals in the organs of fish are determined by the level of pollutants in both water and food (Yilmaz and Dogan, 2008; Rauf, Javed and Ubaidullah, 2009; Tuzen, 2009; Yilmaz, 2009). Chemical elements accumulated in the silt and bottom sediments of water bodies can be released and migrate back into the water, becoming a secondary source of heavy metal pollution (Lacoul & Freedman, 2006; Singh, S.K., Subramanian, V. & Gibbs, R.J., 2009; Wuana and Okieimen, 2011).

Many elemental contaminants eventually become incorporated into the sediments, where they are stored. Any process such as dredging and flooding that stirs up the water, can resuspend the sediments. With resuspenion, the animals in the water, and not just the bottom-dwelling organisms, will be directly exposed to toxic chemicals (Williams, 1964; Knezovich *et al.*, 1987; Giulio *et al.*, 1989).

Different aquatic organisms respond to external contamination in different ways, depending on the quantity and form of the element in water, sediment or food (Kustin & McLeod 1977; Pendias & Mukherjee, 2007). The region of accumulation of heavy metals within fish varies with the route of uptake, the element concerned and the species of fish concerned. The potential use of fish as biomonitors of metals poisoning is significant in the assessment of bioaccumulation and biomagnifications of contaminants within the ecosystem (Peirce *et al.*, 1998; Barwick & Maher, 2003; Malik and Zeb, 2009).

1.3.2 Toxicity of trace elements

Below follows a brief summary of the toxic effects of some elements occurring in industrial effluents such as those encountered in this study.

Humans are primarily exposed to methylmercury through diet, especially fish, and elemental mercury from dental amalgams and occupation hazards such as small-scale mining (Gerhardsson *et. al.*, 1994; Bidone *et. al.*, 1997; Akagi *et. al.*, 2000; Peakall & Burger, 2003; Yokoo *et. al.*, 2003; Scheuhammer *et. al.*, 2007; Mergler *et. al.*, 2007; Feng *et. al.*, 2007; Diez, 2009; Holmes *et al.,* 2009; Zhang *et. al.*, 2010). The effects of Hg include the alteration of genetic enzyme and immune systems and damage to the nervous system (Mergler *et al.,* 2007; Castoldi *et al.,* 2008). Efforts have been made by the Community Strategy Concerning Mercury (European Commission, 2005; Selin & Selin, 2006; Rodrigues *et. al.*, 2006; Ronchetti *et. al.*, 2006; Joas *et. al.*, 2012;

Pereira *et. al.*, 2008) to reduce mercury exposure to humans and consequently the high levels of Hg in the environment.

Arsenic and selenium have become increasingly important in environmental geochemistry because of their significance to human health (Abrahams, 2002; Liu *et al.,* 2007). Their concentrations vary markedly in the environment, partly in relation to geology and partly as a result of human activity (Jain and Ali, 2000; Plant *et al.,* 2001; Civera, Esquivias *et al.,* 2002; Rayman, 2002; Plant *et al.,* 2003; Terlecka, 2005; Fiket *et al.,* 2007). Arsenic is highly toxic and can lead to a wide range of health problems in humans. It is carcinogenic, mutagenic, and teratogenic (Leonard & Lauwerys, 1980; Leonard & Lauwerys, 1990; Gerber *et al.,* 2002; Nordberg, 2007).

Symptoms of arsenicosis include skin lesions and skin cancer. Internal cancers, notably bladder and lung cancer have also been associated with arsenic poisoning. Other health problems include cardiovascular disease, respiratory problems, and diabetes mellitus. There is no evidence of a beneficial role for arsenic (National Research Council, USA, 1999; Salt *et al.,* 2002; Verbeke *et al.,* 2005; Kalia *et al.,* 2005; Ma *et al.,* 2008; Verbruggen *et al.,* 2009). Indeed, the precise nature of the relationship between arsenic dose and carcinogenic effects at low arsenic concentrations remains unresolved (Penrose & Woolson, 2009).

Trace concentrations of Se are essential for human and animal health. Until the late 1980s, the only known metabolic role for selenium in mammals was as a component of the enzyme glutathione peroxidase (GSH-Px), an anti-oxidant that prevents cell degeneration. There is now growing evidence, however, that a seleno-enzyme plays an important part in the synthesis of thyroid hormones (Arthur & Beckett, 1994). Selenium deficiency has been linked to cancer, AIDS, heart disease, muscular dystrophy, multiple sclerosis, osteoarthropathy, immune system and reproductive disorders in humans, and white muscle disease in animals (e.g. sheep and goats) (Plant *et al.*, 2005; Fordyce, 2005; Fordyce, 2013). The deficiency of selenium in humans has also been implicated in the incidence of the heart disease, keshan disease and an osteoathropathic condition known as Kashin-Beck disease (Hollard & Turekian, 2004) in extensive regions of China.

Strontium-90 was extensively dispersed on a world-wide basis during 1950s and 1960s as a consequence of exploding nuclear bombs and releasing toxicity of strontium into the environment (Vohra & Mishra, 1960; Owen, 1997; Richardson, 2004). It is considered to be one of the most hazardous constituents of nuclear waste. The Chernobyl nuclear accident in Russia introduced large quantities of strontium-90 into the

environment (Avery, 1996; Imanaka, 1997; Borovoi & Gagarinskii, 2001; Ryabzev, 2002). Strontium-90 has been dispersed in large quantities over Northern Europe and worldwide. It concentrates in the bones and teeth causing bone cancer, cancer of the soft tissue near the bone and leukemia (Ginzburg & Reis, 1991; Hinton *et al.,* 2007; Anspaugh, 2008).

Cadmium and Cu are also toxic to humans. It has been estimated that about 0.5 million metric ton of Cd and 310 million metric tons of Cu have been mined and ultimately deposited into the biosphere (Gupta, 2011). In many instances, the inputs of these metals from anthropogenic sources exceeded the contributions from natural sources (weathering, volcanic eruptions, and forest fires) by several orders of magnitude (EPA, 2007). These elements are present in the waste of industries such as aluminium smelter, textiles, painting and others.

Various diseases have been associated with toxic concentrations of Al, especially under acidic conditions (Macdonald & Martin, 1988; Campbell, 2002; Kawahara, 2005). Solid Al is solubilized to the hydrated form of $Al^{3-}[(H_20)_6]^{3+}$. The element has been found to be a selective neurotoxin with specific affinity for the brain causing progressive encephalopathy (McLachlan *et. al.*, 1996), neurofibrillary entanglement (Wang *et al.,* 2007), increase in permeability of blood-brain barrier (Huang, Li & Sumner, 2011) and other neurotoxicological diseases (Mohan *et al.,* 2006). It has also a significant effect on fishes for example the gills function less efficiently (Raymond & Felix, 2011).

The emission rate of trace metals into the atmosphere is low due to their low volatility. According to Kersten & Forstner (1995), river sediments, lake sediments and urban particulate matter appear to have between 50 and 70 % m/m of the metal content. Furthermore, with the advent of large scale metal mining and smelting, the emission rate of these metals has increased dramatically. Most of these emissions are released into the atmosphere. As a consequence of these emissions there has been the increase in the occurrence of health problems such as lead poisoning, Cd itai-itai disease, and Cr and Ni carcinogenesis (Odoemelan *et al.,* 2011; Al-Rashdi *et al.,* 2011).

1.4 Types of biomonitoring

Worldwide, various methods for accertaining whether pollution has occurred have been applied[2]. The ease of application and the specificity of these methods also vary. For the purpose of this study the ease of applicability and specificity were divided into four levels. These levels are the community level, micro organism pathogenesis, chemical marks and tissue analysis.

Pollution can be investigated both chemically (i.e. what pollutants are present) and biologically (i.e. the effects of pollutants on organisms and therefore ecosystems).

Direct chemical analyses in water or sediments after most pollution events, substances may be hard to measure or present in minute quantities, and do not tell us what effects they will have on the environment.

Therefore bioassessment is often used. Biomarkers can be at level of

a) whole ecosystem (e.g. analysis of invertebrate or diatom assemblages);
b) individuals (e.g.analysis of loads of heavy metals in muscle and other organisms e.g. eels) or mosses (or other fish);
c) biochemical markers (e.g. cytochrome P450, acetylcholinesterose activity, etc.)

It is necessary to distinguish between use of whole organisms and assemblages (e.g. SASS) and methods assessing chemical components (e.g. cytochomes, acetylcholinesterase of organisms, etc).

1.4.1 Community level

Levels of pollution can be assessed by examining the effects on all the species of a particular kind in an ecosystem for instance, using the South African Scoring System (SASS) (Chutter, 1998). SASS is a biomonitoring system using invertebrates to assess water quality of rivers and streams (Dallas, 1997; Wertz *et al.,* 2004). Such techniques are useful for assessing general levels of pollution but are not able to identify particullar pollutants or to quantify them. Due to their visibility to the naked eye, whole invertebrates are valuable organisms for bioassessment (Dickens &

[2] In this work will be used the term "method" which would indicate a logical procedure for analysis and "technique" where a specific instrument has been used.

Graham, 2002) since the different species respond differently to the effects of past pollution.

According to Becker *et al.* (2007), WHO (2007), Bonanno & Giudice (2010), biological monitoring should not be seen as an alternative to physical and chemical monitoring but they should be seen as useful complementary approaches. Although physical and chemical analyses can identify that many contaminants may be present, biological methods can integrate responses to combinations of all contaminants and to other sources of environmental stress, thereby indicating the overall health of a water body (Cooper, 1993).

It is difficult to ascertain timing of pollution events from any of these bioassessment procedures. For this reason, this work investigated the use of fish scales for assessing environmental contaminants. If differences in concentrations of pollutants (e.g. Al) is discernible in the scale then essentially a history of the pollution events that occurred in the environment of the fish during its lifetime.

1.4.2 Chemical and biological markers

Numerous biochemical makers are used to estimate the degree of pollution by various substances. The induction of cytochrome P450 (Bucheli & Fent, 1995) has been applied various animals to ascertain the extent of pollution. Cytochrome P450 is an enzyme that catalyzes the oxidation of organic substances such as pesticides in lipids. Mosses have been extensively used to monitor trace, minor and major metal concentrations because of their tendency to selectively adsorb heavy metals (Bargagli et al., 1995; Poyy & Turpin, 1998; Vuori et al., 2003; Ogunfowokan et al., 2004). Eels have been largely used to investigate halogenated organic chemicals, which can be absorbed into fatty deposits within the eel (Belpaire & Goemans, 2007).

Organisms such as algae take up nutrients and elements through absorption from the ambient water. These nutrients and elements will have different effects on the organisms depending on their physiology. Many algae and plants for example generally do not respond negatively to a host of elements. Plants and algae may be affected by pollutants. Some fish species feed on the algae containning the pollutants such as heavy metals and concequently become contaminated with these metals.

Animals on the other hand respond more to elevated levels of nutrients and elements and so are affected more so. An animal that consumes a plant or a and algae can be detrimentally affected while the plant/algae itself may not. Furthermore, there are even animals (e.g. mussels and other filter feeders) who are also accumulators of heavy metals while they themselves seen to be unaffected by levels of nutrients/elements. However, the organisms (e.g. fish, etc) that eat these filter feeders can be adversely affected simply because their physiolologies are not adapted to such levels.

Algae and cyanobacteria are tiny organisms that occur naturally in saltwater and freshwater and have been widely used for water quality monitoring e.g. to avaluate eutrophication and turbidity. They are frquently affected by physical and chemical variations in their environment.

1.4.3 Mussels and Pollution

The class Bivalvia comprises sedentary filter-feeding invertebrates that can accumulate pollutants from the environment. Since mussels are a large source of bacterial contamination and pollution by heavy metals, they have been the subject of extensively toxicological investigations (Bayne, 1976; Hunt, 1993; Caussy, *et al.* 2003; Islam, 2004; Morley, 2010). According to Alyakrinskaya (1967), many Bivalvia were identified as being tolerant of a wide range of environmental contaminants.

Mussels were often found as a subject to sewage pollution because of their coastal and estuarine distribution and commercially exploited (Lusher, 1984; Kennish, 2002; Perrow & Davy, 2002; Amaral, 2005). Also mussels can be contaminated with bacterial and viral pathogens particularly when the mussels are eaten raw or only lightly cooked (Crocci *et al.* 2001). When mussels are contaminated with bacteria of non-faecal origen e.g. *Vibrio parahaemolyticus*, was identified as responsible of cases of food poisoning in Japan (Chiang *et al.* 2008). The *Salmonellae* bacterial which include organisms responsible for typhoid fever and other large bacterial species such as *Shigella* which can cause dysentery and viral infective hepatitis associated with shellfish are well- documented (Rippey *et al.* 2005; Ahmed, 2007).

1.4.4 Tissue analysis

Contaminants such as metals and organic compounds can be found in the tissues of organisms (Pohjanvirta & Tuomisto, 1994; Garbarinho et al., 1995; Chapman &

Jackson, 1996; Jarup, 2003; Okey, 2007). Furthermore chemical analysis of the appropriate biological tissues can be used to show the level of contamination in the organism and in some instances monitor the spatial distribution or accumulation of a specific contaminant in the environment (UNEP, 1996; Canesi et al., 1999; Viarengo et al., 1999; WHO, 2006; Van de Berq et al., 2006; Luy et al., 2012).

The determination of body and carcass compositions is important for evaluating growth performance and in predicting energy and nutrient requirements of cattle (AFRC, 1993; NRC, 2000; CSIRO, 2007; Bonilha *et al.*, 2008). The most accurate method for determining animal body composition is through the analysis of the empty body (Howe & Hankins, 1946). However, this method is costly time consuming, and sometime not feasible. However it is therefore necessary to select and find alternative methods that could be used to estimate empty body and carcass compositions with satisfactory accuracy (Brown *et al.*, 1951; Keys & Brozek, 1953; Siri, 1961; Adam & Smith, 1966; Joblin, 1966). Several prediction methods useful in body composition studies were developed (MacNeil, 1983).

For evalution of long-term environmental conditions over a broad area, such as a river stretch or a lake, the monitoring of fish species has several advantages (Chapman, 1996; WHO & UNEP, 1996; Attrill & Depledge, 1997). Fish are relatively long lived and mobile and because different species cover the full range of trophic levels (omnivores, insectivores herbivores, piscivores and planktivores) fish community structure is a good indicator of overall environmental condition (Darwin, 1874; Thomson, 1950; Grosberg & levitan, 1992; Mayr, 1996; Strathmann *et al.,* 2002; Atema *et al.,* 2002). Furthermore fish are an important source of food for humans and it is therefore particularly important to assess potential contamination (Van Dam, 2002; May & Burger, 2006; WHO, 2007).

Various animal body parts have been analyzed to ascertain levels of contamination using nuclear methods. Particle-Induced X-ray emission (PIXE) has been used extensively for elemental concentration analysis of blood sera of breast cancer patients for instance (John *et al.,* 2005; Raju *et al.,* 2006; Guntupalli *et al.,* 2007; Sarita, *et al.,* 2012) because trace elemental imbalance in humans can exert direct or indirect action on the carcinogenic process (Kasprzak*,* 1991). Use of the Tandem Pelletron accelerator at Bhubaneswar Physics Institute, India found a significant variation in the level of most trace elements in the sera of breast cancer patients when compared to sera of control subjects (Irigaray *et al.,* 2007).

Trace elements such as titanium, vanadium, chromium, manganese, iron, cobalt, nickel, copper, zinc, arsenic, selenium and bromine were determined and averaged separately for the normal and cancer group (Foley & Missingham, 1976; Maenhaut, 1988; Panling, 1988; Neff, 2002; Miller, 2004; Kuo, *et al.,* 2002). According to Raju *et al.,* (2005) and Robert *et al.,* (2006), the results obtained for reference materials of bovine liver and apple leaves was used to compare the relative concentration of different elements in the breast cancer patients and with those of healthy controls and showed high level of Cu in the serum of breast cancer patients may cause/increase led with tumor progression (Sawyers *et al.,* 1987; Stohs *et al.,* 1995; Decarli *et al.,* 1996; Nair *et al.,* 2004; Birch *et al.,* 2006). According to Huang *et al.* (1999) and Zowczak *et al.* (2001), the decrease in antioxidant and the decline in immunological competence can influenced the carcinogenic process due to depressed levels of chemical metals such as Zn and Se.

Otoliths or ear stones in fish are hardened calcium carbonates organs, responsible for the senses of gravity and of linear acceleration. The composition determined by Nuclear microprobe (NMP), is relatively pure compared to most biological and mineralogical structures being dominated by calcium carbonate in a non-collagenous organic matrix. The elemental composition is dominated by the major elements calcium, oxygen and carbon, which make up the calcium carbonate ($CaCO_3$) matrix. The elements Na, Sr, K, S, N, Cl and P have been identified in otoliths using PIXE while the bulk of the trace elements are present at concentrations of less than 10 ppm (Aubert *et al.*, 2012). Campana *et al.*, (1977) reported that the otoliths of the fish *Micropogonias ungulates* were composed mainly of calcium carbonate, with traces of inorganic impurities (Edmonds *et al.*, 1992; Campana *et al.*, 1994; Shiller, 1997; Laban & Atkin, 1999; Patterson *et al.,* 1999; Yoshinaga *et al.*, 2000) and protein concentrations (Asano & Mugiya, 1993; Hoff & Fuiman, 1993; Houtman, 1996; Campana *et al.*, 1997).

Nuclear microprobe analysis of muscle biopsies by Moretto *et al.* (2000) demostrated that quantitative information on trace elements and mineral ions could provide information on pathogenesis of certain diseases.

However, experimental preparation of samples is destructive and entails drying and grinding parts of, or the whole body, which it therefore destroyed (Macaire, 2010) and (WHO, 1997). More so, the analysis gives no indication as to when pollution occurred, only that it occured during the life span of the organism (Holt *et al.*, 2011). The outcome is that the timing of pollution events cannot be pinpointed (Nkala *et al.*, 2012). It would therefore be ideal to have methods available that enable non-

destructive preparation and determination of elemental pollutants present in the specimen (Johansson, 1989; Vandecasteele, 1997; IAEA, 2003) and that would allow an estimate of the timing of such events.

1.5 Pollution control in Mozambique

In Mozambique, an industrial revolution has occurred along the Matola River catchment. The increase in pollution in the study country Mozambique is phenomenal (INE, 1994; Chambote & Shankland, 2011) and vast quantities of toxins are being poured into the environment in Mozambique without any notable effort to study their fate or effects (Chorus, 1999; De Villiers, 2001; Bojcevska & Jergil, 2003). It is also uncertain whether the present rates of mobilization and changes of metallic distribution are within pollution control limits (Landrigan *et al.*, 2002; Maas *et al.,* 2005; Swain *et al.,* 2007; Spiegel, 2009; Grant *et al.,* 2009; Watts, 2009; UN, 2011).

Sea water has been strongly affected by microbial pollution along the bay. Industrial pollution associated with port operations and factories also affected the water quality of the western part of the Bay Maputo (Fernandes, 1996; Waelde & Fernandez, 2005; McGranahan *et al.*, 2009; WIO Region, 2009; Ascher, 2009). However, the amount of chemical pollution of the Maputo Bay caused by washed-out pesticides and fertilizers along the Inkomati, Umbeluzi, Futi, Tembe and Maputo rivers which discharge in Maputo Bay, remains unknown (MICOA, 2000; Huhn, 2001).

1.5.1 Contamination of Matola River catchment area

Various industries are found on the banks of the Matola River in southern of Maputo Mozambique. These include an aluminium smelter, textile manufacturers, paint manufacturers, motor vehicle battery manufacturers and plastic, fertilizer, steel and cosmetics industries (Simmons *et al.*, 1978; Jenkins, 2000; Castelo-Branco, 2004; Bhatt, 2006; EPA, 2009). According to Crepeau *et al.* (1992), Chen *et al.* (2000), Akhter & Jowder (1997) and Schintu & Degetto (1999), effluent from aluminium smelters contains significant quantities of Al, S and Ni. The characterization of effluent emanating from the textile industries has been studied in detail (Yusuff & Sonibare, 2004; Sahoo *et al.*, 2012).

Elements, in ionic form, which pose a threat of pollution, include P, S, Hg, Pb, Cd, Cr, Cu, Ni, Zn, Fe and Mn (Kiefer *et al.*, 1995; Wells, 2002; Camara *et al.*, 2004; Le *et. al.*, 2005). These elements, as ions, are also prevalent in the effluents

originating from other manufacturing industries and are disposed of in the river increasing the toxic load (Lokhande *et. al.*, 2011). There are various natural and anthropogenic sources of these heavy metals in the environment (Moore & Rastmanesh, 2011) but mining and smelters industries have become the major sources of metals emissions
into the rivaine and marine environments as tailings and to the atmosphere as metal-rich dust as a result of high-temperature refining processes (Wong, 2006).

1.5.2 Need to evaluate quantities, time and types of metal pollution

Various species of fish are found in the Matola River, the Tembe River, the Espirito Santo Estuary and Maputo Bay and are an important source of proteins for the human consumssion. It is therefore of practical value to evaluate the extent of pollution and to illustrate the applicability of IBA in water pollution. It would be valuable to ascertain types and quantities of pollutants and timing of effluents entering in the rivers. This thesis reports on pilot studies using a novel combination biological material and physical technique such as Proton-Induced X-ray Emission (PIXE), Electron-Induced X-ray Emission (EIXE) also called Scanning Electron Microscopy (SEM), and Proton Backscattering Spectroscopy, also called Backscattering Spectroscopy (BS) to quantify trace elements accumulating in fishes from Maputo Bay.

1.5.3 X-ray emission (XE) techniques

Two non-destructive techniques used in quantification of elements, often heavy metals, are X-ray emission (XE) (Johanson & Johanson, 1996) and backscattering (BS) (Chu *et al.,* 1978). In principle, atoms in the sample matrix are bombarded with a particle that may be a proton, a deuteron or an electron. When the emission of X-rays is induced by protons the term proton-induced X-ray emission (PIXE) is used (Johannson, 1975). However, the "P" in PIXE is normally associated with particles which include protons, deuterium, alpha and other heavy ions and not as protons *per se*. When the emission is induced by electrons the term electron-induced X-ray emissions (EIXE) (Small *et al.*, 2002) is used. EIXE is sometimes also referred to as scanning electron microscopy (SEM). BS is normally induced by protons (Chu *et. al.*, 1978; Malmqvist, 2004; Malmqvist, 2005; Benzeggouta, 2011; Jeynes, 2012) and for this reason BS analysis is done simultaneously with PIXE analysis. Since PIXE and SEM differ in the particle used to induce X-ray emission, these two techniques are not performed simultaneously. Analysis done with the PIXE and BS

techniques is collectively known as Ion Beam Analysis (IBA). Since in SEM analysis a beam of electrons is used, this technique is normally not considered as an IBA technique.

1.6 PIXE

PIXE techniques have been used world-wide to quantify trace and ultra-trace elements (Brown & Milton, 2005) and can provide quantitative analyses of elements in solid materials. The SEM may be used to quantify the major or matrix elements of specimens. The disadvantage of PIXE is that the minimum detection limit realizable is approximately 1 ppm. The most important aspect of PIXE, BS and SEM analyses is that these analytical techniques are non-destructive under most circumstances. Also the location and distribution of the analyte with respect to other elements in the matrix can be ascertained to the nearest micrometer. With PIXE, BS and SEM only elemental analyses can be performed; hence, molecular species such as polyions (nitrates, phosphates, sulphates, acetates, etc.) cannot be determined.

1.6.1 Principles of X-ray emission analysis (XE)

The atom according to Bohr's atomic theory consists of a nucleus at the center with one or more electrons revolving around the nucleus along different energy orbits. The nucleus is fundamentally composed of protons and neutrons, collectively called nucleons (Weisskopf, 1959; Myers, 2003; Escultura, 2010). The electronic structure of the atom according to the Bohr theory states that electrons in an atom rotate around the nucleus in discrete energy orbits or shells. The energy shells, termed K shell, L shell, M shell, N shell, and so forth are stationary and arranged in order of increasing energy. When the transition of an electron occurs from an upper shell to a lower shell, the energy difference between the two shells is released as photon radiation.

If the electron is raised from a lower shell to an upper shell, the energy difference between the two shells is absorbed and must be supplied for the transition to occur. With data obtain from XE analysis, a spectrum of the concentration of the element and the energy can be determined. The principle involved in X-ray emission (XE) is inducing the production of X-rays in the bombardment of the atoms of an element present in a specimen with an intermittent beam of particles such as protons (PIXE) and alphas (AIXE). When an atom is bombarded an inner shell electron is ejected. Then the vacancy is immediately filled with an electron from an outer shell. On return, the atoms emit characteristic X-rays that have a known energy depending

on the atom and the initial or ground energy level. This returning of the electron is termed transition.

According to quantum theory, each shell is designated by a quantum number n, called principal quantum number denoted as an example, 1 for the K shell, 2 for the L shell, 3 for the M shell, 4 for the N shell, and 5 for the O shell. Each energy shell is subdivided into subshells or orbitals, which are normally, termed s, p, d, f and so forth. The transitions filling the vacancies in the innermost shell are called K X-rays and those filling the next shell are L X-rays, whose energies are lower.

The inner-shell vacancy creation is illustrated in **figure 1.1**. A beam of protons is used to eject inner-shell electrons from atoms in a specimen. When the resulting vacancies are filled by outer-shell electrons, characteristic X-rays whose energies identify the particular atom are emitted (Dyson, 1990).

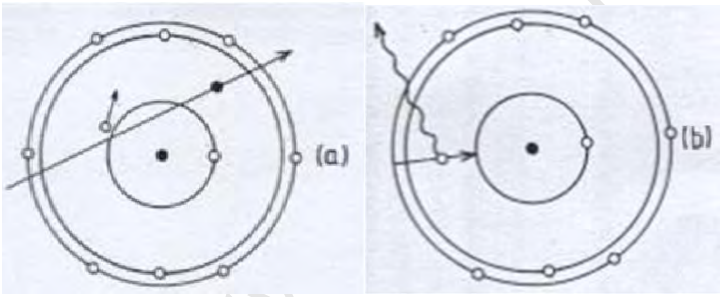

Figure 1-1 Illustration of the a) inner-shell vacancy creation and b) consequent X-ray transition as a result of excitation induced by a beam of particles, such as protons or alphas (Campbell, 1988).

X-ray emission analysis involves both a means of exciting the atoms of a specimen so that they will emit characteristic X-rays and a means of detecting and identifying these so that their intensities can be converted to elemental concentrations in the specimen.

In the process of bombarding a sample with a proton beam, the beam loses some energy while knocking off electrons from the inner shell of the atom resulting into an unstable atomic configuration. During excitation, electrons from higher energy levels fill up the vacancy and characteristic X-rays are generated (Morita, 1973; Garcia, Fortner and Kavanagh, 1973). The bombardment of an atom of low atomic number (Z) yields X-rays of low energy, since transitions of the K shell to the L shell depend on the filling of, for instance, the 2s and 2p orbitals. Therefore high Z atoms produce X-rays of high energies. When an electron returns from L-shell to K-shell the X-ray is called K_α X-ray, and similarly K_β X-ray when electron returns from M-shell to

K-shell. L X-rays are formed when electrons from higher shells return to the L shell and so on for the other lines of X-rays. These transitions are illustrated in **figure 1.2**. The emission of K or L X-rays will depend on the specific inner shell from which the electron is removed. This concentration of the element is proportional to the number of atoms in the specimen. The yield of the concentration is given by the equation of (Johansson & Campbell, 1988) see **Appendix B**.

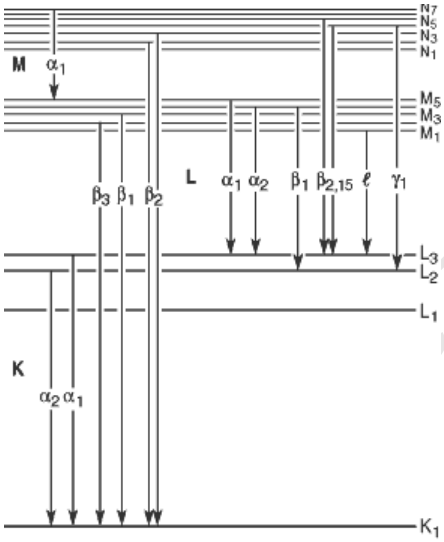

Figure 1-2 Illustration of the transitions that give rise to the various K, L, M and N emission lines (Kortright & Thompson, 2011).

The fundamental theoretical physical principles of PIXE have been detailed by Johannson & Campbell (1988). Furthermore, the background determinations and minimum detection limits (MDLs) have been established (Ishii *et al.,* 1988) for various sample matrices. MDLs (see **Appendix B1D**) of down to 1 ppm were obtained. In addition, applications have been made before. Mars, (2004) investigated matrices such as steel, superconductors and aluminium and zirconate. In that study the MDLs were down to 1 ppm. Recently, Guambe *et al.*, (2012a) and Guambe *et al.*, (2012b) in the determination of Al incorporated into fishscale matrices obtained MDLs in the order of 2-3 ppm. These studies all attest to the applicability of PIXE as an analytical technique. Computational software (GeoPIXE) has been used for quantification of X-ray emission data (Ryan *et al.*, 1995).

The most common detector used for acquiring X-ray emission data from PIXE is a Si (Li) detector with a thin beryllium window. The detector has high efficiency for X-ray energies between 5 and 20 keV, in which most of the elements of interest in

biological analysis lie. The Si (Li) detector is capable of resolving X-ray emissions as closely spaced as 150 eV and as a result 20-30 elements can be readily be quantified at the same time. Filters are absorbing foils normally placed in front of a detector to attenuate the bremsstrahlung background and the dominant low energy X-rays peaks found in biological materials. They are also important in preventing recoiling protons from damaging the Si(Li) detector. Filters can be constructed from several materials such as low atomic number elements such as Na, Mg (Z<10) (Ryan *et al.,* 1995).

1.7 Backscattering spectrometry (BS)

The fundamental physics principles of backscattering spectrometry have been detailed by Chu *et al.* (1978), Borgesen *et al.* (1982), Assmann *et al.* (1994) and Cohen *et al.* (2001) (see details in **Appendix B2E**). Applications for determining MDLs for various matrices have also been extensively applied (Mars, 2004). Computational software for quantification of backscattered data is available (Meyer, 1999).

1.8 Scanning electron microscopy (SEM)

In SEM the principle of analysis is the same as for PIXE. In PIXE, however the bombarding particles are a proton, deuterium, an alpha particle or heavy ions. In SEM the bombarding particles are electrons. The proton is about 2000 times heavier than the electron. This means that the force with which the electrons in the atom are excited is more in the case of PIXE than in SEM. Therefore with SEM mostly light elements such as C, O and N, electrons are excited. Also the bombarding energy of protons is set at 3.0 MeV whereas with electrons it is usually 25 keV.

Furthermore, during the excitation of light elements with protons the X-ray energy is absorbed in the window of the detector and hence X-rays of light elements are not detected in the spectrum of the X-ray emission data. This means that the minimum detection limit of PIXE is much lower (approximately 2000 times) than of SEM. Thus MDLs for SEM are of the order of 0.1% m/m and for PIXE is in order of 1 ppm. Thus trace and ultra-trace elements cannot be determined using SEM.

Hence SEM is used to quantify the major or matrix elements of specimens and PIXE is used to quantify the trace and ultra-trace elements. The Nuclear Microprobe (NMP) houses both PIXE and BS data detection instrumentation and is versatile in that specimens can be analyzed with the two techniques simultaneously (Rutherford, 1911; Goldstein *et al.,* 1959; Themner *et al.,* 1991; Mando *et al.,* 2009), (see **Appen-**

dix B1B). Backscattered particles resulting from the BS analyses can damage the window of the detector of X-ray emissions. However, for this reason and to amplify the X-ray emission data, an absorber (also termed a filter) is placed in front of the PIXE detector.

The most important aspect of PIXE, BS and SEM analyses is that these analytical techniques are multi-elemental, sensitive and non-destructive X-rays characteristics with the advantage of micro-beam scanning ability. This means that the samples once prepared can be analyzed again. Also the location and distribution of the analyte with respect to other elements in the matrix can be ascertained. A major disadvantage of PIXE is that the minimum detection limits realizable is approximately only 0.1 ppm for PIXE.

With regard to toxicity, this disadvantage however only applies to elements that are below this detection limit, such as As. With SEM molecular species such as polyions of nitrogen and carbon can be determined. This means that if NO_3^- ions are to be analyzed, any other nitrogenous substances such as NH_4^+, NO_2^- and organic nitrogen will all be analyzed as N; similarly, for C for the ions CO_3^{2-}, HCO_3^- and so forth.

1.8.1 Limitations of the techniques

The optimum beam energy for PIXE analyses of biological samples is between 2 and 3 MeV depending on the elements of interest (Calligaro *et al.*, 2004). At this energy backscattered particles may damage the detector window. For this reason an absorber is placed between emitted particles and the window of the X-ray detector. The window of the X-ray detector consists of layers of the elements beryllium (Be) with thickness of 8.5 μm, gold (Au) with 0.02 μm of thickness, aluminum (Al), and thickness of silicon (Si) is around 0.018 μm.

This means that the X-rays resulting from the bombardment of atoms of atomic weight between C and Mg are absorbed in the window of the X-ray detector and therefore do not reach the detection system inside the detector. Hence, elements with atomic number lower than and equal to that of Mg cannot be detected. Elements with higher atomic numbers can be detected. Thus, for keratin (KRT) only S can be detected, for calcium carbonate (CCB) only Ca, and for hydroxy-apatite (HAP) only Ca and P can be detected. Hence, elements with lower atomic number for KRT such as C, O and N; for CCB a group of elements C and O and for HAP elements such as C, O and H, it is necessary to apply SEM.

1.8.2 Biological applications of nuclear microscopy

Elements in biological samples such as plant tissues are widely analysed using PIXE (Malmquist, 1990) to determine trace element concentrations due to migration from mineral deposits underground and certain plant species are used as indicators of specific type of mineralization ore deposits (Maenhaut, 1988). A proton beam from a tandem accelerator of the Institute of Physics, Bucharest has been used for determination of major, minor and trace elements in environmental samples (vegetable leaves and soils) (Bancuta*et al.*, 2006; Popescu *et al.*, 2007; Cristache *et al.*, 2008; Ene *et al.*, 2009).

PIXE was able to identify the elements such as S, Cl, K, Ca, Ti, Mn, Fe, Ni, Zn and Sr in vegetable samples and elements such as K, Ca, Mn, Fe, Cu, Zn, Cr, Sr and Mo in soils samples with uncertainties of the order of 10%. Using such techniques it has been showen that the toxic element Sr is high in vegetables and in the surface of the soil and decreases inside the soil (Ene *et al.*, 2001; Olariu *et al.*, 2008; Popescu *et al.*, 2009). Land mammals, birds, fish and insects may be used to identify mineralization (Cannon & Taxon, 1971; Mirzai *et al.*, 1990). PIXE has been used to identify the localization of trace metals in hyper accumulating plant species (Siegele *et al.*, 2008).

Ion Beam Analyses (IBA) may contribute to the improvement of the accuracy of deviation errors of the concentration factors which are expected to be indicators for doses of radiation caused by environmental radioactivity (Ishikawa *et al.,* 1990). It has been found that data obtained from scanning analysis may suggest that elements deposited into the environment are as a result of specific activities or due to the ambient conditions such as environmental pollution by the metals (Ishikawa *et al.,* 1990).

Information on the accumulation of elements especially with regard to age and species, accompanied by information on the growth of organisms may contribute not only to the field of physiology but also to the radiobiology (Davis & Foster, 1958; Whicker & Schultz, 1982; Ishihawa *et al.,* 1990; Hall, 2006) of the organisms of concern. Accumulation of an element may be due to natural bioaccumulation (i.e. part of an organism's natural physiology) or it may be induced by increased ambient concentrations.

PIXE analysis is clearly effective in its ability to detect elements below a few ppm levels, and provides further possibilities for collecting information from bio-medical and environmental samples on trace elements. PIXE as a multi elemental technique

in combination with a high sensitivity permits the determination of many trace elements in one single run. For instance the minimum detection limit in the case of an organic matrix is in order of 10^{-6} -10^{-7} ng/ml.

Although other techniques such as inductive coupled plasma mass spectrometry (ICP-MS), atomic absorption spectrometry (AAS) and ion chromatography (IC), can provide very accurate measures of the concentrations of elements. The sample has to be destroyed as these types of analytical technique require the sample to be dissolved by reaction with strong acids or bases. It is not possible to obtain information on the 3-dymensional distribution of elements in a solid sample.

1.9 Type and composition of fish scales

The scales of teleost (bony) fishes exist in two major forms, cycloid and ctenoid as illustrated in **figure 1.3.** Cycloid scales have smooth margins while ctenoid scales have tiny teeth called ctenii on the posterior edge giving them a rough texture. Scales of both types consist of a layer of acellular bone and an underlying fibrilary plate of collagenous connective tissue. The main constituent of the bony layer is hydroxyapatite crystals consisting chiefly of calcium phosphate (Harder, 1975; Tang *et al.,* 1997; Wojnar, 2011). The lower fibrillar layer has a non-mineralised matrix consisting mainly of collagen and also another protein, isopedine or ichthylepidin (Helfman *et al.*, 2009).

Chemically the fish scale generally consists of keratin (KRT), calcium carbonate $CaCO_3$ (CCB) and hydroxy apatite (HAP) (Jablonski, 2005). The composition of KRT is mostly carbon, hydrogen, oxygen and a small amount of S, about 1% (Geissler *et al.*, 2001). The CCB consist of 40 % of Ca and HAP consists of 40 % m/m of Ca and 20 % of P. Hence in a region where the concentration of calcium is more than twice that of P, the excess Ca is ascribed to CCB. Literature research has shown that was no work has been performed before in applying PIXE in fish scale.

Figure 1-3 Illustration of cycloid scales of *Pomadasys kaakan* and *Lithognathus mormyrus* (on the left) and ctenoid scales of *Lutjanus gibbus* and *Pinjalo pinjalo* (on the right).

Biologically the scale is one of the parts of a fish's body where accumulation occurs by incorporation, of elements directly from the environment (Patel *et al.,* 1975; Finn-Va, 1980; Ishikawa *et al.,* 1984; Van der Perk *et al.,* 2006; IAEA, 2006; Pinder *et al.,* 2011).

Scales are some of the few structures that are accessible for evaluation of chemical composition without killing the fish (Perga & Gerdeaux, 2003). More than that, they can provide composition a time- related indication of environmental condition.

1.9.1 Growth of fish scales

Steinstrup (1861) found that all scales grow throughout life and increase in size as fish size increases. Since scales grow by increasingly larger plates. Mandl, (1839) and Taylor, (1916), found that a combination of the two processes was involved in the development of the scale. In addition to Mandl, Williamson (1851), Baudelot (1873), Iofer (1889), Klaatsch (1890), Ussov (1900) and Hase (1907) studing the histogenesis of scale structures. The outer layer fine scale normally consists of homogeneous proteinaceaus tissue can posed mainey of keratin (KRT) and the remainder consists of amorphous calcium and phosphorus as hydroxyl apatite (HAP) and calcium carbonate (CCB) (Creaser, 1926; Posner & Betts, 1975).

There is considerable evidence that the scales of some fishes cease growing in winter, when the annulus is formed (Weatherley *et al.,* 1987; Casselman, 1990). Pearse (1919) found that adults fish of the species *Pomoziz sparoides* do not appear to feed in the winter. Furthermore, these fish were caught in marine waters. Hence the fish

have spent the first year in a freshwater environment. In addition the average temperature in the gulf region is higher than the temperature in the Indian Ocean and the sub-tropical regions where some of the specimens for this study were caught.

Fish scale incremental patterns possess a unique combination of features. Fish scales are easily available, their preparation for image processing is very simple, and ichthyologists have used fish scale patterns for decades as a source of information about the life history of fish as well as the state of the environmental (Pepin, 1991; Friedland, 1998). A database of results obtained from incremental studies, together with an oceanographic database (Levitus *et al.*, 1998) can provide new methods for studying pollutants of river and ocean life. Fish scales can therefore be used as a source of information which can be used to address important questions in aquatic environment (Beamish *et al.,* 1987; Lund & Hansen, 1991).

1.9.2 Fish scales

The discrete model of the growth of fish scales is a formalization of the 2D anisotropic structure where the growth rate in posterior region is slower than the growth in anterior region (Smolyar & Bromage, 2004). Analyses show that the pattern of anisotropy in fish scales results in less than perfect descriptions of growth rate of 2D fish scale patterns and thus growth-rate variability may only be described in "fuzzy" terms. The index of structural anisotropy is a measure of this fuzziness provided with some perspective on the confidence one may have in the measurements.

Cook & Guthrie (1987) used the problem of fish stock identification to illustrate how the model of the fish scale pattern could contribute to the solution of the problem. For example using a discrete model of fish scale incremental pattern is proposed which takes into account the incremental structure such as the 2-D. Based in this model the representation of the form of the fish scale pattern as a relay network, taking anisotropy in the form of discontinuities and convergences of incremental structural elements into account, and the widths of growth increments in different directions. This model was used for quantification of fish scale growth rate. The capability of the model to analyze objects with similar structures as found in fish scale incremental patterns, opens new challenge such as a comparative study with those found in coral, otoliths, shells, and bones (Popper, Deng, Ramcharitor and Higgs, 2001).

1.10 Application of growth equations

1.10.1 Correlating the length of the fish to the age

The age of a fish is normally determined by its length. Various growth equations have been formulated to account for the growth and the applicability of the growth equations of especially fish and fish populations (von Bertalanffy, 1938; Pauly & Munro, 1984; Tang *et al.*, 1997; Schnute, 1981; Majid & Imad, 1991; Gayanilo *et al.*, 1996; El Husaini *et al.*, 2002; Valinassab *et al.*, 2002; Smolyar & Bromage, 2004; Lei & Zhang, 2006; Falahati *et al.*, 2008). The most applied equations are those of von Bertalanffy (1938) and Schnute (1981). There is no difference in the applicability of these growth equations to the fish scales (Pauly, 1980; Schnute, 1981; Gayanilo *et al.*, 1996; Valinassab *et al.*, 2002; Smolyar & Bromage, 2004; Falahati *et al.*, 2008). For the purpose of this study the von Bertalanffy equation (**Eqn. 1.1**) was chosen on the merit that a seasonalized form (**Eqn. 1.2**) has been evaluated (Fakhri *et al.*, 2011).

$$L_t = L_\infty \left(1 - exp\left(-k(t - t_0)\right)\right) \qquad (1.1)$$

$$L_t = L_\infty \left(1 - exp\left(-k(t - t_0)\right) + \frac{Ck}{2\pi sin\left(2\pi(t - t_s)\right)}\right) \qquad (1.2)$$

In these equations, L_t is the predicted length (cm), L_∞ is the asymptotic (hypothetical length) (cm), k is the growth constant (year^{-1}), t is the time of measurement (year), t_0 is the hypothetical age (year), C is the amplitude of cyclization (seasonality) (year^2) and t_s is the hypothetical age at the onset of the first growth oscillation (year). **Equation 1.2** is given here simply for ease of reference to other investigations, and is not considered in this study since the temperature variation experienced in the geographical area is from 26 to 29°C on average. Based on the philosophical and biochemical basis of the derivation of the von Bertalanffy equation (von Bertalanffy, 1938) temperature variation should not incur growth abnormalities, but would affect the growth rate of the fish.

The values of the parameters for *Pomadasys kaakan* have been discussed by (Fakhri *et al.*, 2011) and are given in **Table 1.1** for ease of reference (Majid & Imad, 1991; Lee *et al.*, 1992; Al-Husaini *et al.,* 2002; Fakhri *et al.*, 2011). For comparison of the different parameter valuesused, the growth performance index (Munro & Pauly, 1983; Pauly & Munro, 1984) is also given. In this table the value of 94 cm for L_∞ and of 0.18 for k provided by (Lee *et al.*, 1992) are not in agreement with the other

values and were not considered in the determination of the age of the fish used in this study.

Table 1-1 Various growth parameters estimated for *Pomadasys kaakan* found in different locations (Fakhri *et al.,* 2011); (Al-Husaini *et al.,* 2002); (Lee *et al.,* 1992) and (Majid and Imad, 1991). L_t is the predicted length (cm), L_∞ is the asymptotic (hypothetical length) (cm), k is the growth constant (year^{-1}), Θ' is the growth performance index (Munro *et al.,* 1983) and (Pauly & Munro, 1984).

L_∞(cm)	k (year^{-1})	Θ'	Locality	Reference
2.20	0.270	3.004	Persian Gulf (Kuwait)	Al-Husaini*et. al.*, (2002)
94.00	0.180	3.200	Persian Gulf (Kuwait)	Lee *et. al.*, (1992)
62.50	0.247	2.980	Coast of Pakistan	Majid&Imad (1991)
64.61	0.240	3.000	Persian Gulf (Iran)	Fakhri*et. al.*, (2011)

1.10.2 Correlating the fish length to scale length

It is now necessary to correlate the growth of the fish to the growth of the scale. For the purpose of this study, two empirical equations (Mars *et al.*, 2012[3]), given in **Table 1.2**, based on independent data (Fry, 1943) were derived to correlate the length and therefore the age of the fish to the scale growth. The growth length considered was that of the diameter of the posterior region of the fish scale.

Table 1-2 Statistical evaluation of two empirical equations used to correlate the growth in length of the fish, and therefore the age of the fish, to the growth in diameter of the posterior region of the fish scale, based on independent data (Fry, 1943), where a and b are the constants determined by the fit to the data, x is the age of the fish and y is the growth in length.

Equation 1	$y^{-1} = a + \frac{b}{x^2}$					
R^2CoefDet	DF Adj R^2	Fit Std Err	F-value			
0.999460765	0.99928102	0.05030925	12974.359			
Parameter and Value		**Std Error**	**t-value**	**95% Confidence Limits**		**p(t)**
a	0.116007	0.002155	53.831712	0.1109112	0.121103	0.00000
b	2055.7518	45.263937	45.416991	1948.719595	2162.784001	0.00000

Equation 2	$ln(y) = a + \frac{b}{x^{0.5}}$					
R^2CoefDet	DF Adj R^2	Fit Std Err	F-value			
0.999028	0.998056	4.899108	3083.505			
Parameter and Value		**Std Error**	**t-value**	**95% Confidence Limits**		**p(t)**
a	7.403507	0.052238	141.725293	7.237261	7.569753	0.00000
b	2055.7518	45.263937	45.416991	-21.493541	-17.807521	0.00006

[3] Mars, J.A., Guambe, J.F. & Day, J. (2012) unpublished data

The parameters in the above table according to Fry, (1943) show an statistical evaluation of two empirical equations used to correlate the growth in length of the fish, and therefore the age of the fish, to the growth in diameter of the posterior region of the fish scale, based on independent data where a and b are the constants determined by the fit to the data, x is the age of the fish and y is the growth in length.

1.10.3 Volumerisation of the scale

The thickness of the scale varies from the focus area to the edge of the scale. This variation in thickness will influence the growth of the scale and the distribution of the elements. The volumerisation of the scale is shown in **figure 1.4**. Since existing data (Fry, 1943) is based on the major area of the scale, formulation of the volumerisation is based on a lateral line that is parallel to the lateral field of the scale and perpendicular to the edge of the scale. The trapezoidal volumerisation is derived based in iteration, correlating the arc length to the radius, establishing the area and then determining the volume as given in **figure 1.4**. It should be noted that the derivation is constrained by $r_i > ½s_i$.

$$i = 1 \,..\, n$$

$$s = r\theta$$

$$IB = \sqrt{(r_2 - r_1)^2 - \left(½(s_2 - s_1)\right)^2}$$

$$Area = IB \times ½(s_2 + s_1)$$

$$volume = area \times ½(t_2 + t_1)$$

$$total\ volume = ¼ \sum_{i=1}^{n} \left(\sqrt{(r_i - r_{i-1})^2 - \left(½(s_i - s_{i-1})\right)^2} \times (s_i - s_{i-1}) \times (t_i - t_{i-1}) \right)$$

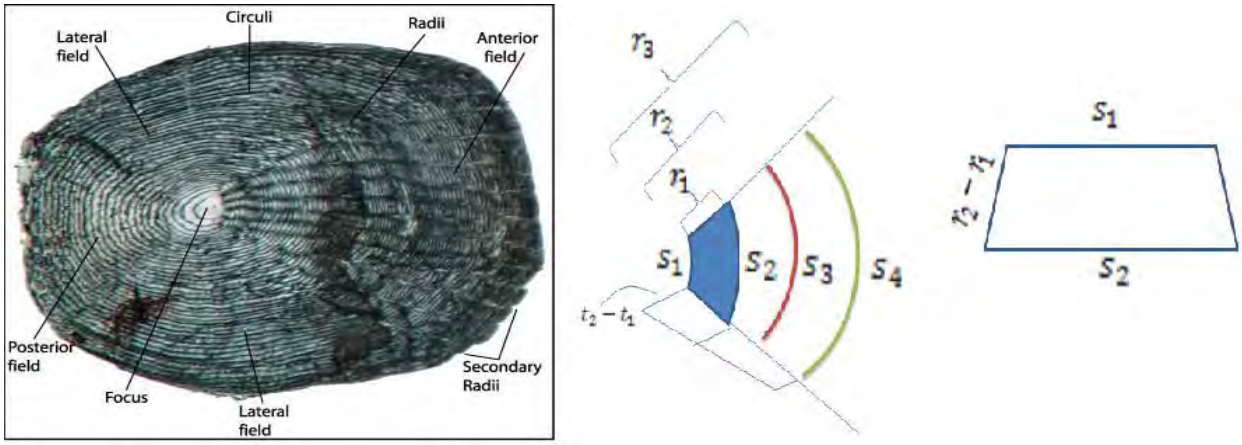

Figure 1-4 Trapezoidal volumerisation of the fish scale. $t^{\cdot}_i$, $r^{\cdot}_i$ and $s^{\cdot}_i$ are respectively the thickness, radius and the arc lengths.

1.11 Statistics and minimum detection limit (MDL)

The information in this section is provided for the benefit of the readers who are not familiar with PIXE techniques. The "p" values for the data were determined using Statistical software version 9 (Greenberg, *et al.,* 1978). A "p" value of 0.05 was accepted as indicating significance.

In any measurement of a physical system there are, inevitably, sources of both systematic and random error. The former are usually associated with systematic defect in the measuring equipment and can often be compensated for by careful calibration of the equipment against a known standard. The latter can be much more subtle, involving both the measuring equipment and the physical process being measured. When measuring small physical properties, in particular electronic or other signals, the random noise on the signals determines the ultimate detection limit on the measurement of a real physical occurrence/event. A signal that exceeds this threshold detection limit is assumed not to be due to noise.

In practice a number of different "detection limit" criteria have been defined. These include the "Instrument Detection" Limit (IDL), the "Practical Quantification Limit" (PQL), and the "Method on Minimum Detection Limit" (MDL), which includes all the steps in the analysis of the data (see for example chapters 3-5). In this latter method, which is used in the present work, the results of a set of fifty or sixty measurements are analyzed and the standard deviation, σ, for the noise signal is estimated. This may be determined from raw data for the noise alone i.e. in the absence of the wanted/real signal, or otherwise estimated by a variety of means (see

Appendix B). Any signal with a value (amplitude or number) greater than 2σ may then be considered to be real with a confidence limit of 95% (see **Appendix B1D**).

To facilitate the analysis of a continuum of data as a function of some variable, for example the PIXE spectrum, it is necessary to transform the data into a histogram format. Thus the total spectral energy range (dependent variable) is divided into a fixed number of equally spaced portions or "bins" into which the measured data is electronically stored. The MDL analysis is then done separately on the average (i.e. over the seven measurements) data in each bin.

An example of a single PIXE spectrum (showing peaks for the Fe K_α is emitted at 6.39 keV and that of molybdenum (Mo) K_α at 17.478 keV lines) is given in **figure 1.5** where the spectrum energy range has been divided into 511 bins. However, the energy of 6.39 keV is collected in bin 150. The emission spectra results from an absorption/bombardment-emission process, as in PIXE, the total area under the peak is proportional to the cross section for the process and to the concentration of the absorbing atomic species.

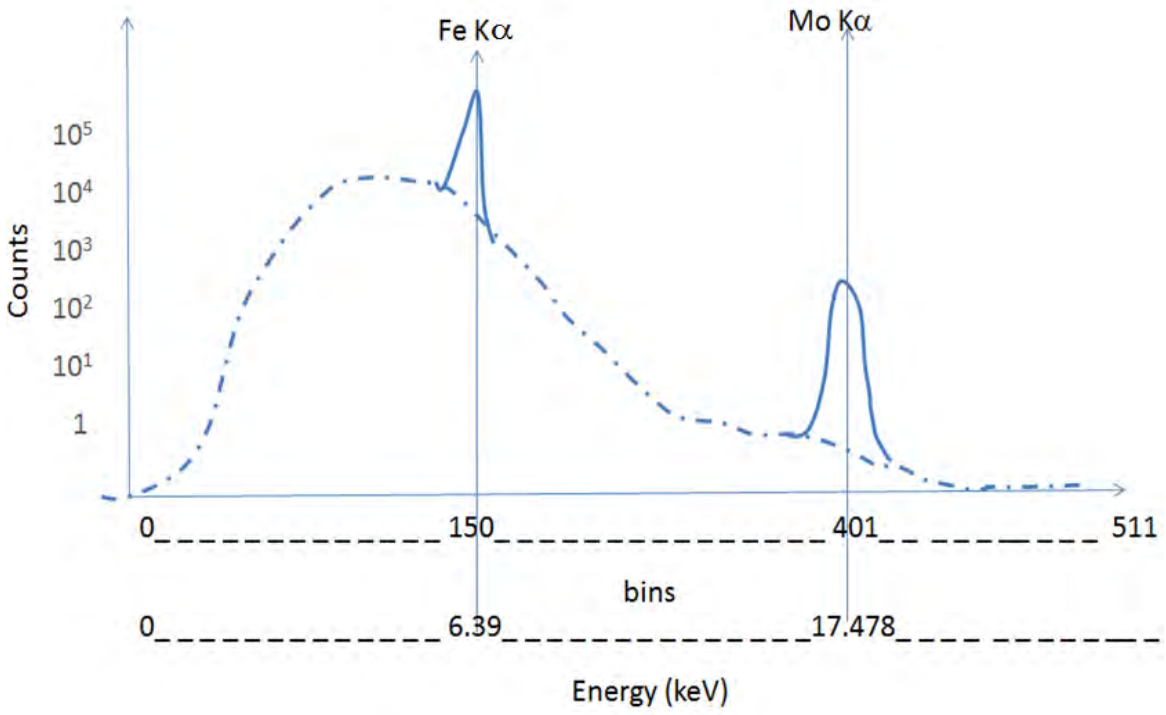

Figure 1-5 Illustration of the determination of X-ray data of the energy versus the counts. The dotted line is the background based on equations (with references) given in Appendix B1B. Bins are based on the registers of the electronic istruments, based on which a calibrate value for energies of emitted X-rays are determined.

As an example, let's assume there are 100 ppm of Fe and 10 ppm of Mo present in a sample. When the beam of particles strikes the sample excitations of electrons in the atoms occur. As soon as the electrons are ejected out of the atom and other electrons fill the vacancies and return to the initial position, giving off X-rays.

The intensity of the X-rays is proportional to the number of electrons excited which is proportional to the number of atoms present. The number of atoms present is proportional to the concentration. Say the counts for Fe K_α and Mo K_α for the first emission are 1500 and 150. With the second and third beam bombardment the counts are 1510 and 148 and then 1495 and 151, and so forth. Each count, for X-ray energy is done every 10 milliseconds. These are then repeated for a period of 2.5 hours. These counts are then averaged. Hence the average counts after the duration of 2.5 hours are displayed. Using the equations for bremsstrahlung (see **Appendix B**), the background when plotted as the 10^x of the X-ray energy is given by dotted line in the figure below. Thus 10000 counts would be 10^4, etc.

From visual inspection, the Fe K_α peak seems smaller than the Mo K_α peak and hence the area of the Fe peak should be less than that of Mo and so the concentration. However the background at the energy of Fe K_α is about 10^4 more than the background at the energy of Mo K_α. Similarly, the K_β X-rays energies are exhibited. In the case of a compound, i.e. where there is more than one emitting atomic species with a fixed concentration ratio among them, then the ratio of their characteristic PIXE peak areas must scale with the concentration of the compound.

The correlation of concentrations is necessary to identity component structure. For example, if a sample such as HAP consists of Ca and P then, if Ca is formed in a certain area of the sample, the P should also be formed in that area. Then the correlation will be linear. The slope of the line representing the correlation will depend on the composition of Ca and P in HAP. The slope will however not affect the linearity. If the correlation is diffused, then Ca and P are present but not as HAP, rather as another type of compound. Because of the concentrations can at times be in the parts per million ranges, the logarithm of the concentration is plotted.

1.12 Pile-up

A particular source of error, known as "Pile-up" error, occurs when obtaining a spectrum of intensity (i.e. fluency of photons) as a function of their energy (by measuring the pulse height amplitude of "pulses" produced by a detector of the photons) and results when a pulse arrives at the detector at a time when the detector base line, following a preceding pulse, has not yet been fully restored (O'Meara & Campbell, 2004). For this reason the beam is intermittently propagated. This is done by a beam on demand electronic system. This error leads to a decrease in energy resolution and may be minimized by one of two means, namely:

(i) By the application, in the electronic measurement system, of a "dead-time, or period of time which starts at the beginning of each pulse detected and ends when the base line is restored. During this dead-time period no other pulse is analyzed.

(ii) By limiting the intensity of the photon source such that the average time separation distance between successive pulses is much larger than the pulse time width. In the present case this is done by reducing the intensity (fluency) of the incident radiation onto the specimen).

The silicon escape peak arises from the K X-rays escape of silicon as a result of photo-electric interactions close to the surface window of the detector (Campbell *et al.,* 1987; Fraser *et al.,* 1994). Its intensity is 1% or even less of its parent peak for e.g. the escape peak of Fe K_α at 4.65 keV, overlaps the Ti K_α in the energy range of 4.51 keV (Goulding & Jaklevic, 1973; Johansson *et al.,* 1988; Campbell *et al.,* 1998).

Chapter Two
2 Materials and Methods

2.1 Geography of the study area

Mozambique is located in the south eastern part of Africa (**figure 2.1**). It is bordered to the east by the Mozambique Channel, which is part of the warm Indian Ocean. For this reason, the country's climate is predominantly tropical to sub-tropical with average temperatures around 28^0 C along the coast even in mid-winter July. Rainfall is predominantly in summer from October to April illustrated in **Appendix G**. To the north it is borders with Tanzania (Rovuma River), Zambia, Zimbabwe and Malawi of which Lake Nyasa forms an integral part on the west and South Africa and Swaziland on the south. Maputo is the capital of the country and also the largest municipal area. It has a population approximately 1 million (INE, 2007). According to the 2009 census (INE, 2009), the population of Mozambique is about 23 million. Annual population growth rate is 1.9 % (INE, 2009). Mozambique is mainly agricultural, being dominated by small-scale cultivating farms with an average area of 100 to 500 m^2. Several rivers meet in the Espirito Santo estuary to the south of the Maputo city and drain into the Indian Ocean. Except for the Matola River, discussions and images of the other sampling area are given in **Appendix D**.

Many people have very low incomes and rely on these rivers for fish as a major source of protein.

The Matola River drains into the Espirito Santo estuary which in turn drains into Maputo Bay. The inflow of the river into the Espirito Santo estuary lies 12 kilometers to the west of the Maputo Central in the intersection of the Incomati and Umbeluzi basins. The river is approximately 70 km in length. The width varies from 1.8 to 2 km and depth from 2 to 6 meters more details see **Appendix F**.

The vegetation is predominantly degraded Miombo Savannah, as it has been used for subsistence agriculture until fairly recently. Most of the woody vegetation has therefore been cleared, and the area is dominated by relatively open grassland with scattered shrubs and small trees, many of which have grown from remaining root stock. Many industries drain their effluents into the Matola River hence the particular attention of the study of this river. Precipitation averages 761 mm per year.

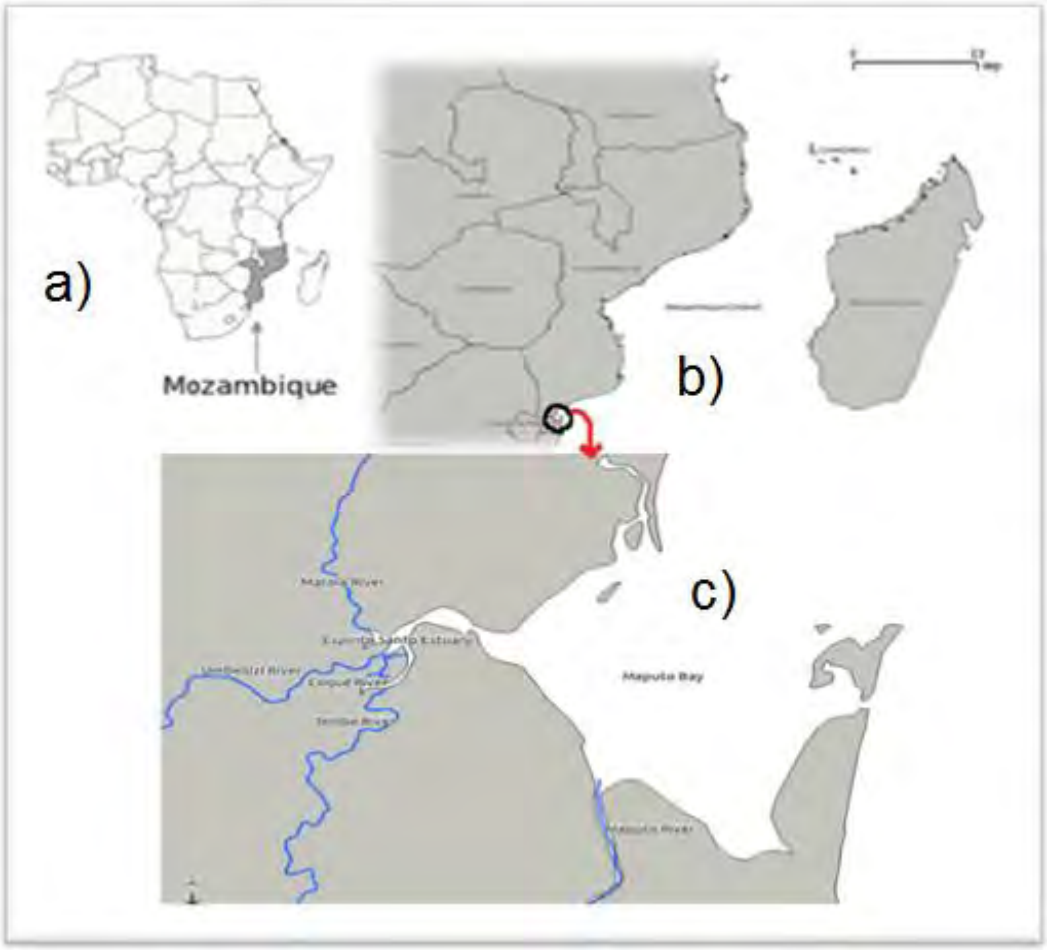

Figure 2-1 Geographic location of Mozambique in the African continent a). To the north it is bordered by Tanzania through the Rovuma River; to the west is bordered with Malawi, Zambia and Zimbabwe and to the south by South Africa and Swaziland. To the east it is bordered by the Mozambique Channel which is part of the Indian Ocean, b). Matola River, Umbeluze River, Coque River, Tembe River, Espirito Santo Estuary, Maputo River and Maputo Bay are the sampling areas, c). The country is typical flat land and only the borders with South Africa, Zimbabwe and Zambia are mountainous.

The river is typically mangrove channels and corals. The Mozambique aluminium smelter industry (MOZAL), sampling point A5, is approximately 15 km from Matola harbour. A few hundred meters north east of the MOZAL plant and immediately west of the Matola River lies 60 hectare of the future GS Cimentos, Cement Factory and Limestone mine, Mozambique see **Appendix D1**.

Figure 2.2 shows sampling points A1, A2, A3, A4, A5, A6, A7, and A8 along the Matola River where most of the industries discharge their effluents. Samplinges were taken between 2007 and 2009.

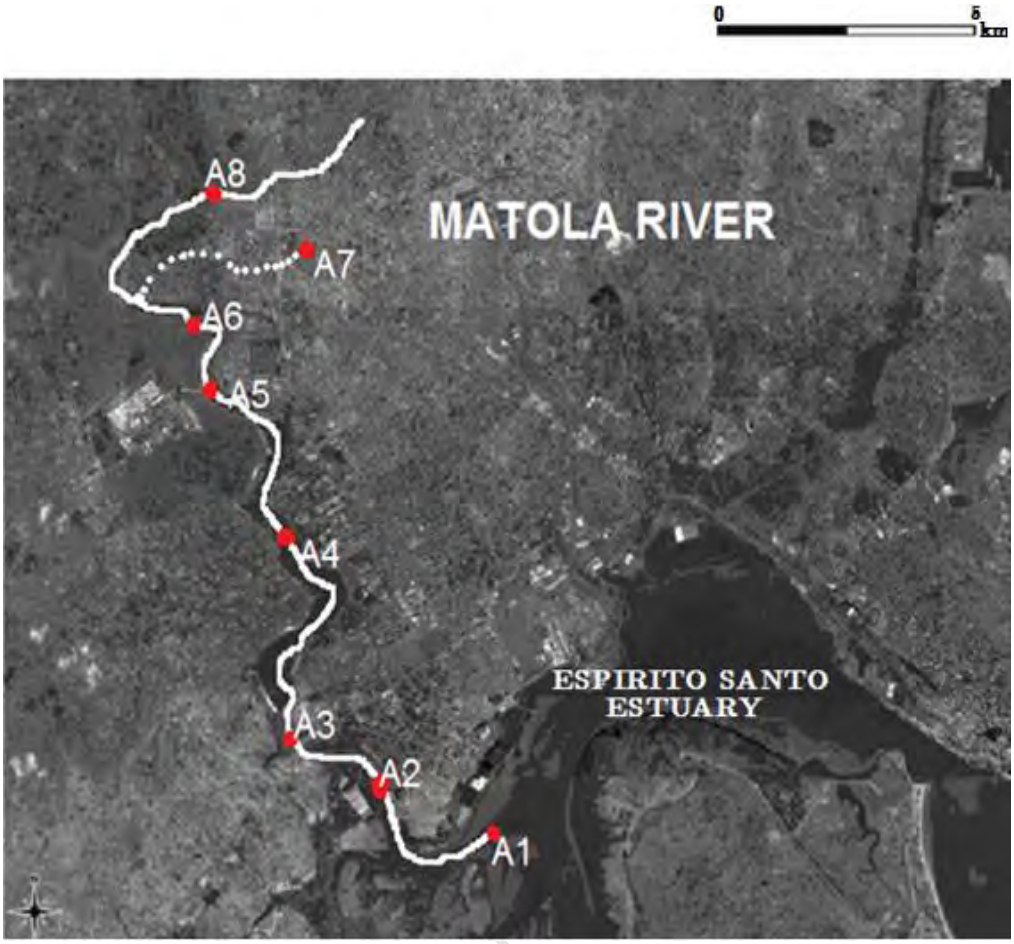

Figure 2-2 Sampling points along the Matola River in the period 2007-2009. An aluminium smelter is located near to sampling point A5. QGIS 2007, http://qgis.org, accessed 2008-12-24.

2.2 Fish scales

Fish such as *Pomadasys kaakan* (the javelin grunter)*, Pinjalo pinjalo*, *Lutjanus gibbus* and *Lithoguaths mormyrus* are mostly often caught for human consumption along the Matola River, Tembe River, Espirito Santo Estuary and Maputo Bay with more details **Appendix E5**. In **Appendix C** is presented the sampling points coordinates of the different fish species. These fish species spend the first year of life in a freshwater environment (Gerking, 1959; Weatherley, 1987). During this period they do not reproduce (Humphries *et al.,* 1999), only reproducing when may migrates to the sea (Quinn *et al.*, 2009). The scales of teleost fishes exist in two forms: cycloid and ctenoid. They consist of a layer of acellular bone and an underlying fibrilary plate of collagenous connective tissue. The main constituent of the bony layer is hydroxyapatite crystals comprising chiefly of calcium phosphate (Harder, 1975; Tang *et al.,* 1997; Wojnar, 2011).

The lower fibrillar layer has a non-mineralised matrix comprising mainly of collagen and also a special protein, isopedine or ichthylepidin (Helfman *et al.*, 2009).

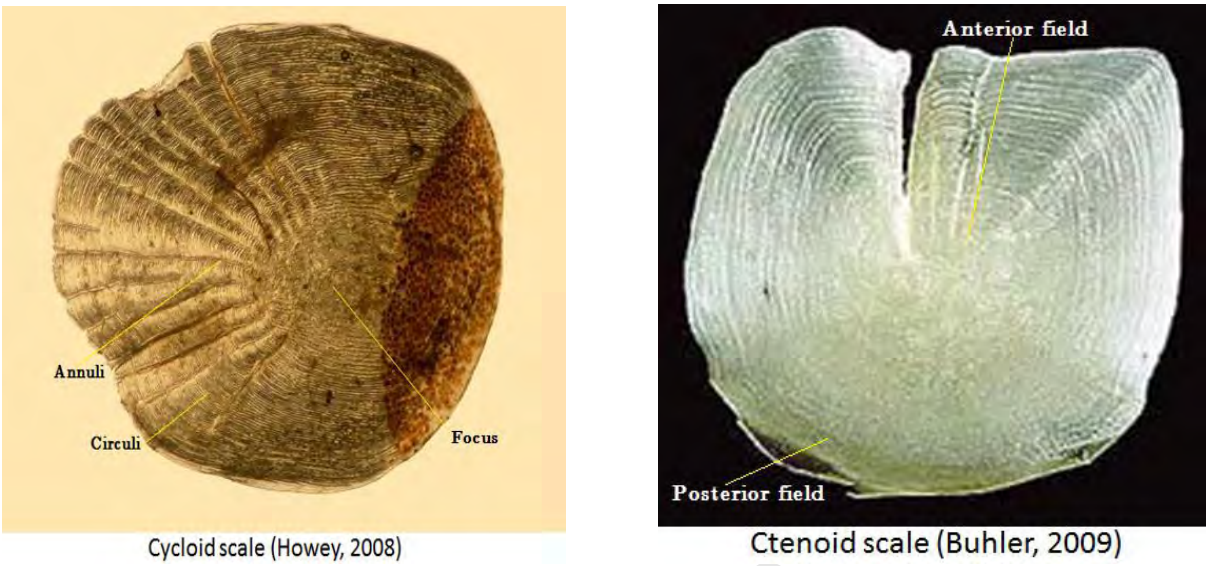

Cycloid scale (Howey, 2008)

Ctenoid scale (Buhler, 2009)

Figure 2-3 Scales of the types cycloid (Howey, 2008) and ctenoid (Buhler, 2009).

The fish scale generally consists of keratin (KRT), calcium carbonate (CCB) and hydroxy apatite (HAP) (Jablonski, 2005; Guambe *et al.*, 2012). The composition of KRT is mostly carbon, hydrogen, oxygen and a small amount of S, about 1% (Geissler *et al.*, 2001). The CCB consist of 40 % of Ca and HAP consists of 40 % m/m[4] of Ca and 20 % of P. Hence in a region where the concentration of calcium is greater than twice that of P, then the excess Ca is ascribed to CCB. **Appendix D & E** are showing the concentrations of ions from water analysis.

2.3 Analytical techniques and applicability

The principal aim of this study is to find a useful method for assessing pollution of natural resources by metals. This means that instruments with which the concentrations of substances will be determined should be applicable to the analysis of the substances. More importantly, the smallest amount of the substance present should be determinable with the particular instrument. The smallest amounts of substance that can be determined with an instrument are referred to as the minimum detection limit (MDL) and depend on the sample nature. In this study fish scales, sediment and water were analyzed. Since fish scales and sediments are solid in nature, the

[4] In SI unit: 1% m/m=10 000 ppm= 10 000 mg/kg= 10 g/kg

applicable techniques for analysis were particle induced X-ray emission (PIXE), backscattering spectrometry (BS) and electron-induced X-ray emission, normally referred to as scanning electron microscopy (SEM).

2.4 Specimen sampling procedures

2.4.1 Water

The water samples were collected using a Van Dorn Water Sampling apparatus (Duncan & Associates, Cumbria, United Kingdom) see **Appendix H3** in the different geographic points along Matola River, Umbeluze River, Coque River, Tembe River, Espirito Santos Estuary, Maputo River, Maputo estuary, and Maputo Bay (see **Appendix D**). The pH was determined with a Crison micro pH meter (Allele, Barcelona, Spain), and the results are shown in **Appendix D & E**. The water sample was then cooled to 4^0C and stored at this temperature until analysis. Additional water parameters such as depth (meters), conductivity ($mS.m^{-1}$), visibility, nephelometric turbidimetric (NTU), salinity (parts per million (practical salinity units (PSU) and temperature (^{0}C) were measured *in situ* with the CTD probe (Hart Scientific, American fork, Utah, USA). The CTD probe was secured in a cage as shown in see **Appendix H4**.

The sampling points from which the fish were collected are given in **table 2.1**.

Table 2-1 Sampling points where the fish was caught. The area, the species and the sampling points and the GPS coordinates (degrees, minutes and seconds) are given.

Area	Fish	Sampling point	GPS coordinates	
Matola River	*Pomadasys kaakan*	A3	25 58 29	32 26 14
Tembe River	*Pinjalo pinjalo*	D3	26 03 18	32 28 30
Espirito Santo Estuary	*Lutjanus gibbus*	E4	26 58 00	32 29 46
Maputo Bay	*Lithoguathos mormyrus*	G13	25 54 07	32 9 52

The geographic coordinates and sampling points for water and sediment samples and fish scales are given in **Appendix C** and **Appendix D**.

Sediments and fish scales were analyzed using Particle Induced X-ray Emission (PIXE), Backscattering spectrometry (BS) and Scanning electron microscopy (SEM).

The water samples were analyzed using Inductively Coupled Plasma Mass Spectrometry (ICP-MS), Flame Atomic Absorption Spectrometry (FAAS) and Ion Chromatography (IC) see **Appendix D** and **E** for results.

2.4.2 Sediments

The different geographic sampling points for sediments are illustrated in **Appendix C** and **D**. The sediment sampler used was a Van Veen grab sampler (Rickly Hydrological Co., Columbus, Ohio, USA) in the field see **Appendix H5**. The sediments samples were transported in 500 mL plastic containers to the laboratory where the samples were removed from the plastic containers and spread over a surface area. The samples were then left to dry under dust-free conditions for a period of 5-10 days. The samples were then coated with a layer approximately 10 nanometers' thick of carbon see **Appendix H2**.

2.4.3 Fish scales

In this study 22 fish scales were sampled, two from cach of 11 specimens (2 from each) see **Appendix C** and **Appendix F** and caught by fish net **Appendix H7**. But for the present work were presented the results for four fish scales because of morphometric similarity. After being caught, the fishes were stored at 4^0 C and taken to the Institute of Fisheries IIP, *Instituto Nacional de Investigaçao Pesquiera* (National Institute of Fisheries) in Maputo, Mozambique, for identification. Scales were removed immediately, and washed with copious amounts of distilled water to remove adhering impurities such as salts. The scales were afterwards submerged in ethanol (100%) and then placed an ultrasonic bath for 30 minutes and washed again with distilled pure water. The weight of the scales were 140 ± 20 mg.

After washing the scales were wrapped in filter paper and clamped between two Perspex plates. This was done to minimize curving of the scale. Each scale was glued to an aluminum stub of 11 mm × 22 mm, with holes of 8 mm diameter and then coated in a sputter coater with layer of approximately 10 nanometres thick of carbon for electron conduction see **Appendix H2**. In the **Appendix E2** is showing the table contain detailed information related to fish species studied.

Microscope images were obtained with a Nikon SMZ 1500 (Nikon, Tokyo, Japan). The microscope images were necessary as the minimum magnification with the

scanning electron microscope was 25 times and detailed full image was needed for verification purposes.

2.5 Analytical sample preparation and instrumental procedures

2.5.1 X-ray emission analysis

Proton-induced X-ray emission analyses were performed only on the fish scales and sediments. Fish scales were mounted on the aluminium stub of 11 mm × 22 mm with hole of 12 mm diameter and fixed with carbon glue. The samples were then coated in the same manner as with the sediment. Immediately after drying, the sediments were placed on aluminium pin stubs of 12 mm diameter containing conductive carbon glue. The sample was coated in sputter coater (Balzers BVC 010, Balzers, Liechtenstein) with a 4.0 nanometer thick layer of carbon for conductivity of current and see **Appendix H2**. The samples were stored in dust-free environment until analysis.

The PIXE analysis was performed with a proton particle beam. A schematic of the Van de Graaff accelerator is provided in **Appendix H1** and of the NMP in **figure 2.4** layout at the Material Research Department (MRD), NRF-iThemba LABS, South Africa. Proton beam of energy 1.500 ± 0.001 MeV was used to scan the scale specimens. The Si(Li) PIXE detector was mounted at an angle of 135 ° to the incoming beam. Beryllium absorbers of thicknesses 25 μm and 125 μm were used to obtain an elemental spectrum from Al to Pb. The resolution of the detector was 146 eV X-ray at Mn K_α line. The beam spot size was 1.5 μm × 1.5 μm and the duration of each analysis was 150-180 minutes until a charge of 1 micro coulomb has been collected. Data were quantified with the GeoPIXE software program (Ryan *et al.*, 1995).

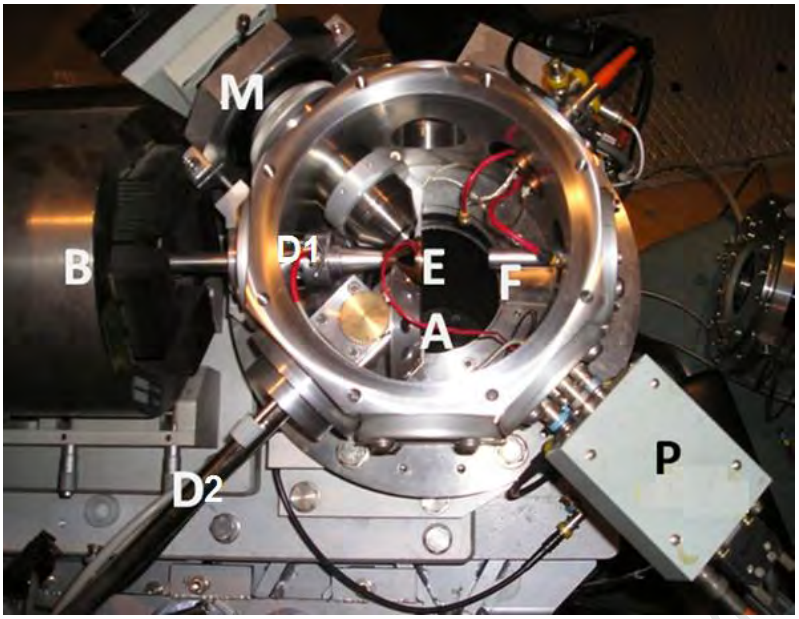

Figure 2-4 The Nuclear Microprobe (NMP) chamber at Material Research Department, iThemba LABS, Somerset West, South Africa. Inside the chamber RBS detector (D1); copper ring (E); optical microscope (M); Faradays cup (F); Preamplifier for RBS detector (P); filters (A); Si(Li) detector (D2) and on vertical position the motor with holder sampler.

2.5.2 Backscattering spectrometry

Because of the versatility of the NMP chamber, the PIXE and BS determinations were done simultaneously. The detector used for BS analyses was a solid surface barrier detector (ORTEC, USA). The detector was mounted at an angle of 176 ° to the incoming beam. Data were quantified with the RUMP software, UK, 1991.

2.5.3 Scanning electron microscopy

Light microscope is a type of microscope based on visible light thru a group of lenses to magnify images of particularly small samples. In this technique, largely produces an image by applying electrons instead forms an image. In **Appendix H3** is illustrated a photo of Leica/LEO-Stereoscan S440 microscopic Scanning Electron Microscope Unit at University of Cape Town was used. The energy of the electron beam for SEM analysis was 25 keV. The tilt was 0.00°; the take-off was 39.43°, and the amplitude 50.00. The detector used was a super ultrathin window sapphire (SUTW) with a resolution of 145.2 eV. The analysis duration was 180 live seconds. Data were evaluated with the manufacture's EDAX software program, UK, 1998.

2.5.4 Inductively coupled plasma mass spectrometry (ICP-MS)

The water sample was filtered through Whatman No. 2 filter paper to remove any suspended matter. Ten microliter of 5% vol/vol HNO_3 (65% m/v) was added to 100 µL of sample. The ICP-MS used in this study was a Thermo Scientific X series 2 (Bremen, GmbH, Germany), with a Cetac ASX-120 autosampler (Timberline Instruments, Boulder, Colorad, USA).

2.5.5 Flame absorption spectrometry (FAAS)

The water sample was filtered through Whatman No. 2 filter paper to remove any suspended matter. One milliliter of 5% vol/vol HNO_3 (65% m/v) was added to 100 mL of sample. The FAAS used in this study was a SpectrAA-400 Zeeman spectrometer with a platform-equipped furnace sourced from Agilent, Santa Clara, California, USA.

2.5.6 Ion chromatography (IC)

The water samples were filtered through a 0.45 µm filters paper before analysis. The IC used was a Dionex system unit (Dionex Corporation, Sunny Vale, California, USA.) with an Eluant Degas Module (Cations) and Conductivity Detector; on the right DIONEX Basic chromatography Module (Anions); DIONEX CSRS, ULTRA II 4 mm. Ten milliliters of sample was used for analaysis. The column used for anion analysis was AS14 (4 mm diameter) and for cations, CG12 (4 mm in diameter). The eluent for anion determination was 2.4 mM Na_2CO_3 and 1 mM Na_2HCO_3. For cations the eluent was 2.2 mM H_2SO_4. The sample loop volume varied between 50 µL for anions and 25 µL for cations. The anion and cation guard columns were AG14 and CG12 respectively. The suppressors used were ASRS-I-4 mm and CSRS-Ultr-4 mm with the eluent flow rates 1.2 $mL.min^{-1}$ and 10 $mL.min^{-1}$, all respectively.

Chapter Three
3 Results: Two- and three dimensional analyses of a fish scale

3.1 Introduction

This chapter provides the results of analyses of the two dimensional and three dimensional aspects of the fish scale.

Pollution events that occurred are at times difficult to detect because of the continuous river flow. However, changes in the chemical composition of the water are incorporated into the matrix of fish scales as growth occurs. Hence, pollutants in the water may be identified by the analysis of fish scale.

Concentration levels of various metals in the aquatic environment through anthropogenic sources such as domestic sewage, industrial and agricultural effluents, and natural resources groundwater as such become a source of several environmental and ecological impacts (Javed, 2004).

Fish have been used widely as an important indicator of metals contaminants of the aquatic ecosystems (Venugopal *et al.,* 2009 & Sekabira *et al.,* 2010). Metal concentrations can affect fisheries and health of the people consuming fish.

In the PIXE analyses, the peaks representing the emission of the X-ray data are overlaid on the background that consists of the bremsstrahlung continuum (see **Appendix B**). The scans shown are the quantitative elemental concentration distributions (QECDs) of the elements present in the fishscale matrix.

In the BS spectra the locations of the elements are those when these elements are located at the surface of the fish scale. The physics principles on which BS theory is based does not account for deviations of the data and the computation at low energies. However, since the energy of C, the lowest atomic number element of interest, is three orders of magnitude greater than these low energies, these low-energy deviations are not significant.

3.2 Results of the two dimensional (2-D) analysis

3.2.1 Morphometry of the scale

The 2-D and 3-D analyses reported here are based on results for a single scale of a specimen of the fish *Pomadasys kaakan*. The fish weighed 2750 g and had a fork length of 420 mm. The age was determined as 12 ± 1 month. The thickness of the scale varies from 340 μm, near the focus, to 200 μm at the distal edge of the scale. The length of the scale from the focus to the edge is 5.620 mm.

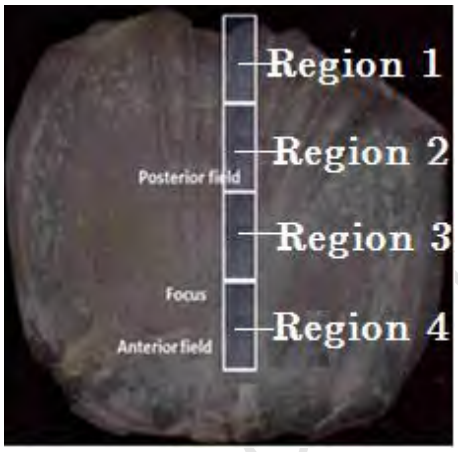

Figure 3-1 Illustration of the four areas of the fish scale of *Pomadasys kaakan* that was scanned and the posterior field, focus and the anterior field. Region 1 corresponds to figs 3.5, 3.6, 3.7, 3.8 and 3.9. Region 2 corresponds to figs 3.18, 3.19 and 3.20. Region 3 corresponds to figs 3.26, 3.27 and 3.28 and Region 4 corresponds to figs 3.34, 3.35 and 3.36.

The length is scanned as four individual sections since the maximum attainable focused beam size is 1.76 mm × 1.76 mm.

The dimensions of the scanned areas are 340 μm × 200 μm, and then for three sections, 1760 μm × 400 μm. The scanned areas are indicated in **figure 3.1**. This section reports on the 2-D analysis of these four scanned areas.

The total spectrum, based on the X-ray emission data, for this scanned area, is shown in **figure 3.2**. In the spectrum the only peaks for both the K_α and the K_β emission lines of the elements Ca and Sr are observable. The peak of the K_β line emission data of the lower atomic number elements coincides and therefore overlaps with the peak of the K_α line emission data of the higher atomic number elements. It means that for two elements the energy of K_α emission line of the element with the higher atomic number will coincide with the energy of the K_β emission line of the element

with the lower atomic number, e.g. K_β of Ni will coincide with the K_α emission line of Zn.

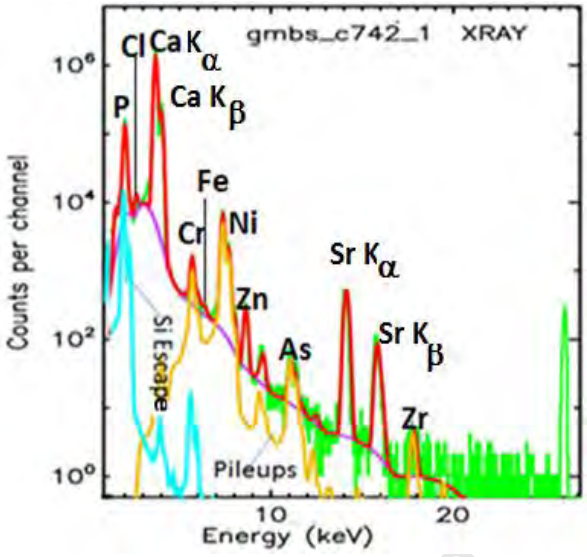

Figure 3-2 Total spectrum, based on the proton-induced X-ray emission data, for the entire scanned area of region 1, 340 μm × 200 μm (length by width), of the scale of *Pomadasys kaakan*. The green line represents the X-ray data, the red line the fit to the data, the purple line the background, the blue line Si escape peaks and yellow line is the pileup from the data.

The total spectrum, based on the proton-induced backscattered data, for the scanned area of 340 μm × 200 μm, is shown in **figure 3.3**. The peaks of the elements C, N and O are indicated.

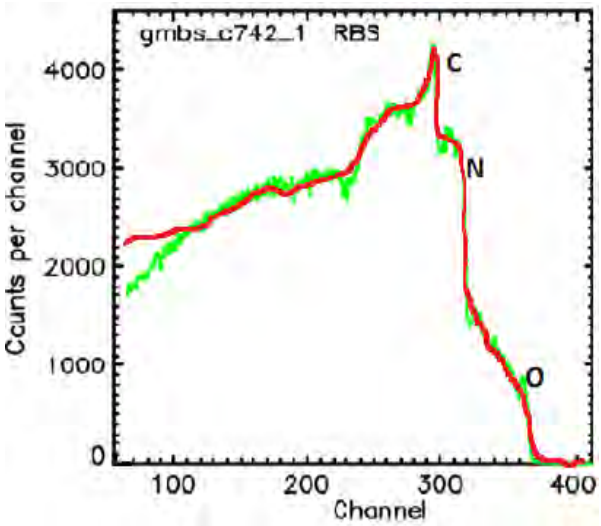

Figure 3-3 Total spectrum, based on the backscattered data, for the entire scanned area 340 μm × 200 μm of the scale of the fish *Pomadasys kaakan.* The green line represents the data and the red line the fit to the data. The peaks for C, N and O are indicated.

The difference between the data and the fit to the data at the low energy ranges is due to the inadequate description of the cross sections in the backscattering theory at these low energies.

The total spectrum, based on the electron-induced X-ray emission data, for the entire scanned area of 340 μm × 200 μm, is shown in **figure 3.4**.

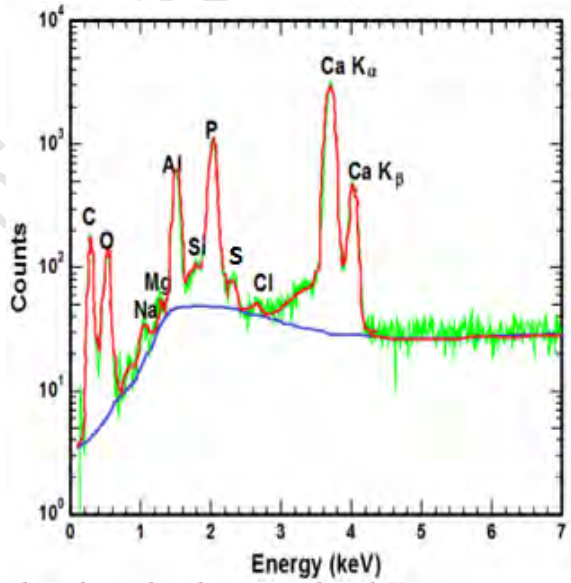

Figure 3-4 Total spectrum, based on the electron-induced X-ray emission (SEM) data, for the entire scanned area of 340 μm × 200 μm of the scale of the *Pomadasys kaakan.* The green line represents the data, the red line the fit to the data and the blue line the background.

Region 1

Four growth areas in region 1 are discernible and are indicated in **figure 3.5,** which shown the quantitative elemental concentration distributions of Ca and P. In area 1 in the growth pattern, based on both the Ca and P quantitative elemental concentration distributions, indicates low P and Ca concentrations for the first 30 µm of the scanned area.

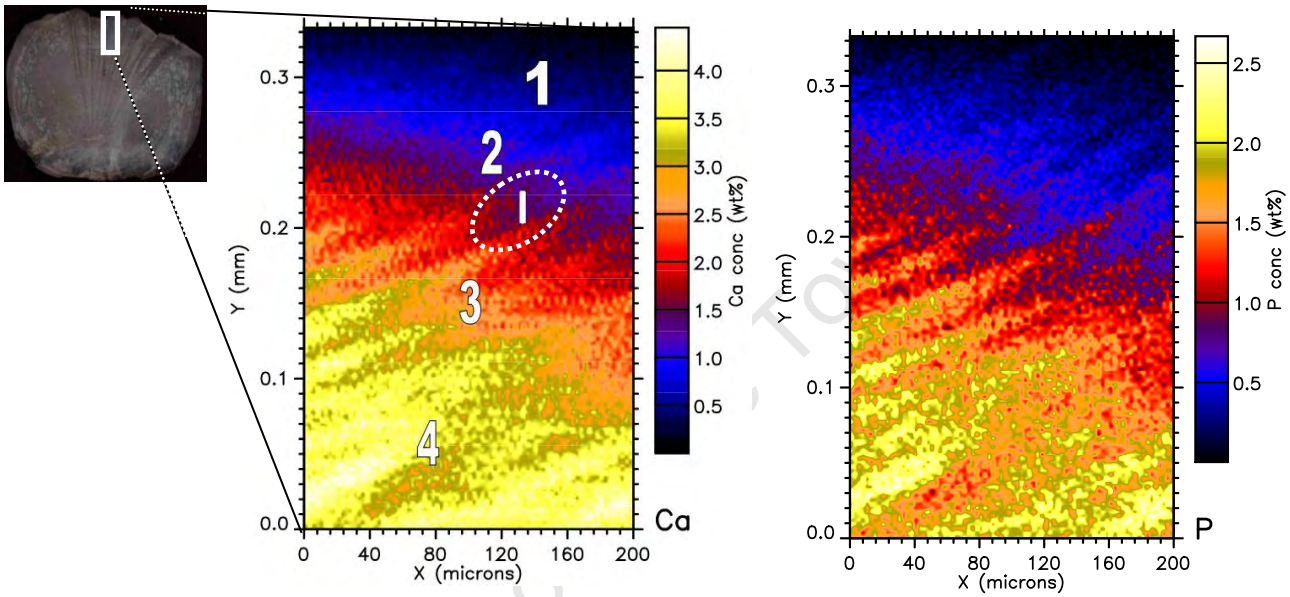

Figure 3-5 Scale of *Pomadasys kaakan* (inset) showing the scanned area of 340 µm × 200 µm (length by width). The quantitative elemental concentration distributions based on the X-ray emission data, of the elements Ca and P in the scanned area. The four concentration areas discernible are indicated by the numbers. "I" indicates ingrowths from the region nearer to the edge (0.0 µm), of the scale, to the succeeding region.

Hence in this region of the fish scale matrix the concentrations of calcium carbonate (CCB) and hydroxyl-apatite (HAP) are low. Thus the region consists primarily of keratin, implying that in the initial stage of scale growth only keratin is formed.

However from **figure 3.5**, based on the Ca quantitative elemental concentration and distribution, in-growths of P are found in the corresponding region of the P quantitative elemental concentration distribution. HAP consists of 40% m/m of Ca and 20% m/m of P HAP which yields 2.0 as a ratio of these concentrations. When the P concentration is less than that of Ca, that is, the concentration ratio is greater than 2, and then the excess Ca is assumed to be present in a chemical form other than HAP. The only matrix composition is that of CCB.

When P is present in excess then it is assumed that the P is present as ALP. Since the corresponding Ca quantitative elemental concentration distribution is very low

(less than 0.1 % mass/mass) and that of P relatively higher (greater than 1.05 mass/mass), P is present in a chemical composition other than HAP. The only composition possible is that with Al of aluminium phosphate ($AlPO_4$).

In area 2 region 1, the Ca QECD forms a semi-homogeneous distribution. The corresponding region in the P quantitative elemental concentration and distribution consists of various in-growth strands, growing from the edge of the scale towards the focus of the scale. Hence, some of these strands indicate a corresponding higher concentration of Ca to a corresponding lower concentration of P. For the Al quantitative elemental concentration and distribution the growth in the corresponding region is homogeneous. Therefore, $AlPO_4$ also can be present. Hence in these strands the Ca is present as both CCB and HAP.

The P QECD in area 3 region 1 is inhomogeneous and consists mostly of in-growing strands, of length 80 μm. The degree of homogeneity of the Ca quantitative elemental concentration distribution in area 3 is greater than the degree of homogeneity of the P quantitative elemental concentration distribution in this area. The lengths of the strands here are about 30 μm long. This means that for a distance of about 50 μm the ratio of concentrations of Ca to P is about 5:1. Since the ratio of Ca:P in HAP is 2.0, it means that only about 20% of this in-growth consists of HAP.

Hence in the growth strand area the matrix is predominantly CCB and keratin. Since the concentration of S in keratin is 0.01% m/m, the corresponding S concentration in the scanned area is expected to be low. As with area 3, quantitative elemental concentration distribution of P in area 4 region 1 is also ill-defined, and similarly in the Ca quantitative elemental concentration distribution. However, the concentrations of P and Ca are the highest in this area, and therefore the keratin concentration should be relatively low and hence a low S concentration is expected.

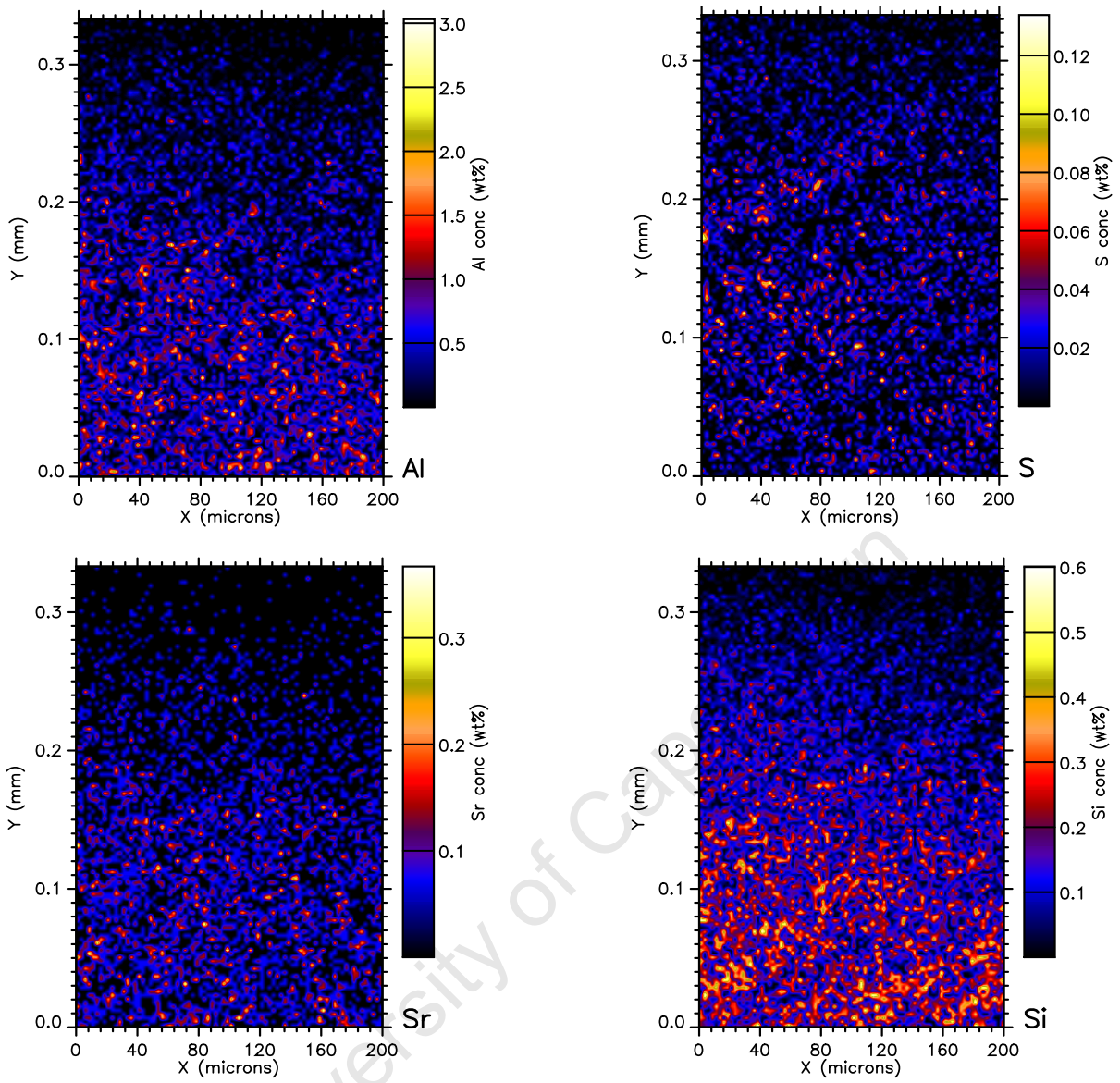

Figure 3-6 Quantitative elemental concentration distributions, based on the X-ray emission data, of the elements Al, S, Sr and Si in the first 340 µm from the edge (0.0 µm) in the direction to the focus, of the scale of *Pomadasys kaakan* (Region 1).

The S quantitative elemental concentration distribution is relatively higher than the expected S concentration. This indicates that S excess may be due to pollutants.

In the Al QECD three regions are distinguishable (**figure 3.6**). For the first 40 µm from the edge of the scale, Al is undetectable. This correlates with the P and Ca QECDs and therefore this region can be considered and consist mainly of keratin. Since Al has been identified as a contaminant it means that keratin growth occurs firstly and the Al is only incorporated afterwards. In the S QECD (**figure 3.6**) only two regions are distinguished. The first region contains small amounts of S and in the second region higher amounts of S. As S is a element in keratin, this therefore

again confirms that the initial growth matrix consists mainly of keratin. The higher concentration in the second region may indicate that S contamination also took place.

Only three regions are distinguishable in the QECDs of Sr and Si (**figure 3.6**). In the Sr and Si maps quantitative elemental concentration and distribution the first region aproximately 40 μm contains no Sr and Si. This confirms that the matrix consists entirely of keratin. By comparison the gradient of the QECD of Sr is lower than that of Si. Since Sr and Ca are in the same periodic group it is assumed that Sr is incorporated as the carbonate, $SrCO_3$. Silicious matter is assumed to be incorporated as silicon oxides and/or hydroxides.

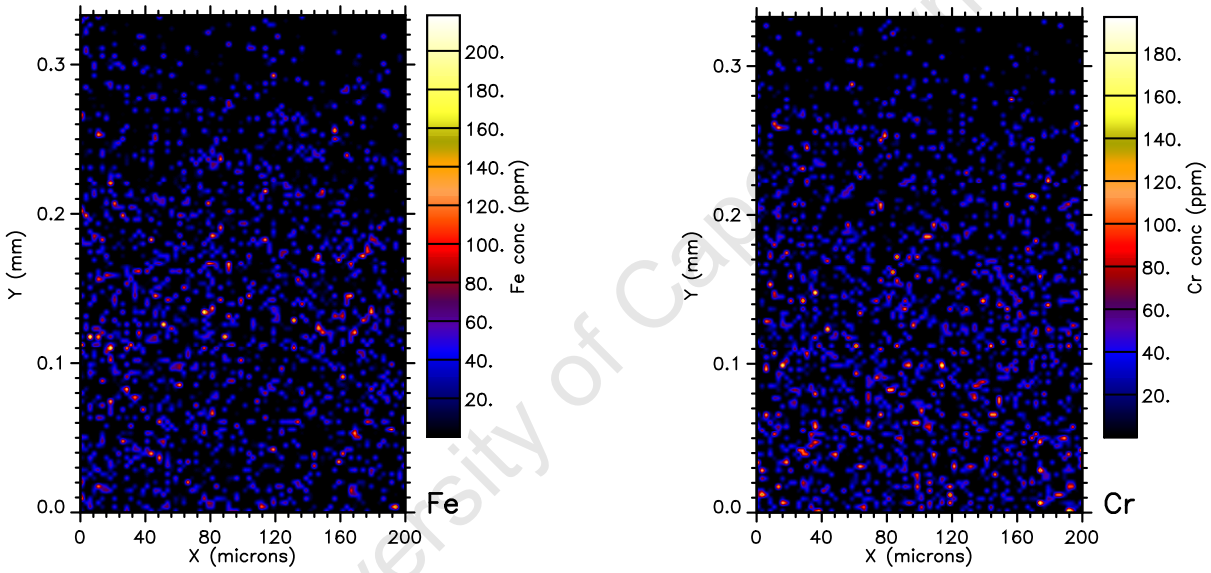

Figure 3-7 Quantitative elemental concentration distributions, based on the X-ray emission data of the elements Fe and Cr in the first 340 μm from the edge of the scale of *Pomadasys kaakan*.

The quantitative elemental concentration distributions (QECDs) of Fe and Cr based on the X-ray emission data are shown in **figure 3.7**. Only two regions are observed in each. The first region is about 80 μm long. Important here is that even though these elements are present in trace amounts in the matrix, these elements are present in the region where the matrix is composed predominantly of keratin. This indicates that during the initial growth periods, these elements are incorporated into the matrix. After this 80 μm the concentration gradients of the two elements do not change and hence no further incorporation of these elements occurred. This indicates that even though the concentrations of these elements in the parts per million ranges, the quantitative elemental concentration distribution are not affected by the previously mentioned elements.

The QECDs of Ti, V, Mn and Ni, based on the X-ray emission data are shown in **figure 3.8**. In the Ti QECD the concentration of the element is low in the first 340 μm. Afterwards the concentration increases and remains the same for the remaining area in the region. Similar trends are observable in the QECDs of V and Mn. The elements are therefore incorporated into the scale matrix in the initial growth stages. In the Ni QECD, incorporation into the matrix also started in the initial growth stages. However, three growth regions are observable.

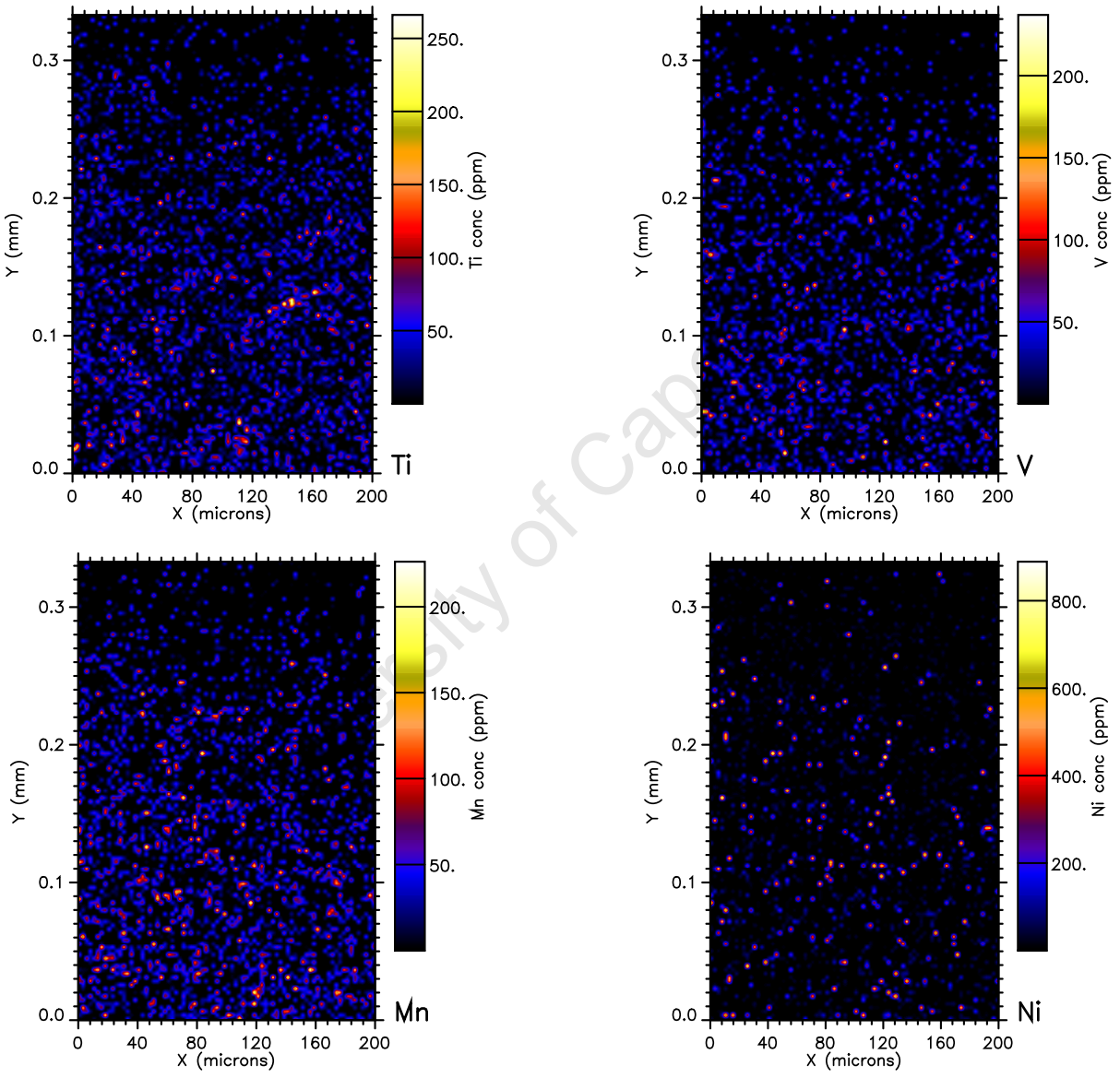

Figure 3-8 Quantitative elemental concentration distributions of the elements Ti, V, Mn and Ni in the first 340 μm from the edge of the scale of *Pomadasys kaakan*.

The first region (distance of 80 μm from the edge) shows similar trends as in the QECDs of Ti, V and Mn. In the second growth region the concentration of Ni is relatively small (less than 5 ppm). There is thus a significant decrease in the

concentration of Ni. This means that the Ni pollution of the natural resources was intermittent. The concentration of Ni in the third region is homogeneous with no concentration gradient.

The QECDs of Cu, Zn and Se are shown in **figure 3.9**. As is distinguishable from these QECDs the incorporation of Cu and Zn also assumes the pattern of low concentrations in the first 80 μm and then an increase in the concentrations that remains for the rest of the region. Se incorporation is homogeneous throughout the distance of 340 μm. This concentration indicates that Se contamination was constant through the time period for this length of the fish scale.

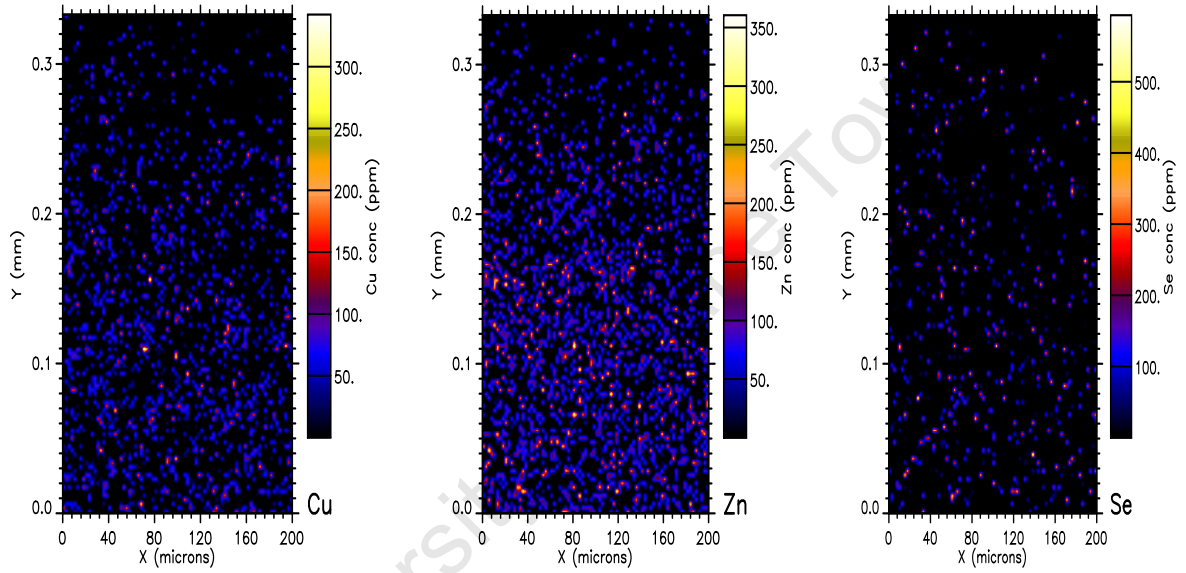

Figure 3-9 Quantitative elemental concentration distributions, based on the X-ray emission data, of the elements Cu, Zn and Se in the first 340 μm from the edge of the scale of *Pomadasys kaakan.*

These QECDs can now be correlated with one another. This was achieved by performing a quantitative linear traverse analysis (LTA) across the area of interest and is shown in **figure 3.10** for the elements Al, Si, P, Ca and Sr. The distance 340 μm is at the edge of the scale. The standard deviation in concentration in the Al LTA is relatively high. This is due to the dispersed homogeneous distribution of the element, which is observable in the Al QECD. Similar relatively high standard deviation in concentration for Si is also visible and is also due to the dispersed but homogeneous distribution of the elements. The linear correlation between the concentrations of P and Ca in the linear traverse analyses is observable by following the trends of the concentrations.

The low concentration of the elements in the region of 340 μm to 250 μm range is indicative of the scale matrix consisting predominantly of keratin, that is low in S concentration. The relatively high Sr concentration can be seen. This means that in the growth of the scale, Sr is included in the keratin matrix. It is assumed that the element is incorporated in the carbonate form, as $SrCO_3$. The concentration of the elements however levels off at the 100 μm growth stage, that is, after a growth distance of 240 μm the incorporation of HAP and CCB are constant. The growth data can be used to determine the kinetics of the incorporation of the elements Al, Si, P, Ca and Sr.

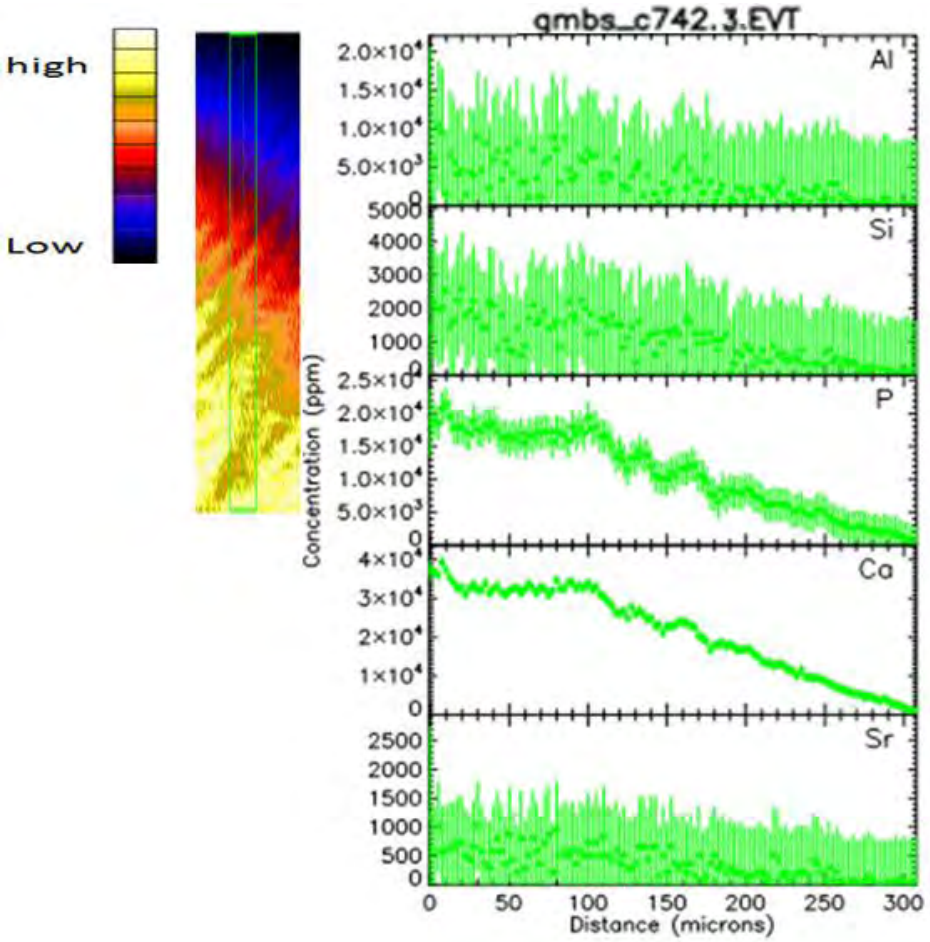

Figure 3-10 Quantitative linear traverse analysis (LTA), based on the X-ray emission data, of the corresponding elements Al, Si, P, Ca and Sr in the first 340 μm from the edge of the scale of *Pomadasys kaakan*. The 340 μm distance is located at the edge of the scale. The width of the LTA was 200 μm. The standard deviation of the concentration is illustrated. Where the deviation is not visible it indicates that the value of the deviation with respect to the value of the concentration is small.

The linear traverse analyses, based on the X-ray emission data, of the elements Ti, V, Mn, Ni and Se (to the left) and of Cr, Fe, Cu and Zn (to the right) in the first 340 μm from the edge of the fish scale of *Pomadasys kaakan* are shown in **figure 3.11**.

The width of the LTA was 200 μm. There are no linear correlations among the concentrations of the elements in the linear traverse analyses. Hence it can be assumed that the QECDs of these elements are not affected by one another.

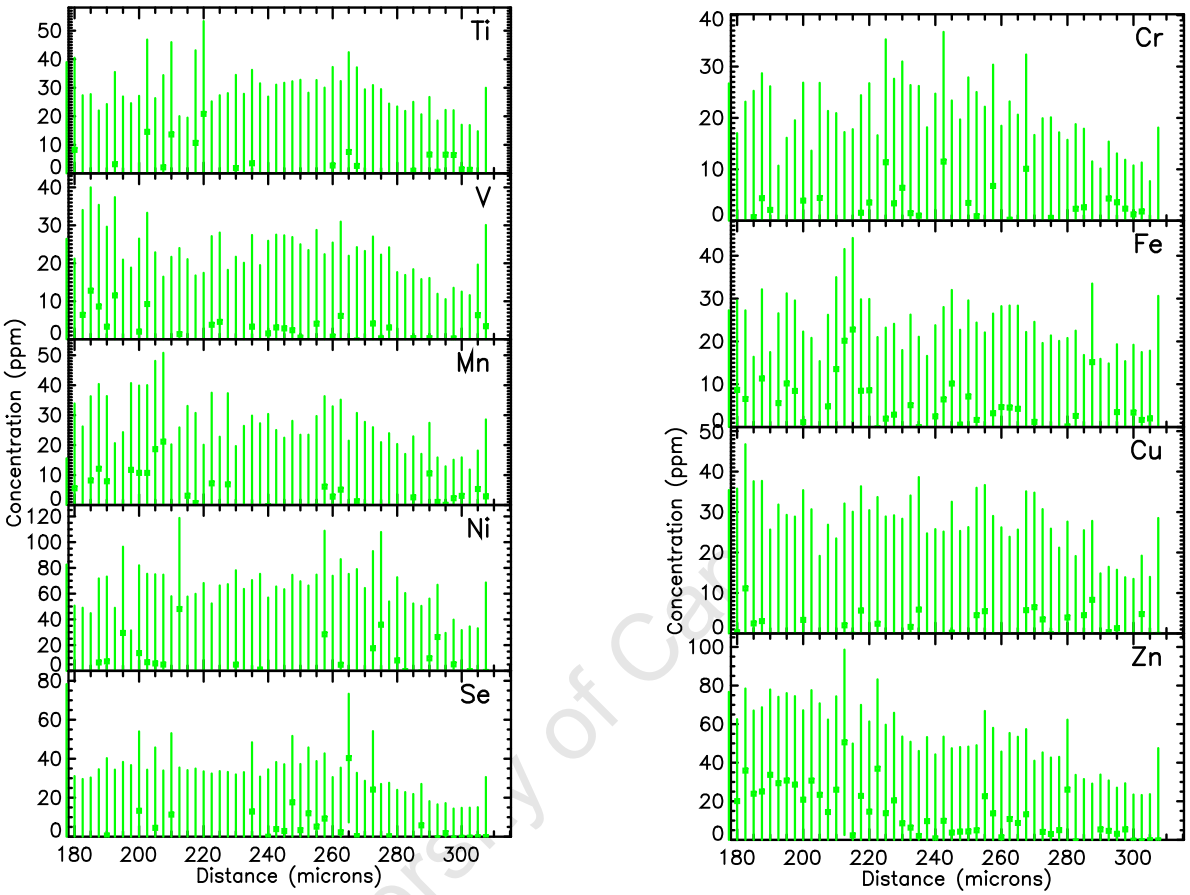

Figure 3-11 Linear traverse analysis, based on the X-ray emission data, of the elements Ti, V, Mn, Ni and Se (to the left) and of Cr, Fe, Cu and Zn (to the right) in the first 340 μm from the edge of the scale of *Pomadasys kaakan*. The width of the LTA was 200 μm.

The correlation of the concentrations (as the log of ppm) of the elements P and Ca, P and Al, Si and Al, Al and Ca are shown in **figure 3.12**. The correlation between the concentrations of P and Ca is linear since these elements together constitute the HAP component of the fish scale matrix.

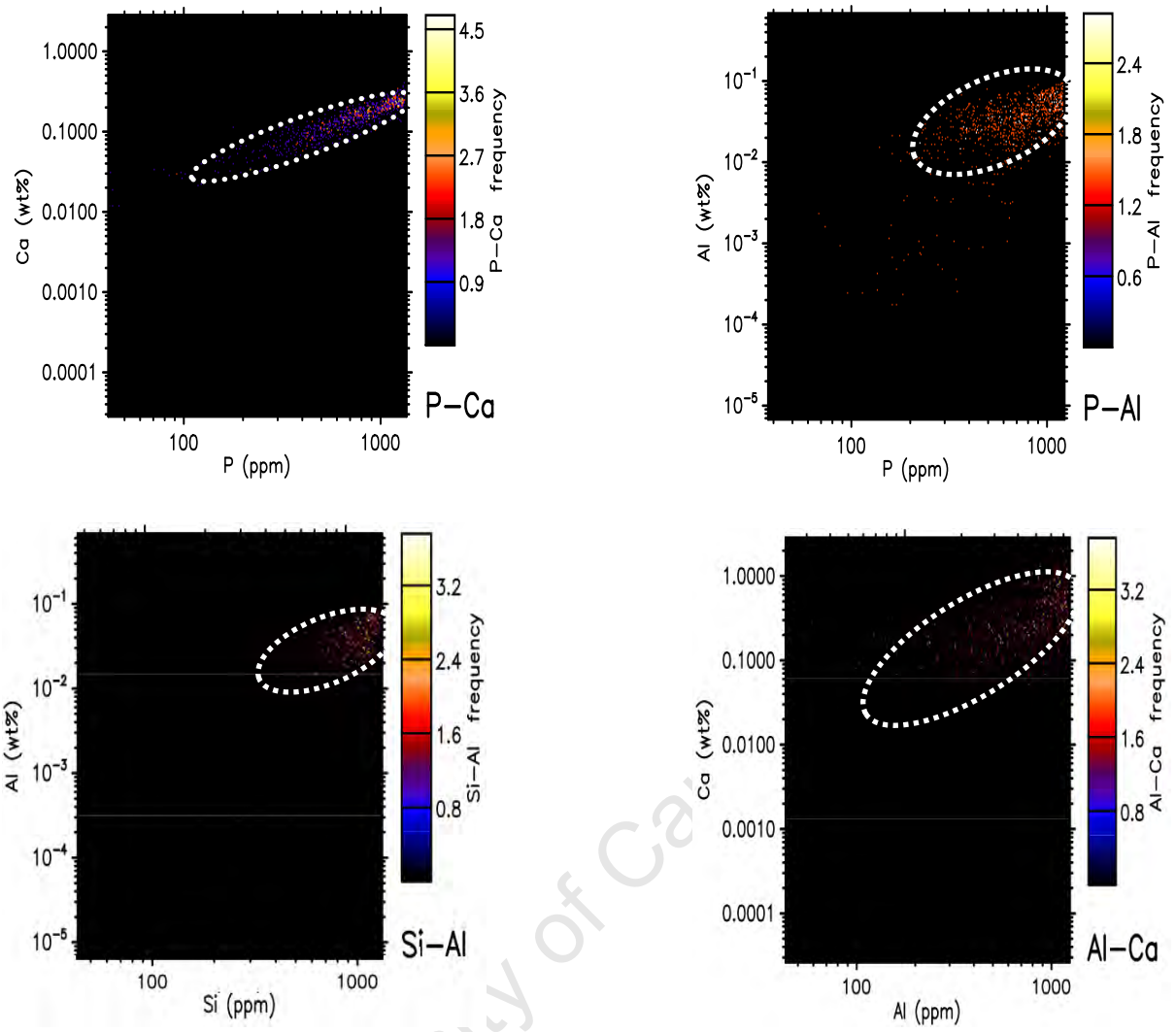

Figure 3-12 The concentrations (in log of ppm value) correlations of the corresponding elements P-Ca, P-Al, and Si-Al, Al-Ca in the first 340 µm from the edge of the scale of *Pomadasys kaakan.* The dotted ellipses show the positions of the corresponding correlations.

The correlation of P and Al shows a linear trend but is slightly dispersed. This is due to the inclusion of Al and P as $AlPO_4$ in the scale matrix. Both the correlations of Si and Al and Al and Ca are dispersed. This indicates that the incorporation of Si into the matrix is not affected by the incorporation or Al and that the Al incorporation is not affect by that of Ca.

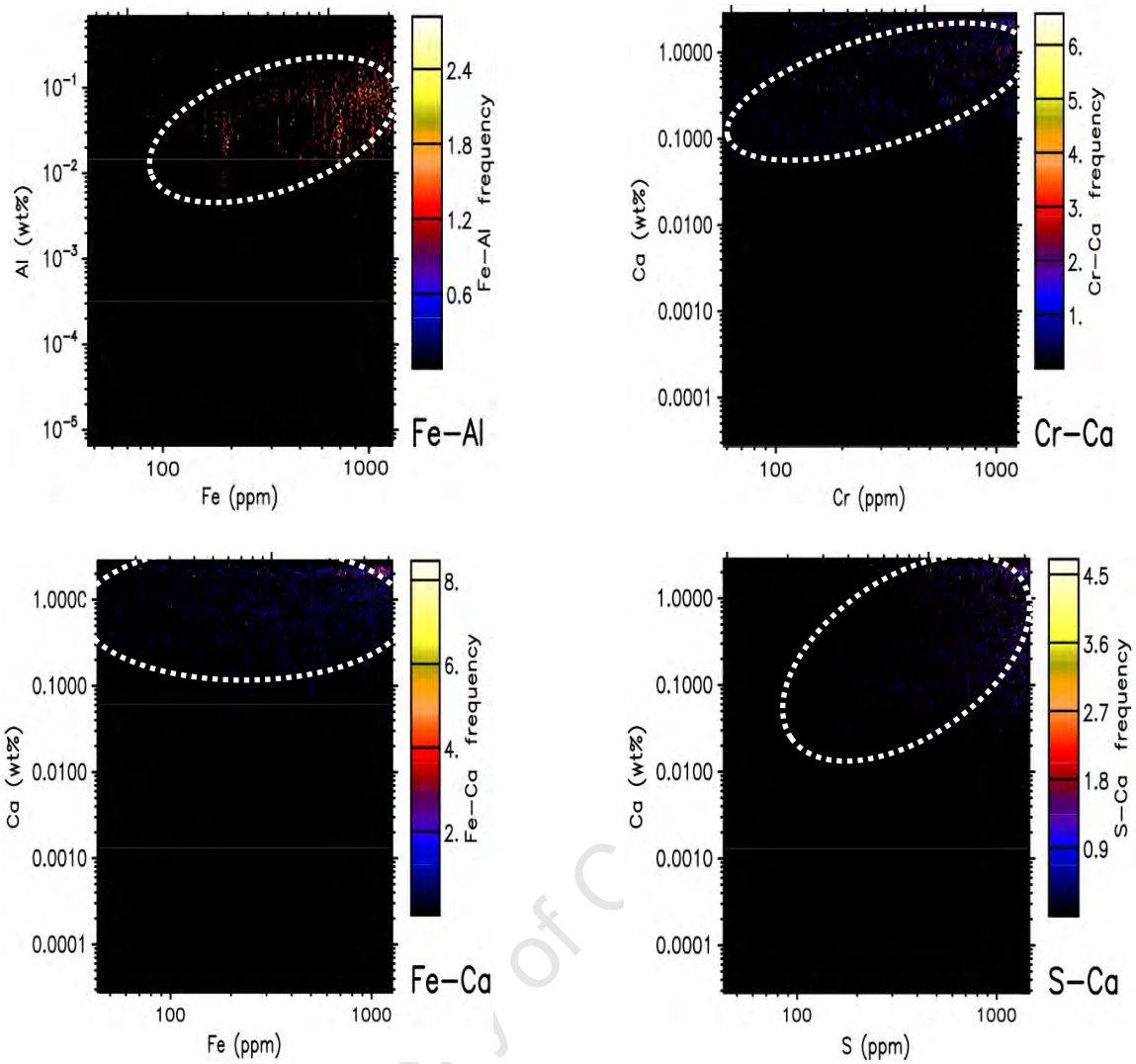

Figure 3-13 The concentrations (in log of ppm value) correlations, based on the X-ray emission data, of the corresponding elements Fe-Al, Cr-Ca, and Fe-Ca, S-Ca in the first 340 μm from the edge of the scale of *Pomadasys kaakan*.

The correlation of the concentrations (as the log of ppm) of the elements Fe and Al, Cr and Ca, Fe and Ca, and of S and Ca are shown in **figure 3.13**. These correlations are all dispersed and therefore these elements do not affect one another's incorporation into the fish scale matrix. The correlations of the concentrations (as the log of ppm) of the elements Si-Ca, Sr-Ca, and Fe-Cr in the first 340 μm from the edge of the fish scale of *Pomadasys kaakan* are shown in **figure 3.14**.

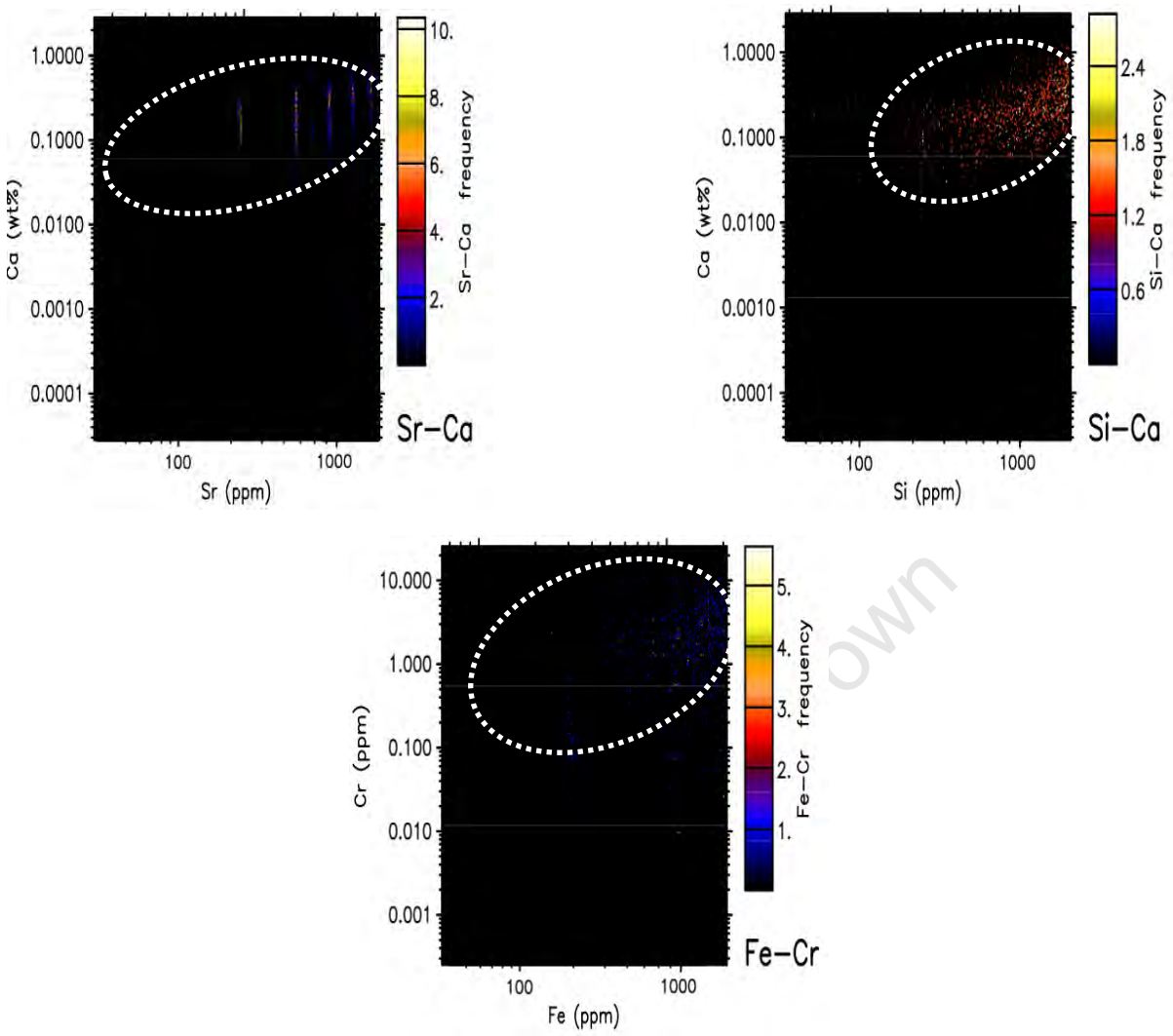

Figure 3-14 The correlation of the concentrations (as the log of ppm), based on the X-ray emission data, of the elements Si-Ca, Sr-Ca, and Fe-Cr in the first 340 μm from the edge (0,0 μm) of the scale of *Pomadasys kaakan*.

The concentrations correlations of all these elements are dispersed. Therefore the incorporations of these elements into the fish scale matrix do not affect one another.

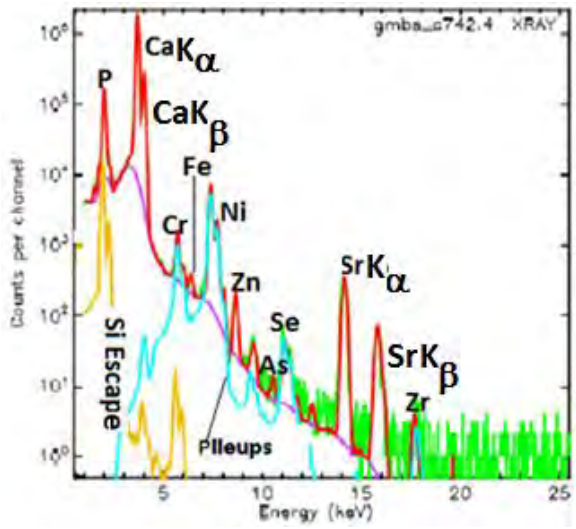

Figure 3-15 Total spectrum, based on the proton-induced X-ray emission data for the entire scanned area of 1760 μm × 400 μm (length by width), that is, for the distance length of 340 μm to 2100 μm (Region 2). The green line represents the X-ray data, the red line the fit to the data, the purple line the background; the blue line Si escape peaks and the yellow line the pileup from the data.

The total spectrum, based on the proton-induced X-ray emission data for the entire scanned area of 1760 μm × 200 μm (length by width), that is, for the distance length of 340 μm to 2100 μm, is shown in **figure 3.15**.

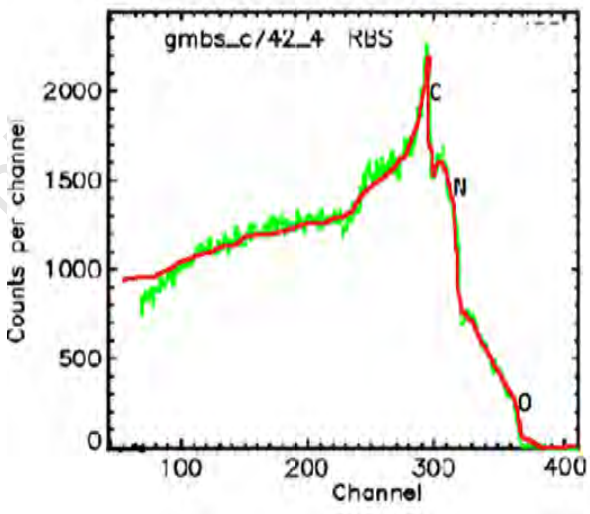

Figure 3-16 Total spectrum, based on the backscattered data for the entire scanned area of 1760 μm × 400 μm, that is, in the distance length of 340 μm to 2100 μm, of the scale of the *Pomadasys kaakan*. The green line represents the data and the red line the fit to the data. The peaks for C, N and O are indicated.

The total spectrum, based on the backscattered data for the corresponding scanned area of 1760 μm × 200 μm, that is, in the length distance of 340 μm to 2100 μm, of the scale of the fish *Pomadasys kaakan* is shown in **figure 3.16**.

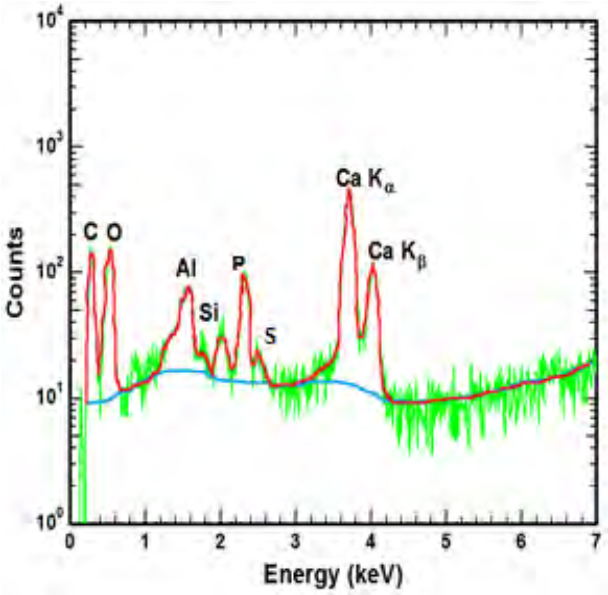

Figure 3-17 Total spectrum, based on the electron-induced X-ray emission data, for the entire scanned area of 1760 μm × 400 μm, that is, for the distance length of 340 μm to 2100 μm, of the scale of the *Pomadasys kaakan*. The green line represents the data, the red line the fit to the data and the blue line the background.

The total spectrum, based on the electron-induced X-ray emission data, of the entire scanned area of 1760 μm × 400 μm for the length distance 340 μm to 2100 μm (Region 2) of the scale is shown in **figure 3.17**.

Region 2

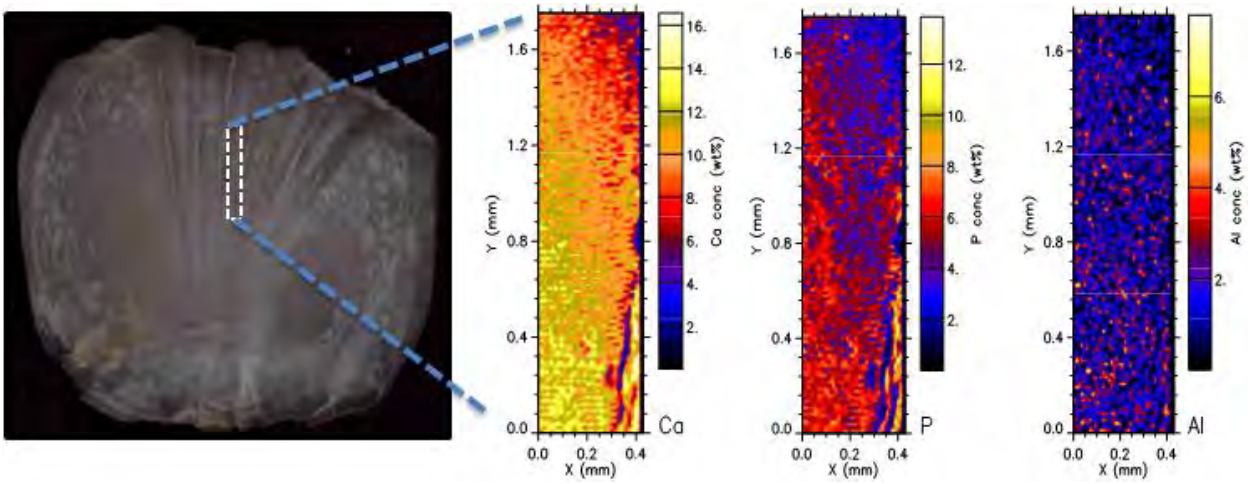

Figure 3-18 Scale of the *Pomadasys kaakan* (inset) showing the scanned area of 1700 µm × 400 µm (length by width) for the length distance of 340 µm to 2100 µm. In the alongside three images the 1700 µm corresponds to the 340 µm and the 0 µm corresponds to 2100 µm. The distribution of the elements is discussed from the 1700 µm mark to the 0 µm mark. The quantitative elemental concentration distribution based on the X-ray emission data, of the elements Ca, P and Al in the scanned area. Various concentration regions are discernible in the scanned area.

Scale of the fish *Pomadasys kaakan* (inset) showing the scanned area of 1760 µm × 400 µm (length by width) for the length distance of 340 µm to 2100 µm (Region 2). The quantitative elemental concentration distributions are based on the X-ray emission data, of the elements Ca, P and Al in the scanned area are shown in **figure 3.18**.

There is continuity between the QECD of Ca in this scanned area to the QECD of Ca in the initial scanned area. There is however an increase in Ca concentration for the length distances from 1300 µm to 2100 µm in the scanned area. The low Ca concentration located on the right-side of the scanned area represents the annulus, in which the concentration of the element is low. More so, the concentration of Ca decreases in the vicinity of the annulus. Similar trends in the QECD of P are observable, except that the concentrations are lower than those for Ca. The relatively low concentration of P to the right-hand side of the QECD is also representative of the annulus, in which the P concentration is low.

There is no discernible concentration region or demarcation in the Al QECD, suggesting that the Al contamination occurs throughout the scale, including in the annuli.

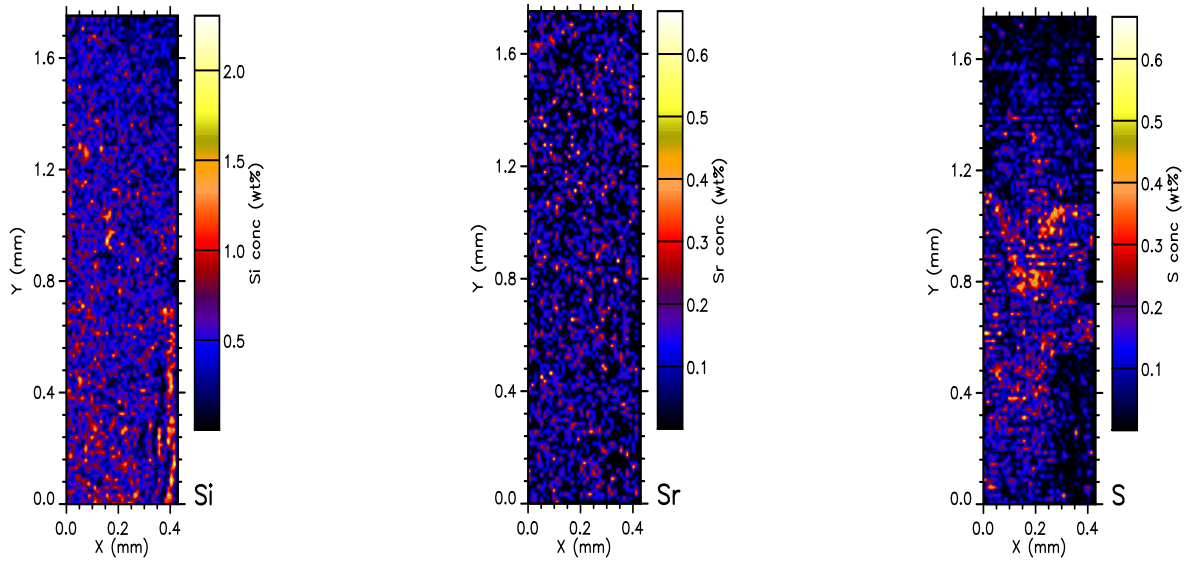

Figure 3-19 Quantitative elemental concentration distribution, based on the X-ray emission data, of scanned area of 1760 μm × 400 μm, of the elements Si, Sr and S in the length distance of 340 μm to 2100 μm.

The quantitative elemental concentrations distributions, based on the X-ray emission data, of the elements Si, Sr and S in the length distance of 340 μm to 2100 μm are shown in **figure 3.19**. Two concentration regions are discernible in the QECD of Si. From the length distance of 820 μm to about 900 μm there is an increase in the concentration. From 900 μm onwards the concentration is homogeneous and there is no increase in Si. In contrast to the Ca and P concentrations there is a discernible increase of Si in the annulus region.

In the Sr QECD there are no visible concentration regions and is homogeneously distributed throughout the scanned area. This means that Sr is also found in the annulus of the fish scale (see chapter 5).

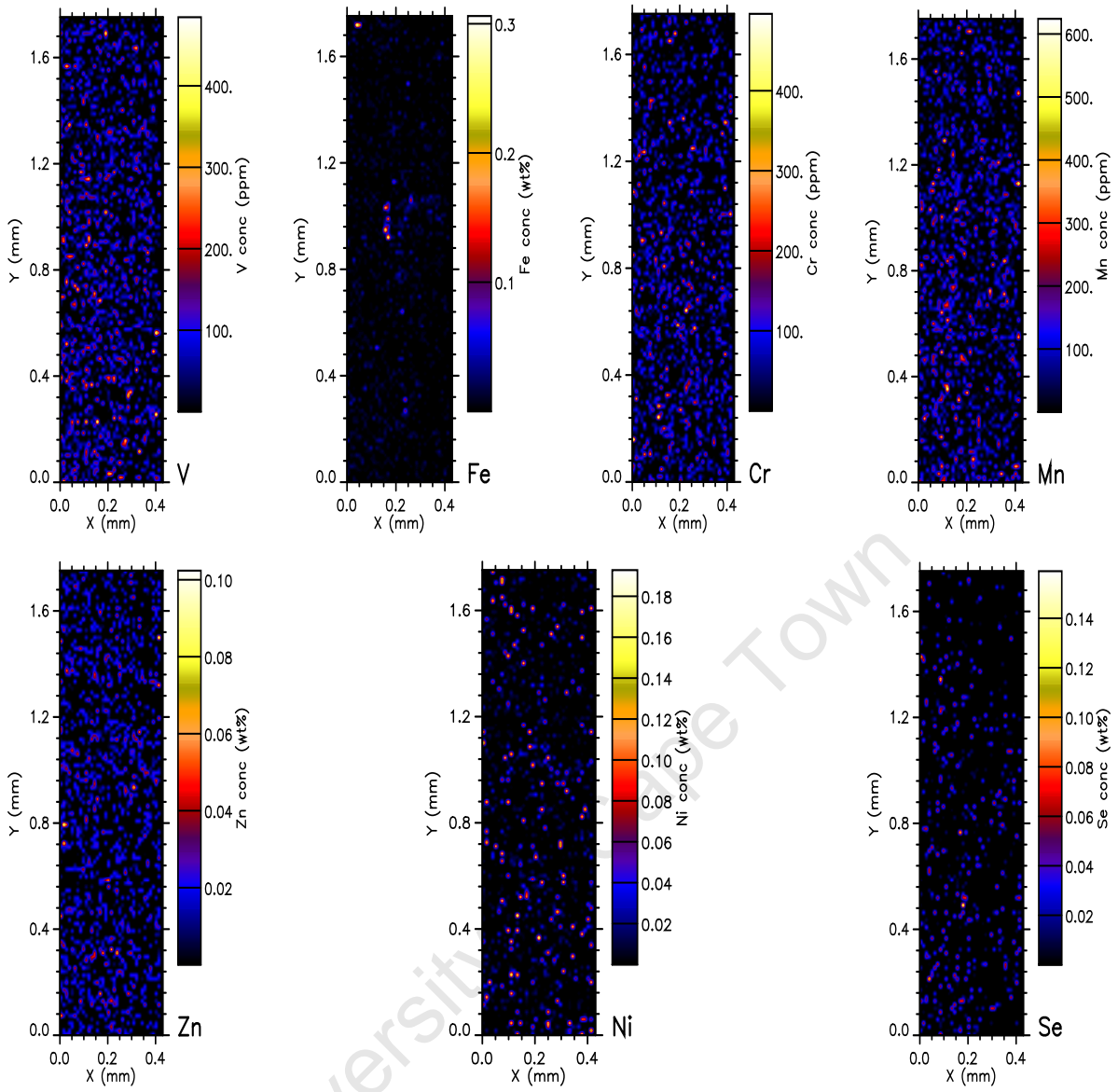

Figure 3-20 **Quantitative elemental concentration distributions, based on the X-ray emission data, of the scanned area of 1760 μm × 400 μm, of the elements V, Fe, Cr, Se, Mn, Ni and Zn in the length distance 340 μm to 2100 μm of the scale of *Pomadasys kaakan*.**

The S QECD in the region 1500 μm is irregular and relatively low. In the region 1080 μm to 1520 μm there is an increase in S concentration. Since S is contained in keratin (KRT), but in relatively smaller amounts (0.002 % m/m) it can now be postulated that this excess S is due to pollution. The QECD for S is also relatively low in the region of the annulus.

The QECDs, based on the X-ray emission data, of the elements V, Fe, Cr, Se, Mn, Ni and Zn in the length distance of 340 μm to 2100 μm of the fish scale of *Pomadasys kaakan* are shown in **figure 3.20**. The QECDs of all these elements with the

exception of Fe are homogeneous. It seems, therefore, when this part of the scale was laid down, that the pollution levels were constant and low.

The Fe QECD indicates that in the length distances 1060 μm to 1220 μm and 1440 μm (Region 4) to 1540 μm, Fe levels in the ambient water increased on occasion.

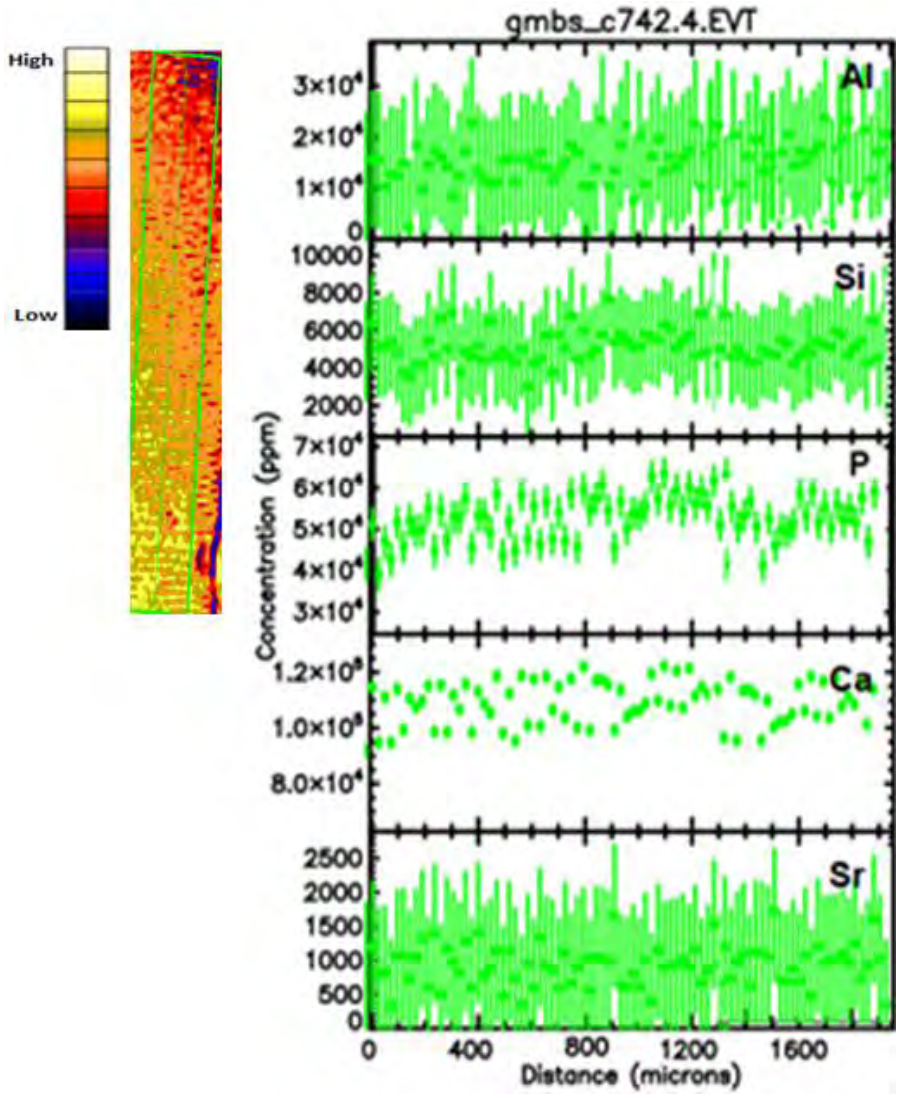

Figure 3-21 Quantitative linear traverse analysis (LTA), based on the X-ray emission data, of the corresponding elements such as Al, Si, P, Ca and Sr in the length distance 340 μm to 2100 μm, of the scale of *Pomadasys kaakan*. The width of the LTA was 200 μm.

The correlations of QECDs can now be achieved by performing a quantitative linear traverse analysis (LTA) across the area of interest as is shown in **figure 3.21** for the elements Al, Si, P, Ca and Sr. The standard deviation in concentration in the Al LTA is relatively high. This is due to the dispersed homogeneous distribution of the element, which is observable in the Al QECD. Similar relatively high standard deviation in concentration for Si is also visible and is also due to the dispersed but

homogeneous distribution of the elements. The linear correlation can be seen between the concentrations of P and Ca in the linear travesrse analyses.

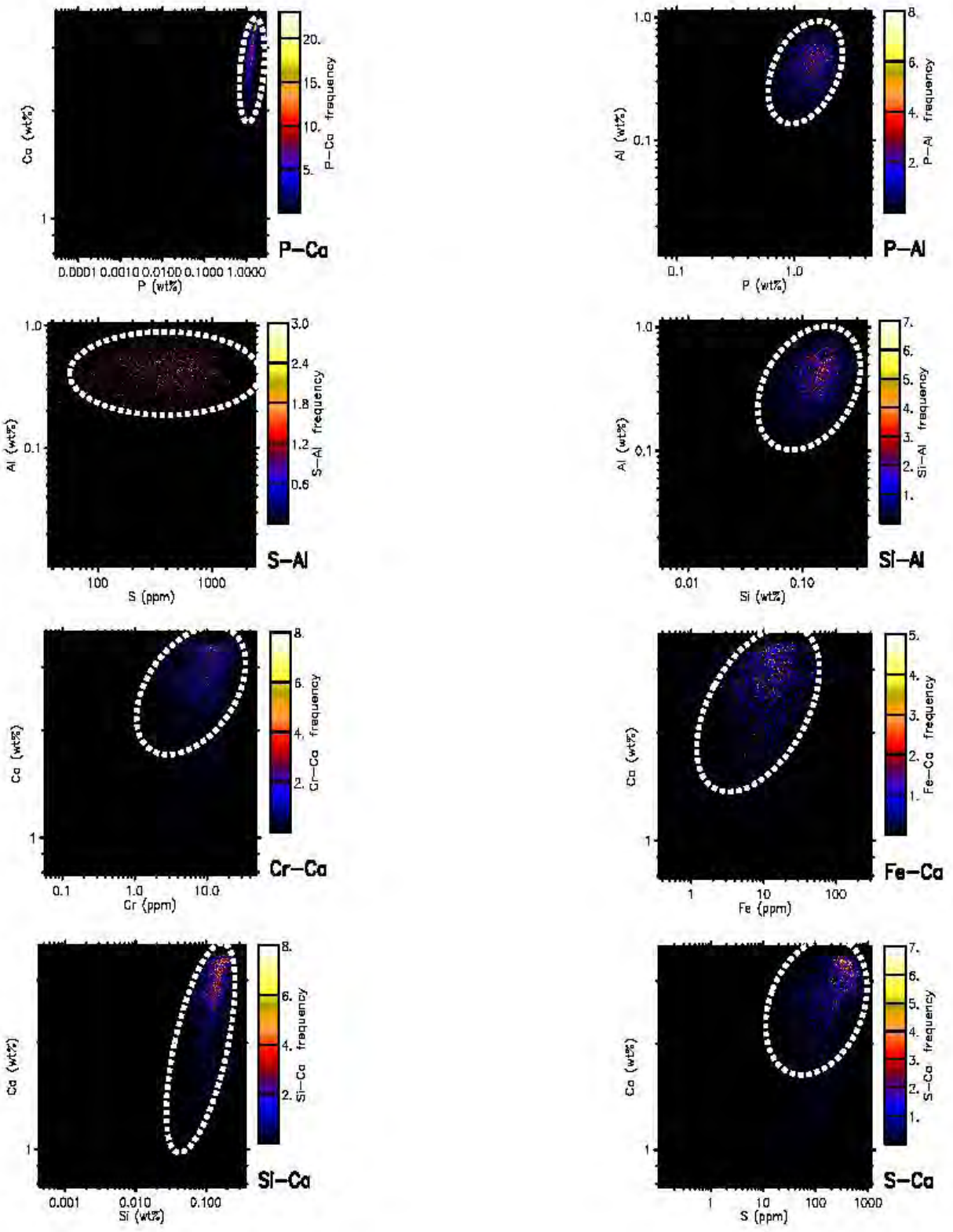

Figure 3-22 Correlations between concentrations, based on the X-ray emission data, of the corresponding elements P-Ca, P-Al, Si-Al, S-Al, Cr-Ca, Fe-Ca, Si-Ca and S-Ca in the length distance 340 µm to 2100 µm from the edge of the scale of *Pomadasys kaakan*.

Correlations, based on the X-ray emission data of the concentrations of the corresponding elements P-Ca, P-Al, and Si-Al, S-Al, Cr-Ca, Fe-Ca, Si-Ca and S-Ca in the length distance 340 μm to 2100 μm from the edge of the fish scale of *Pomadasys kaakan* are shown in **figure 3.22**.

The high degree of linearity in the P-Ca correlation is observable, and is due to the presence of HAP. The low degree of inter-correlation for the other elements suggests that these elements are not affected by the presence of the others.

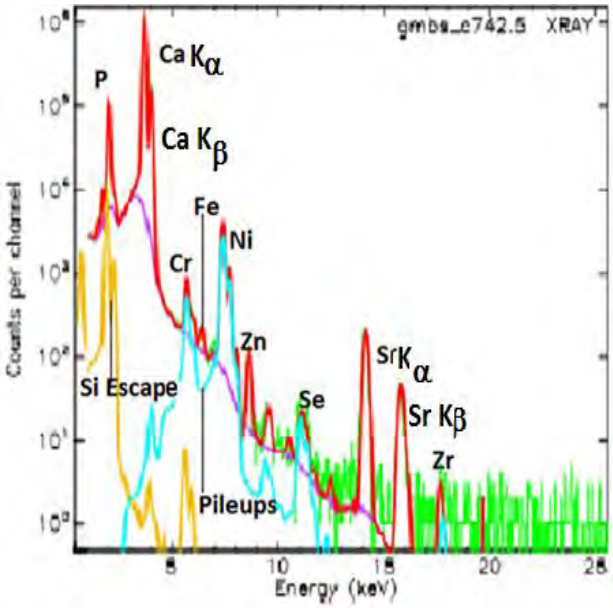

Figure 3-23 Total spectrum, based on the proton-induced X-ray emission data for the entire scanned area of 1760 μm × 400 μm (length by width), that is, for the distance length of 2100 μm to 3860 μm. The green line represents the X-ray data, the red line the fit to the data, the purple line the background, the blue line Si escape peaks and yellow line is the pileup from the data.

The total spectrum, based on the proton-induced X-ray emission data for the entire scanned area of 1760 μm × 400 μm (length by width), that is, for the distance length of 2100 μm to 3860 μm (Region 3), is shown in **figure 3.23**.

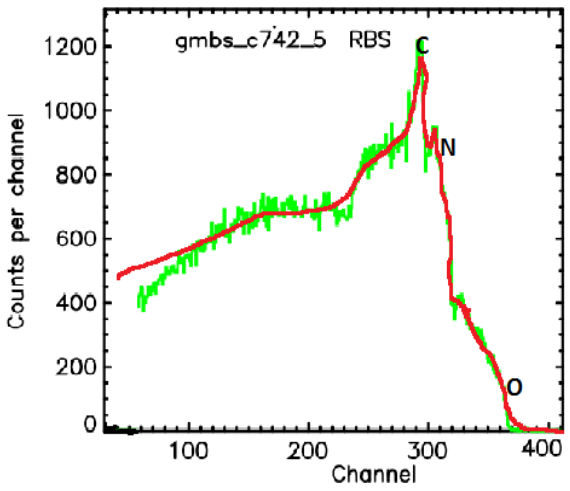

Figure 3-24 Total spectrum, based on the backscattered data for the entire scanned area of 1760 μm × 400 μm, that is, in the distance length of 2100 μm to 3860 μm, of the scale of the *Pomadasys kaakan.*

The total spectrum, based on the backscattered data for the entire scanned area of 1760 μm × 400 μm, that is, in the distance length of 2100 μm to 3860 μm, of the scale of the fish Pomadasys kaakan, is shown in **figure 3.24**.

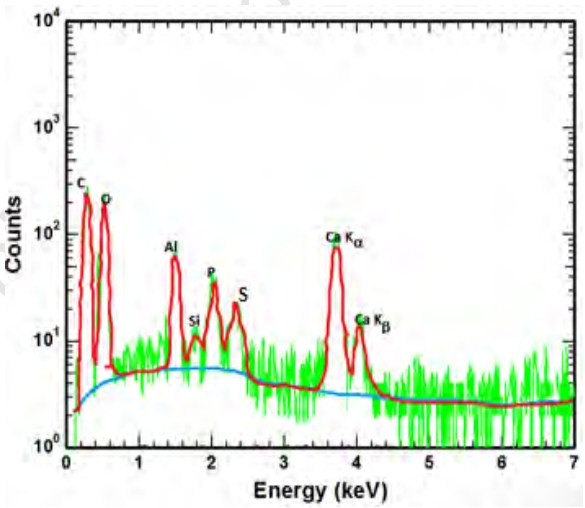

Figure 3-25 Total spectrum, based on the electron-induced X-ray emission data, for the entire scanned area of 1760 μm × 400 μm, that is, for the distance length of 2100 μm to 3860 μm, of the scale of the *Pomadasys kaakan.* The green line represents the data, the red line the fit to the data and the blue line the background.

The total spectrum, based on the electron-induced X-ray emission data, for the entire scanned area of 1760 μm × 400 μm, that is, for the distance length of 2100 μm to 3860 μm, of the scale of the fish *Pomadasys kaakan*, is shown in **figure 3.25**. The K_α

emission line of Sr is not observed in the SEM spectrum since its concentration is below the MDL for this element in SEM.

Region 3

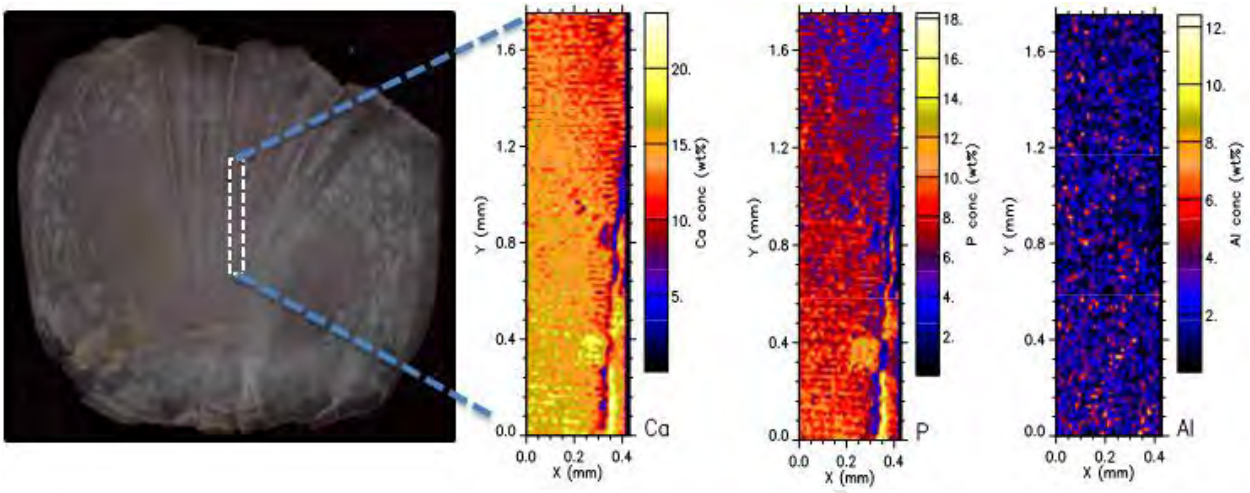

Figure 3-26 Scale of the *Pomadasys kaakan* (inset) showing the scanned area of 1760 µm × 400 µm (length by width) for the length distance of 2100 µm to 3860 µm (Region 3). In the alongside three images the 2100 µm corresponds to the 1700 µm and the 0 µm corresponds to 3860 µm. The distribution of the elements is discussed from the 1700 µm mark to the 0 µm mark. The quantitative elemental concentration distributions based on the X-ray emission data, of the elements Ca, P and Al in the scanned area. Various concentration regions are discernible in the scanned area.

The QECDs, based on the X-ray emission data, of Ca, P and Al in the length distance of 2100 to 3860 µm (Region 3) are shown in **figure 3.26**. There is continuity between the QECD of Ca in this scanned area and the QECD of Ca in the initial scanned area. There is however an increase in Ca concentration for the length distances from 2100 µm to 3860 µm in the scanned area. The low Ca concentration located on the right-hand side of the scanned area represents the annulus, in which the concentration of the element is low. More so, the concentration of Ca decreases in the vicinity of the annulus. Similar trends in the QECD of P are observable, with the exception that the concentrations are lower than those for Ca. The relatively low concentration of P to the right-side of the QECD is also representative of the annulus, in which the P concentration is low. There is no discernible concentration region or demarcation in the Al QECD. This means that the Al contamination also occurs in the annuli of the fish scale. The QECDs, based on the X-ray emission data, of Sr, Si and S in the length distance region of a 2100 µm to 3860 µm are shown in **figure 3.27**. The QECD of Sr is homogeneously distributed.

In constrast to the QECDs of Ca and P, the Sr is also found in the annulus of the scale. In the Si QECD two regions are observable. In the first region, that is for the

length distance of 2100 μm to 3380 μm, the concentration is constant. The concentration however increase in the region 3380 μm to 3860 μm. In the S QECD two concentration regions are discernible. The concentration is high in the region 2100 μm to 3380 μm and low region 3380 μm to 3860 μm.

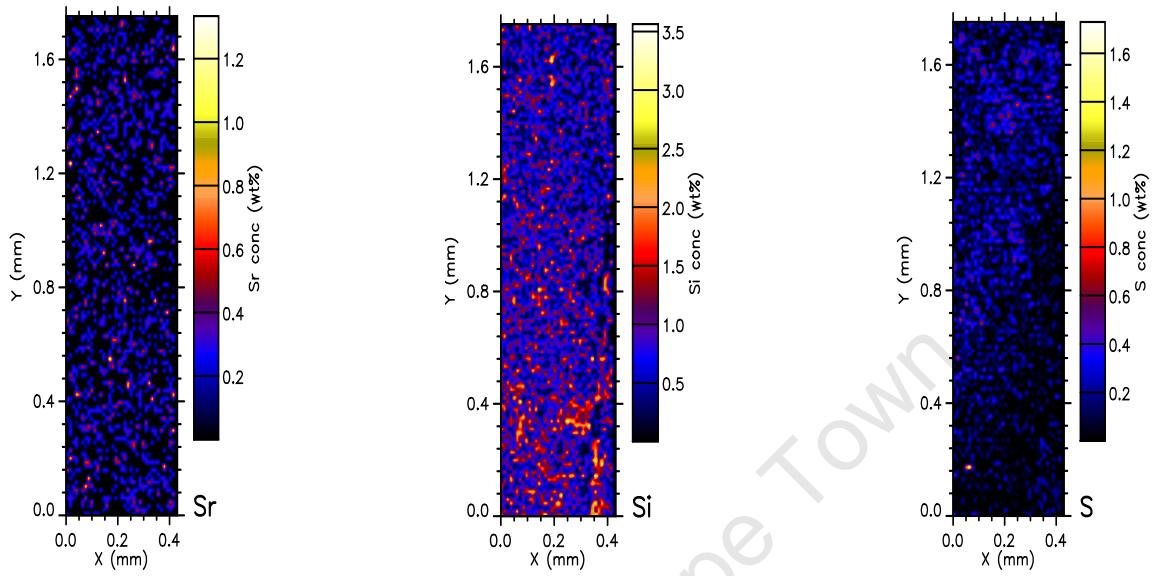

Figure 3-27 The quantitative elemental concentration distributions, based on the X-ray emission data, of the elements Sr, Si and S in the length distance region of a 2100 μm to 3860 μm from the edge of the scale of *Pomadasys kaakan*.

The QECDs, based on the X-ray emission data, of the elements Fe, Mn, V, Ti, Se, Ni and Cr in the length distance region of a 2100 μm to 3860 μm, are shown in **figure 3.28**. There are no observable concentration regions for these elements in the scanned area. It is therefore assumed that the uptake of the elements was constant and low.

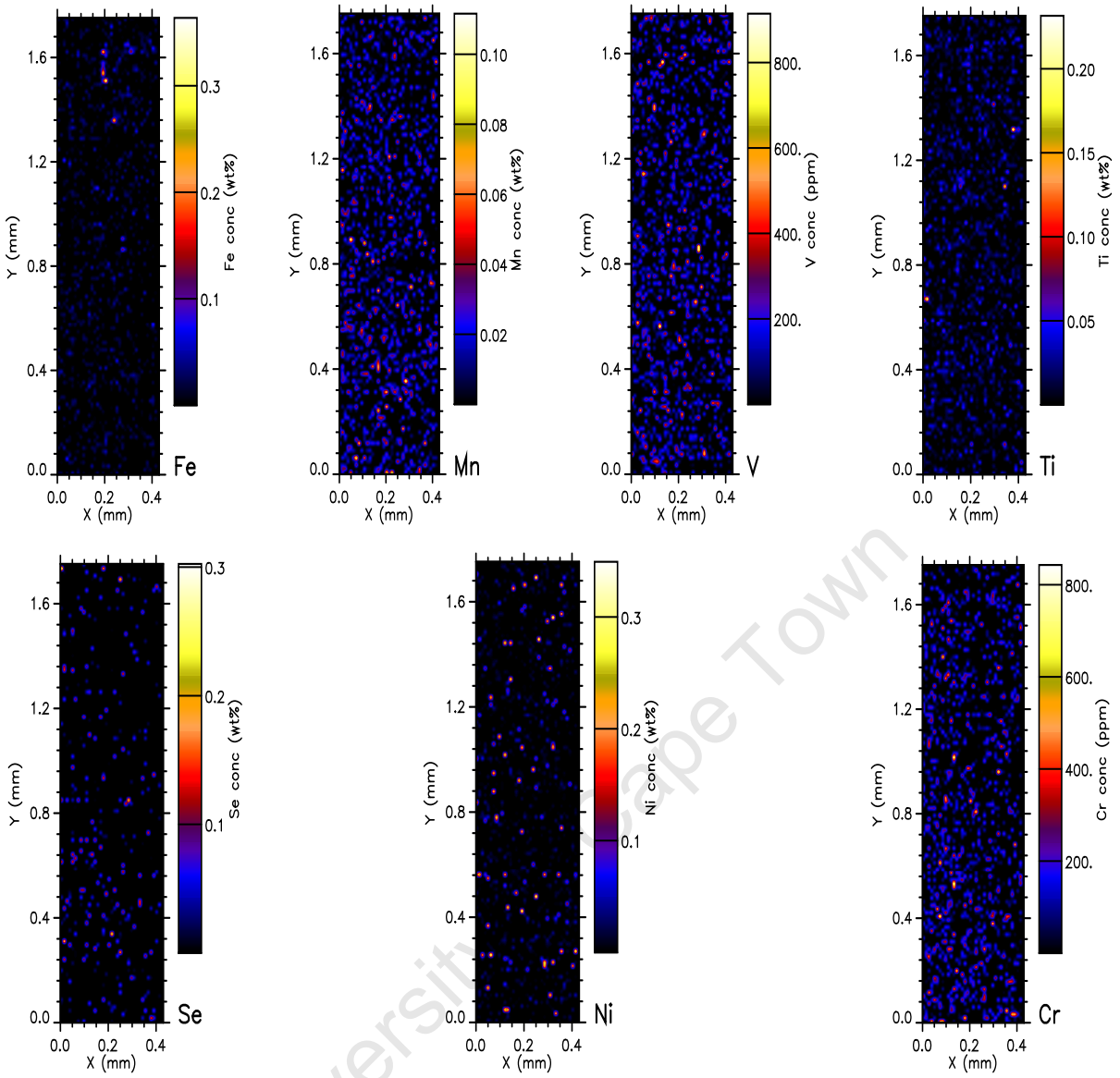

Figure 3-28 The quantitative elemental concentration distributions, based on the X-ray emission data, of the elements Fe, Mn, V, Ti, Se, Ni and Cr in the length distance region of 2100 μm to 3860 μm from the edge of the scale of *Pomadasys kaakan*.

Concentration correlations, based on the X-ray emission data, of the corresponding elements P-Ca, P-Al, and Si-Al, S-Al, Cr-Ca, Fe-Ca, Si-Ca and S-Ca in the length distance 340 μm to 2100 μm from the edge of the fish scale of *Pomadasys kaakan* are shown in **figure 3.29**. The linear correlation of P and Ca is not as strong as in the previous regions. Since this region is near to the focus of the fish scale. The poor correlation indicates that here the scale is in the beginning stages of formation or incorporation of HAP.

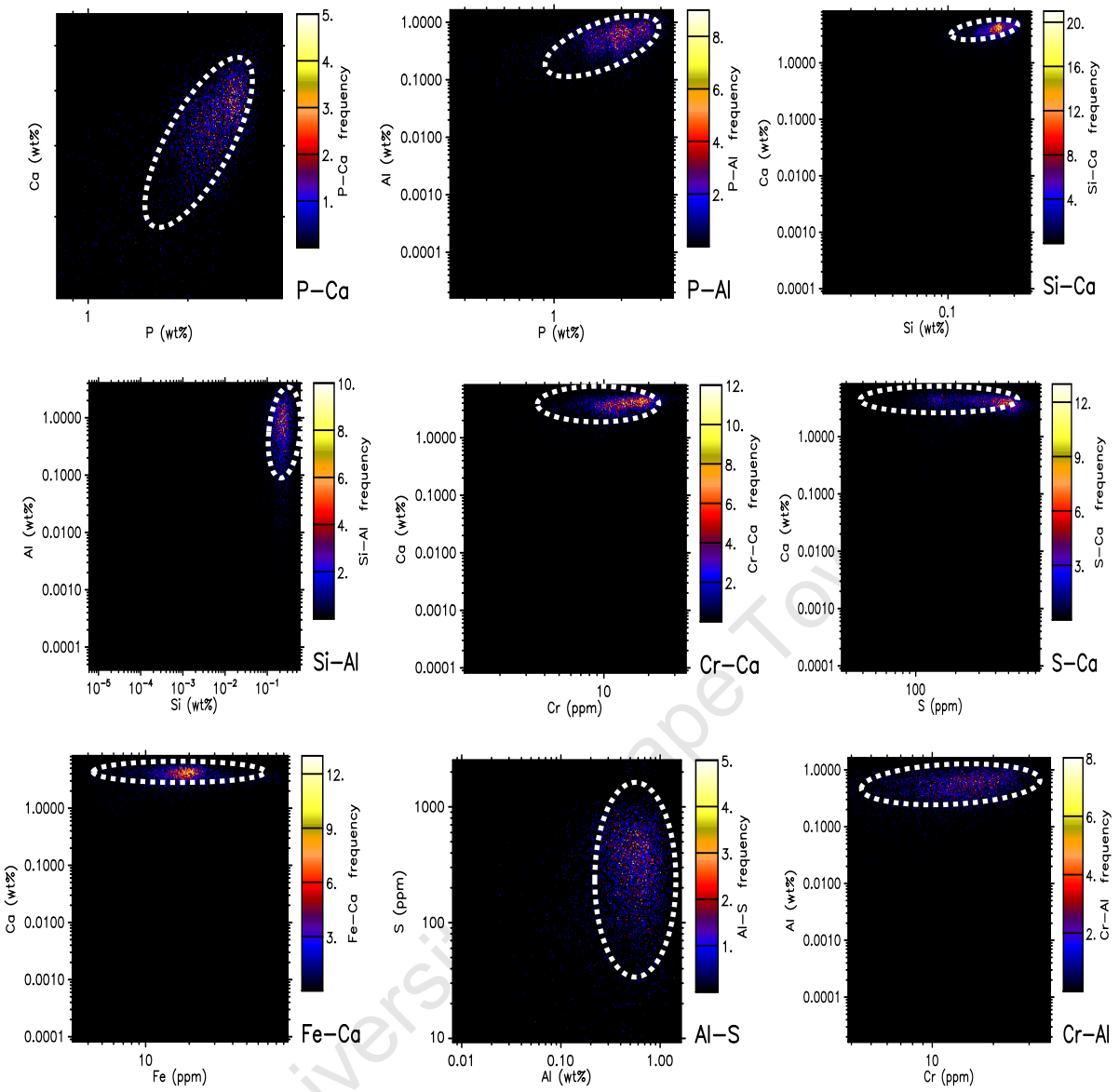

Figure 3-29 Concentrations correlations, based on the X-ray emission data, of the corresponding elements P-Ca, P-Al, Si-Al, Al-S Cr-Ca, Fe-Ca, Si-Ca and S-Ca in the length distance 2100 µm to 3860 µm from the edge of the scale of *Pomadasys kaakan*.

No linearity exists for each of the other inter-element comparisons. Hence we can infer that some of these elements were taken up independently of the others and then incorporated into the fish-scale matrix.

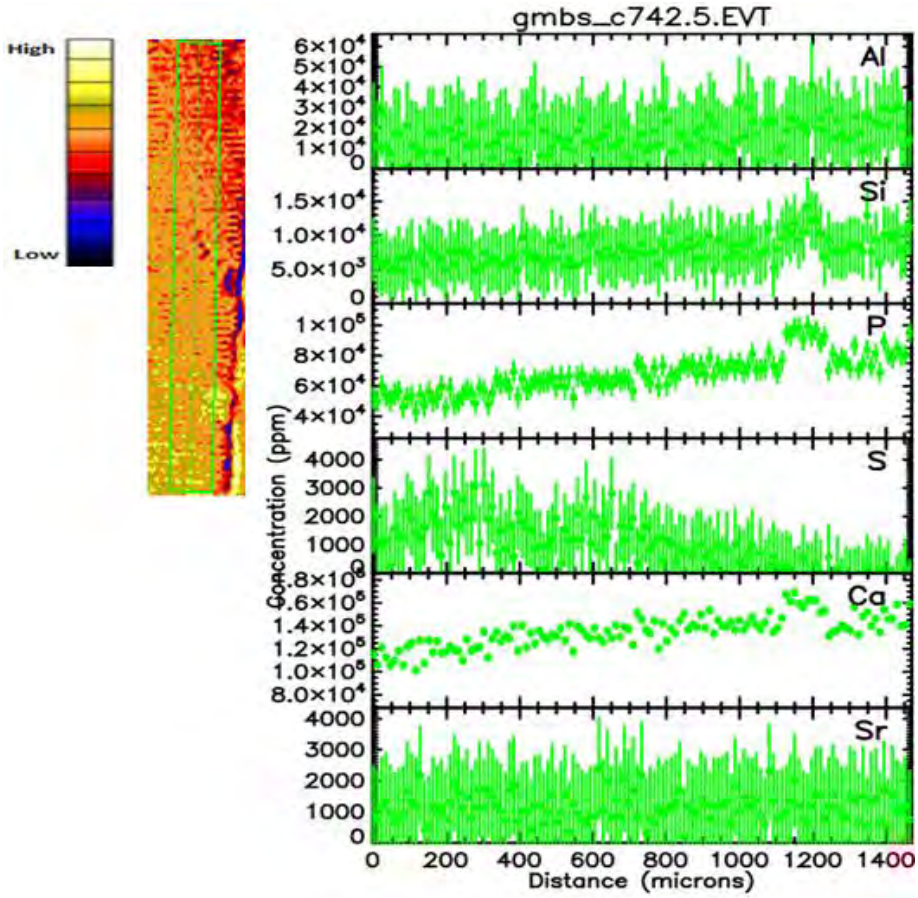

Figure 3-30 Quantitative linear traverse analyses (LTA), based on the X-ray emission data, of the corresponding elements such as Al, Si, P, Ca and Sr in the first 340 μm from the edge of the scale of *Pomadasys kaakan*. The width of the LTA was 200 μm.

Quantitative linear traverse analysis (LTA), based on the X-ray emission data, of the corresponding elements such as Al, Si, P, Ca and Sr in the first 340 μm from the edge of the fish scale of *Pomadasys kaakan*, is shown in **figure 3.30**. The width of the LTA was 200 μm.

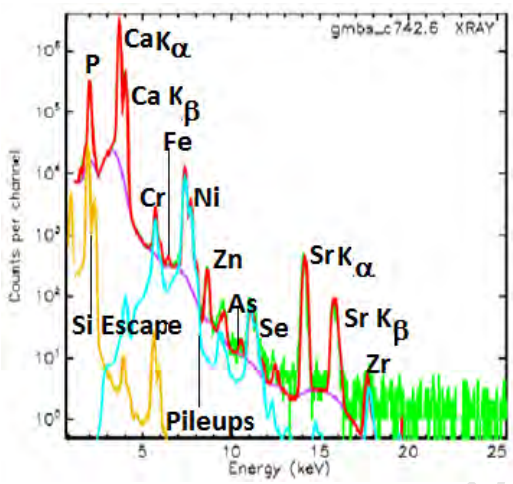

Figure 3-31 Total spectrum, based on the proton-induced X-ray emission data for the entire scanned area of 1760 μm × 400 μm (length by width), that is, for the distance length of 3860 μm to 5620 μm. The green line represents the X-ray data, the red line the fit to the data, the purple line the background, the blue line Si escape peaks and yellow line is the pileup from the data.

The total spectrum, based on the proton-induced X-ray emission data for the entire scanned area of 1760 μm × 400 μm (length by width), that is, for the distance length of 3860 μm to 5620 μm, is shown in **figure 3.31**.

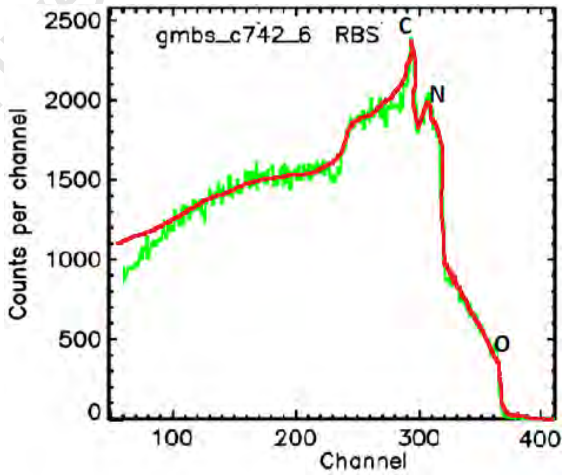

Figure 3-32 Total spectrums, based on the backscattered data for the entire scanned area of 1760 μm × 400 μm, that is, in the distance length of 3860 μm to 5620 μm, of the scale of the *Pomadasys kaakan*.

The total spectrum, based on the backscattered data for the entire scanned area of 1760 μm × 400 μm, that is, in the distance length of 3860 μm to 5620 μm, of the scale, is shown in **figure 3.32**.

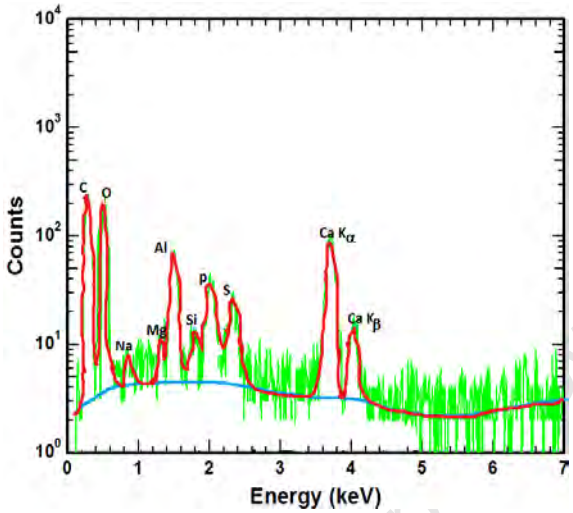

Figure 3-33 Total spectrum, based on the electron-induced X-ray emission data, for the entire scanned area of 1760 μm × 400 μm, that is, for the distance length of 3860 μm to 5620 μm, of the scale of the *Pomadasys kaakan*. The green line represents the data, the red line the fit to the data and the blue line the background.

Region 4

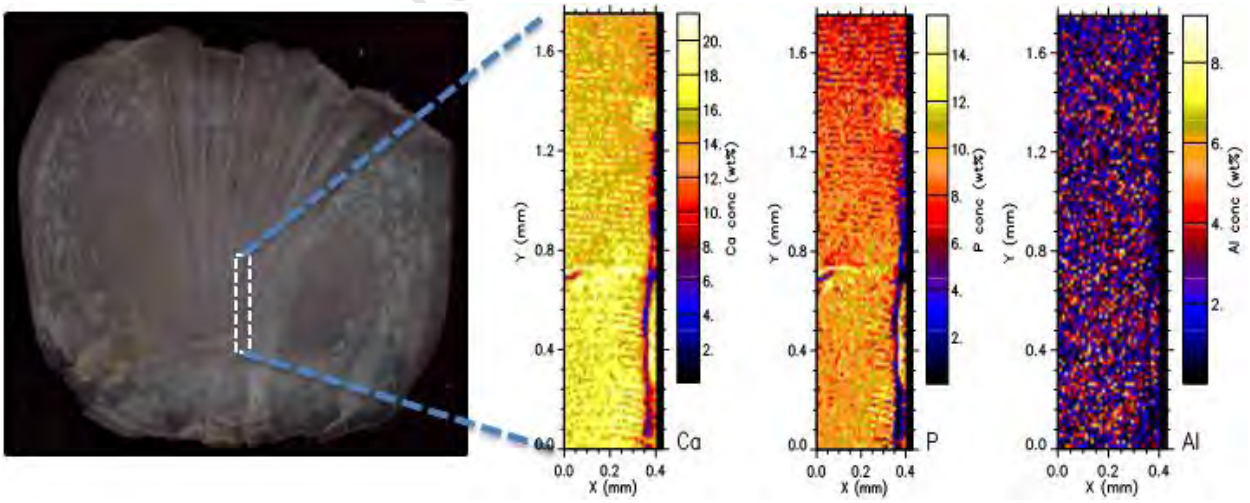

Figure 3-34 Scale of the fish *Pomadasys kaakan* (inset) showing the scanned area of 1760 μm × 400 μm (length by width) for the length distance of 3860 μm to 5620 μm (Region 4). In the alongside three images the 1700 μm corresponds to the 3860 μm and the 0 μm corresponds to 5620 μm. The distribution of the elements is discussed from the 1700 μm mark to the 0 μm mark. The quantitative elemental concentration distributions based on the X-ray emission data, of the elements Ca, P and Al in the scanned area. Various concentration regions are discernible in the scanned area.

The total spectrum, based on the electron-induced X-ray emission data, for the entire scanned area of 1760 μm × 400 μm, that is, for the distance length of 3860 μm to 5620 μm (Region 4), of the scale of the fish *Pomadasys kaakan*, is shown in **figure 3.33**.

The QECDs, based on the X-ray emission data, for the elements Ca, P and Al for the length distance of 3860 μm to 5620 μm for the fish *Pomadasys kaakan*, is shown in **figure 3.34**. This length distance, from 4900 μm to 5620 μm, includes the focus region of the fish scale.

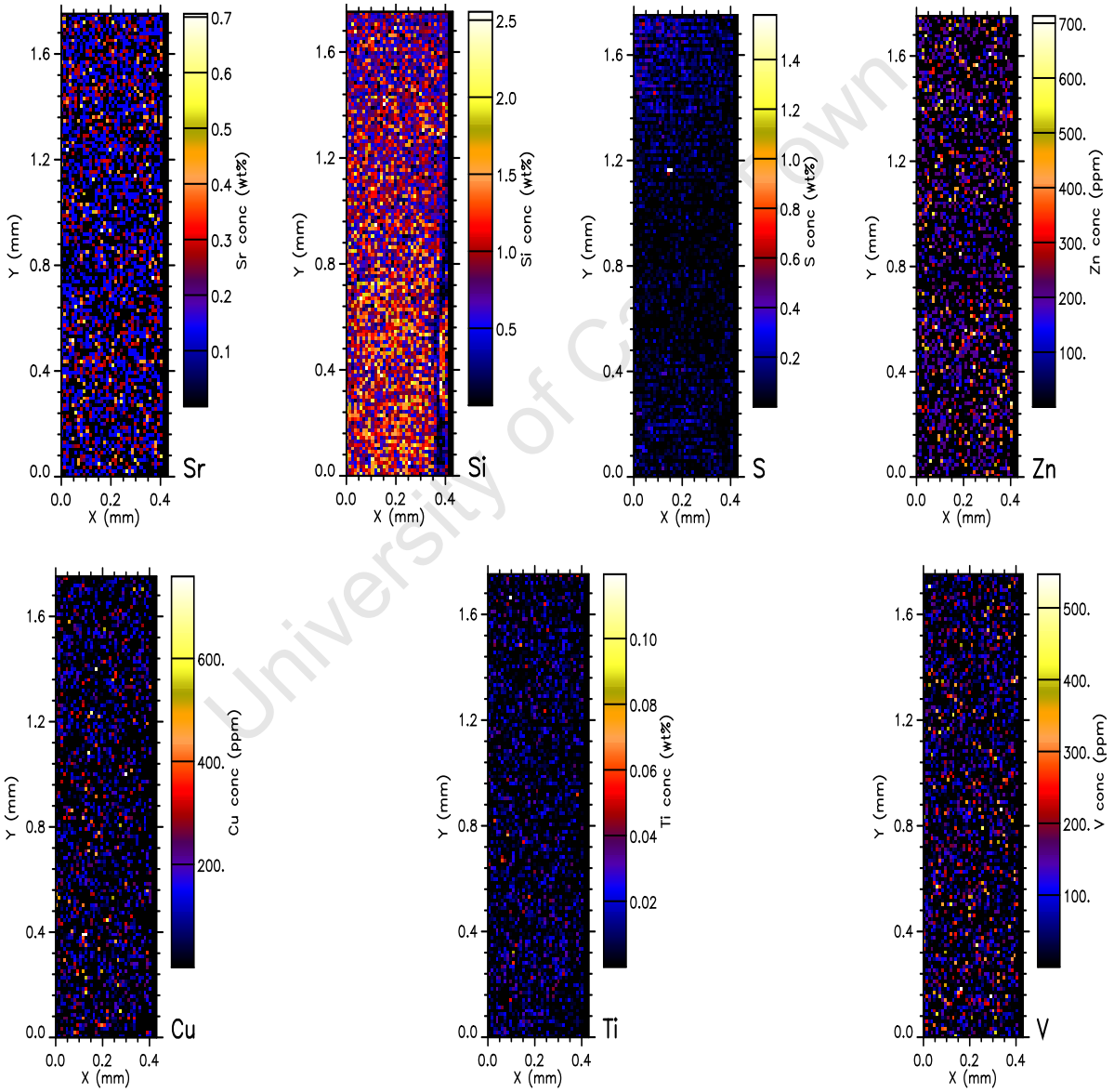

Figure 3-35 The quantitative elemental concentration distributions, based on the X-ray emission data, of the elements Sr, Si S, Zn, Cu, Ti and V in the length distance region of a 3860 μm to 5620 μm from the edge of the scale of *Pomadasys kaakan*.

Three regions are distinguishable in the Ca QECD. There is however very little concentration difference between the Ca in the field posterior to the focus and Ca in the focus. The area of low concentration on the right-side of the Ca QECD is the region of the annulus.

The QECD of P is similar to that of Ca, that is, the concentration of P in the field posterior to the focus to that in the focus. The Al QECD is however homogeneously distributed throughout this scanned area. In addition, the concentration of Al in this region is relatively higher that in the previous scanned area (2100 μm to 3860 μm).

This means that relatively high levels of Al were present in the river from the very onset of the fish's life. This degree of pollution only abated during the growth of the scale in the previous length distance. The QECDs, based on the X-ray emission data, of the elements Sr, Si, S, Zn, Cu, Ti and V in the length distance region of a 3860 μm to 5620 μm, are shown in **figure 3.35**. There are no observable concentration regions for these elements in the scanned area. The QECDs, based on the X-ray emission data, of the elements Fe, Mn, Ni, and Se in the length distance region of a 3860 μm to 5620 μm, are shown in **figure 3.36**.

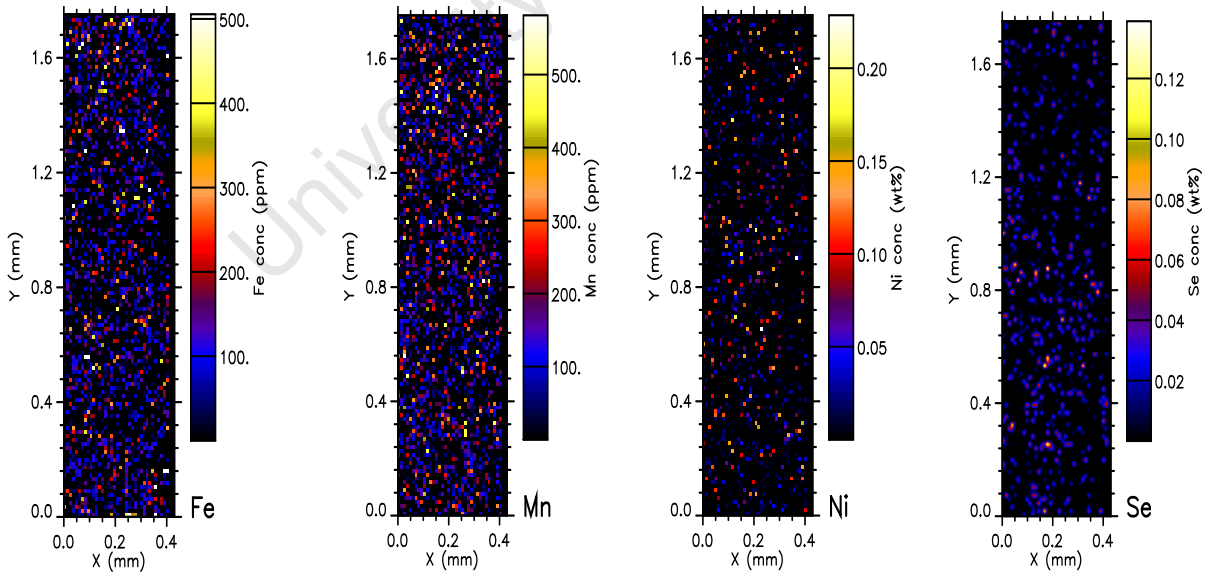

Figure 3-36 The quantitative elemental concentration distributions, based on the X-ray emission data, of the elements Fe, Mn, Ni and Se in the length distance region of a 3860 μm to 5620 μm, of the scale of *Pomadasys kaakan*.

There are no observable concentration regions for these elements in the scanned area. Quantitative linear traverse analysis (LTA), based on the X-ray emission data, of the

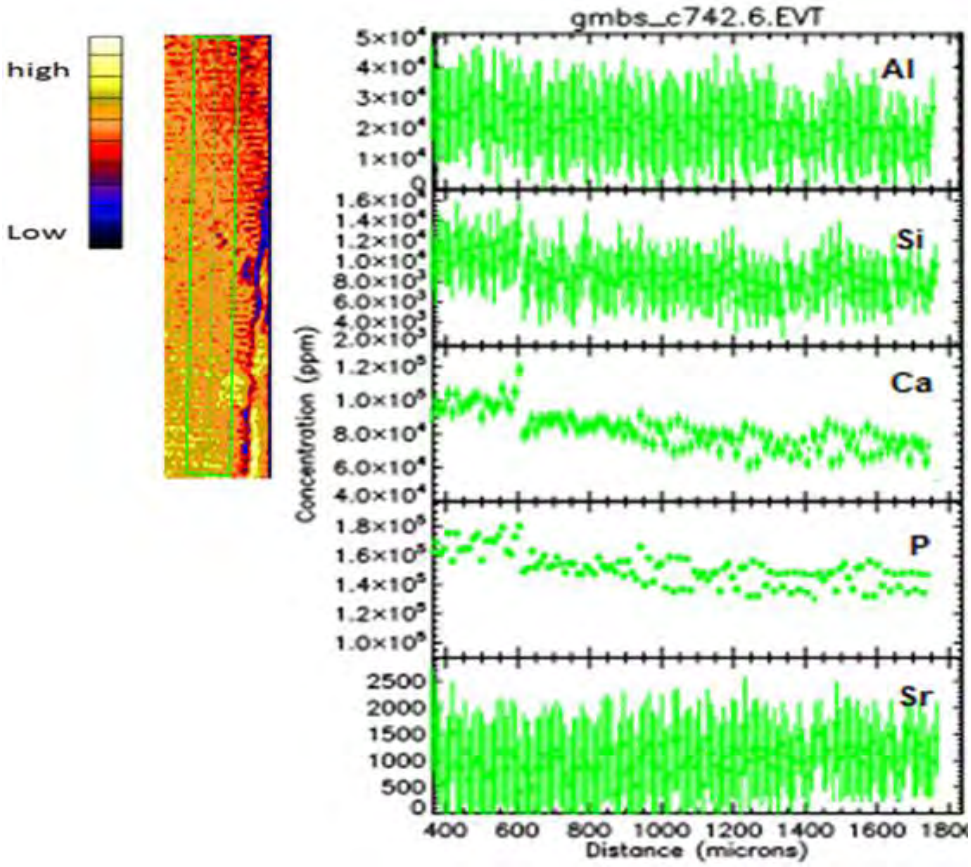

Figure 3-37 Quantitative linear traverse analysis (LTA), based on the X-ray emission data, of the corresponding elements such as Al, Si, P, Ca and Sr in in the length distance region of a 3860 μm to 5620 μm of the scale of *Pomadasys kaakan*. The width of the LTA was 200 μm.

corresponding elements such as Al, Si, Ca, P, and Sr in the in the length distance region of a 3860 μm to 5620 μm of the fish scale of *Pomadasys kaakan*, is shown in **figure 3.37**. The width of the LTA was 200 μm.

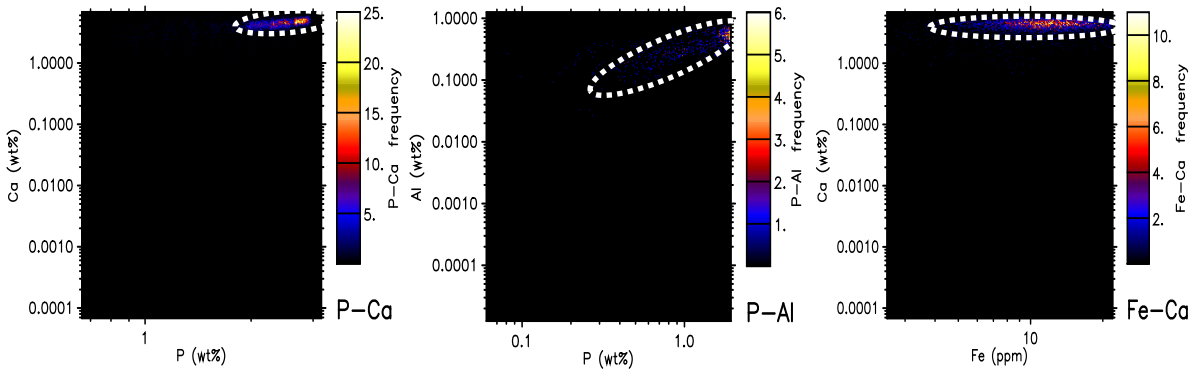

Figure 3-38 Concentrations correlations, based on the X-ray emission data, of the corresponding elements P-Ca, P-Al, and Fe-Ca in the length distance 3860 µm to 5620 µm from the edge of the scale of *Pomadasys kaakan*.

Concentrations correlations, based on the X-ray emission data, of the corresponding elements P-Ca, P-Al, and Fe-Ca in the length distance 3860 µm to 5620 µm of the fish scale of *Pomadasys kaakan* are shown in **figure 3.38**.

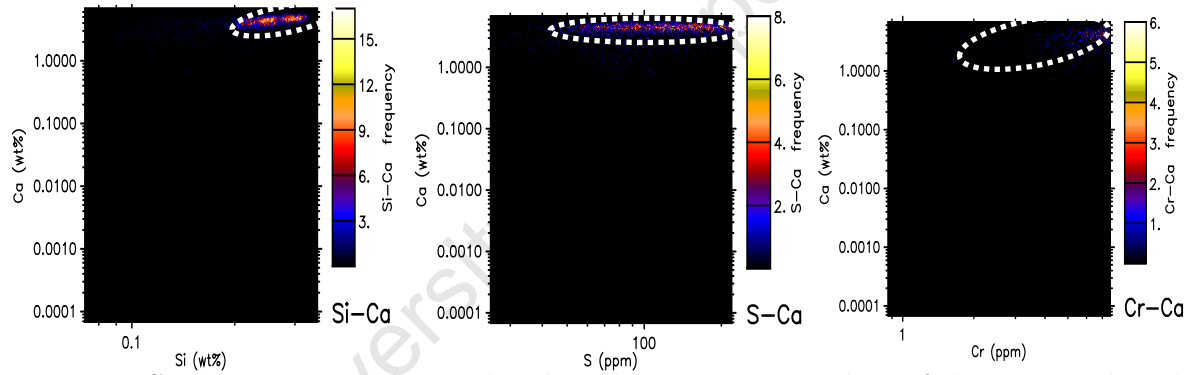

Figure 3-39 Concentrations correlations, based on the X-ray emission data, of the corresponding elements Si-Ca, S-Ca and Cr-Ca in the length distance 3860 µm to 5620 µm from the edge of the scale of *Pomadasys kaakan*.

The linear correlation of P and Ca is weaker than in the previous regions. Since this region is near to the focus of the fish scale it indicates that in the beginning stages of growth HAP is either formed or incorporated into the matrix.

Concentration correlations, based on the X-ray emission data, of the corresponding elements Si-Ca, S-Ca and Cr Ca in the length distance 340 µm to 2100 µm from the edge of the fish scale of *Pomadasys kaakan* are shown in **figure 3.39**.

The linear correlation of P and Ca is weaker than in the previous regions. Since this region is near to the focus of the fish scale, it indicates that in the beginning stages the formation or incorporation of HAP was homogeneous.

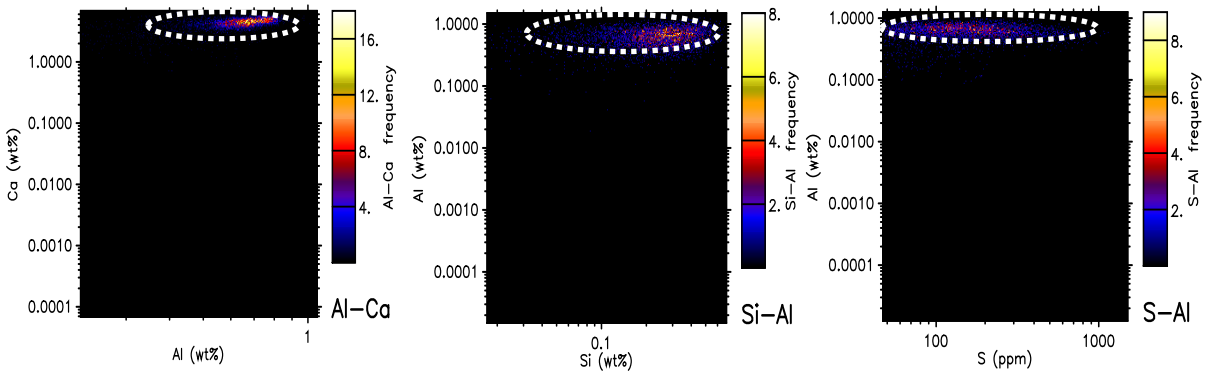

Figure 3-40 Concentrations correlations, based on the X-ray emission data, of the corresponding elements Al-Ca, Si-Al and S-Al in the length distance 3860 µm to 5620 µm from the edge of the scale of *Pomadasys kaakan*.

No linearity exists for each of the other inter-element comparisons. Hence these elements did not affect each others incorporation into the fish scale matrix. Concentrations correlations, based on the X-ray emission data, of the corresponding elements Al-Ca, Si-Al and S-Al in the length distance 3860 µm to 5620 µm of the fish scale of *Pomadasys kaakan* are shown in **figure 3.40**.

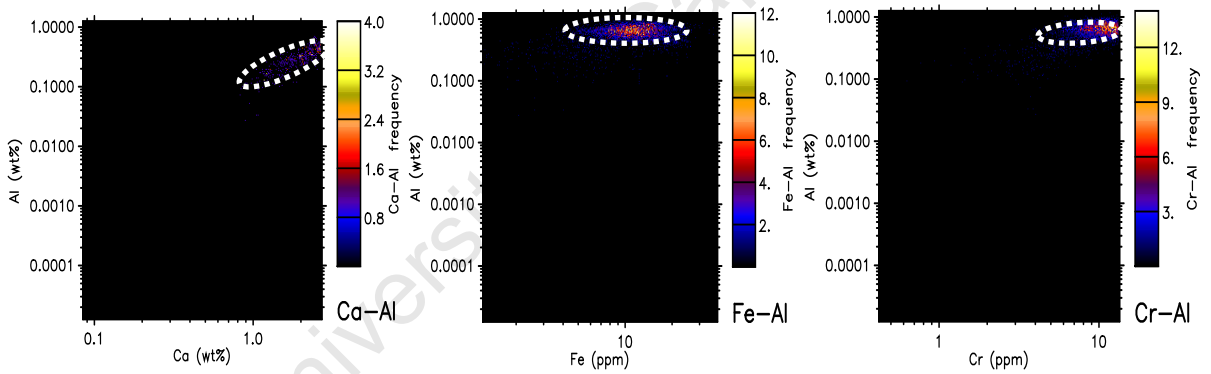

Figure 3-41 Concentrations correlations, based on the X-ray emission data, of the corresponding elements Ca-Al, Fe-Al and Cr-Al in the length distance 3860 µm to 5620 µm of the scale of *Pomadasys kaakan*.

Concentrations correlations, based on the X-ray emission data, of the corresponding elements Ca-Al, Fe-Al, and Cr-Al in the length distance 3860 µm to 5620 µm of the fish scale of *Pomadasys kaakan* are shown in **figure 3.41**.

3.3 Three dimensional (3-D) analysis of the fish scale.

In the previous section 3.1 the 2-D analysis of the fish scale was discussed and it was found that some of the elements have been incorporated homogeneously and others heterogeneously. In this section the cross-sectional quantitative elemental concentration and distributions of the elements are discussed. The dimensions of the scanned areas are 150 μm × 200 μm, and then for three sections, 600 μm × 2300 μm. The scanned areas are indicated in **figure 3.42**.

The quantitative elemental concentration distribution of the elements Ca, P and Al are shown in **figure 3.43**. From the quantitative elemental concentration distributions it is evident that HAP is formed predominantly in the core of the scale. Towards the ends of the edge the matrix consists mostly of KRT. However, from the correlation the Ca and P quantitative elemental concentration distributions, which should be in the concentration ratio of 2:1, it is evident that the ratio is less than 2:1. This means that the concentration of P is relatively more hence P is probably also present as $AlPO_4$. Aluminium (ALM) is also incorporated into this core area. In the width length of 150 μm the concentrations of all Ca, Al and P are relatively low. This means that areas of KRT are formed in the core of the fish scale. The linear traverse analyses across the cross-sectional area of Ca, P and Al and of the trace elements are shown in **figure 3.45**.

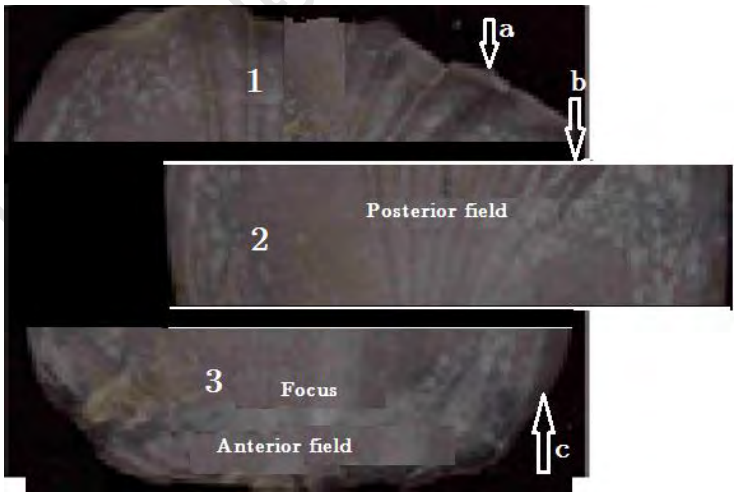

Figure 3-42 Illustration of three areas (1, 2 & 3) of the fish scale of *Pomadasys* kaakan that was cut and scanned along the surface as indicated in (a, b & c).

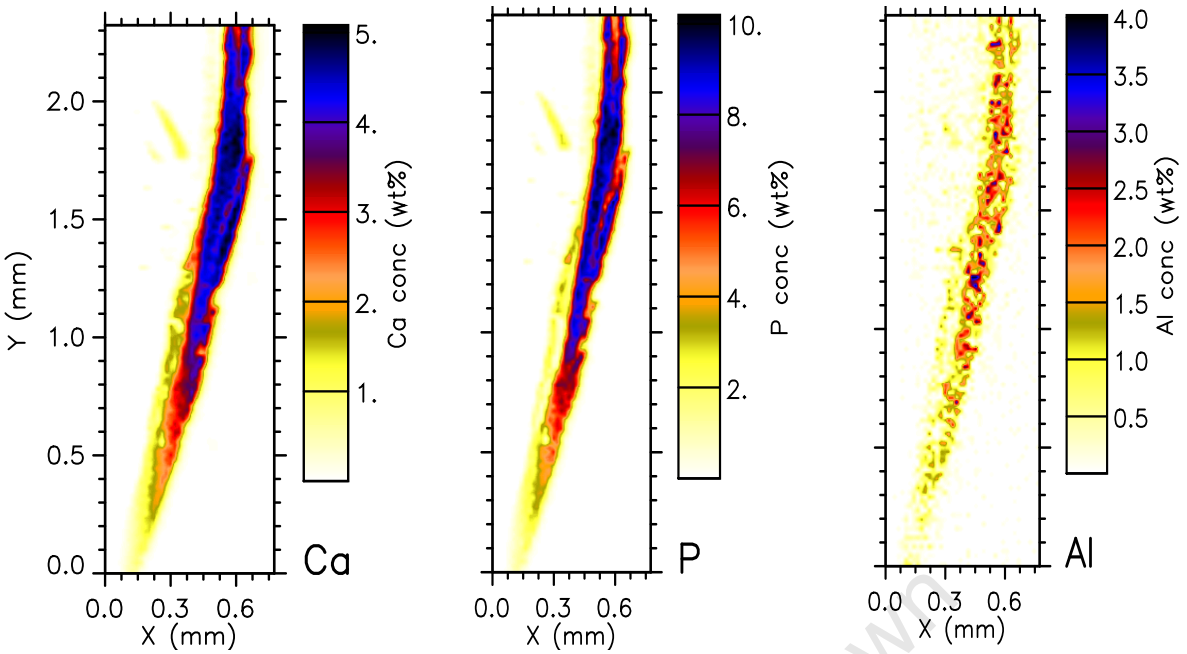

Figure 3-43 Quantitative elemental concentration distributions (QECDs) of Ca and P, the major elements, and of Al a pollutant, found in the cross-section of the fish scale matrix. The QECDs are based on X-ray emission data. The right side of the cross-sectional areas is the front side facing the water and the left side is attached to the body.

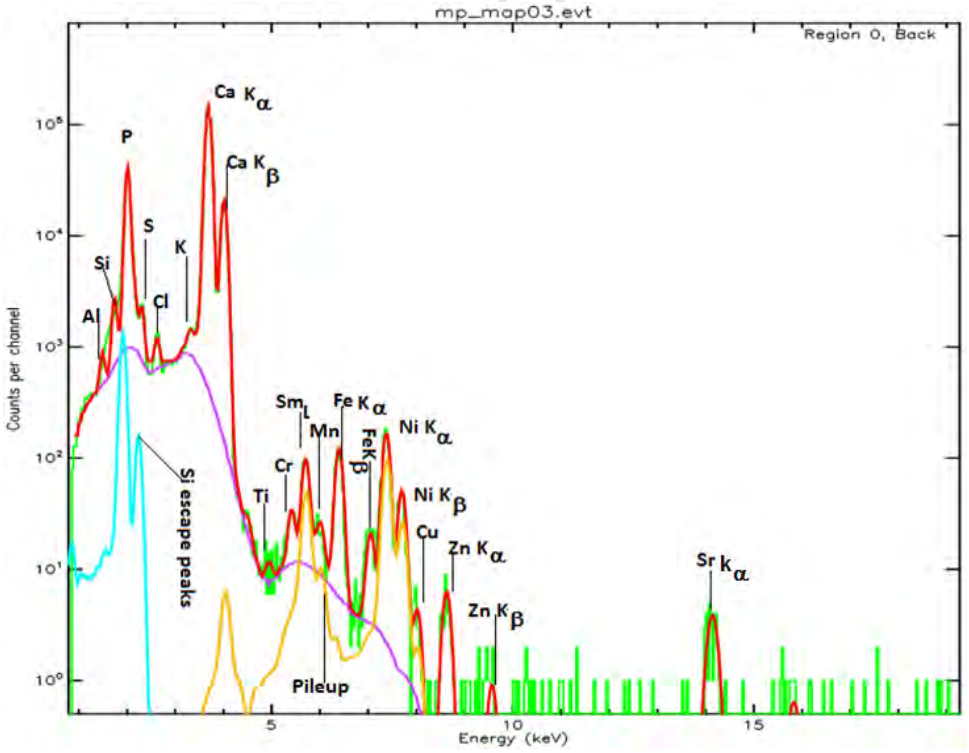

Figure 3-44 Total spectrum, based on the proton-induced X-ray emission data for the entire scanned area of 150 µm × 250 µm (length by width). The green line represents the X-ray data, the red line the fit to the data, the purple line the background, the blue line Si escape peaks and yellow line is the pileup from the data.

The quantitative elemental concentration distributions of Ca and P show the same trend. The quantitative elemental concentration distributions of the minor and trace elements, with the exception of Sr, are heterogeneous and therefore these elements do not affect the distribution of the major elements. More so, distributions of these elements are sporadic and at certain length intervals are present below the minimum detection limit.

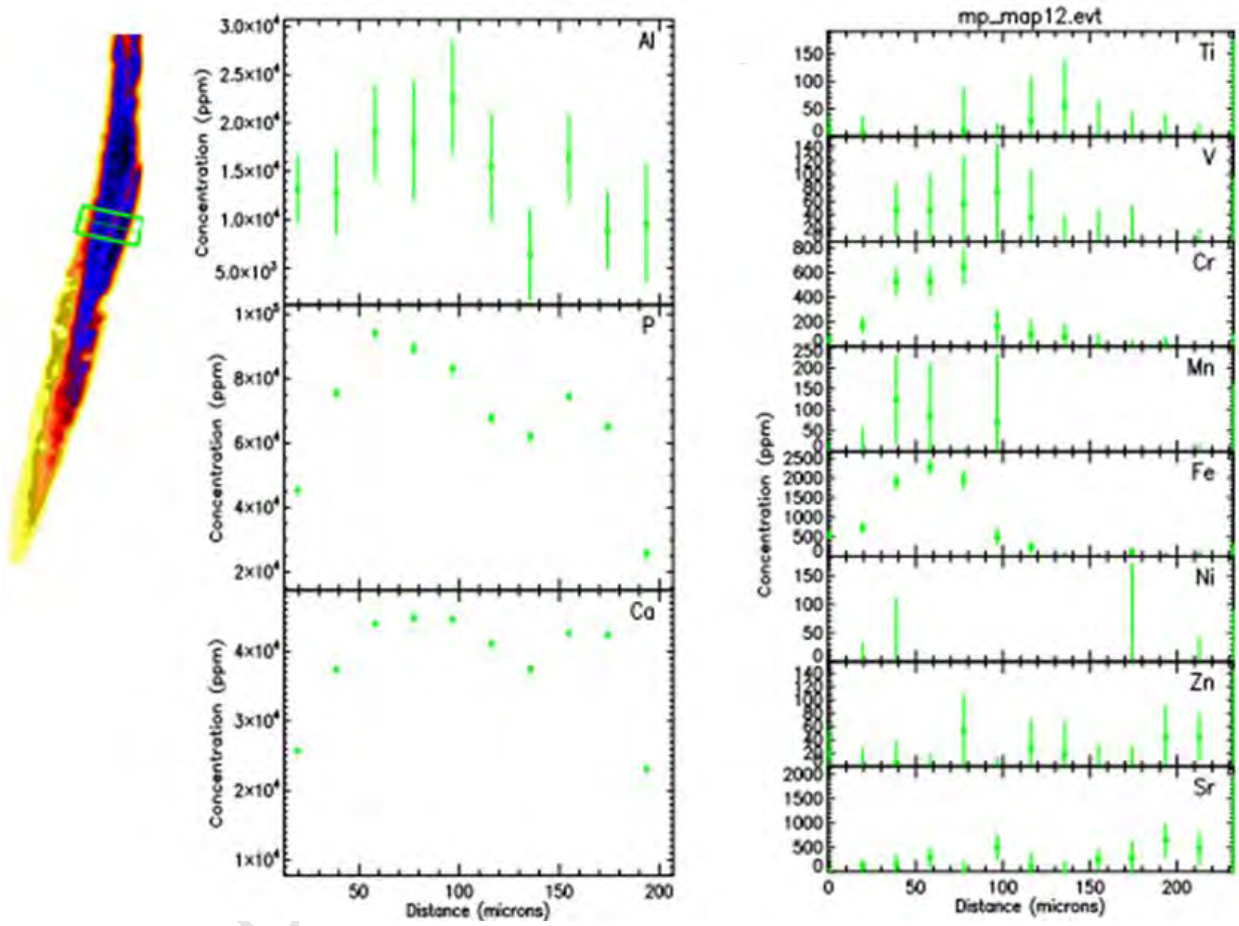

Figure 3-45 The quantitative linear traverse analysis (LTA), based on the X-ray emission data, across the length of the cross-sectional area of the fish scale. To the left are the LTAs of the major elements Ca and P and Al. To the right are the LTAs of the heavy metals to indicate any correlation with those of the major elements and Al. The inset is the quantitative elemental concentration distribution of Ca. The width of the LTA was 200 μm.

Correlations between the concentrations of the elements Ca and P and Fe and Al are shown in **figure 3.45**. From the trend of the correlation of Ca and P it is evident that these elements are linearly correlated in the region of high concentration.

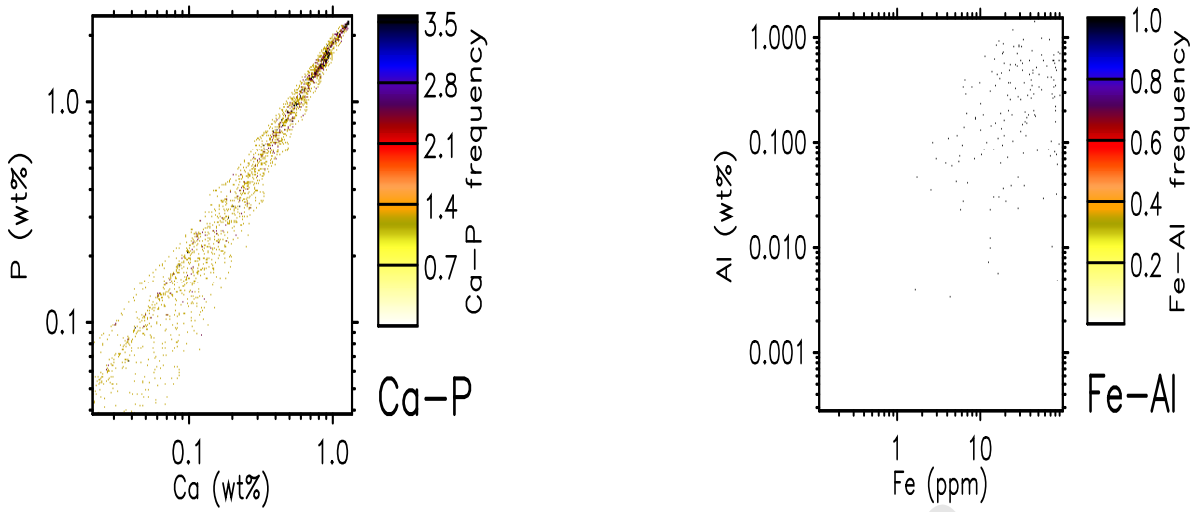

Figure 3-46 The quantitative concentration correlations of Ca and P (to the left) and of Fe and Al (to the right). The correlations are based on the X-ray emission data generated by GeoPIXE softwar.

The concentration correlation trend of Fe and Al is diffused, which means that these elements are not co-distributed and hence do not affect the QECDs of each other's.

To illustrate the chemical formation of Al with P, the P and Al QECDs are overlaid on one another, as shown in **figure 3.47**. From these maps it is evident that $AlPO_4$ is mostly formed in the core of the fish scale than on the periphery.

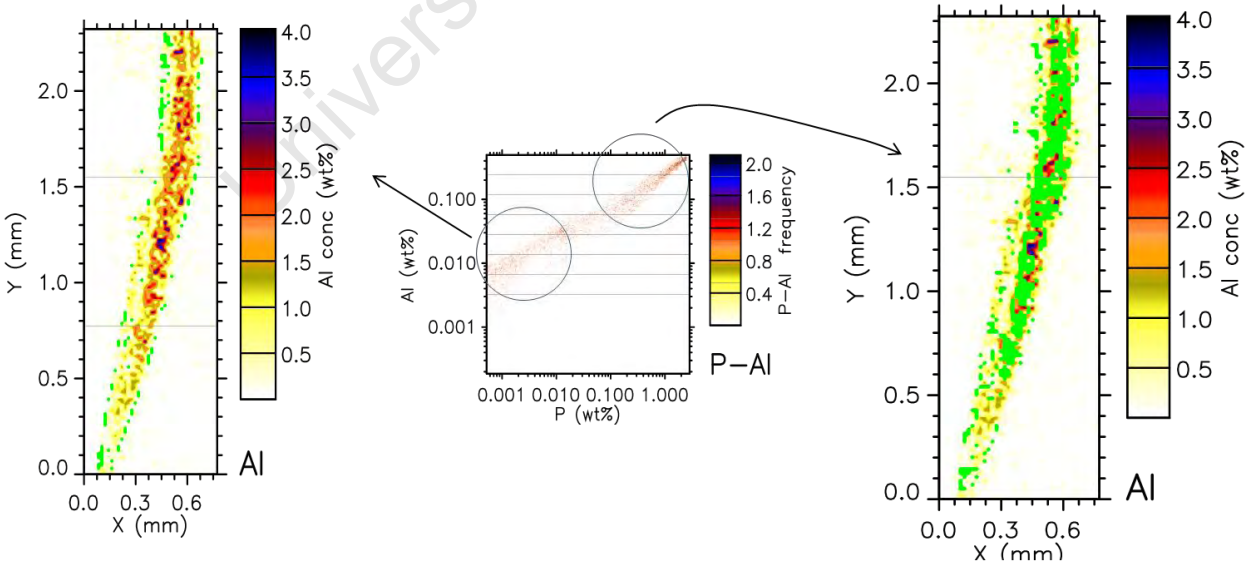

Figure 3-47 The graphic representation of quantitative concentration correlations of Al and P (in the centre) to show any hetero- or homogeneity. The correlations are based on the X-ray emission data and are overlaid on the Al quantitative elemental concentration distribution.

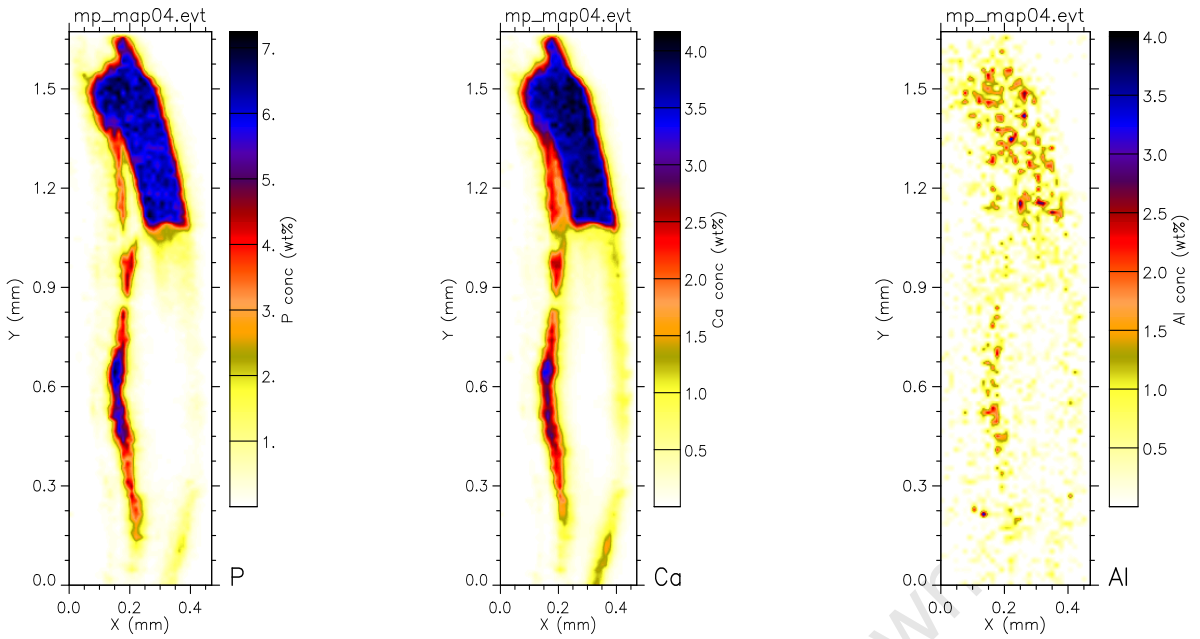

Figure 3-48 Quantitative elemental concentration distributions (QECDs) of P and Ca, the major elements, and of Al found in the cross-section "a" in figure 3.42 of the fish scale matrix. The QECDs are based on X-ray emission data.

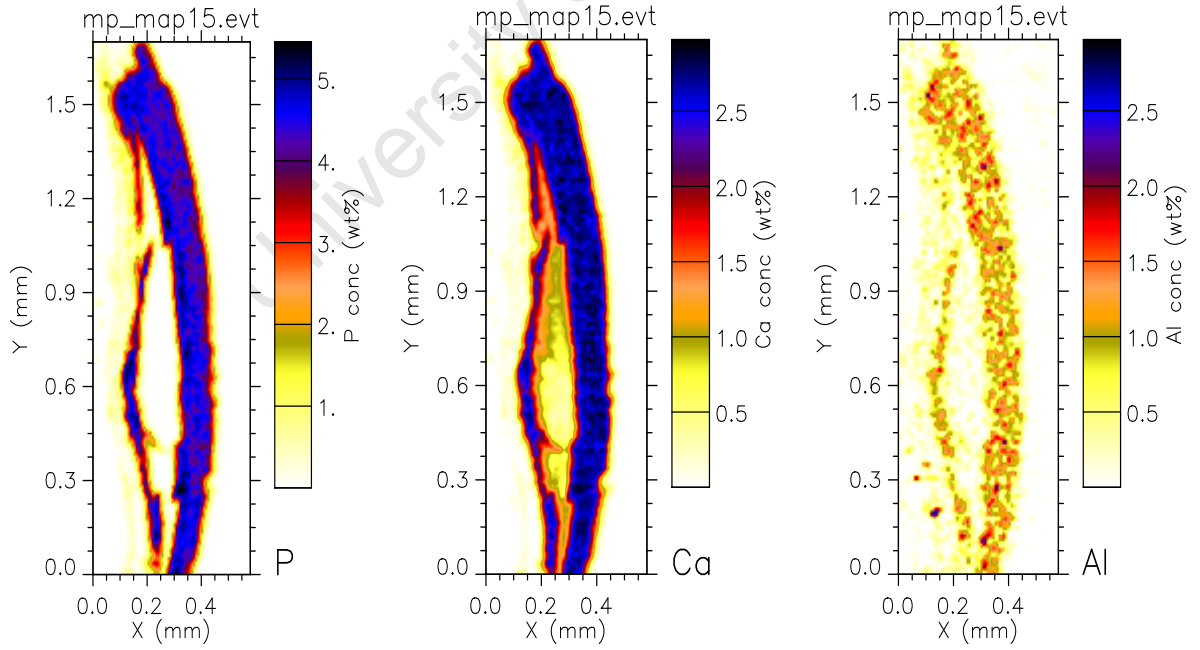

Figure 3-49 Quantitative elemental concentration distributions (QECDs) of P and Ca, the major elements, and of Al found in the cross-section "b" in figure 3.42 of the fish scale matrix. The QECDs are based on X-ray emission data.

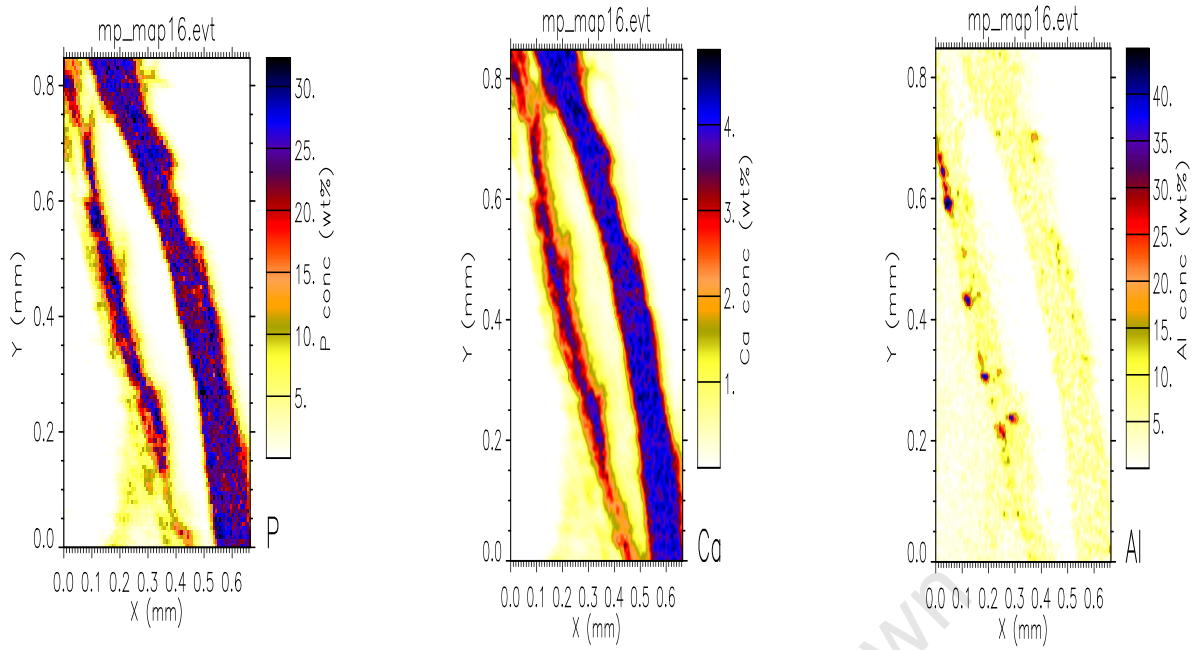

Figure 3-50 Quantitative elemental concentration distributions (QECDs) of P and Ca, the major elements, and of Al, the pollutant, found in the cross-section "c" in figure 3.42 of the fish scale matrix. The QECDs are based on X-ray emission data.

3.4 Discussion

The region 1 of the fish scale scanned was that from the edge of the scale where growth must be happening where the scale joins the body. The edge of the scale was set as 340 μm and the end of the distance 0 μm.

In the 2-Dimensional analysis of the fish scale it was found that the incorporation of HAP and CCB is constant only after the first 100 μm of growth from the edge of the scale.

In the region of 340 μm to 250 μm range there is clear indication that the scale matrix consists mostly of keratin.

The homogeneous distribution of Al QECD for the scan area e. g. Region 4 from the edge of the fish scale of *Pomadasys kaakan* indicates that Al contamination was constant.

No significant inter-element correlation was found. This is due to irregular distribution of the elements. It is important to note with regard to the QECD that Al in area of Region 4 is relatively higher than in the area 2100 μm to 3860 μm presumable due to relatively high levels of Al presence in the river from the very onset of the fish's life. This amount of Al QECD only it was found along a growth of the scale in the length distance. In the region of the focus was found clear indication of the

beginning stages of the formation either incorporation of HAP as part integrant in matrix composition of the fish scale.

In the linear traverse analysis (LTA) the correlation between the concentrations of P and Ca is irregular in some regions due to dispersed distribution of the elements. It was found that there is no discernible concentration region or demarcation in the Al QECD suggesting that the Al contamination also occurs in the annuli of the fish scale. The standard deviation of Si is high due to heterogeneous distribution of the elements in different regions.

On the base of the three dimensional analyses it was found that the quantitative elemental concentration and distributions of the elements such as Ca and P were similar. The trace and minor elements except Sr are heterogeneously distributed although the distributions of the major elements are not affected. It was shown that at certain length intervals the distribution of these elements are not detectable and they are present in quantities below the minimum detection limit.

Chapter Four
4 Comparative analysis of scales of four different fish species

4.1 Introduction

Elemental distribution in a single scale of *Pomadasys kaakan* was described in chapter three. This chapter compares quantitative elemental concentration distribution patterns in the scales of three other species of fish to see if there are obvious differences in pattern. This data will allow us to see if a particular species of fish would be especially useful in further studies. A cycloid scale of the type found in *Pomadasys kaakan* and *Lithognathus mormyrus* (to the left) and a ctenoid scale of type found in *Lutjanus gibbus* and *Pinjalo pinjalo* (to the right) are illustrated in **figure 4.1**.

Figure 4-1 Illustration of the scanned area of cycloid scales of *Pomadasys kaakan* and *Lithognathus mormyrus* (on the left) and scanned areas of the ctenoid scales of *Lutjanus gibbus* and *Pinjalo pinjalo* (on the right). "A" indicates the scanned areas of the scales.

The aim of this section of the work was to see if the morphology of the scales is similar in different species and if the apparent degree of uptake of metals would be comparable. The three species used for comparisons were *Lutjanus gibbus*, *Pinjalo pinjalo* and *Lithognathus mormyrus*. Geographic coordinates of the positions where the fishes were caught are given in **table 4.1**. These species and localities were chosen since residential areas are located close to these rivers and the four species of fish form a major part of the diet of the local inhabitants.

Table 4-1 Localities in terms of GPS coordinates, where the specimen fish were caught.

Type of fish	GPS Coordinates	Place	Mass (g)	Length (cm)	Age (days)
Pomadasys kaakan	25^0 58" 29' and 32^0 26" 14'	Matola River	2700	42	365±30
Lithognathus mormyrus	25^0 54" 07' and 32^0 49" 52'	Maputo Bay	2000	39	365±35
Lutjanus gibbus	26^0 58" 00' and 32^0 29" 46'	Espirito Santo Estuary	2500	40	365±35
Pinjalo pinjalo	26^0 03" 18' and 32^0 28" 30'	Tembe River	3000	41	365±25

In the previous sections, the elements analysed were Ca, P, Al, S, Sr, Si, Fe, Cr, Ti, V, Mn, Ni, Cu, Zn, and Se. In this chapter the elemental distribution of Ca, P, Al, S, Fe and Cr are examined because these are the elements shown to have interesting distributions.

4.2 Results of PIXE analysis

4.2.1 The comparison of hydroxyl apatite (HAP), keratin (KRT) and calcium carbonate (CCB)

The quantitative elemental concentrations and distributions extracted from μ-PIXE of Ca, P, Al, S, Fe and Cr are indicated in the corresponding **figures 4.2 to 4.7.**

Hydroxylapatite consists of Ca (40%) and P (20%). Hence if Ca and P are present in the ratio of 2:1, then the composition is pure hydroxyl apatite. If the concentration ratio is greater than 2:1, then the Ca is present in a comparatively higher concentration. Hence the composition would be HAP and calcium carbonate (CCB), $CaCO_3$. If the Ca concentration is less than 40%, and the P concentration is less than 20%, then the reminder of the composition is keratin. If the Ca:P ratio is less than 2:1, then P is combined with another element (e.g. Al, as $AlPO_4$).

The scan of *Pomadasys kaakan* in **figure 4.2A** shows that only keratin is formed in the first 40 μm of growth. The first 40 μm has low concentrations of both Ca and P. The concentration of Ca is approximately 1% and that of P is approximately 0.5%. This yields a concentration of HAP of 2.5%. Hence the $CaCO_3$ composition is low (<1.0%). Therefore this area predominantly consists of approximately 97.0% keratin.

The scan of the scale of *Lithognathus mormyrus* **figure 4.2B** shows that the first 5 μm growth is predominantly keratin and that the Ca concentration is very high in comparison with that of *Pomadasys kaakan* due to the fact that Ca and P constitute

the major part of the scale matrix. The concentrations of Ca and P in the first 5 μm are 5 % and 2 % respectively. Considering the P concentration, then the concentration of HAP is approximately 10%. The excess of Ca is 5 % and hence the $CaCO_3$ concentration is approximately 1.25 %. Therefore the concentration of keratin in this region is approximately 89 %.

In the first growth of the scale of *Lutjanus gibbus* **figure 4.2C** Ca and P are present in high percentages and keratin is located primarily in the annuli.The edge region for about 400 μm consists of a maximum of 25% Ca and a maximum of 12% P. Hence the region consists of a maximum of 68% HAP and 32% keratin. Moreover, the Ca and P are predominantly located in the circuli of the scale (maximum 25% and 12.5%) and to a less extent in the annulis (maximum 5% and 2.5% respectively). Note that the distance between consecutive circuli is about 25 μm.

In *Pinjalo pinjalo*, **figure 4.2D** Ca and P comprise the major part of the scale matrix. In the scale of *Pinjalo pinjalo*, the distance between consecutive circuli is about 300 μm. In the first approximately 100 μm from the edge the Ca concentration is about 16 % and the P concentration about 8%. This yields an HAP concentration of about 40% and keratin concentration of about 60%.

Note that the results for *P. kaakan* and *P. pinjalo* do not indicate the absence of keratin in the matrix but merely that the percentage of keratin is low relative to the concentrations of Ca and P.

4.2.2 The concentration of Al and S

The Al concentration is exceptionally high only in the scale of *Pomadasys kaakan* (note differences in concentration in the vertical axis of **figure 4.4A**). In the scales of the other three species the Al concentration is in the parts per million ranges. Furthermore, higher concentrations of S, approximately 2%, were found in *Pomadasys kaakan* than in the other scales.

4.2.3 Comparison of Fe and Cr concentrations

For both Fe and Cr distributions, the concentrations of both Fe and Cr are higher by and order of magnitude in *L. gibbus* than in the other three species.

4.3 Discussion

The life cycle of *Lithognathus mormyrus* can be diadromous (catadromous fish species are born in fresh water and live there for the first year of the life cycle and then migrate to seawater to spawn while anadromous-fish species that spend all or part of the adult life cycle in seawater, but migrate to freshwater areas to spawn) (Koutrakis *et al.*, 2005; Malavasi, 2004) hence this species spent part of their lives in saltwater and other part in freshwater. *Lithognathus mormyrus* is born in salt water areas and migrate to freshwater environment where growing occurs (Smith, 1938). At maturity the species return to marine water to spawn. *Lutjanus gibbus* has the same anadromous migration as *Pomadasys kaakan* FAO (1997). *Pinjalo pinjalo* is typically catadromous hence it is born in marine environment and migrated to freshwater areas where spend their lives growing and as adults they return to the sea for breeding (FAO, 1997). Hence catadromous species are best for studying pollution as these species spend the first year of the life cycle in freshwater.

Differences in QEDCs in the different species could be a result of various factors.
The obvious and most important factor is the concentrations of the pollutants in the ambient environment. *P. kaakan* spends the first year of its life cycle in the Matola River into which at times residential and industrial effluent is discharged. It is expected that the elemental concentrations would be relatively higher in comparison to those in scale of the fish *P. pinjalo* that spent part of its life cycle in Tembe River. There are no industrial manufacturers on the periphery of the Tembe and the population is small. Also, the Fe and Cr concentrations in *P. kaakan* should be lower than the concentrations of these elements in *L. gibbus* which was caught in the Espirito Santo Estuary.

- The kinetics of the physiological uptake might also differ from species to species, and hence the concentrations would also differ;
- The fishes might also have been exposed to effluents with different chemical compositions at different time intervals;
- It is possible, but unlikely that pollutants such as Al are not found in all the scales of a simple fish specimen.

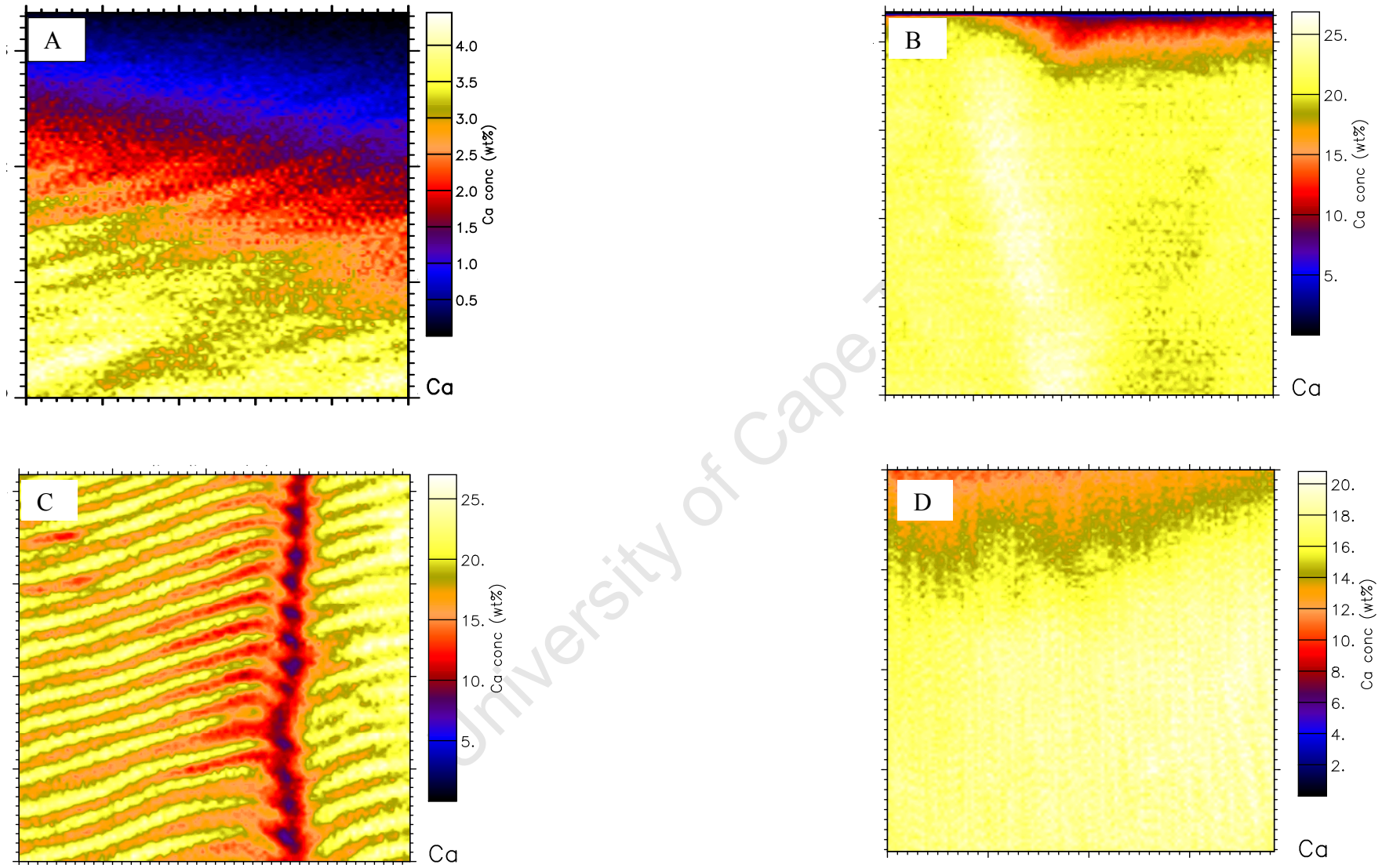

Figure 4-2 Comparative analysis of Ca in the scales of the fish *Pomadasys kaakan* (A), *Lithognathus mormyrus* (B) the *Lutjanus gibbus* (C) and *Pinjalo pinjalo* (D). The scanning area is 400 µm × 400 µm

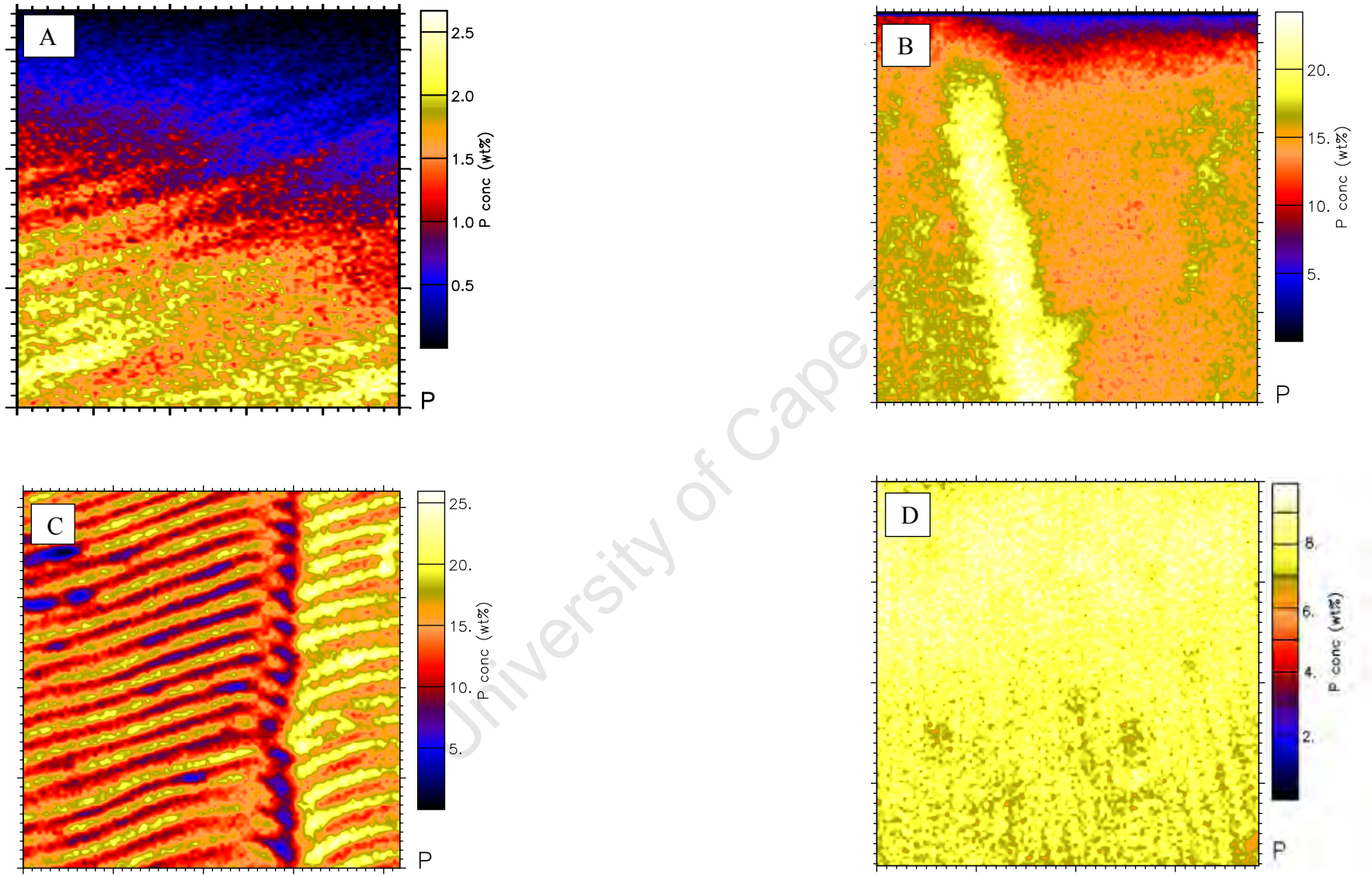

Figure 4-3 Comparative analysis of P in the scales of the fish *Pomadasys kaakan* (A), *Lithognathus mormyrus* (B) the *Lutjanus gibbus* (C) and *Pinjalo pinjalo* (D). The scanning area is 400 µm × 400 µm.

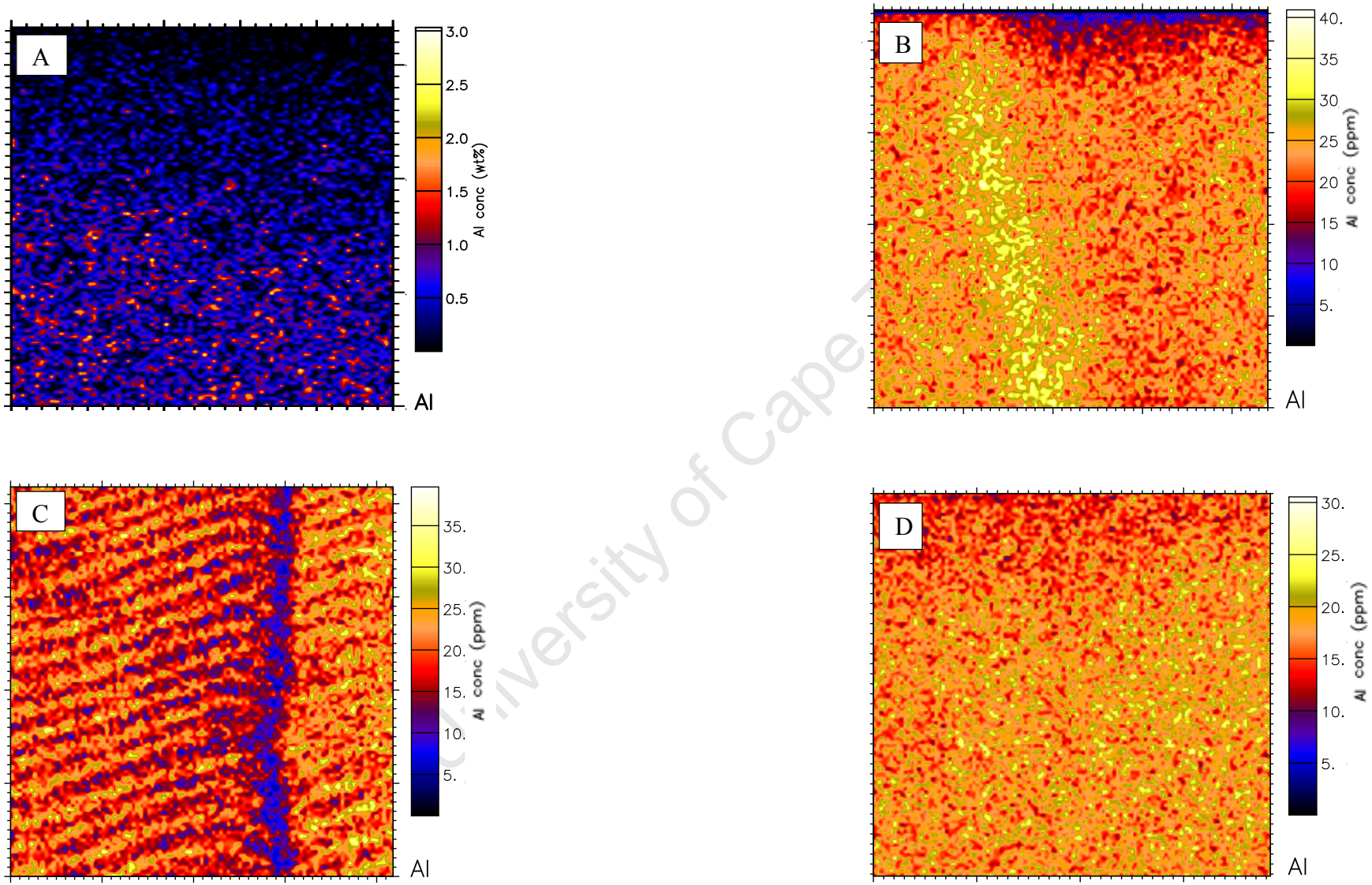

Figure 4-4 Comparative analysis of Al in the scales of the fish *Pomadasys kaakan* (A), *Lithognathus mormyrus* (B) the *Lutjanus gibbus* (C) and *Pinjalo pinjalo* (D). The scanning area is 400 µm × 400 µm. Note that the concentration of Al in *P. kaakan* is in % mass/mass.

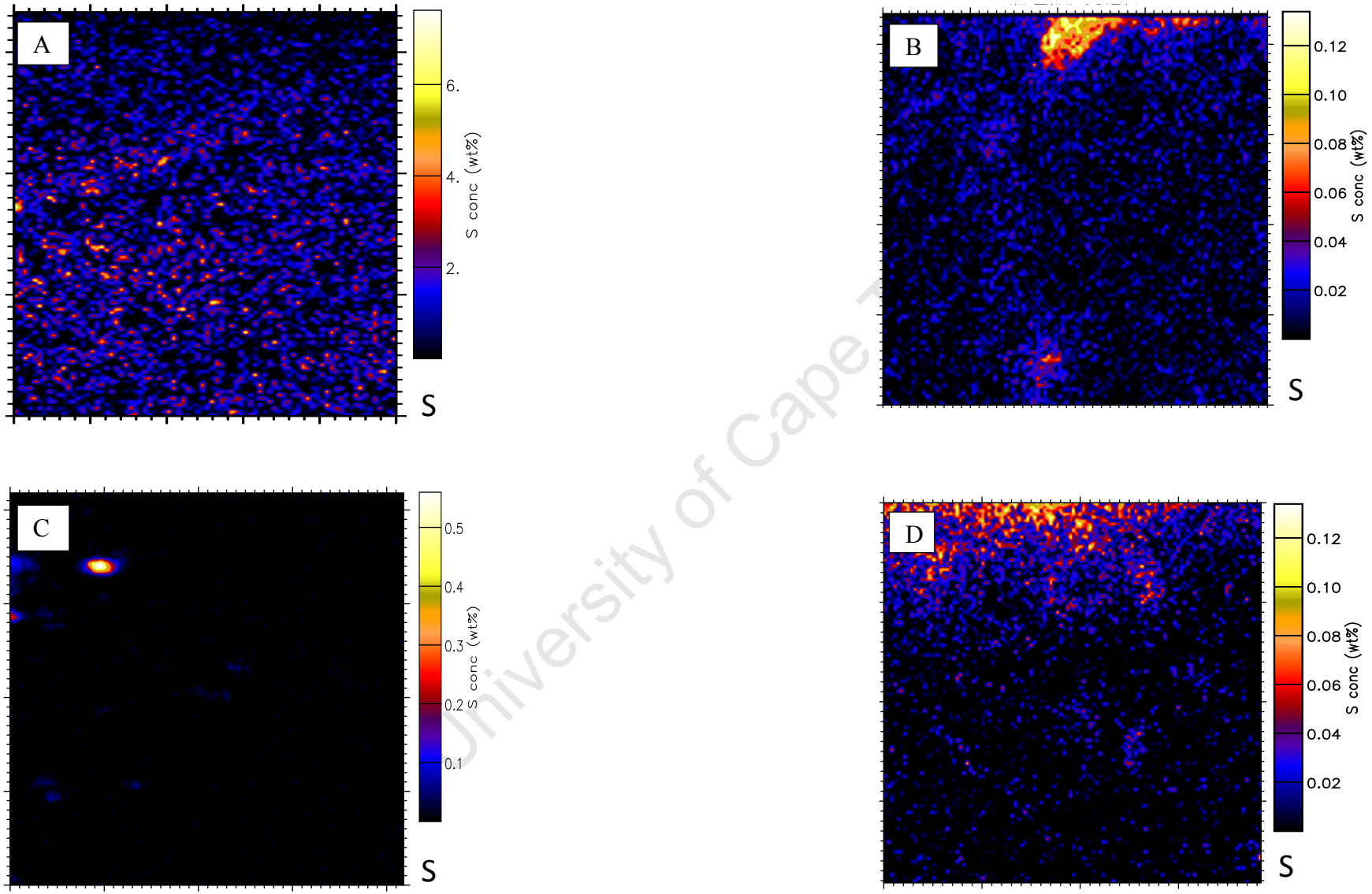

Figure 4-5 Comparative analysis of S in the scales of the fish *Pomadasys kaakan* (A), *Lithognathus mormyrus* (B) the Lutjanus gibbus (C) and *Pinjalo pinjalo* (D). The scanning area is 400 μm × 400 μm.

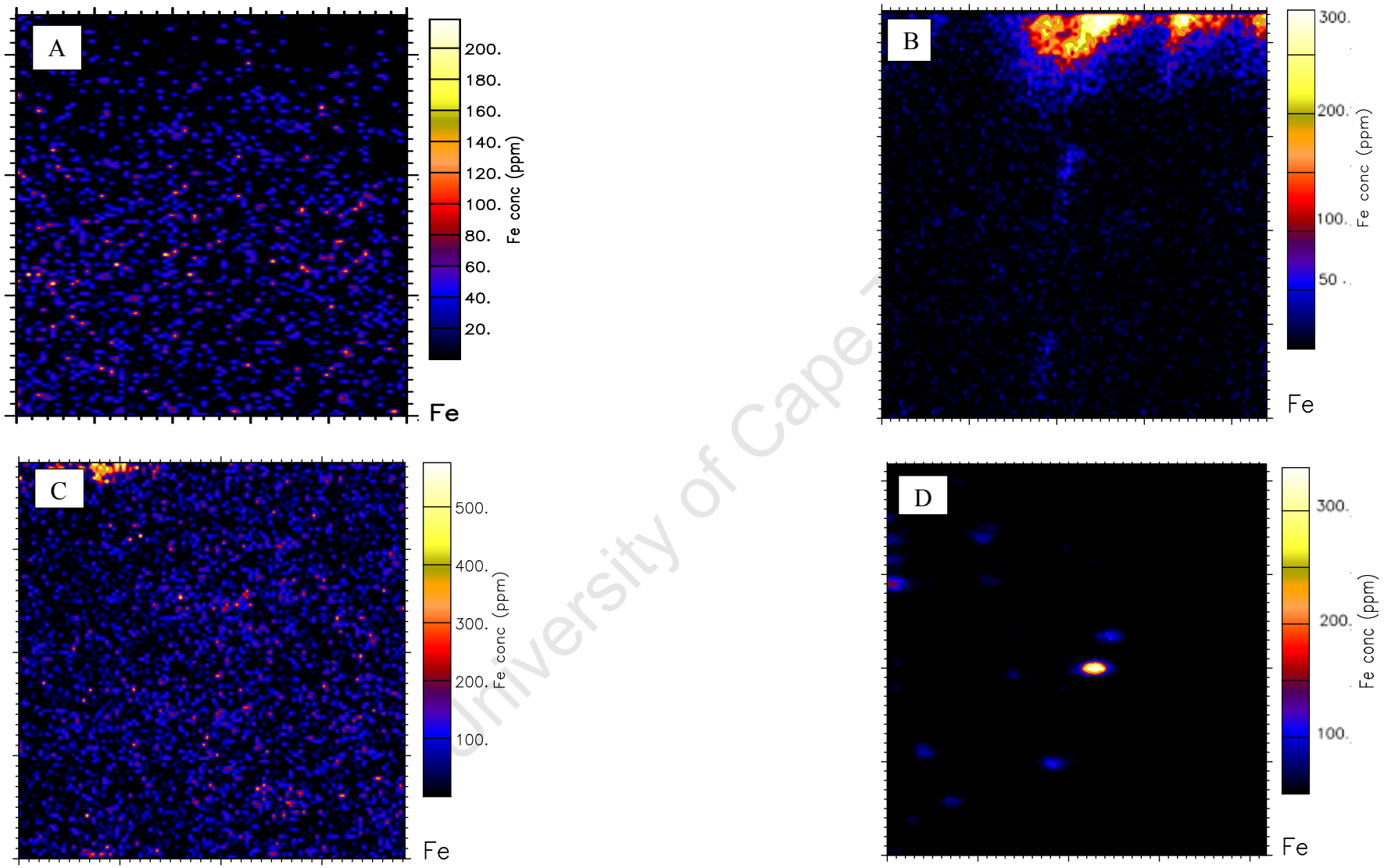

Figure 4-6 Comparative analysis of Fe in the scales of the fish *Pomadasys kaakan* (A), *Lithognathus mormyrus* (B) the *Lutjanus gibbus* (C) and *Pinjalo pinjalo* (D). The scanning area is 400 μm × 400 μm.

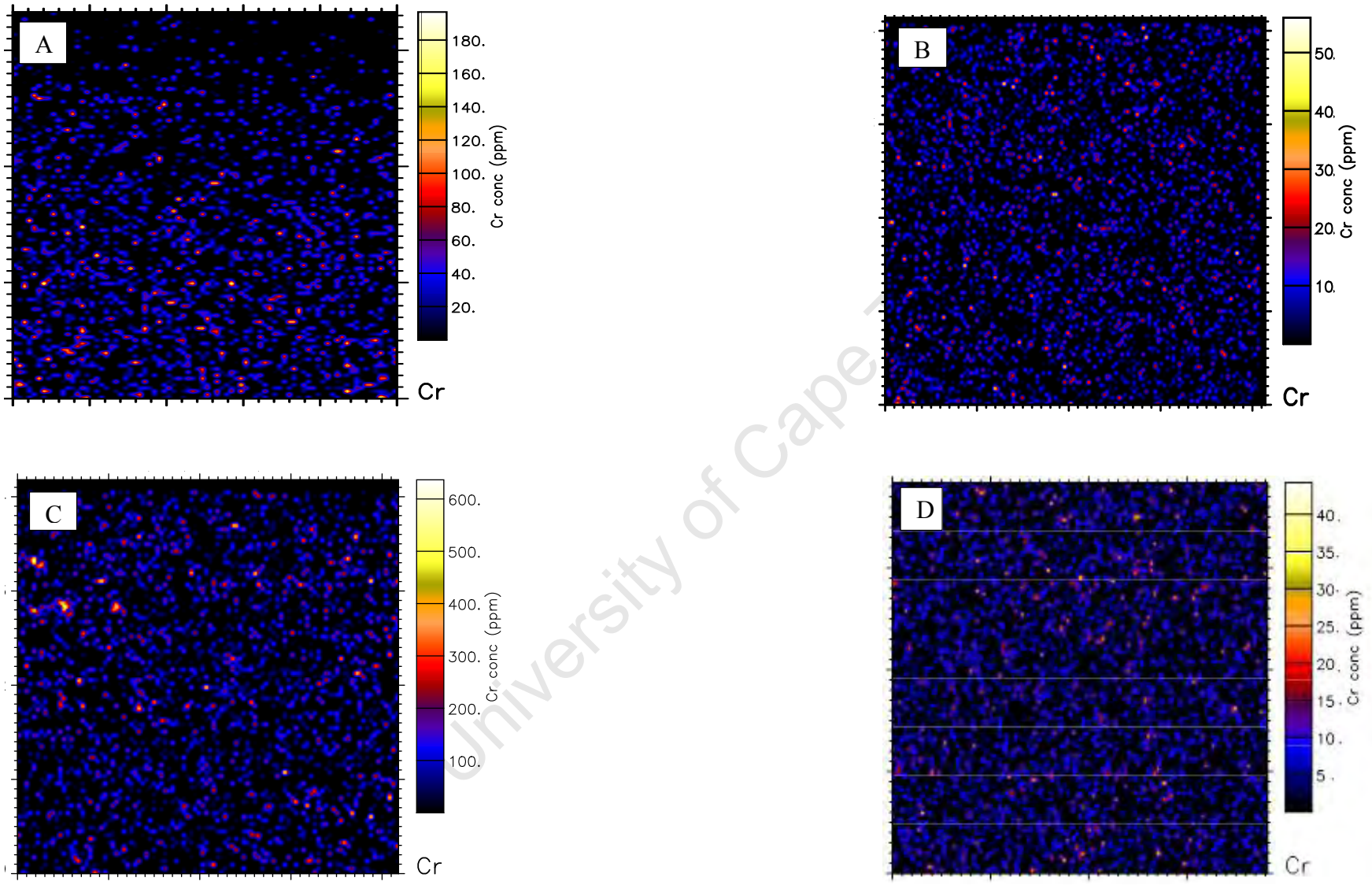

Figure 4-7 Comparative analysis of Cr in the scales of the fish *Pomadasys kaakan* (A), *Lithognathus mormyrus* (B) the *Lutjanus gibbus* (C) and *Pinjalo pinjalo* (D). The scanning area is 400 µm × 400 µm.

Chapter Five
5 Results: Growth patterns of fish scales

5.1 Introduction

In this chapter the elemental quantification of the incremental growth patterns in the fish scale is discussed. Although these patterns have been described mathematically, the aim of this chapter is to quantify the patterns chemically.

5.2 Quantification of growth patterns

The growth pattern of fish scales is characteristically anisotropic (Smlyar & Bromage, 2004). More so, the respective growth patterns are at times also intermittent, convergent, divergent, continuous or discontinuous. Because of anisotropy, the fish scale growth has previously been described in fuzzy mathematical terms (Smlyar & Bromage, 2004). This Smlyar & Bromage model does not take into account the elemental chemical compositions displayed in these types of growth pattern. The Smlyar & Bromage model has been extensively applied for scales of fish, contributing to environmental data bases and information about the life history of fishes based on the work of Pepin (1991) and Friedland (1998). Incremental patterns of growth can be used for environmental purposes such as pinpointing pollution events by examining metal concentrations in fish scales.

The growth of fish scales results in rhythmically constructed rings, termed circuli, which are demarcated by annuli (**figure 5.1**). The regions between two circuli are termed incremental bands (IBs) which exhibit characteristically anisotropic growth. This is important as it encrypts events, such as pollutants in the ambient water, into the fish scales.

Each analysis was repeated five times (n=5). Only the carbon mass percentage was used in this evaluation.

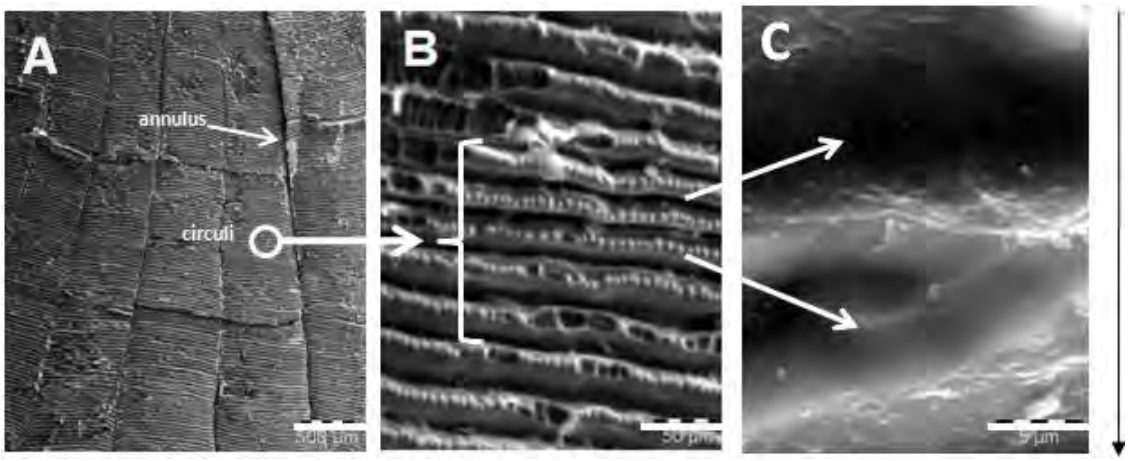

Figure 5-1 Original scanning electron micrographs of the fish scale of *Pomadasys kaakan*. In A the annuli and circuli are indicated (bar equals 500 µm). The frontal growth and the incremental band (IB) are shown in B (bar equals 50 µm). In C are shown the incremental band and the frontal growth on a smaller scale to emphasize the size (bar equals 5 µm). The arrow indicates the direction of growth. In B the complete and disrupted circulus is observable.

In **figure 5.1**(**A**) the circuli and annuli are shown. In (**B**) the curculi are shown at a higher magnification. In (**C**) the incremental band and the frontal growth are shown on a higer magnification (smaller scale) to emphasize the size of the band and the circulus.

To provide a quantitative description of variation in growth over time, a discrete conceptual model based on the fuzziness of anisotropic growth has been developed by Smolyar & Bromage (2004). Various transverse growth patterns (**figure 5.2**), such as discontinuous (**#1**) or continuous (**#2** to **#5**), which may be convergent (**#2** to **#4**) or divergent (**#5**), have been proposed (Smolyar & Bromage, 2004). As this model is purely mathematical, it does not address the effects of various factors.

These factors are:

1) The elemental concentration distributions of trace elements present in the matrix and if these distributions affect those of the major elements;

2) The growth characteristics within the incremental band, that is, as the IB1 is traversed from the preceding circulus to the succeeding circulus;

3) The effect of circulus width on IB size and growth characteristics in that area;

4) The position in terms of the gates (a discontinuation of the growth pattern) of the IB and in terms of distance from the demarcation;

5) For continuous growth (**#2** to **#5**), for which the composition should be statistically similar. Furthermore, the effects of exogenous factors, such as (pollution) events that occurred during the fish life history, could be detailed. These factors can be quantified in terms of the chemical composition as they are fundamentally of a chemical nature.

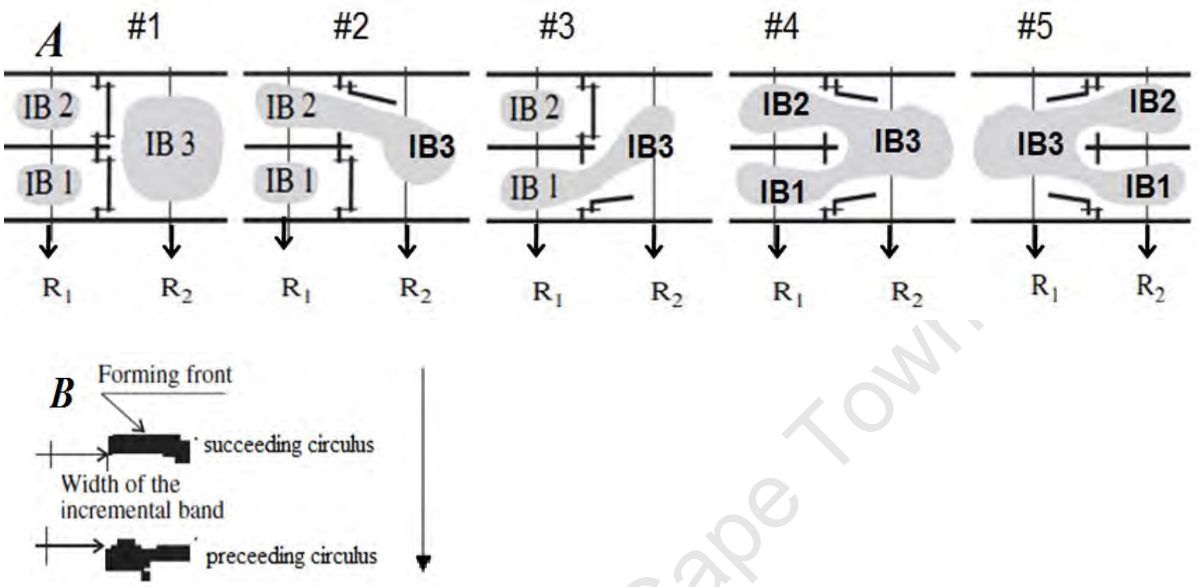

Figure 5-2 Models of the various anisotropic growth patterns (A) of the fish scale represented as a relay net-work of incremental bands (IBs), adopted from (Smolyar & Bromage, 2004). R_n are transects. The arrows indicate the direction of growth. B show the model of the incremental band used in this study.

5.3 Results

Pattern **#1** in **figure 5.2** shows that the carbon composition of IB1 and IB2 cannot be related to that of IB3 ($p<0.05$ in both instances) different and that the composition of IB1 is not the same as the composition of IB2 ($p<0.05$) significantly differ. In **#2**, the growth pattern assumes continuity between concentrations of IB2 and IB3 and hence $p>0.05$. However, $p<0.05$ when comparing the concentrations of IB1 and IB2 and also for IB1 and IB3. For #3, the continuity between IB1 and IB3 is assumed and the concentrations should be similar ($p>0.05$), but not for IB1 and IB2 ($p<0.05$) and for IB1 and IB3 ($p<0.05$).

The patterns **#4** and **#5** are both representative of a continuous growth pattern and $p>0.05$ for all comparisons.

The elemental concentrations (c), as % m/m, are defined as c_i^j, for $i = \{KRT, CCB, HAP, ALM, T\}$, where T is the total concentration of the element in the matrix, and $_j = \{C, O, N, P, S, Ca, Al\}$. N is found only in the keratin, hence c_{KRT}^N can be used to determine the percentage composition of KRT in the matrix. The concentrations of the other elements C, O, and N, in keratin that is c_{KRT}^C, c_{KRT}^O and c_{KRT}^N can then be calculated (Tang *et. al.*, 1997). Sulphur (S), possibly a pollutant, environment may then be calculated by difference ($c_T^S - c_{KRT}^S$). Similarly, the percentage composition of the components of HAP can be calculated from c_{HAP}^P , since P is only present in HAP and from this concentration c_{HAP}^O and c_{HAP}^{Ca} can be calculated. Also the component percentage concentration of ALM can be determined from the aluminium concentration, c_{ALM}^{Al}, and afterwards c_{ALM}^O can be calculated. Since O is not considered a pollutant, it can be determined by difference ($c_O^T - c_{KRT}^O - c_{ALM}^O - c_{KRT}^O$) and afterwards c_{CCB}^C and c_{CCB}^{Ca} can be calculated.

These calculations can now be applied to the various incremental bands, IB_n. In the demarcation of IB_n, that is, between the initial growth (and of the preceding circulus), to the frontal growth (beginning of the succeeding circulus), it is assumed that the chemical compositions, based on the C % m/m, of the circuli are similar to each other, but markedly different from the chemical composition of the IB. This is shown in **figure 5.3**. Hence, the growth characteristics of component c_{KRT}^C in the IB area are conceived as a saddle region and for the purpose of this study the asymmetric double sigmoidal function (Mitchell, 1997) is used to determine the length of the IB region. This function has two maxima (high C % m/m of the circuli, which consists mostly of KRT) and a region (in µm) where the composition of c_{KRT}^C does not change drastically (at the 95% confidence level).

The asymmetric double sigmoidal function is expressed by the equation below:

$$c_{KRT}^C = k_1 + \frac{k_2}{1+exp\left(-\frac{d-k_3}{k_5}\right)}\left(1 - \frac{1}{1+exp\left(-\frac{d-k_4}{k_6}\right)}\right) \qquad (5.1)$$

where c_{KRT}^C is the concentration and d the distance, k_i are constants determined by the fit to the data. The constraints to the equation are k_i: $i \neq 0$; $i \varepsilon N$. The growth patterns are transverse to the growth direction of the fish scale and hence to the frontal movement. To verify whether two chemical concentrations are statistically different, a value for $p<0.05$ was chosen because is very commonly used in biology.

The values of i, σ, the 95% confidence limits (CL) and p for k_i are given in **table 5.1**. All values are significant (p<0.05).

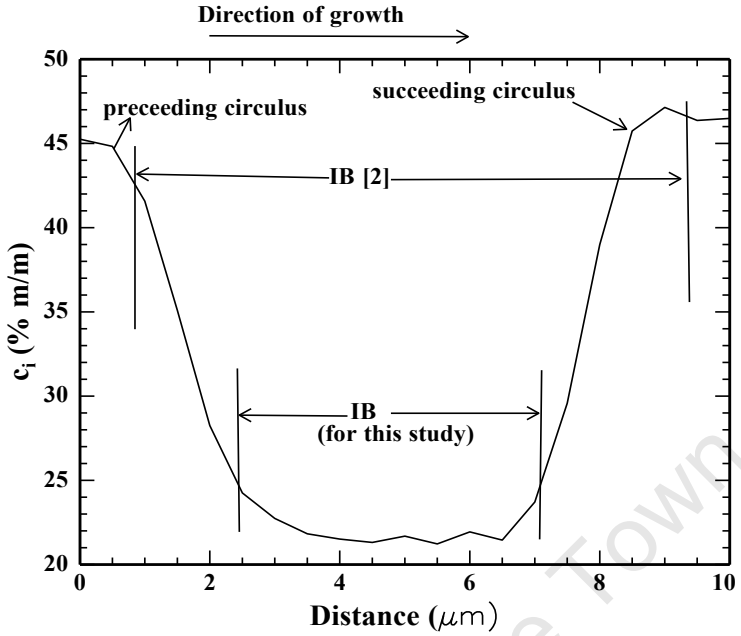

Figure 5-3 A schematic representation of the incremental band (IB) used in this study. The IB for the mathematical conceptual model (Smolyar, 1997) is also indicated. ci is the concentration as % m/m of the component used to demarcate the IB. The incremental band is based on the double sigmoidal function with two maxima at distance 0 μm and 9 μm.

The statistical evaluation of the parameters contained in **equation 5.1** that was used for the determination of the incremental band area, is given in **table 5.1**. The incremental band region was found to be 8 μm ± 3 μm.

The annuli and circuli are indicated in **figure 5.1** (**A**). The frontal growth and the incremental band (IB) are shown in (**B**). Disruptions in the structure of the circuli are visible. Furthermore, granular structures are located on the circuli. These granular structures have the same chemical composition and consist mostly of KRT and were not present in the areas where there was structural disruption.

Table 5-1 Statistical evaluation of the parameters of equation 5.1 used to calculate the region distance of the incremental band. The concentration of C (% m/m) in the matrix component used was for c^{C}_{KRT}. σ is the standard error and CL is the confidence limits.

k_i	Value	σ	95% CL		p
1	47.31	0.49	46.28	48.33	<0.001
2	-32.56	0.73	-34.09	-31.03	<0.001
3	4.84	0.03	4.78	4.90	<0.001
4	6.02	0.07	5.87	6.17	<0.001
5	0.57	0.05	0.46	0.67	<0.001
6	0.25	0.03	0.19	0.31	<0.000

Furthermore, the chemical compositions of the granule and the inter-granular areas were significantly different, 85% and 92% KRT respectively with $p<0.05$. For this reason the region selected for the evaluation of equation 1 was from the inter-granular area to the preceding circulus to the inter-granular area of the succeeding circulus.

The **figure 5.1** shows the incremental band and the frontal growth on a smaller scale to emphasize the size correlation between the band and the circulus. The graphical representations of the PIXE, SEM and BS data (energy and counts), as spectra, are shown in **figures 5.4**, 5.5 and 5.6. The spectrum of the SEM data is shown in **figure 5.4** in the energy region 0 to 5 keV. The elements with X-ray emission energies greater than 5 keV are present in the fish scale matrix in parts per million ranges.

These concentrations are below the minimum detection limit of the technique and are therefore not shown. The energy region displayed is from 0 to 5 keV since the elements in the matrix with X-emission energy higher than 5 keV are present in the parts per million ranges which are below the detection limit of the technique. The data were quantified using the manufacturer's computational software (JEOL, Japan).

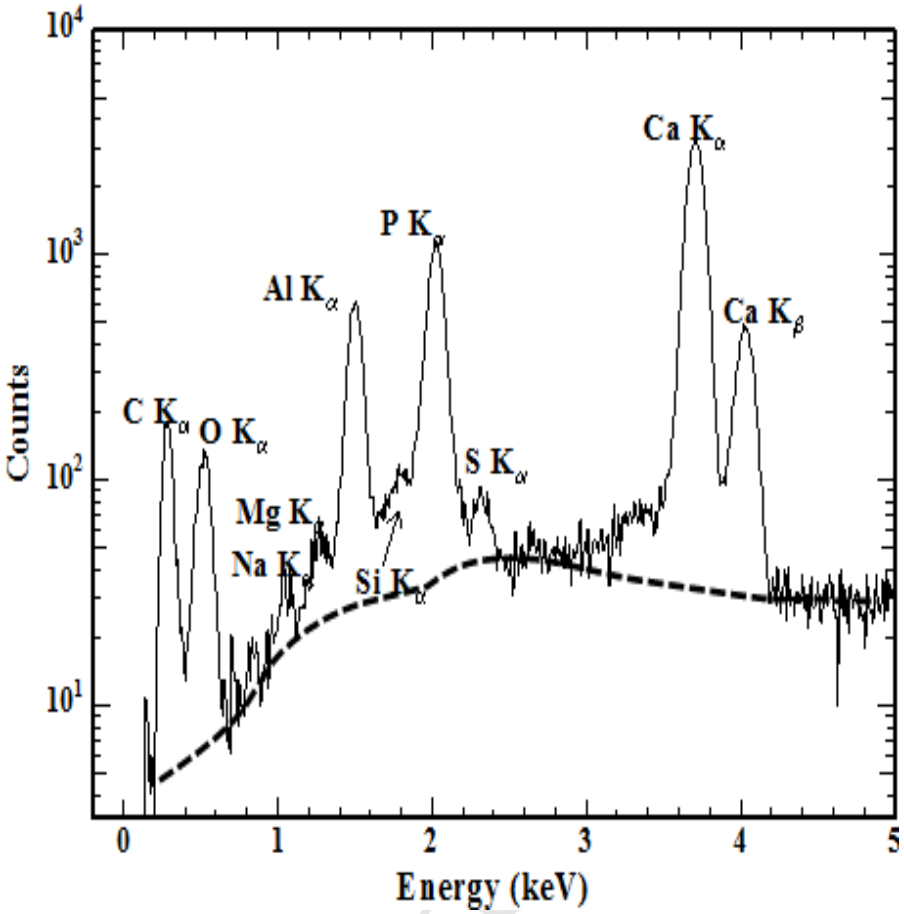

Figure 5-4 Graphic representations, as a spectrum, of the SEM X-ray emission. The fit to the data is represented by a continuous line, the data by ▪▪▪ and the background by —. The data are those accumulated over the entire region of 80 μm × 80 μm.

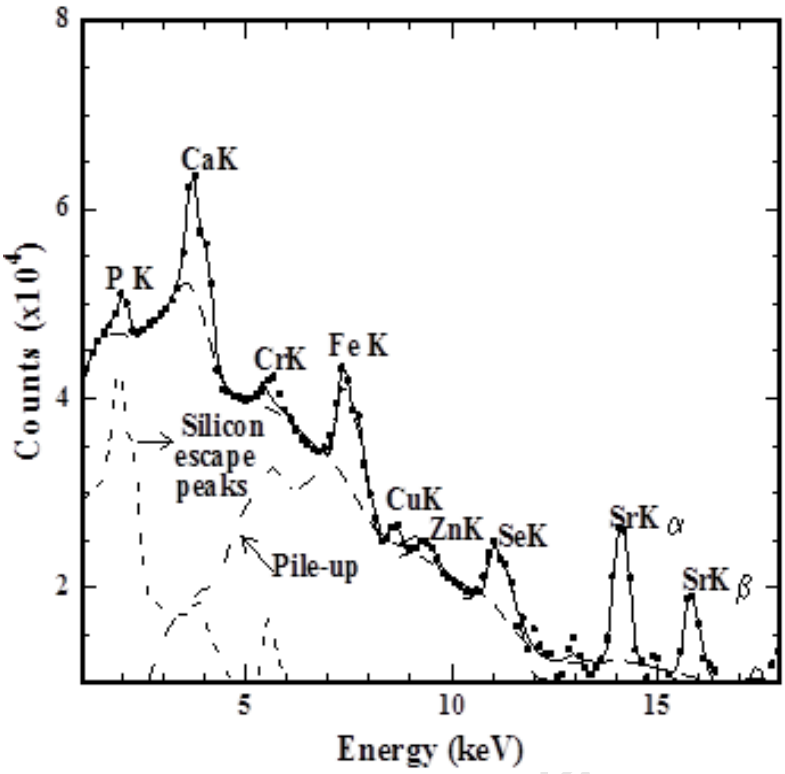

Figure 5-5 A spectrum of the PIXE , X-ray emission data obtained by proton bombardment. The fit to the data is represented by a continuous line, the data by ▪▪▪ and the background by - - -. The pile-up from the spectrum and the Si escape peaks are also shown. The data are those accumulated over the entire region of 80 μm × 80 μm.

In **figure** 5.5 the spectrum of the PIXE data is shown. Since the minimum detection limit of PIXE is in the parts per million ranges, the trace amounts of elements of high atomic number (Z > 0) can be seen. In **figure 5.6** the spectrum of the BS data is shown. The arrows indicate the positions of the elements when located at the surface of the specimen.

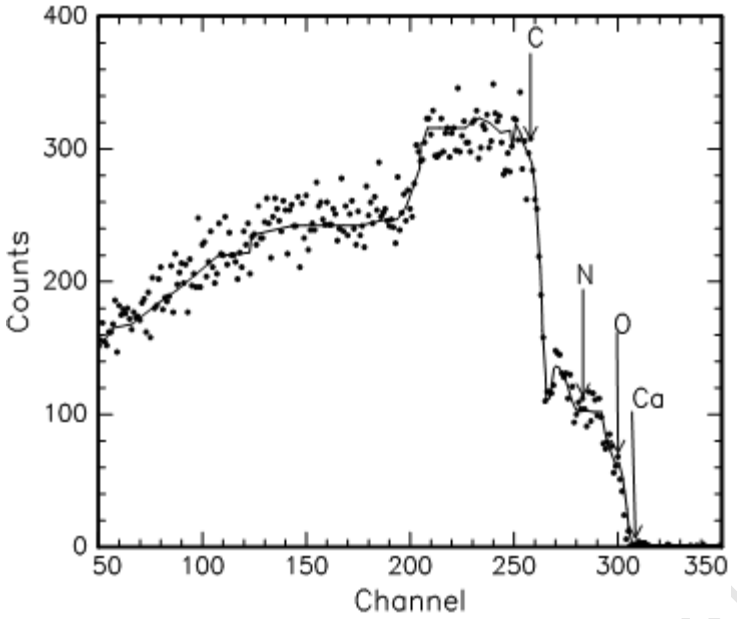

Figure 5-6 The spectrum of the BS data is shown. The fit to the data is represented by a continuous line, the data by ▪▪▪ and the background by —. The data are those accumulated over the entire region of 80 μm × 80 μm.

The QECD of Ca as a major matrix element, Cr as a trace element and Al, a contaminant, are shown in **figure 5.7**.

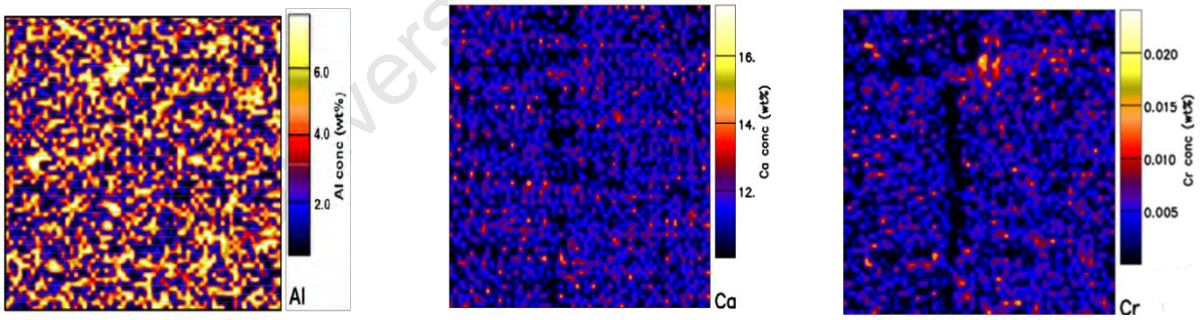

Figure 5-7 The micro-PIXE quantitative elemental concentration distributions (QECDs) of the elements Al, Ca, Cr and in the fish scale matrix. The discrete dark (black) areas in th e Ca and Cr region quantitative elemental concentration distributions represent the annuli. In the Al QECD the distribution of the element is homogenous. The data are those accumulated for the entire of 80 μm × 80μm.

From the quantitative elemental distribution of Ca it can be seen that Ca is predominantly present in the incremental band with less in the circuli and mostly absent from the annuli. The distribution of Cr is similar to that of Ca in the incremental bands but less so in the annuli. The QECD of Al is homogeneous throughout the matrix of the fish scale.

The average concentrations and minimum detection limits, based on PIXE and BS data, for the scanned area of other elements found in the matrix are given in **table 5.2**.

Table 5-2 Average concentrations and minimum detection limits (MDLs) based on PIXE and BS data, for the scanned area 80 μm × 80 μm, of the elements Ca, Cr and Al and other elements detected in the fish scale matrix. Values as mass per mass are indicated in parts per million (ppm). The other values are in ppm concentrations. ND indicates that the elements are present in concentrations below the detection limit.

El	Al	P	S	Ca	Cr	Mn	Fe	Ni	Cu	Zn	Se	Br	Sr	Mo
Conc	36400	79900	50000	128000	52	208	20	29	ND	18	35	49	11500	ND
MDL	10000	285	83	500	2	17	17	26	13	17	24	13	83	35

For the incremental band area the data obtained could be fitted with the saddle function. This indicates that there is a marked difference in chemical composition between that of the area of the circulus and that in the incremental band. It was also found that in the regions of the circuli, where structure disruption occurred, and the incremental band area is smaller (see **figure 5.1B**). However, the chemical composition demarcation still exists. There is no significant difference between keratin composition of the annuli and the circuli.

Most noticeably, the degree of aluminium incorporated in the annuli and circuli is nearly an order of magnitude lower than the aluminium incorporated into the IBs. For growth pattern **#1** (discontinuous growth), the chemical compositions of IB1 and IB2 are not significantly different and these compositions differ significantly from IB3. Thus, the growth pattern of #1 is applicable. For **#2** the compositions of IB2 and IB3 should not differ significantly as these two areas represent a continuum. This is however not the case and hence the growth pattern is not applicable.

For **#3** the compositions of IB1 and IB3 should also not differ significantly as these two areas represent a continuum. This is however not the case and hence the growth pattern is not applicable. In the case of **#4** the average chemical composition of IB1 and IB2 should not differ from that of IB3. This is however the case and hence the growth pattern is applicable. For **#5** the average chemical composition of IB1 and IB2 should not differ significantly from that of IB3; since this is the case, the growth pattern is applicable.

For the purpose of this study the incremental band region (**figure 5.1B**) was different from the fuzzy model in that in this conceptual model it was based on the frontal movement from the edge of the preceding forming front to the edge of the succeeding

forming front. Thus, the area of the succeeding annulus was incorporated into the model. As indicated in **table 5.2**, the chemical compositions of KRT in the annulus and the incremental band are vastly different and cannot be incorporated into a chemical model.

5.4 Discussion

In this study it was shown that the mathematical model for the anisotropic growth in fish scales can to an extent be correlated with the chemical composition model given in **table 5.3**.

Furthermore, the incremental band structure is confined to the area in between two circuli and not from the forming front of the preceding circulus to the forming front of the succeeding circulus.

The mathematical function presented in 5.1 allows us to make some comparisons between the different structures of the fish scales. It was found that the anisotropy pattern of the elemental distribution in fish scale results in a description growth in two dimensions and can be described as fuzzy.

The incremental pattern of growth of the fish scale shows a unique combination of useful features. Fish scales can easily being accessed and their preparation for analysis is quite simple. They can thus be used to report on the life history of both the fish and the environment (Pepin, 1991; Friedland, 1998 & Guambe *et al.,* 2012).

The similarities between fish scale incremental patterns and other such patterns from diverse biological samples were discussed by (Smolyar and Bromage, 2004):

The incremental bands of different incremental patterns represent one cycle of growth. The length of incremental band is a measure of the growth rate of the incremental pattern.

A growth rate of incremental patterns was found as a function of internal factors. Incremental patterns may therefore be used in identifying the growth-rate variability as has been applied in the fish scales of *Pomadasys kaakan*, the javelin grunter, in the present work.

The structure of incremental band can be used as a source of diagnostic information about events in the life history of incremental patterns of fish.

This work identifies differences in chemical composition between the area of the circulus and the area of the incremental bands due to the anisotropic pattern of growth of the fish scale.

In the region of the circuli where disruption of pattern occurs the incremental band area is smaller and chemical composition demarcation still exists.

The composition of keratin of the annuli and circuli was slightly different. However, the degree of incorporation of aluminium into the annuli and circuli is lower than the aluminium incorporated into the IBs. In chapter 3, aluminium was identified as a major pollutant in the fish scale of *Pomadasys kaakan*. In the present section the values of aluminium oxide (Al_2O_3) found in the incremental bands are shown in the **table 5.3**. This implies that Al is incorporated more strongly in the IB than in the circulus.

The growth pattern #1 (discontinuous growth) and the chemical composition of IB1 and IB2 are not significantly different and slightly differ with the IB3.

It was found that the growth of fish scales is anisotropic and can be correlated with the chemical composition of the elements. However the continuous divergent growth pattern cannot be accounted for. More so, the incremental band structure is confined to the area in between two circuli and not from the forming front of the preceding circulus to the forming front of the succeeding circulus.

Table 5-3 Matrix component compositions and standard deviations in the compositions (σ), based on SEM, PIXE and BS data, of keratin (KRT), hydroxy-apatite (HAP), calcium carbonate (CCB) and aluminum oxide (ALM) found in the incremental bands, the circuli and annuli. The composition is expressed in percentage mass per mass. p_{IBn} values are also given. The p value for the annuli and circuli, $p_{a,c}$ is also given.

#	IB	KRT % ± σ	p_{IBn}	HAP % ± σ	p_{IBn}	CCB % ± σ	p_{IBn}	ALM % ± σ	p_{IBn}
1	IB1	26.1 ± 0.4	$p_{1,2}$=0.03	42.2 ± 0.9	$p_{1,2}$=0.006	20.3 ± 0.4	$p_{1,2}$=0.002	12.5 ± 0.3	$p_{1,2}$=0.006
	IB2	25.3 ± 0.7	$p_{2,3}$<0.001	36.4 ± 0.9	$p_{2,3}$<0.005	27.2 ± 0.9	$p_{2,3}$=0.004	11.4 ± 0.4	$p_{2,3}$=0.003
	IB3	20.1 ± 0.5	$p_{1,3}$<0.001	40.5 ± 1.2	$p_{1,3}$<0.001	24.6 ± 0.7	$p_{1,3}$<0.001	14.8 ± 0.6	$p_{1,3}$=0.005
2	IB1	12.4 ± 0.4	$p_{1,2}$<0.001	38.1 ± 0.8	$p_{1,2}$<0.001	36.1 ± 0.8	$p_{1,2}$<0.001	12.6 ± 0.4	$p_{1,2}$<0.001
	IB2	22.5 ± 0.8	$p_{2,3}$=0.006	32.8 ± 0.9	$p_{2,3}$<0.001	30.4 ± 0.7	$p_{2,3}$=0.006	14.3 ± 0.4	$p_{2,3}$=0.002
	IB3	25.4 ± 0.7	$p_{1,3}$=0.007	30.2 ± 0.7	$p_{1,3}$=0.007	29.2 ± 0.8	$p_{1,3}$<0.001	16.2 ± 0.7	$p_{1,3}$=0.002
3	IB1	14.3 ± 0.7	$p_{1,2}$=0.002	37.1 ± 0.9	$p_{1,2}$=0.006	38.1 ± 1.0	$p_{1,2}$=0.003	10.9 ± 0.4	$p_{1,2}$=0.005
	IB2	22.8 ± 0.8	$p_{2,3}$=0.006	35.7 ± 1.1	$p_{2,3}$<0.001	26.7 ± 0.7	$p_{2,3}$<0.001	14.8 ± 0.4	$p_{2,3}$<0.001
	IB3	27.4 ± 0.7	$p_{1,3}$=0.005	26.8 ± 0.9	$p_{1,3}$=0.003	29.1 ± 0.9	$p_{1,3}$=0.006	16.7 ± 0.6	$p_{1,3}$=0.004
4	IB1	43.7 ± 0.4	$p_{1,2}$=0.009	22.3 ± 0.8	$p_{1,2}$=0.002	19.5 ± 0.8	$p_{1,2}$=0.002	14.5 ± 0.4	$p_{1,2}$=0.002
	IB2	36.1 ± 0.7	$p_{2,3}$=0.005	20.4 ± 0.9	$p_{2,3}$<0.001	21.4 ± 0.8	$p_{2,3}$=0.002	22.1 ± 0.5	$p_{2,3}$=0.006
	IB3	42.8 ± 1.1	$p_{1,3}$=0.003	28.4 ± 0.7	$p_{1,3}$=0.006	10.1 ± 0.4	$p_{1,3}$=0.006	18.7 ± 0.6	$p_{1,3}$<0.001
5	IB1	42.6 ± 0.8	$p_{1,2}$=0.003	25.4 ± 0.9	$p_{1,2}$=0.006	15.6 ± 0.8	$p_{1,2}$=0.004	16.4 ± 0.4	$p_{1,2}$<0.001
	IB2	36.3 ± 0.7	$p_{2,3}$=0.004	22.4 ± 0.7	$p_{2,3}$=0.008	23.9 ± 0.4	$p_{2,3}$=0.003	18.4 ± 0.4	$p_{2,3}$=0.003
	IB3	38.4 ± 0.8	$p_{1,3}$=0.004	29.1 ± 0.4	$p_{1,3}$=0.006	17.9 ± 0.4	$p_{1,3}$=0.003	14.6 ± 0.3	$p_{1,3}$=0.002
Annuli		96.2 ± 1.5	$p_{a,c}$=0.45	0.6 ± 0.2	$p_{a,c}$=0.150	1.2 ± 0.5	$p_{a,c}$=0.770	2.0 ± 0.6	$p_{a,c}$=1.00
Circuli		95.8 ± 1.2		0.9 ± 0.2		1.3 ± 0.6		2.0 ± 0.5	

Chapter Six
6 Discussion and Recommendations

6.1 Discussion

The major findings of this work concern both the chemical nature of fish scales and also the usefulness or otherwise of ion beam techniques for analysing them. As hypothesized, the small-scale chemical inhomogeneities in the fish scale matrix could be characterized. More so, the minimum detection limits achieved were in the order of parts-per-million concentration ranges.

6.1.1 Chemichal nature of the fish scales

Fish scales of four species found in different aquatic environments were analyzed. Some of these environments contain high concentrations of metal pollutants (as ions) while others did not contain metal ion pollutants present in measurable quantities.

In the instance of *P. kaakan*, from the linear traverse analysis performed across the scale, illustrated in **figure 3.10**, the growth of the fish scale begins with keratin. Calcium carbonate and hydroxyapatite are only incorporated into the scale after a growth in length of about 40 μm. As an example, in the growth of length 250 ± 2 μm, measured over a width of 2 μm (**figure 3.10**), the concentrations (as mass per mass) of 1.1% of Ca and 0.4% of P are present in the fish scale. Based on the chemical composition of hydroxyapatite, the ratio of the concentrations of Ca to P is 2:1. This means that for 0.4% of P there should be 0.8% of Ca. Since Ca constitutes 40% of hydroxyapatite, the concentration of hydroxyapatite at this distance is 2%. However, there is 1.1% of Ca present thus 0.3% of calcium remains. This calcium therefore is contained in calcium carbonate. The calcium composition in calcium carbonate is 40%. Hence the remaining 0.3% of calcium yields 0.8% calcium carbonate. The amount of Al present at this growth is 0.3%. It was assumed that the Al is present as aluminum oxide. This yields a composition of Al_2O_3 of 0.6%. Keratin would then constitute the remainder (96.6%) of the matrix composition. Similarly at a distance of 340 μm the keratin compositon would only be approximatelly 78%. However, aluminium is not normally present in the fishscale matrix in the percentage mass per mass concentration range. Based on the data in **Table 5.3**, the total composition of keratin, hydroxyapatite and calcium carbonate in the matrix are respectively 34.4 ± 0.8%, 36.8 ± 1% and 29.2 ± 0.8%, when excluding aluminium oxide.

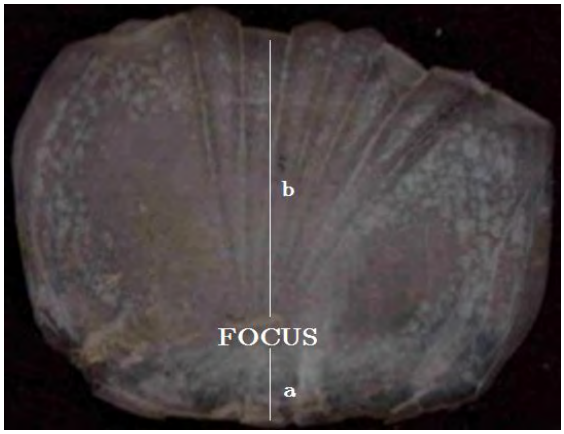

Figure 6-1 Illustration of the fish scale of *Pomadasys kaakan* that was scanned and the posterior field, focus and the anterior field where "a and b" represent the growth lengths from the focus.

The growth-lengths **a** and **b** (**figure 6.1**) of the *P. kaakan* fish scale occurred both over a period of about (12 ± 1) months. As these growth lengths differ significantly, it cannot be assumed that these growth lengths are linear with time. These can be rather assumed to be either logarithmic or exponential. Futheremore, once the pollutant containing effluent reaches the river water it is immediately diluted by the river water volume. In addition, the river flows constantly and thus the time the fish is exposed to toxic effluents depends on the flow and on the marine tide. During high tide the river water flow is slower than during low tide. Hence at high tide the fish will be exposed to the pollution for a longer time than during low tide. This is also only applicable should the fish remains static for a considerable period of time. The latter is however unlikly.

In the case of *L. mormyrus*, only a growth length distance of 20 μm (**figure 4.2B**) consists primarily of keratin. The QECD of P is given in (**figure 4.3B**). In the growth length of 20-60 μm the concentrations of hydroxylapotite and calcium carbonate are increased to approximately 31% and 26% respectively. For the remainder of the growth length of the scale these concentrations increased to 37% and 34% respectively. Aluminum concentration is in ppm ranges, (**figure 4.4B**) and aluminum oxide is approximately 40 ppm. From (**figure 4.3B**) it is evident that hydroxylapotite and calcium carbonate concentrations are relatively higher in the annulus.

In the case of *L. gibbus* the hydroxylapotite and calcium carbonate concentrations are relatively lower in the circule than in the rest of the fishscale matrix (**figure 4.2C** and **figure 4.3C**). The concentration of aluminum (**figure 4.4C**) is also is ppm ranges. In the case of *P. pinjalo* hydroxylapotite and calcium carbonate are present in the fish scale matrix (**figure 4.2D** and **figure 4.3D**). However, in the first 100 μm of

growth length, the concentration of calcium is linear with the concentration of P. In this region the calcium concentration is 12% wheres as the phosphorus concentration is approxixately 8% (**figure 4.D**).

In the species *Pomadasys kaakan* the Fe concentration is approximately 40 ppm, whereas in the species *Lithognathus mormyrus* and *Pinjalo pinjalo* the Fe concentration is well below 40 ppm (approximately 20 ppm). In contrast, the Fe concentration in the scale of *Lutjanus gibbus* that was caught in the Maputo estuary, where a lot of ship wrecks are found, is approximately 150 ppm. More so, this concentration occurs throughout the fishscale matrix, which is not the case with the fish scales of the other species. It is therefore evident that that *L. gibbus* was present in this environment throughout its life span.

The concentration of Cr (**figure 4.7A, B, C** and **D**) in the fish scale of *P. kaakan* is approximately 40 ppm, for *L. mormyrus* is approximately 15 ppm, in *L. gibbus* the Cr concentrations is approximately 150 ppm. The Cr concentration in *P. pinjalo* is about 7 ppm. For *L. gibbus* the relatively higher concentration of Cr corresponds to the relatively high Fe concentration might be due to the presence of shipurecks in the aquatic environment. More so, the quantitative elemental concentration distributions of Fe and Cr are homogeneous which could imply that the fish spent most of the year of life in this environment and /or that pollution by Fe and Cr is more or less constant.

Futhermore, it can be implied that pollution of the natural environment might not have occurred continuously, as with *L. gibbus*. Hence there was no continuous incorporation of pollutants into the fishescale matrix. Only the specific areas contained the polluting heavy metal ions. In addition, the incorporation of the pollutants into the fish scale matrix only occurs while the fish is present in the polluted aquatic environment. This is shown in **figure 4.6 (page 94)**.

This thesis examined the potential for using IBA techniques for pollution studies using fish scales. The results suggest that the time and duration of the pollution event can be determined using PIXE. Moreover, the percentage composition of any pollutant should be proportional to the total pollution the fish experienced throughout its time in the aquatic environment.

Furthermore, the distributions and concentrations of elements such as Al, S, Fe and Cr, which are not normally incorporated into the scale in measurable quantities, can be characterized because of the relatively narrow width of the beam of particles.

Growth regions can be discerned and the concentrations in these regions of the contaminants can be characterized. Comparative analysis of scales from different species of fish showed that both the distribution and the concentrations of a number of elements differ among species. Lastly, the presence of elements such as Al and Cr in the scales allows up to hypothesize that the fish had been exposed to pollutants in the environment in which they lived but the data presented in this thesis are not of the kind that can confirm this hypothesis. Methods for addressing this issue are discussed in section 6.2 below.

6.2 The advantages of PIXE techniques

6.2.1 High sensitivity

Compared to electron-based x-ray analytical techniques such as energy dispersive spectroscopy (EDS), commonly called scanning electron microscopy (SEM), PIXE offers better peak to noise ratios and consequently much higher trace element sensitivities, as seen in the spectra in chapter 5. Absolute sensitivity to a given trace element is dependent upon a number of factors, such as matrix composition, detector efficiency and overlap of peaks. PIXE has a resolution of approximately 1.5 μm. This resolution permits the characterisation and quantification of small size inhomogeneties. Furthermore, the minimum detection limits are in the order of 1 ppm concentration range.

6.2.2 Multi-element capability

Elemental analyses are performed for any element from sodium to uranium in a single spectrum on the NMP system. X-rays from elements of atomic masses lighter than sodium cannot be seen because these X-rays are absorbed in either the detector window, between the sample and the detector, or through any filters used. For trace element analysis, we choose a filter to attenuate the X-rays at the energies of the major elements allowing the detector to measure the trace elements with greater sensitivity. Usually these filters will cause insensitivity to higher elements, but will allow simultaneous analysis of any element above the filter's absorption edge.

Hence, in summary, the techniques allow very fine resolution, identification of amall quantities of an element, and simultaneous analysis of many elements.

6.3 Constraints to the use of PIXE in pollution studies

The instrumentation needed in theses analyses is costly (in the excess of USD 3 million) so it would be unlikely to be acquired only for studies such as this one. However, because of the versatility of a Nuclear Microprobe (NMP) facility, solid samples of various kinds, not only biological but also geological and archaeological as well as those used by arts conservators, medical researchers and others, can be probed to help answer questions of provenience, dating and authenticity.

The instruments require well trained dedicated technicians to oversee their use, and a qualified person to be responsible for the training of users. Furthermore, sample preparation is time-consuming and a person to assist with this should be available.

The actual process of scanning a sample is time-consuming: the duration of a single analysis is normally 2 hours per sample per demarcated area on the sample. The time taken to analyse the results of a single scan is dependant on the area of interest. However, the minimum time to completely characterize and quantify an area on the sample is about 2 hours.

The computing power is depending of the version of the software program GeoPIXE used. However, the latest version of the software allows more in depth characterization. Futhermore GeoPIXE is dependant on the software package IDL.

Only elemental analysis and not ionic analysis can be done. As examples, only the calcium atom, Ca, and not the ion Ca^{2+}, can be determined. Polyionic substances cannot be determined, especially where oxygen is present in the matrix.

So in summary because of all these constrains regarding a complex of machine, costs, and time nuclear methods are not recommended for simple analyse. But on the other hand this technique can provide a better interpretation of the QECDs.

6.4 Recommendations

It is difficult to envisage ion beam analysis being used in routine analyses of pollutants because of the cost and difficulty of the analyses. The data presented in this thesis show, however, that IBA is capable of providing some very useful results. In particular, there is potential for pinpointing the timing of pollution events, a feature that can be important forensically.

I therefore recommended that this project should be continued with the objective of calibrating elemental concentrations, particularly of pollutants such as Al and Cr, in the scales of one or more fish species. To attain this objective it will be necessary to perform the following types of experiments and other analyses. Most of the following will require laboratory experiments in which fish are grown under controlled conditions.

- Under laboratory conditions, ascertaining growth kinetics of fish scales of one or more species from birth until adulthood (at least one year) so as to correlate the time interval(s) of scale growth with season and the age of the fish. The matrix composition can then be determined for each growth interval.
- Ascertaining the relationship between concentrations and distributions of polluting elements in the environment and in scales of fish under laboratory conditions (i.e. bioaccumulation studies). Additional data may need to be generated on the effects on scale growth rates of these contaminants at toxic concentrations.
- It is necessary to grow fish in the lab at different concentrations of the trace elements of interest to relate concentrations in water to concentrations in scales and to find out how long it takes from first contamination until the pollutant can be seen in the scale.
- Because only scales need to be examined, the some fish can be used throughut the length of each experiment.

When these parameters have been determined then an environmental forensic profile can be established. Validation of such a profile can be used as a legal tool to assess pollution levels and more particularly, discrete pollutions events.

In this work it has been shown, by applying NMP techniques that fish scales contain elements bioaccumulated from the water in which they live. Furthermore, accumulated elements in fish scales are differentially distributed throughout the scale. Most importantly, PIXE can be used to quantify the distribution of elemental concentrations in fish scales at a sufficiently fine spatial scale to pinpoint differences in bioaccumulation over time. The fine-scale distribution of elements can be used to model growth patterns in fish scales and so determine the time interval during which the pollution occurred. With these quantifications of the distribution of elemental concentrations and growth patterns a forensic pollution profile can be established.

In summary:

- *The ease of access of the scale of fish for timing pollution studies.*

- *The advantage of using the scales instead of the organs is that in using the organs, the fish has to be killed and this would necessitate having more than one fish available for the study.*

- *In the techniques such as AAS and ICP-MS, the sample must be digested, that is the matrix integrity of the sample and the distribution of the elements in the scale would be lost.*

- *A cross-sectional analysis of the scale was done to show that the incorporation of the elements into the scale is homogeneous.*

- *Samples analysed in Heavy Ion ERDA must be very smooth. This is the main limitation when it comes to fish scales because they are generally not smooth. One cannot get reliable depth profiles from rough surfaces. If you try to make them smooth then you destroy the surface you want to analyse.*

- *Another problem is the sensitivity of the ERDA technique can vary from 0.1 to 1.0 atomic percentage. It is not much sensitive as PIXE (ppm). Beam damage can also be a problem when using heavy ions such as ERDA, which means we use a very low current to minimise this damage.*

- *This work can be used as a reference for further studies regarding to fish scale growth patterns and the incorporation of pollution events that occurred in the immediate environment.*

References

Abrahams, P.W. 2002, Soils: their implications to human health, *Science of the Total Environment*, vol. 291, pp. 1-32.

Addison, R.F. 1996, The use of biological effects monitoring in studies of marine pollution. *Environmental Reviews*, vol. 4, no. 3, pp. 225-237.

Agrawal, P., Mittal, A., Kumar, M. & Tripathi, S. 2008, "Mercury Exposure in Indian Environment due to Coal Fired Thermal Power Plants and Existing Legislations-a Review", *Indian Journal of Forensic Medicine and Pathology,* vol. 1, no. 2, pp. 41-46.

Alonso G., F. Casati, H. Kuno and V. Machiraju 2004, Web Services. Concepts, Architectures and Applications. Springer, Berlin.

Ahlberg, M. & Akselsson, R. 1976, "Proton-induced X-ray emission in the trace analysis of human tooth enamel and dentine", *The International Journal of Applied Radiation and Isotopes,* vol. 27, no. 5, pp. 279-290.

Ahmed, F.E. 2007. Assessing and managing risk due to consumption of sea food contaminated with microorganisms, parasites, and natural toxins in the US. *International Journal of Food & Technology*, vol.27, no. 3, pp. 243-260.

Aiuppa, A., Allard, P., D'Alessandro, W., Michel, A., Parello, F., Treuil, M. & Valenza, M. 2000, "Mobility and fluxes of major, minor and trace metals during basalt weathering and groundwater transport at Mount Etna volcano, Sicily", *Geochimica et Cosmochimica Acta,* vol. 64, no. 11, pp. 1827-1841.

Akagi, H., Castillo, E.S., Cortes-Maramba, N., Francisco-Rivera, A.T. & Timbang, T.D. 2000, "Health assessment for mercury exposure among schoolchildren residing near a gold processing and refining plant in Apokon, Tagum, Davao del Norte, Philippines", *Science of the Total Environment,* vol. 259, no. 1, pp. 31-43.

Akhter, M.S. & Al-Jowder, O. 1997, "Heavy metal concentrations in sediments from the coast of Bahrain", *International Journal of Environmental Health Research,* vol. 7, no. 1, pp. 85-93.

Al-Husaini, M. & Aquaculture, F. 2003, "Fishery of shared stock of the silver pomfret, *Pampus argenteus*, in the Northern Gulf; a case study", *Papers presented at the*

Norway-FAO Expert Consultation on the Management of Shared Fish Stocks: Bergen, Norway, 7-10 October 2002, no. 695, pp. 44-56.

Amaral, A.C.Z. & Jablonski, S. 2005. Conservation of marine and coastal biodiversity in Brazil. *Conservation Biology*, vol. 19, no. 3, pp. 625-631.

Anderson, D.M., Glibert, P.M. & Burkholder, J.M. 2002, "Harmful algal blooms and eutrophication: nutrient sources, composition, and consequences", *Estuaries and Coasts,* vol. 25, no. 4, pp. 704-726.

Anspaugh, L. 2008, "Environmental Consequences of the Chernobyl accident and their remediation: 20 years of experience Chernobyl: Looking back to go forward. Proceedings of the International Conference on Chernobyl, 6-7 September, 2005, Vienna, pp. 47-76.

Arthur, J.R. & Beckett, G.J. 1994, Newer aspects of micronutrients in at risk groups. New metabolic roles fro selenium, *Proceedings of the Nutrition Society*, vol. 53, pp. 615-624.

Assmann, W., Huber, H., Steinhausen, C., Dobler, M., Glückler, H. & Weidinger, A. 1994, "Elastic recoil detection analysis with heavy ions". *Nuclear Instruments and Methods in Physics Research Section B,* vol. 89, no. 1, pp. 131-139.

Attrill, M.J. & Depledge, M.H. 1997, "Community and population indicators of ecosystem health: targeting links between levels of biological organisation", *Aquatic Toxicology,* vol. 38, no. 1, pp. 183-197.

Avery, S.V. 1996, "Fate of cesium in the environment: distribution between the abiotic and biotic components of aquatic and terrestrial ecosystems", *Journal of Environmental Radioactivity,* vol. 30, no. 2, pp. 139-171.

Bailey, S.E., Olin, T.J., Bricka, R.M. & Adrian, D.D. 1999, "A review of potentially low-cost sorbents for heavy metals", *Water Research,* vol. 33, no. 11, pp. 2469-2479.

Baker, A., McGrath, S., Reeves, R. & Smith, J. C., 2000, "Metal hyperaccumulator plants: a review of the ecology and physiology of a biological resource for phytoremediation of metal-polluted soils", *Phytoremediation of Contaminated Soil & Water, Lewis Publishers Boca Raton, Florida USA.*

Bandeira, S.O., Paula e Silva, R., Paula, J., Macia, A., Hernroth, L., Guissamulo, A.T. & Gove, D.Z. 2002, "Marine biological research in Mozambique: past, present

and future", *AMBIO: A Journal of the Human Environment,* vol. 31, no. 7, pp. 606-609.

Banlaoi, R.C. 2005, "Maritime terrorism in Southeast Asia", *Naval War College Review, vol.* 58, pp. 63-80.

Bargagli, R., Brown, D. & Nelli, L. 1995, "Metal biomonitoring with mosses: procedures for correcting for soil contamination", *Environmental Pollution,* vol. 89, no. 2, pp. 169-175.

Bartschat, K., Burke, P.G. & Crowe, A. 2009, Electron Scattering by Atoms, Ions, and Molecules, *Encyclopedia of Applied Physics*, pp. 211-282.

Barwick, M. & Maher, M. 2003, Biotransference and biomagnification of selenium copper, cadmium, zinc, arcenic and lead in a temperate seagrass ecosystem frm Lake Macquarie Estuary, NSW, Australia, *Marine Environmental Research*, vol. 56, pp. 471-502.

Bayne 1976. Marine mussels their ecology and physiology, *Cambridge University Press, London UK*

Beamish, R., Mahnken, C. & Neville, C. 2004, "Evidence that reduced early marine growth is associated with lower marine survival of coho salmon", *Transactions of the American Fisheries Society,* vol. 133, no. 1, pp. 26-33.

Becker, T., Hitzmann, B., Muffler, K., Portner, R., Reardon, K., Stahl, F. & Ulber, R. 2007, "Future aspects of bioprocess monitoring", *White Biotechnology,* vol. 105, pp. 249-293.

Beckman, D. 2012, Marine environmental biology and conservation, *Journal of Environmental Law*, vol. 22, pp. 301-314.

Benzeggouta, D., Vickridge, I., Barradas, N.P., Doebeli, M., Jeynes, C., & Vantomme, A. 2011, "Handbook on best practice for minimising beam-induced damage during IBA", *Spirit Damage Handbook*, *Paris Contributors NP Barradas*, version 1.0, 1 March 2011, pp. 16-20.

Bertalanffy, L. 1938, "A quantitative theory of organic growth (inquiries on growth laws II)", *Human Biology,* vol. 10, no. 2, pp. 181-213.

Bhatia, N.P., Walsh, K.B., Orlic, I., Siegele, R., Ashwath, N. & Baker, A.J.M. 2004, "Studies on spatial distribution of nickel in leaves and stems of the metal hyperaccumulator Stackhousia tryonii bailey using nuclear microprobe (micro-PIXE) and EDXS techniques", *Functional Plant Biology,* vol. 31, no. 11, pp. 1061-1074.

Bhatt, J.D. 2006, The strategic use of small scale water providers: an analysis of private-sector participation in peri-urban Maputo. *The World Bank, 1818 H Stret, NW, Washington, DC 20433 USA,* pp. 8-17.

Bidone, E., Castilhos, Z., Santos, T.J.S., Souza, T.M.C. & Lacerda, L. 1997, "Fish contamination and human exposure to mercury in Tartarugalzinho River, Amapa State, Northern Amazon, Brazil. A screening approach", *Water, Air & Soil Pollution,* vol. 97, no. 1, pp. 9-15.

Birch, N., Wang, X. & Chong, H.S. 2006, "Iron chelators as therapeutic iron depletion agents", *Chemical Biology*, vol. 16, pp.1533-1556.

Bjorklund, E., Nilsson, T., Bowadt, S., Pilorz, K., Mathiasson, L. & Hawthorne, S.B. 2000, "Introducing selective supercritical fluid extraction as a new tool for determining sorption/desorption behavior and bioavailability of persistent organic pollutants in sediment", *Journal of Biochemical & Biophysical Methods,* vol. 43, no. 1, pp. 295-311.

Blaauw, M., Campbell, J., Fazinic, S., Jaksic, M., Orlic, I. & Van Espen, P. 2002, "The 2000 IAEA intercomparison of PIXE spectrum analysis software", *Nuclear Instruments and Methods in Physics Research B,* vol. 189, no. 1, pp. 113-122.

Bodansky, D. 2009, The art and craft of international environmental law, *Georgia Journal of International and Comparative Law*, vol. 38, pp. 511-524.

Boer, B. 1993, "Environmental and Resource Law in Australia", *Osgoode Hall Law Journal,* vol. 31, pp. 297-305.

Borgesen, P., Behrisch, R. & Scherzer, B. 1982, "Depth profiling by ion-beam spectrometry", *Applied Physics A: Materials Science & Processing,* vol. 27, no. 4, pp. 183-195.

Borovoi, A. & Gagarinskii, A.Y. 2001, "Emission of radionuclides from the destroyed unit of the Chernobyl nuclear power plant", *Atomic Energy,* vol. 90, no. 2, pp. 153-161.

Bojcevska, C. & Jergil, E. 2003, Removal of cyanobacterial toxins (LPS endotoxins and microcystin) in drinking-water using the biosand household water filter. Minor field study in Mozambique. Uppsala University, Sweden.

Brack, W., Bandow, N., Schwab, K., Schulze, T. & Streck, G. 2009, "Bioavailability in effect-directed analysis of organic toxicants in sediments", *TrAC Trends in Analytical Chemistry,* vol. 28, no. 5, pp. 543-549.

Brey, T. 1999, "Growth performance and mortality in aquatic macrobenthic invertebrates", *Advances in Marine Biology,* vol. 35, pp. 153-223.

Bryceson, D.F. & Mbara, T. 2003, "Petrol pumps and economic slumps: rural-urban linkages in Zimbabwe's globalisation process", *Tijdschrift voor Economische & Sociale Geografie,* vol. 94, no. 3, pp. 335-349.

Bucheli, T.D. & Fent, K. 1995, Induction of cytochrome P450 as a biomarker for environmental contamination in aquatic ecosystems. *Critical Reviews in environmental Science & Technology,* vol.25, no.3, pp. 201-268.

Burton, J.G.A. 2002, "Sediment quality criteria in use around the world", *Limnology,* vol. 3, no. 2, pp. 65-76.

Bush, A.I. 2000, "Metals and neuroscience", *Current Opinion in Chemical Biology,* vol. 4, no. 2, pp. 184-191.

Bush, M.B., Silman, M.R. & Urrego, D.H. 2004, "48,000 years of climate and forest change in a biodiversity hot spot", *Science,* vol. 303, no. 5659, pp. 827-829.

Caddy, J. 1987, "Size-frequency analysis for Crustacea: moult increment and frequency models for stock assessment", *Kuwait Bulletin of Marine Science,* vol. 9, pp. 43-61.

Calamari, D. 1994, Review of pollution in the African aquatic environment, *Food and Agriculture Organization of the United Nations*, Rome, Italy.

Camara, C., Madrid, Y., de Embun, P.X., Echevarria, G., Shallari, S., Gerard, E., Denys, S., Morel, J.L., Gonnelli, R.G.C. & Gawronski, S. 2001, "Toxic metals", *International Journal of Photoremediation*, vol. 3, no. 4, pp. 369-379.

Camargo, J.A. & Alonso, A. 2006, "Ecological and toxicological effects of inorganic nitrogen pollution in aquatic ecosystems: A global assessment", *Environment International,* vol. 32, no. 6, pp. 831.

Campbell, G.S. 1985, *Soil physics with BASIC: transport models for soil-plant systems,* Elsevier Science B.V., Sara Burgerhartstraat 25, AE Amsterdam, The Netherlands.

Campbell, J., Perujo, A. & Millman, B. 1987, "Analytic description of Si (Li) spectral lineshapes due to monoenergetic photons", *X-Ray Spectrometry,* vol. 16, no. 5, pp. 195-201.

Campbell, J. 1988, "Assessment of a self-consistent theoretical data base for L X-Ray relative intensities in proton-induced X-Ray emission analysis", *Nuclear Instruments and Methods in Physics Research B,* vol. 31, no. 4, pp. 518-524.

Campbell, J. 1989, "The study of atomic inner shell transitions using solid state X-ray spectrometers", *Canadian Journal of Physics,* vol. 67, no. 8, pp. 806-812.

Campbell, J., Cauchon, G., Lepy, M.C., McDonald, L., Plagnard, J., Stemmler, P., Teesdale, W. & White, G. 1998, "A quantitative explanation of low-energy tailing features of Si (Li) and Ge X-ray detectors, using synchrotron radiation", *Nuclear Instruments and Methods in Physics Research A,* vol. 418, no. 2, pp. 394-404.

Campbell, J., Babaluk, J., Cooper, M., Grime, G., Halden, N., Nejedly, Z., Rajta, I. & Reist, J. 2002, "Strontium distribution in young-of-the-year Dolly Varden otoliths: Potential for stock discrimination", *Nuclear Instruments and Methods in Physics Research B,* vol. 189, no. 1, pp. 185-189.

Campbell, A. 2002, "The potential role of aluminium in Alzheimer's disease", *Nephrology Dialysis Transplantation,* vol. 17, no. suppl 2, pp. 17-20.

Campbell, J. 2003, "Fluorescence yields and Coster-Kronig probabilities for the atomic L subshells", *Atomic Data & Nuclear Data Tables,* vol. 85, no. 2, pp. 291-315.

Canesi, L., Viarengo, A., Leonzio, C., Filippelli, M. & Gallo, G. 1999, "Heavy metals and glutathione metabolism in mussel tissues", *Aquatic Toxicology,* vol. 46, no. 1, pp. 67-76.

Cannon, H.L. 1971, "The use of plant indicators in ground water surveys, geologic mapping, and mineral prospecting", *Taxonomy,* vol. 20, pp. 227-256.

Cao, L., Huang, W., Shan, X., Xiao, Z., Wang, Q. & Dou, S. 2009, "Cadmium toxicity to embryonic-larval development and survival in red sea bream *Pagrus major*", *Ecotoxicology & Environmental Safety,* vol. 72, no. 7, pp. 1966-1974.

Casselman, J.M. 1990a, "Growth and relative size of calcified structures of fish", *Transactions of the American Fisheries Society,* vol. 119, no. 4, pp. 673-688.

Castel-Branco, C.N. 2004, "What is the experience and impact of South African trade and investment on growth and development of host economies? A view from Mozambique", *HSRC Conference on "Stability, Poverty Reduction & South African Trade and Investment in Southern Africa*, pp. 29.

Castoldi, A.F., Johansson, C., Onishchenko, N., Coccini, T., Roda, E., Vahter, M., Ceccatelli, S. & Manzo, L. 2008, Human developmental neurotoxicity of methylmercury: Impact of variable and risk mod*ifiers, Regulatory Toxicology and Pharmacology*, vol. 51, pp. 201-214.

Caussy, D., Godifeld, M. *et al.* 2003. Lessons from case studies of metals investigating exposure bioavailability, and risk. *Ecotoxicology and Environmental Safety*, vo. 56, no. 1, pp. 45-51.

Chakalall, B., Mahon, R., McConney, P., Nurse, L. & Oderson, D. 2007, "Governance of fisheries and other living marine resources in the Wider Caribbean", *Fisheries Research,* vol. 87, no. 1, pp. 92-99.

Chapman, D.V. 1996, Water quality assessments: a guide to the use of biota, sediments, and water in environmental monitoring*, University Press,* Cambridge, UK.

Chapman, D.V. 1996, Water quality assessments: a guide to the use of biota, sediments, and water in environmental monitoring*, Spon Press,* London, UK.

Chebbo, G. 1999, "Characterisation of urban runoff pollution in Paris", *Water Science Technology,* vol. 39, no. 2, pp. 1-8.

Chen, C.M., Lee, S.Z. & Wang, J.S. 2000, "Metal contents of fish from cultureponds near scrap metal reclamation facilities", *Chemosphere,* vol. 40, no. 1, pp. 65-69.

Chen, M.H. 1990, "X-ray and Auger transitions in atoms and ions", *AIP Conference Proceedings*, Knoxville, Tennessee, USA.

Chiang, Y.C., Liao, W.W. & Fan, C.M. 2008. PCR detection of *Staphylococcal enterotoxins* (SEs) and survey of SE types in *Staphylococcus aureus isolates* from food-poisoning cases in Taiwan, *International Journal of Food Microbiology,* bl. 121, no. 1-15, pp. 66-73.

Chojnacka, K., Chojnacki, A. & Gorecka, H. 2004, "Trace element removal by *Spirulina sp.* from copper smelter and refinery effluents", *Hydrometallurgy,* vol. 73, no. 1, pp. 147-153.

Chorus, I., Falconer, I.R., Salas, H.J. & Bartram, J. 2000, "Health risks caused by freshwater cyanobacteria in recreational waters", *Journal of Toxicology & Environmental Health Part B: Critical Reviews,* vol. 3, no. 4, pp. 323-347.

Chu, Wei-Kan, Mayer, J.M, Nicolet, Marc-A. 1978, Backscattering Spectrometry, Academic Press, New York, USA.

Civera, R.G., Esquivias, G.B., Blanc, J.J., Brignole, M., Mitjans, A.M.I., Granell, R.R. and Wieling, W. 2002, *Blackwell Science Ltd*, Malden, USA, pp.12-23.

Clarkson, T.W. 1997, "The toxicology of mercury", *Critical Reviews in Clinical Laboratory Sciences,* vol. 34, no. 4, pp. 369-403.

Cloete, T. & Muyima, N. 1997, *Microbial community analysis: the key to the design of biological wastewater treatment systems,* International Water Association, Scientific and Technical Report No. 5, pp. 4-22.

Codd, G.A., Morrison, L.F. & Metcalf, J.S. 2005, "Cyanobacterial toxins: risk management for health protection", *Toxicology & Applied Pharmacology,* vol. 203, no. 3, pp. 264-272.

Cohen, D.D., Bird, R., Dytlewski, N. & Siegele, R. 2001, "Ion beams for materials analysis", *Encyclopedia of Physics and Science & Technology,* vol. 1-11, pp. 1265.

Collins, C.J.W. 1884, "Result of the Introduction of Gill-Nets into the American Cod-Fisheries", *Transactions of the American Fisheries Society,* vol. 13, no. 1, pp. 212-228.

Cook, R. & Guthrie, I. 1987, "In-season stock identification of sockeye salmon (Oncorhynchus nerka) using scale pattern recognition", *Sockeye salmon stock biology and future management, Canadian Species Public Fish Aquatic Sciences,* vol. 39, no. 96, pp. 611-617.

Cordain, L., Eaton, S.B., Sebastian, A., Mann, N., Lindeberg, S., Watkins, B.A., O'Keefe, J.H. & Brand-Miller, J. 2005, "Origins and evolution of the Western diet: health implications for the 21st century", *The American Journal of Clinical Nutrition,* vol. 81, no. 2, pp. 341-354.

Cornelissen, G., Gustafsson, O., Bucheli, T.D., Jonker, M.T.O., Koelmans, A.A. & van Noort, P.C.M. 2005, "Extensive sorption of organic compounds to black carbon, coal, and kerogen in sediments and soils: Mechanisms and consequences for distribution, bioaccumulation, and biodegradation", *Environmental Science & Technology,* vol. 39, no. 18, pp. 6881-6895.

Craft, C.D., Pearson, R.M. & Hurcomb, D. 2007, "Mineral Dissolution and Dam Seepage Chemistry–The Bureau of Reclamation Experience", *Proceedings of the 2007 National Meeting, Dam Safety 2007.*

Craig, R.K. 2005, "Urban Runoff and Ocean Water Quality in Southern California: What Tools Does the Clean Water Act Provide", *Chapman Law Review,* vol. 9, pp. 313-363.

Creaser, C.W. 1926, "The structure and growth of the scales of fishes in relation to the interpretation of their life-history, with special reference to the sunfish *Eupomotis gibbosus*". *Museum of Zoology, University of Michigan*, USA, vol. 17, pp. 1-82.

Criss, J. & Birks, L. 1968, "Calculation methods for fluorescent x-ray spectrometry. Empirical coefficients versus fundamental parameters", *Analytical Chemistry,* vol. 40, no. 7, pp. 1080-1086.

Cristache, C., Duliu, O., Ricman, C., Toma, M., Dragolici, F., Bragea, M. & Done, L. 2008, "Determination of elemental content in geological samples", *Romanian Journal of Physics,* vol. 53, no. 7-8, pp. 941.

Crocci, L., De Medici, D.*, et al.* 2005. Resistance of hepatitis A virus in mussels subjected to different domestic cookings. *International Journal of Food*, vol. 105, no.2, pp. 139-144.

Dallas, H.F. 1997, A preliminary evaluation of aspects of SASS (South African Scoring System) for the rapid bioassessment of water quality in rivers, with particular reference to the incorporation of SASS in a national biomonitoring programme. *Journal of Aquatic Science*, vol. 23, no. 1, pp. 79-94.

Dallas, H.F. 2004, Seasonal variability of macroinvertebrate assemblages in two regions of South Africa: Implications for aquatic bioassessment. *Journal of Aquatic Science*, vol. 29, no. 2, pp. 173-184.

Dasch, E.J. 1969, "Strontium isotopes in weathering profiles, deep-sea sediments, and sedimentary rocks", *Geochimica et Cosmochimica Acta,* vol. 33, no. 12, pp. 1521-1552.

Davidson, P.W., Myers, G.J. & Weiss, B. 2004, "Mercury exposure & child development outcomes", *Pediatrics,* vol. 113, no. 3, pp. 1023-1029.

Davis, J. & Foster, R. 1958, "Bioaccumulation of radioisotopes through aquatic food chains", *Ecology,* vol. 39, no.7, pp. 530-535.

Dietzel, K.I. 2000, "On-line X-ray fluorescence analysis applied to industrial processes and environmental monitoring". *Journal of Analytical Atomic Spectrmetry*, vol. 92, no. 4, pp. 672-678.

Diez, S. 2009, "Human health effects of methylmercury exposure", *Reviews of Environmental Contamination & Toxicology,* vol. 198, pp. 111-132.

Dondeyne, S., Ndunguru, E., Rafael, P. & Bannerman, J. 2009, "Artisanal mining in central Mozambique: Policy and environmental issues of concern", *Resources Policy,* vol. 34, no. 1, pp. 45-50.

Doolittle, I.R. 1986, Pollution effects on stone benches of the eagle warriors precinct at the major temple, *Nuclear Instruments and Methods in Physics Research B,* vol. 15, pp. 227.

Douay, F., Pruvot, C., Roussel, H., Ciesielski, H., Fourrier, H., Proix, N. & Waterlot, C. 2008, "Contamination of urban soils in an area of Northern France polluted by dust emissions of two smelters", *Water, Air & Soil Pollution,* vol. 188, no. 1, pp. 247-260.

Duda, A.M. & Sherman, K. 2002, "A new imperative for improving management of large marine ecosystems", *Ocean & Coastal Management,* vol. 45, no. 11, pp. 797-833.

Eckstein, W. & Mayer, M. 1999, "Rutherford backscattering from layered structures beyond the single scattering model", *Nuclear Instruments and Methods in Physics Research B,* vol. 153, no. 1, pp. 337-344.

Eisenberg, D., Soller, J., Sakaji, R. & Olivieri, A. 2001, A methodology to evaluate water and wastewater treatment plant reliability, *Water Science & Technology*, vol. 43, pp. 91-99.

Ene, A., Popescu, I., Stihi, C., Gheboianu, A., Pantelica, A. & Petre, C. 2010, "PIXE analysis of multielemental samples", *Romanian Journal of Physics,* vol. 55, no. 7-8, pp. 806-814.

EPA 1999, Wastewater Technology Fact Stree*t, United States Environmental Protection Age*ncy, Washington, USA.

EPA 2007, Framework for Metals Risk Assessment, *United States Environmental Protection Age*ncy, Washington, USA.

Escultura, E. 2010, "Qualitative model of the atom, its components and origin in the early universe", *Nonlinear Analysis: Real World Applications,* vol. 11, no. 1, pp. 29-38.

European Commission 2005, "Communication from the commission to the Council and the European Parliament-Community Strategy Concerning Mercury-SEC (2005) 101", *European Community, Brussels,* pp. 1-11.

Evans, C.A. Jr. & Blattner, R.J. 1978, Modern experimental methods for surface and thin-film chemical analysis, *Materials Science*, vol. 8, pp. 181-214.

Fakhri, A., Pazira, A., Rastgoo, A. & Shadi, A. 2011, "Mortality, Exploitation and Yield per Recruit of Javelin Grunter, Pomadasys kaakan, in the Iranian Waters of the Persian Gulf", *Middle-East Journal of Scientific Research,* vol. 9, no. 1, pp. 64-67.

Fanning, L., Mahon, R. & McConney, P. 2009, "Focusing on living marine resource governance: The Caribbean Large Marine Ecosystem and adjacent areas project", *Coastal Management,* vol. 37, no. 3-4, pp. 219-234.

Feng, X., Li, P., Qiu, G., Wang, S., Li, G., Shang, L., Meng, B., Jiang, H., Bai, W. & Li, Z. 2007, "Human exposure to methylmercury through rice intake in mercury mining areas, Guizhou Province, China", *Environmental Science & Technology,* vol. 42, no. 1, pp. 326-332.

Feyerabend, F., Fischer, J., Holtz, J., Witte, F., Willumeit, R., Drucker, H., Vogt, C. & Hort, N. 2010, "Evaluation of short-term effects of rare earth and other elements used in magnesium alloys on primary cells and cell lines", *Acta Biomaterialia,* vol. 6, no. 5, pp. 1834-1842.

Field, R., Borst, M., O'Connor, T.P., Stinson, M.K., Fan, C.Y., Perdek, J.M. & Sullivan, D. 1998, "Urban wet-weather flow management: research directions", *Journal of Water Resources Planning & Management,* vol. 124, no. 3, pp. 168-180.

Fiket, Z., Roje, V., Mikac, N. & Kniewald, G. 2007, "Determination of arsenic and other trace elements in bottled waters by high resolution inductively coupled plasma mass spectrometry", *Croatica Chemica Acta,* vol. 80, no. 1, pp. 91-100.

Finn, D.P. 1980, "Ocean disposal of radioactive wastes: The obligation of international cooperation to protect the marine environment", *Journal of International Law,* vol. 21, pp. 621.

Flora, S., Bhadauria, S., Kannan, G. & Singh, N. 2007, "Arsenic induced oxidative stress and the role of antioxidant supplementation during chelation: a review", *Journal of Environmental Biology,* vol. 28, no. 2, pp. 333.

Foley, P. & Missingham, G. 1976, "Monitoring of community water supplies", *Journal American Water Works Association,* vol. 2*,* pp. 105-111.

Fordyce, F. 2005, "Selenium deficiency and toxicity in the environment", *Natural Environment Research Council*, vol. 81, pp. 527-533.

Fordyce, F. 2013, "Selenium deficiency and toxicity in the environment", *Springer-Veilag, Netherlands*, vol. 81, pp. 375-416.

Fraser, G., Abbey, A., Holland, A., McCarthy, K., Owens, A. & Wells, A. 1994, "The X-ray energy response of silicon Part A. Theory", *Nuclear Instruments and Methods in Physics Research A,* vol. 350, no. 1, pp. 368-378.

Freeman III, A.M. 1990, "Water pollution policy", *Public Policies for Environmental Protection,* Published by New York Press, Albany, pp. 97-150.

Friedland, K.D. 1998, "Ocean climate influences on critical Atlantic salmon (Salmo salar) life history events", *Canadian Journal of Fisheries & Aquatic Sciences,* vol. 55, no. S1, pp. 119-130.

Froese, R. & Binohlan, C. 2003, "Simple methods to obtain preliminary growth estimates for fishes", *Journal of Applied Ichthyology,* vol. 19, no. 6, pp. 376-379.

Game, Fish Commission of Minnesota & Minnesota Commission of Fisheries 1892, *Annual report of the Game & Fish Commission of Minnesota,* Harrison & Smith, printers, vol. 2, pp. 76-106.

Garman, E.F. & Grime, G.W. 2005, "Elemental analysis of proteins by micro-PIXE", *Progress in Biophysics & Molecular Biology,* vol. 89, no. 2, pp. 173-205.

Gayanilo, F. 1997, FAO-ICLARM stock assessment tools*: reference manual, Food & Agriculture Organization of the United Nations* Rome Italy, pp. 336-389.

Geldreich, E.E. 1978, "Bacterial populations and indicator concepts in feces, sewage, stormwater and solid wastes", *Indicators of Viruses in Water and Food,* pp. 51-97.

Gerber, G., Leonard, A. & Hantson, P. 2002, "Carcinogenicity, mutagenicity and teratogenicity of manganese compounds", *Critical Reviews in Oncology/Hematology,* vol. 42, no. 1, pp. 25-34.

Gerhardsson, L., Oskarsson, A. & Skerfving, S. 1994, "Acid precipitation-effects on trace elements and human health", *Science of the Total Environment,* vol. 153, no. 3, pp. 237-245.

Ginzburg, H.M. & Reis, E. 1991, "Consequences of the nuclear power plant accident at Chernobyl", *Public Health Reports,* vol. 106, no. 1, pp. 32.

Gilbert, P.M., Anderson, D.M., Gentien, P., Graneli, E. & Sellner, K.G. 2005, "The global, complex phenomena of harmful algal blooms" Paris, vol. 18, pp. 236-266.

Giulio, R.T.D., Washbum, P.C., Wenning, R.J., Winston, G.W. and Jewell, C.S. 1989, Biochemical responses in aquatic animals: A review of determinants of oxidative stress, Toxicology and chemistry, vol.8, pp. 1103-1123.

Goldman, L.R. & Shannon, M.W. 2001, "Technical report: mercury in the environment: implications for pediatricians", *Pediatrics,* vol. 108, no. 1, pp. 197-205.

Goodier, J. 1984, "The Nineteenth-Century Fisheries of the Hudson's Bay Company Trading Posts on Lake Superior: a Biogeographical Study", *Canadian Geographer/Le Geographe Canadien,* vol. 28, no. 4, pp. 341-357.

Goulding, F. & Jaklevic, J. 1973, "Photon-excited energy-dispersive X-ray fluorescence analysis for trace elements", *Annual Review of Nuclear Science,* vol. 23, no. 1, pp. 45-74.

Goyer, R.A. & Clarkson, T.W. 1996, "Toxic effects of metals", *Casarett & Doull's Toxicology. The Basic Science of Poisons, McGraw-Hill Health Professions Division,* New York, USA.

Greenberg, Bernard, G., Cox, G.M., Mason, David, D., Grizzle, J.E., Johnson, N.L., Jones, L.V., Monroe, J. & Simmons, D. Jr. 1978, "Statistical Training and Research: The University of North Carolina System", *International Statistical Review*, vol. 46, pp. 171-207.

Grime G. W. 1996, The "Q factor" method: quantitative micro PIXE analysis using RBS normalisation. *Nuclear Instruments & Methods in Physics Research B*, vol. 109, pp. 170-174.

Guambe, J.F., Mars, J.A. & Day, J. 2012, "Application of Particle-Induced X-ray Emission, Scanning Electron Microscopy and Backscattering spectrometry in the Elemental quantification of incremental patterns in scales of the fish *Pomadasys kaakan*: A 2-d study. *International Journal of PIXE,* vol. 22, pp. 185.

Guambe, J.F., Mars, J.A. & Day, J. 2012, "Application of PIXE in pollution control of the Matola River in Mozambique-analysis of fish scales", *Nuclear Instruments and Methods in Physics Research B,* vol. 273, pp. 171-172.

Gumbo, R.J., Ross, G. & Cloete, E.T. 2010, "Biological control of Microcystis dominated harmful algal blooms", *African Journal of Biotechnology,* vol. 7, no. 25, pp. 4765-4773.

Guntupalli, J.N.R., Padala, S., Gummuluri, A.V.R.M., Muktineni, R.K., Byreddy, S.R., Sreerama, L., Kedarisetti, P.C., Angalakuduru, D.P., Satti, B.R. & Venkatathri, V. 2007, "Trace elemental analysis of normal, benign hypertrophic and cancerous tissues of the prostate gland using the particle-induced X-ray emission technique", *European Journal of Cancer Prevention,* vol. 16, no. 2, pp. 108-115.

Guo, C., Stetzenbach, K.J. & Hodge, V.F. 2005, "Determination of 56 trace elements in three aquifer-type rocks by ICP-MS and approximation of the relative solubilities for these elements in a carbonate system by water-rock concentration ratios", *Rare Earth Elements in Groundwater Flow Systems,* vol. 51, pp. 39-65.

Gupta, R.C. 2011, Reproductive and Developmental Toxicology, *Academic Press*, London, UK.

Hammer, D.A. 1992, "Designing constructed wetlands systems to treat agricultural nonpoint source pollution", *Ecological Engineering,* vol. 1, no. 1, pp. 49-82.

Hanson, H.L., Donermeyer, D.L., Ikeda, H., White, J.M., Shankaran, V., Old, L.J., Shiku, H., Schreiber, R.D. & Allen, P.M. 2000, "Eradication of Established Tumors by CD8, T Cell Adoptive Immunotherapy", *Immunity,* vol. 13, no. 2, pp. 265-276.

Hanson, J.M. & Courtenay, S.C. 1997, Seasonal Distribution, maturity, condition, and feeding of smooth flounder (*Pleuronectes putnami*) in the Miramichi estuary, southern Gulf of St. Lawrence. *Canadian Journal of Zoology*, vol.75 no. 8, pp. 1226-1240.

Hasanuzzaman, M. & Fujita, M. 2012, "2 Heavy Metals in the Environment", *Phytotechnologies: Remediation of Environmental Contaminants,* CRC Press, New York, USA.

Hatcher, C.O., Ogawa, R.E. & Poe, T.P. 1992, "Trace elements in lake sediment, macrozoobenthos, and fish near a coal ash disposal basin", *Journal of Freshwater Ecology,* vol. 7, no. 3, pp. 257-269.

Heidarsson, T., Antonsson, T. & Snorrason, S.S. 2006, "The relationship between body and scale growth proportions and validation of two back-calculation methods using individually tagged and recaptured wild Atlantic salmon", *Transactions of the American Fisheries Society,* vol. 135, no. 5, pp. 1156-1164.

Herbert, M. 2008, *Developmental Problems of Childhood and Adolescence: Prevention, Treatment and Training,* Wiley-Blackwell, Malden, USA, pp. 13-231.

Hinrichsen, D. 1999, *Coastal waters of the world: trends, threats, and strategies,* Island Press, Covelo, USA.

Hinton, T.G., Alexakhin, R., Balonov, M., Gentner, N., Hendry, J., Prister, B., Strand, P. & Woodhead, D. 2007, "Radiation-induced effects on plants and animals:

Findings of the United Nations Chernobyl Forum", *Health Physics,* vol. 93, no. 5, pp. 427-440.

Hofmann, T.A. & Mason, C.F. 2005, "Habitat characteristics and the distribution of Odonata in a lowland river catchment in eastern England", *Hydrobiologia,* vol. 539, no. 1, pp. 137-147.

Hollard, H.D., & Turekian, K.K. 2004, Environmental Geochemistry, *Amsterdam*, The Netherlands.

Holmes, P., James, K.A.F. & Levy, L.S. 2009, Is low-level environmental mercure of concer to human health? *Science of the Total Environment*, vol. 408, pp. 171-182.

Huang, P.M., Li, Y. & Sumner, M.E. 2011, Resource Management and Environmental Impacts, *Critical Reviews in Environmental Control Press*, Madison, USA.

Huhn, E., Lincoln, R., Pandozi, E., Pertuz, J., Anderson, P., Brownstein, J., Confalonieri, U., Causey, D., Chan, N. & Ebi, K.L. 2006 "Climate change futures", *The Center for Health & the Global Environment*, *American Bar Association*, USA.

Hugentobler, M., Iosifescu-Enescu, I. & Hurni, L. 2009, Implementing cartographic services for environmental management based on QGIS. *Prague, Czech Republic, January 19-22, 2009.*

IMANAKA, I.A.R.T. 1997, "Legislation and research activity in Russia about the radiological consequences of the Chernobyl accident", *Environment Review,* vol., pp. 203-205.

Ishii, K. & Morita, S. 1988, "Theoretical estimation of PIXE detection limits", *Nuclear Instruments & Methods in Physics Research B,* vol. 34, no. 2, pp. 209-216.

Ishikawa, M., Ishii, T. & Kitao, K. 1990, "Pixe scanning analysis across the scale of a sea-bass, la *Teolabrax japonicus*, *Nuclear Instruments & Methods in Physics Research B,* vol. 49, no. 1, pp. 485-489.

Islam, S. & Tanaka, M. 2004. Impact of pollution on coastal and marine ecosystems including coastal and marine fisheries and approach for management. *Marine Pollution Bullentin,* vol. 48, no.7-8, pp. 624-649.

Jain, C.K. and Ali, I. 2000, Arsenic: occurrence, toxicity and speciation techniques, *Water Research*, vol. 34, pp. 4304-4312.

Jammer, M. 1999, Concepts of mass in contemporary physics and philosophy*, Princeton University Press, Princeton, USA.*

Janvier, C., Villeneuve, F., Alabouvette, C., Edel-Hermann, V., Mateille, T. & Steinberg, C. 2007, "Soil health through soil disease suppression: Which strategy from descriptors to indicators?" *Soil Biology &Biochemistry,* vol. 39, no. 1, pp. 1-23.

Jenkins, P. 2000, "City profile: Maputo", *Cities,* vol. 17, no. 3, pp. 207-218.

Jeynes, C. 2012, "Elastic Backscattering of Ions for Compositional Analysis", *Characterization of Materials,* vol. 25, no. 1, pp. 171-191.

Jeynes, C., Barradas, N., Marriott, P., Boudreault, G., Jenkin, M., Wendler, E. & Webb, R. 2003, "Elemental thin film depth profiles by ion beam analysis using simulated annealing-a new tool", *Journal of Physics,* vol. 36, no. 7, pp. R97.

Joas, R., Casteleyn, L., Biot, P., Kolossa-Gehring, M., Castano, A., Angerer, J., Schoeters, G., Sepai, O., Knudsen, L.E. & Joas, A. 2012, "Harmonised human biomonitoring in Europe: Activities towards an EU HBM framework", *International Journal of Hygiene & Environmental Health,* vol. 215, no. 2, pp. 172-175.

Johansson, S.A.E. 1988, "PIXE: A novel technique for elemental analysis", *Endeavour,* vol. 13, no. 2, pp. 48-53.

Johansson, S.A.E. & Johansson, T.B. 1976, "Analytical application of particle induced X-ray emission", *Nuclear Instruments & Methods in Physics Research B,* vol. 137, no. 3, pp. 473-516.

Johansson, T.B., Van Grieken, R.E., Nelson, J.W. & Winchester, J.W. 1975, "Elemental trace analysis of small samples by proton induced X-ray emission", *Analytical Chemistry,* vol. 47, no. 6, pp. 855-860.

Kalia, K. & Flora, S.J.S. 2005, "Strategies for safe and effective therapeutic measures for chronic arsenic and lead poisoning", *Journal of Occupational Health,* vol. 47, no. 1, pp. 1-21.

Kalipeni, E. 2000, "Health and disease in southern Africa: a comparative and vulnerability perspective", *Social Science & Medicine,* vol. 50, no. 7, pp. 965-983.

Khan, S.J. & McDonald, J.A. 2010, Quantification human exposure to contaminants for multiple-barrier water reuse systems, *Water Science & Technology*, vol. 61, pp. 77-83.

Kawahara, M. 2005, "Effects of aluminum on the nervous system and its possible link with neurodegenerative diseases", *Journal of Alzheimer's Disease,* vol. 8, no. 2, pp. 171-182.

Keener, S., Luengo, M. & Banerjee, S., 2009, Provision of water to the poor in Africa. *The World Bank,* NW, Washington, DC 20433 USA.

Kersten, M. & Forstner, U. 1995, Speciation of trace metals in sediments and combustion waste. *In chemica Speciation in the Environmental*, London, UK.

Keunish, M.J. 2002. Environmental threats and environmental future of estuaries. *Environmental Conservation*, vol. 29, no. 1, pp.78-107.

Klaus, J.S., Frias-Lopez, J., Bonheyo, G.T., Heikoop, J.M. & Fouke, B.W. 2005, "Bacterial communities inhabiting the healthy tissues of two Caribbean reef corals: interspecific and spatial variation", *Coral Reefs,* vol. 24, no. 1, pp. 129-137.

Klumb, R.A., Bozek, M.A. & Frie, R.V. 1999, "Proportionality of body to scale growth: validation of two back-calculation models with individually tagged and recaptured smallmouth bass and walleyes", *Transactions of the American Fisheries Society,* vol. 128, no. 5, pp. 815-831.

Knapp, J., Banks, J. & Brice, D. 1994, "Trace contamination measurements using heavy ion backscattering spectrometry", *MRS Proceedings* Cambridge University Press, Cambbridge, UK.

Knapp, J., Barbour, J. & Doyle, B. 1992, "Ion beam analysis for depth profiling", *Journal of Vacuum Science & Technology A,* vol. 10, no. 4, pp. 2685-2690.

Knezovich, J.P., Harrison, F.L. and Wilhelm, R.G. 1987, The bioavailability of sediment-sorbed organic chemicals: *A review, Water, Air, and Soil Pollution*, vol. 32, pp.233-245.

Kolak, J.J., Long, D.T., Beals, T.M., Eisenrich, S.J. & Swackhamer, D.L. 1998, "Anthropogenic inventories and historical and present accumulation rates of copper in Great Lakes sediments", *Applied Geochemistry,* vol. 13, no. 1, pp. 59-75.

Koppe, P., Stozek, A. & Neitzel, V. 2008, "Municipal Wastewater and Sewage Sludge", *Biotechnology,* vol. 11a, pp. 159-189.

Krantz, D.S. & McCeney, M.K. 2002, "Effects of psychological and social factors on organic disease: A Critical Assessment of Research on Coronary Heart Disease", *Annual Review of Psychology,* vol. 53, no. 1, pp. 341-369.

Kustin, K. & McLeod, G.C. 1977, Interations between metal ions and living organisms in water, *Inorganic Biochemistry II,* vol. 69, pp. 1-37.

Langworth, S., Sallsten, G., Barregard, L., Cynkier, I., Lind, M.L. & Soderman, E. 1997, "Exposure to mercury vapor and impact on health in the dental profession in Sweden", *Journal of Dental Research,* vol. 76, no. 7, pp. 1397-1404.

Lacoul, P. & Freedman, B. 2006, Environmental influences on aquatic plants in freshwater ecosystems, *Environmental reviews*, vol. 14, pp. 89-136.

Lech, T. 2002, "Suicide by sodium tetraoxoselenate (VI) poisoning", *Forensic Science International,* vol. 130, no. 1, pp. 44-48.

Lee, C.S., Tamaru, C.S., Kelley, C.D., Moriwake, A. & Miyamoto, G.T. 1992, "The effect of salinity on the induction of spawning and fertilization in the striped mullet, *Mugil cephalus*" *Aquaculture,* vol. 102, no. 3, pp. 289-296.

Leland, H.V., Copenhaver, E.D. & Corrill, L.S. 1974, "Heavy metals and other trace elements", *Journal of the Water Pollution Control Federation,* vol. 46, no. 6, pp. 1452-1476.

Leland, H.V., Luoma, S.N., Elder, J.F. & Wilkes, D.J. 1978, "Heavy metals and related trace elements", *Journal of the Water Pollution Control Federation,* vol. 50, no. 6, pp. 1469-1514.

Lemly, A.D. 2002, *Selenium assessment in aquatic ecosystems: a guide for hazard evaluation and water quality criteria,* Springer-Verlag, New York, USA.

Leonard, A. & Lauwerys, R. 1990, "Mutagenicity, carcinogenicity and teratogenicity of cobalt metal and cobalt compounds", *Mutation Research/Reviews in Genetic Toxicology,* vol. 239, no. 1, pp. 17-27.

Leonard, A. & Lauwerys, R. 1980, "Carcinogenicity, teratogenicity and mutagenicity of arsenic", *Mutation Research/Reviews in Genetic Toxicology,* vol. 75, no. 1, pp. 49-62.

Leonard, A. & Lauwerys, R. 1987, "Mutagenicity, carcinogenicity and teratogenicity of beryllium", *Mutation Research/Reviews in Genetic Toxicology,* vol. 186, no. 1, pp. 35-42.

Levitus, S., Antonov, J.I., Boyer, T.P. & Stephens, C. 2000, "Warming of the world ocean", *Science,* vol. 287, no. 5461, pp. 2225-2229.

Liu, G., Zheng, L., Duzgoren-Aydin, N.S., Gao, L., Liu, J. & Peng, Z. 2007, Health Effects of arsenic, fluorine, and selenium from indoor burning of Chinese coal, *Reviews of Environmental Contamination & Toxicology*, vol. 189, pp. 89-106.

Lund, R. & HANSEL, L. 1991, "Identification of wild and reared Atlantic salmon, Salmo salar L., using scale characters", *Aquaculture Research,* vol. 22, no. 4, pp. 499-508.

Luoma, S.N. 1996, The developing framework of marine ecotoxicology: Pollutants as a variable in marine ecosystems? *Journal of Experimental Marine Biology & Ecology*, vol. 200, pp. 29-55.

Lusher, J.A. 1984. Water quality criteria for the South African coastal zone. *Foundation for Research Development CSIR, Report 94*, pp. 56.

Luster, M.I. & Rosenthal, G.J. 1993, "Chemical agents and the immune response.", *Environmental Health Perspectives,* vol. 100, pp. 219.

Luy, N., Gobert, S., Sartoretto, S., Biondo, R., Bouquegneau, J.M. & Richir, J. 2012, "Chemical contamination along the Mediterranean French coast using *Posidonia oceanica* (L.) Delile above-ground tissues: a multiple trace element study", *Ecological Indicators,* vol. 18, pp. 269-277.

Ma, J.F., Yamaji, N., Mitani, N., Xu, X.Y., Su, Y.H., McGrath, S.P. & Zhao, F.J. 2008, "Transporters of arsenite in rice and their role in arsenic accumulation in rice grain", *Proceedings of the National Academy of Sciences,* vol. 105, no. 29, pp. 9931-9935.

McDonald, S.J., Willett, K.L., *et al.,* 1996, Sublethal detoxification responses to contaminant exposure associated with offshore production platforms. *Canadian Journal of Fisheries & Aquatic Sciences*, vol. 53, no. 11, pp. 2606-2617.

Macdonald, T.L. & Bruce Martin, R. 1988, "Aluminum ion in biological systems", *Trends in Biochemical Sciences,* vol. 13, no. 1, pp. 15-19.

Maenhaut, W. 1988, "Applications of ion beam analysis in biology and medicine, a review", *Nuclear Instruments & Methods in Physics Research B,* vol. 35, no. 3, pp. 388-403.

Majid, A. & Imad, A. 1991, "Growth of *Pomadasys kaakan* (Haemulidae) off the coast of Pakistan", *Fishbyte,* vol. 9, no. 2, pp. 19-20.

Makundi, I.N. 2001, Toxic hazardous substances & environmental Engineering. *Journal of Environmental Science & Health*, vol. 36, pp. 909-921.

Malavasi, S., Fiorin, R., Franco, A., Franzoi, P., Granzotto, A., Riccato, F. & Mainardi, D. 2004, "Fish assemblages of Venice Lagoon shallow waters: an analysis based on species, families and functional guilds", *Journal of Marine Systems,* vol. 51, no. 1, pp. 19-31.

Malik, R.N. and Zeb, Naila 2009, Assessment of environmental concentration using feathers of *Bubulcus ibis* L., as a biomonitor of heavy metal pollution, Pakis*tan, Ecotoxicology*, vol. 18, pp. 522-536.

Malko, M.V. 1998, "Assessment of the Chernobyl radiological consequences", *Research activities on the radiological consequences of the Chernobyl NPS accident and social activities to assist the sufferers from the accident, KURRI-KR-21 Kyoto University, Kyoto* , Japan.

Malmqvist, K.G. 2004, "Accelerator-based ion beam analysis-an overview and future prospects", *Radiation Physics and Chemistry,* vol. 71, no. 3, pp. 817-827.

Malmqvist, K. 2005, "Ion Beam Analysis", *Electrostatic Accelerators,* Springer Berlin Heidelberg.

Malmqvist, K. 1996, "Bio-PIXE: present status and future prospects", *International Journal of PIXE,* vol. 6, pp. 3-18.

Mars, J., Gihwala, D., Przybyleowicz, W., Bladergroen, B. & Linkov, V. 2004, "μ-IBA analysis of Al_2O_3-ZrO_2 tubes to be used in wastewater purification", *Radiation Physics & Chemistry,* vol. 71, no. 3, pp. 799-800.

Maret, T.R. and Skinner, K.D. 2000, Concentrations of Selected Trace Elements in Fish Tissue and Streambed Sedment in the Clark Fork-Pend Oreille and Spokane River Basins, *United State Geological Survey*, Boire, Idoho, USA.

Martin, S. & Griswold, W. 2009, "Human health effects of heavy metals", *Center for Hazardous Substance Research, Kansas State University, Manhattan USA.*

Mason, C.F. 2002, Biology of freshwater pollution, *Freshwater Biology*, vol. 47, pp. 1696-1706.

Massuti, E., Morales-Nin, B. & Stefanescu, C. 1995, "Distribution and biology of five grenadier fish (Pisces: Macrouridae) from the upper and middle slope of the north-western Mediterranean", *Deep Sea Research Part I: Oceanographic Research Papers,* vol. 42, no. 3, pp. 307-330.

Massuti, E., Morales-Nin, B. & Moranta, J. 2000, "Age and growth of blue-mouth, *Helicolenus dactylopterus* (Osteichthyes: Scorpaenidae), in the western Mediterranean", *Fisheries Research,* vol. 46, no. 1, pp. 165-176.

May, H. & Burger, J. 2006, "Fishing in a polluted estuary: fishing behavior, fish consumption, and potential risk", *Risk Analysis,* vol. 16, no. 4, pp. 459-471.

Maenhaut, W., Applications of ion beam analysis in biology and medicine, a review, *Nuclear Instruments & Methods in Physics Research B,* vol. 35, no. 3, pp. 388-403.

Mayer, M. 1999, SIMNRA, a simulation program of the analysis of NRA, RBS and ERDA, *American Journal of Physics*, vol. 475, pp. 541-544.

McLachlan, D., Bergeron, C., Smith, J., Boomer, D. & Rifat, S. 1996, "Risk for neuropathologically confirmed Alzheimer's disease and residual aluminum in municipal drinking water employing weighted residential histories", *Neurology,* vol. 46, no. 2, pp. 401-405.

McLachlan, D., Bergeron, C., Smith, J., Boomer, D. & Rifat, S. 1996, "Risk for neuropathologically confirmed Alzheimer's disease and residual aluminum in municipal drinking water employing weighted residential histories", *Neurology,* vol. 46, no. 2, pp. 401-405.

Mears, A.J., Jordan, T., Mirzayans, F., Dubois, S., Kume, T., Parlee, M., Ritch, R., Koop, B., Kuo, W.L. & Collins, C. 1998, "Mutations of the forkhead gene in patients ", *The American Journal of Human Genetics,* vol. 63, no. 5, pp. 1316-1328.

Mergler, D., Anderson, H.A., Chan, L.H.M., Mahaffey, K.R., Murray, M., Sakamoto, M. & Stern, A.H. 2007, "Methylmercury exposure and health effects in humans: a worldwide concern", *AMBIO: Journal of the Human Environment,* vol. 36, no. 1, pp. 3-11.

Meyers, G.D. 1992, "Surveying the Lay of the Land, Air, and Water: Features of Current International Environmental and Natural Resources Law, and Future Prospects for the Protection of Species Habitat to Preserve Global Biological Diversity", *Colorado Journal of International Environmental Law & Policy,* vol. 3, pp. 479.

Mezzasalma, S.A. 2008, "Chapter Two The Special Theory of Brownian Relativity", *Interface Science and Technology,* vol. 15, pp. 79-135.

Miller, R. 2004, "The Elements, 21st Century", *Global Change Biology*, vol. 8, pp. 695-709.

Mirzai, A., McKee, J., Yeo, Y., Gallop, D. & Medved, J. 1990, "Leaf analysis as an exploratory tool in mineralogy", *Nuclear Instruments & Methods in Physics Research B,* vol. 49, no. 1, pp. 313-317.

Mistry, P., Gomez-Morilla, I., Grime, G., Webb, R., Gwilliam, R., Cansell, A., Merchant, M., Kirkby, K., Teo, E. & Breese, M. 2005, "New developments in the applications of proton beam writing", *Nuclear Instruments & Methods in Physics Research B,* vol. 237, no. 1, pp. 188-192.

Misund, A., Frengstad, B., Siewers, U. & Reimann, C. 1999, "Variation of 66 elements in European bottled mineral waters", *Science of the Total Environment,* vol. 243, pp. 21-41.

Mitchell, E., Frisbie, S. & Sarkar, B. 2011, Exposure to multiple metals from groundwater-a global crisis; Geology, climate change, health effects, testing, and mitigation, *Metallomics*, vol. 3, pp. 874-908.

Mittelmark, M.B. 2001, "Promoting social responsibility for health: health impact assessment and healthy public policy at the community level", *Health Promotion International,* vol. 16, no. 3, pp. 269-274.

Mohr, P.J., Taylor, B.N. & Newell, D.B. 2008, "CODATA Recommended Values of the Fundamental Physical Constants: 2006". Review Modern Physics, vol. 80, pp. 633-730.

Monosson, E. & Stegeman J.J. 1994, Induced cytochrome P4501A in winter flounder, *Pleuronectes americanus*, from offshore and coastal sites. *Canadian Journal of Fisheries & Aquatic Sciences*, vol. 51, no. 4, pp. 933-941.

Monperrus, M., Point, D., Grall, J., Chauvaud, L., Amouroux, D., Bareille, G. & Donard, O. 2005, "Determination of metal and organometal trophic bioaccumulation in the benthic macrofauna of the Adour estuary coastal zone (SW France, Bay of Biscay)", *Journal at Environmental Monitoring,* vol. 7, no. 7, pp. 693-700.

Moolenaar, S.W. & Lexmond, T.M. 1998, "Heavy metal balances, part I", *Journal of Industrial Ecology,* vol. 2, no. 4, pp. 45-60.

Moore, S.H., Smith, M.R. & Cochran, H.B. 1986, *Process for the purification of effluents and purge streams containing trace elements,* US Patent 4, 578, 195, pp. 1-12.

Moriarty, F. 1988, "Ecotoxicology", *Human & Experimental Toxicology,* vol. 7, no. 5, pp. 437-441.

Morley, N.J. 2010. Interactive effects of infectious diseases and pollution in aquatic molluscs. A*quatic Toxicology*, vol. 96, no. 1-21, pp.27-36.

Munro, J. & Pauly, D. 2012, "A simple method for comparing the growth of fishes and invertebrates", *The World Fish Center Working Papers,* vol.19, no. 6, pp. 376-379.

Mvungi, A., Hranova, R. & Love, D. 2003, "Impact of home industries on water quality in a tributary of the Marimba River, Harare: implications for urban water management", *Physics & Chemistry of the Earth, Parts A/B/C,* vol. 28, no. 20, pp. 1131-1137.

Mytilineou, C. & Sarda, F. 1995, "Age and growth of *Nephrops norvegicus* in the Catalan Sea, using length-frequency analysis", *Fisheries Research,* vol. 23, no. 3, pp. 283-299.

Naga Raju, G., John Charles, M., Bhuloka Reddy, S., Sarita, P., Seetharami Reddy, B., Rama Lakshmi, P. & Vijayan, V. 2005, "Trace elemental analysis in cancer-

afflicted tissues of penis and testis by PIXE technique", *Nuclear Instruments & Methods in Physics Research B,* vol. 229, no. 3, pp. 457-464.

Ng, J.C., Wang, J., Shraim, A. 2003, A global health problem caused by arsenic from natural sources, *Environmental & Public-Health Management*, vol. 52, pp. 1353-1359.

Nair, U., Bartsch, H. & Nair, J. 2004, "Alert for an epidemic of oral cancer due to use of the betel quid substitutes gutkha and pan masala: a review of agents and causative mechanisms", *Mutagenesis,* vol. 19, no. 4, pp. 251-262.

Neff, J.M. 2002, *Bioaccumulation in marine organisms: effect of contaminants from oil well produced water,* Elsevier Science Limited, Amsterdam, The Netherland.

Nordberg, G.F., Fowler, B.A., Nordberg, M. & Friberg, L., 2007, *Handbook on the Toxicology of Metals,* Academic Press, San Diego, California, USA.

Olariu, A., Badica, T., Alexandrescu, E. & Avram, A. 2008, "Archaeometric study of a bronze age sword discovered at Giurgiu, Romania", *Romanian Reports in Physics,* vol. 60, no. 3, pp. 563-570.

O'Meara, J.M. & Campbell, J.L. 2004, "Corrections to the conventional approach to Si (Li) detector efficiency", *X-Ray Spectrometry,* vol. 33, no. 2, pp. 146-157.

Oreskes, N. & Conway, E.M. 2010, *Merchants of doubt: How a handful of scientists obscured the truth on issues from tobacco smoke to global warming,* Bloomsbury Press, California, USA.

Ormerod, S. 2003, "Current issues with fish and fisheries: editor's overview and introduction", *Journal of Applied Ecology,* vol. 40, no. 2, pp. 204-213.

Owen, L.A. 1997, *An introduction to global environmental issues,* Routledge, New York, USA.

Paerl, H.W. 1988, "Nuisance phytoplankton blooms in coastal, estuarine, and inland waters", *Limnology and Oceanography,* vol. 32, pp. 823-847.

Paerl, H.W., Xu, H., McCarthy, M.J., Zhu, G., Qin, B., Li, Y. & Gardner, W.S. 2011, "Controlling harmful cyanobacterial blooms in a hyper-eutrophic lake (Lake Taihu, China): The need for a dual nutrient (N & P) management strategy", *Water Research,* vol. 45, no. 5, pp. 1973-1983.

Palamiappan, M., Gleick, P.M., Allen, L., Cohen, M.J., Smith,, J.C. & Smith, C. 2011, Water Quality, Island Press, pp.45-72.

Parr, L. & Mason, C. 2003, "Long-term trends in water quality and their impact on macroinvertebrate assemblages in eutrophic lowland rivers", *Water Research,* vol. 37, no. 12, pp. 2969-2979.

Patel, B., Mulay, C. & Ganguly, A. 1975, "Radioecology of Bombay Harbour-A tidal estuary", *Estuarine & Coastal Marine Science,* vol. 3, no. 1, pp. 13-42.

Pauling, L. 1988, "General chemistry"*, Dover Publications*, Mineola, New York USA.

Pauly, D. 1980, "On the interrelationships between natural mortality, growth parameters, and mean environmental temperature in 175 fish stocks", *Journal du Conseil International pour L'Exploration de la Mer,* vol. 39, no. 2, pp. 175-192.

Pauly, D. & Munro, J. 1984, "Once more on the comparison of growth in fish and invertebrates", *Fishbyte,* vol. 2, no. 1, pp. 21.

Peakall, D. and Burger, J. 2003, Methodologies for assessing exposure to metals: speciation, bioavailability of metals, and ecological host factors, *Ecotoxicology & Environmental Saf*ety, vol. 56, pp. 110-121.

Peirce, J.J., Weiner, R.F. and Vesilind, P.A. 1998, Environmental pollution and control, Butterworth-Heinemann, USA, pp. 31-57.

Pendias, A.K. & Mukherjee, A.B., 2007, Trace elements from soil to human, Springer-Verlag Berlin Heidelberg pp. 9-39.

Penrose, W.R. & Woolson, E.A. 2009, Arsenic in the marine and aquatic environments: Analysis, occurrence, and significance, *Critical Reviews in Environmental Control*, vol. 4, pp. 465-482.

Pepin, P. 1991, "Effect of temperature and size on development, mortality, and survival rates of the pelagic early life history stages of marine fish", *Canadian Journal of Fisheries & Aquatic Sciences,* vol. 48, no. 3, pp. 503-518.

Pereira, E., Rodrigues, S., Otero, M., Valega, M., Lopes, C., Pato, P., Coelho, J., Lillebo, A., Duarte, A. & Pardal, M. 2008, "Evaluation of an interlaboratory proficiency-testing exercise for total mercury in environmental samples of soils, sediments and fish tissue", *TrAC Trends in Analytical Chemistry,* vol. 27, no. 10, pp. 959-970.

Perrow, M.R. & Davy, A.J. 2002. Handbook of ecological restoration: Restoration in practice. *Cambridge University Press,* Cambridge, UK.

Pinckney, J.L., Richardson, T.L., Millie, D.F. & Paerl, H.W. 2001, "Application of photopigment biomarkers for quantifying microalgal community composition and in situ growth rates", *Organic Geochemistry,* vol. 32, no. 4, pp. 585-595.

Pinder, J., Hinton, T., Taylor, B. & Whicker, F. 2011, "Cesium accumulation by aquatic organisms at different trophic levels following an experimental release into a small reservoir", *Journal of Environmental Radioactivity,* vol. 102, no. 3, pp. 283-293.

Plant, J., Smith, D., Smith, B. & Williams, L. 2001, "Environmental geochemistry at the global scale", *Applied Geochemistry,* vol. 16, no. 11, pp. 1291-1308.

Plant, J., Kinniburgh, D., Smedley, P. & Fordyce, F. 2005, "and BA Klinck British Geological Survey, Keyworth, Nottingham, UK", *Environmental Geochemistry,* vol. 9, pp. 17.

Plant, J., Kinniburgh, D., Smedley, P., Fordyce, F. & Klinck, B. 2003, "Arsenic and selenium", *Treatise on Geochemistry,* vol. 9, pp. 17-66.

Pleiter, M.G., Palomares, S.G.I.R, Rosal, F.L.R., Boltes, K., Marco, E. & Pinas, F.F. 2013, Toxicity of five antibiotics and their mixtures towards photosynthetic aquatic organisms: Implications for environmental risk assessment, *Water Research Journal,* vol. 47, pp. 2050-2064.

Popescu, B.F.G., George, M.J., Bergmann, U., Garachtchenko, A.V., Kelly, M.E., McCrea, R.P.E., Lüning, K., Devon, R.M., George, G.N. & Hanson, A.D. 2009, "Mapping metals in Parkinson's and normal brain using rapid-scanning X-ray fluorescence", *Physics in Medicine & Biology,* vol. 54, no. 3, pp. 651.

Potts, D. 2005, "Counter-urbanisation on the Zambian copperbelt? Interpretations and implications", *Urban Studies,* vol. 42, no. 4, pp. 583-609.

Pouria, S., De Andrade, A., Barbosa, J., Cavalcanti, R., Barreto, V., Ward, C., Preiser, W., Poon, G.K., Neild, G. & Codd, G. 1998, "Fatal microcystin intoxication in haemodialysis unit in Caruaru, Brazil", *The Lancet,* vol. 352, no. 9121, pp. 21-26.

Prozesky, V., Przybylowicz, W., Van Achterbergh, E., Churms, C., Pineda, C., Springhorn, K., Pilcher, J., Ryan, C., Kritzinger, J. & Schmitt, H. 1995, "The NAC

nuclear microprobe facility", *Nuclear Instruments & Methods in Physics Research B,* vol. 104, no. 1, pp. 36-42.

QGIS 2007, http://qgis.org, accessed 2008-12-24

QGIS mapserver 2008, http://karlinapp.ethz.ch/qgis˙wms, accessed 2008-12-24

Qin, B., Zhu, G., Gao, G., Zhang, Y., Li, W., Paerl, H.W. & Carmichael, W.W. 2010, "A drinking water crisis in Lake Taihu, China: linkage to climatic variability and lake management", *Environmental Management,* vol. 45, no. 1, pp. 105-112.

Rajta, I., Borbely-Kiss, I., Morik, G., Bartha, L., Koltay, E. & Kiss, Œ.Z. 1996, "The new ATOMKI scanning proton microprobe", *Nuclear Instruments & Methods in Physics Research B,* vol. 109, pp. 148-153.

Raju, G., Sarita, P., Kumar, M.R., Murty, G., Reddy, B.S., Lakshminarayana, S., Vijayan, V., Lakshmi, P., Gavarasana, S. & Reddy, S.B. 2006, "Trace elemental correlation study in malignant and normal breast tissue by PIXE technique", *Nuclear Instruments & Methods in Physics Research B,* vol. 247, no. 2, pp. 361-367.

Rakestraw, A. 2012, "Open Oceans and Marine Debris: Solutions for the Ineffective Enforcement of MARPOL Annex V", *Hastings International & Company Law Review,* vol. 35, pp. 383-451.

Rakocinski, C.F., Brown, S.S., Gaston, G.R., Heard, R.W., Walker, W.W. & Summers, J.K. 1997, "Macrobenthic responses to natural and contaminant-related gradients in northern Gulf of Mexico estuaries", *Ecological Applications,* vol. 7, no. 4, pp. 1278-1298.

Rauch, S., Morrison, G.M. & Monzon, A. 2009, *Highway and urban environment: proceedings of the 9th Highway & Urban Environment Symposium,* Springer New York USA.

Rauf, A., Javed, M. and Ubaidullah, M. 2009, Heavy metal levels in three major carps (*Catla catla, Labeo rohita and Cirrhina mrigala*) from the river ravi, *Pakistan Veterinary Journal*, vol. 29, pp. 24-26.

Rayman, M.P. 2002, The argument for increasing selenium intake, *Proceedings of the Nutrition Society*, vol. 61, pp. 203-215.

Region, W.I.O., 1999, "United Nations Global Environment Programme Facility Transboundary Diagnostic Analysis of Land-based Sources and Activities in the Western Indian Ocean Region", *UNEP*, TDA/SAP-WIO, Maputo, pp.16-35.

Repavich, W.M., Sonzogni, W.C., Standridge, J.H., Wedepohl, R.E. & Meisner, L.F. 1990, "Cyanobacteria (blue-green algae) in Wisconsin waters: acute and chronic toxicity", *Water Research,* vol. 24, no. 2, pp. 225-231.

Richardson, M. 2004, *A time bomb for global trade: Maritime-related terrorism in an age of weapons of mass destruction,* Institute of Southeast Asian Studies, Singapore, pp. 28-108.

Riegl, B., Bruckner, A., Coles, S.L., Renaud, P., Dodge, R.E. 2009, Coral Reefs, *Annals of the New Yourk Academy of Sciences*, vol.1162, pp. 136-186.

Risher, J.F. & Amler, S.N. 2005, "Mercury exposure: evaluation and intervention: the inappropriate use of chelating agents in the diagnosis and treatment of putative mercury poisoning", *Neurotoxicology,* vol. 26, no. 4, pp. 691-699.

Rispin, A., Farrar, D., Margosches, E., Gupta, K., Stitzel, K., Corr, G., Greene, M., Meyer, W. and McCell, D. 2002, Alternative Methods for the Median Lethal Dose (LD_{50}) Test: The up-and-Down Procedure for Acute Oral toxicity, *Institute for Laboratory Animal Research Journal*, vol. 43, pp. 233-243.

Ritter, L., Solomon, K., Sibley, P., Hall, K., Keen, P., Mattu, G. & Linton, B. 2002, "Sources, pathways, and relative risks of contaminants in surface water and groundwater: a perspective prepared for the Walkerton inquiry", *Journal of Toxicology & Environmental Health Part A,* vol. 65, no. 1, pp. 1-142.

Roach, E.S., Golomb, M.R., Adams, R., Biller, J., Daniels, S., Ferriero, D., Jones, B.V., Kirkham, F.J., Scott, R.M. & Smith, E.R. 2008, "Management of stroke in infants and children a scientific statement from a special writing group of the American heart association stroke council and the council on cardiovascular disease in the young", *Stroke,* vol. 39, no. 9, pp. 2644-2691.

Roberts, J.R. 1999, "Metal toxicity in children", *Training manual on pediatric environmental health: Putting it into practice,* Children's Environmental Health Network, San Francisco, California, USA.

Rodrigues, S., Pereira, M., Duarte, A., Ajmone-Marsan, F., Davidson, C.M., Grčman, H., Hossack, I., Hursthouse, A.S., Ljung, K. & Martini, C. 2006, "Mercury in urban soils: a comparison of local spatial variability in six European cities", *Science of the Total Environment,* vol. 368, no. 2, pp. 926-936.

Rogers, J.J.W., Ghuma, M.A., Nagy, R.M., Greenberg, J.K. & Fullagar, P.D. 1978, "Plutonism in Pan-African belts and the geologic evolution of northeastern Africa", *Earth & Planetary Science Letters,* vol. 39, no. 1, pp. 109-117.

Ronchetti, R., Zuurbier, M., Jesenak, M., KOPPE, J.G., AHMED, U.F., Ceccatelli, S. & VILLA, M.P.I.A. 2006, "Children's health and mercury exposure", *Acta Paediatrica,* vol. 95, pp. 36-44.

Roux, D., Van Vliet, H. & Van Veelen, M. 1993, "Towards integrated water quality monitoring: assessment of ecosystem health", *Water S.A.,* vol. 19, no. 4, pp. 275-280.

Rutherford, E.1911, "LXXIX. The scattering of α and β particles by matter and the structure of the atom", *The London, Edinburgh and Dublin Philosophical Magazine & Journal of Science,* vol. 21, no. 125, pp. 669-688.

Ruus, A., Schaanning, M., Oxnevad, S. & Hylland, K. 2005, "Experimental results on bioaccumulation of metals and organic contaminants from marine sediments", *Aquatic Toxicology,* vol. 72, no. 3, pp. 273-292.

Ryabzev, I.A. 2002, "Epidemiological studies in Russia about the consequences of the Chernobyl APS accident", *Institute of Problem of Ecology & Evolution, Russian Academy of Sciences Leninky st. D-33, Moscow 117071, Russia*.

Ryan, C.G., Cousens, D.R., *et al.*, 1990, Quantitative PIXE microanalysis of geological material using the CSIRO proton microprobe, *Nuclear Instruments & Methods in Physics Research B*, vol. 47 no. 1-4, pp. 55-71.

Ryan, C.G. & Jamieson, D.N. 1993, Dynamic analysis: on-line quantitative PIXE microanalysis and its use in overlap-resolved elemental mapping, *Nuclear Instruments & Methods in Physics Research B*, vol. 77, pp. 203-214.

Ryan, C.R., Heinrich, C.A. & Memagh, T.P. 1993, PIXE microanalysis of fluid inclusions and its application to study ore metal segregation between magmatic brine and vapor, *Nuclear Instruments & Methods in Physics Research B*, vol. 77 no. 1-4, pp. 463-471

Ryan, C., Jamieson, D., Churms, C. & Pilcher, J. 1995, "A new method for on-line true-elemental imaging using PIXE and the proton microprobe", *Nuclear Instruments & Methods in Physics Research B,* vol. 104, no. 1, pp. 157-165.

Ryan, C.G., van Achterbergh, E., *et al.*, 1996 Overlap corrected on-line PIXE imaging using the proton microprobe, *Nuclear Instruments & Methods in Physics Research B,* vol. 109/110, pp. 154-160.

Ryan, C. 2000, "Quantitative trace element imaging using PIXE and the nuclear microprobe", *International Journal of Imaging Systems & Technology,* vol. 11, no. 4, pp. 219-230.

Ryan, C.G. 2001, "Developments in Dynamic Analysis for quantitative PIXE true elemental imaging", *Nuclear Instruments & Methods in Physics Research B,* vol. 181, no. 1, pp. 170-179.

Ryan, C., Van Achterbergh, E., Yeats, C., Drieberg, S., Mark, G., McInnes, B., Win, T., Cripps, G. & Suter, G. 2002, "Quantitative, high sensitivity, high resolution, nuclear microprobe imaging of fluids, melts and minerals", *Nuclear Instruments & Methods in Physics Research B,* vol. 188, no. 1, pp. 18-27.

Ryan, C., Van Achterbergh, E. & Jamieson, D. 2005, "Advances in Dynamic Analysis PIXE imaging: Correction for spatial variation of pile-up components", *Nuclear Instruments & Methods in Physics Research B,* vol. 231, no. 1, pp. 162-169.

Ryan, C.G. 2011, "PIXE and the nuclear microprobe: Tools for quantitative imaging of complex natural materials", *Nuclear Instruments & Methods in Physics Research B,* vol. 269, no. 20, pp. 2151-2162.

Ryding, S.O. 1994, *Environmental management handbook,* IOS Press Amsterdam, Netherlands.

Salt, D.E., Prince, R.C. & Pickering, I.J. 2002, "Chemical speciation of accumulated metals in plants: evidence from X-ray absorption spectroscopy", *Microchemical Journal,* vol. 71, no. 2, pp. 255-259.

Santos, P.L., Gouvea, R.C. & Dutra, I.R. 1995, Human occupational radioactive contamination from the use of phosphate fertilizers. *Science of the Total Environmental,* vol. 162, pp. 19-22.

Sarma, H., Deka, S., Deka, H. & Saikia, R.R. 2011, "Accumulation of heavy metals in selected medicinal plants", *Reviews of Environmental Contamination & Toxicology,* 214, pp. 63-86.

Saunders, D., Meeuwig, J. & Vincent, A. 2002, "Freshwater protected areas: strategies for conservation", *Conservation Biology,* vol. 16, no. 1, pp. 30-41.

Scheuhammer, A.M., Meyer, M.W., Sandheinrich, M.B. & Murray, M.W. 2007, "Effects of environmental methylmercury on the health of wild birds, mammals, and fish", *AMBIO: A Journal of the Human Environment,* vol. 36, no. 1, pp. 12-19.

Schintu, M. & Degetto, S. 1999, "Sedimentary records of heavy metals in the industrial harbour of Portovesme, Sardinia (Italy)", *Science of the Total Environment,* vol. 241, no. 1, pp. 129-141.

Schmidt, R.L. & Forster, W.O. 1977, "Copper in the marine environment", *Critical Reviews in Environmental Science & Technology,* vol. 8, no. 1-4, pp. 101-152.

Shumway, S.E., Allen, S.M., Boersma 2003, Marine birds and harmful algal blooms: sporadic victims or under-reported events? *Science Direct*, vol. 2, pp.1-17.

Schnute, J. 1981, "A versatile growth model with statistically stable parameters", *Canadian Journal of Fisheries & Aquatic Sciences,* vol. 38, no. 9, pp. 1128-1140.

Selin, N.E. & Selin, H. 2006, "Global Politics of Mercury Pollution: The Need for Multi-Scale Governance", *Review of European Community & International Environmental Law,* vol. 15, no. 3, pp. 258-269.

Senesil, G.S., Baldassarre, G., Senesi, N. & Radina, B. 1999, "Trace element inputs into soils by anthropogenic activities and implications for human health", *Chemosphere,* vol. 39, no. 2, pp. 343-377.

Sheehy, B. 2005, "Does international marine environment law work? An Examination of the Cartagena Convention for the Wider Caribbean Region", *Georgetown International Environmental Law Review*, vol. 16, no. 3, pp. 441-472.

Sheehy, B.C. 2003, "International marine environment law: A case study in the Wider Caribbean Region", *Journal of Environmental Law,* vol. 31, no. 3, pp. 140-149.

Shugart, L.R., McCarthy, J.F. & Halbrook, R.S. 1992, "Biological markers of environmental and ecological contamination: an overview", *Risk Analysis,* vol. 12, no. 3, pp. 353-360.

Siegele, R., Kachenko, A., Bhatia, N., Wang, Y., Ionescu, M., Singh, B., Baker, A. & Cohen, D. 2008, "Localisation of trace metals in metal-accumulating plants using PIXE", *X-Ray Spectrometry,* vol. 37, no. 2, pp. 133-136.

Sigman, H. 2000, "Hazardous waste and toxic substance policies", *Public Policies for Environmental Protection,* vol. 56, pp. 215-259.

Sims, N.A. 1994, "Growth of wild and cultured black-lip pearl oysters, *Pinctada margaritifera* (L.)(Pteriidae; Bivalvia), in the Cook Islands", *Aquaculture,* vol. 122, no. 2, pp. 181-191.

Simpson, S.L., Batley, G.E., Chariton, A.A., Stauber, J.L., King, C.K., Chapman, J.C., Hyne, R.V., Gale, S.A., Roach, A.C. & Maher, W.A. 2005, *Handbook for Sediment Quality Assessment* (CSIRO: Bangor, NSW).

Singh, R. 2004, "Water for all: Is privatisation the only solution?"", *Combat Law,* vol. 3, pp. 2.

Singh, S.K., Subramanian, V. & Gibbs, R.J. 2009, Hydrous FE and MN oxides-scavengers of heavy metals in the aquatic environment, *Critical Reviews in Environmental Control*, vol. 14, pp.1984-1993.

Smith, J.L.B. 1938, "The South African fishes of the families Sparidae and Denticidae", *Transactions of the Royal Society of South Africa,* vol. 26, no. 3, pp. 225-305.

Smolyar, I.V. & Bromage, T.G. 2004, "Discrete model of fish scale incremental pattern: a formalization of the 2D anisotropic structure", *ICES Journal of Marine Science: Journal du Conseil,* vol. 61, no. 6, pp. 992-1003.

Sobsey, M., Khatib, L., Hill, V., Alocilja, E. & Pillai, S. 2001, "Pathogens in animal wastes and the impacts of waste management practices on their survival, transport and fate"*, Journal of Environmental Quality,* vol, 25, pp. 53-88.

Sparre, P. & Venema, S. 1999, "Introduction to tropical fish stock assessment Part 2: Exercises", *FAO Fisheries Technical Paper,* vol. 306, pp. 2.

Spehar, R., Holcombe, G., Carlson, R., Drummond, R., Yount, J. & Pickering, Q. 1979, "Effects of pollution on freshwater fish", *Journal of the Water Pollution Control Federation,* vol. 51, no. 6, pp. 1616-1694.

Speller, S., Heiland, W. & Schleberger, M. 2001, "1. Surface characterization: Composition, structure and topography", *Experimental Methods in the Physical Sciences,* vol. 38, pp. 1-109.

Spiegel, S.J. & Veiga, M.M. 2005, "Building capacity in small-scale mining communities: health, ecosystem sustainability, and the Global Mercury Project", *Eco Health,* vol. 2, no. 4, pp. 361-369.

Spies, M. 2009, "Potentials for Migration and Mobility Among Oil Workers in the Russian North", *Geografiska Annaler: Series B, Human Geography,* vol. 91, no. 3, pp. 257-273.

Spohn, H. 2004, Dynamics of charged particles and their radiation field, Cambridge university press.

Stamatopoulos, C. & Caddy, J. 1989, "Estimation of von Bertalanffy growth parameters: a versatile linear regression approach", *Journal of Marine Science,* vol. 45, no. 2, pp. 200-208.

Stastny, P. 1964, "Persistence of acquired tolerance in cells transferred to an antigen-free environment", *The Journal of Immunology,* vol. 92, no. 4, pp. 626-629.

Steffens, W. 1997, "Effects of variation in essential fatty acids in fish feeds on nutritive value of freshwater fish for humans". *Aquaculture*, vol.151, pp.97-119.

Stegemen, J.J., Teng, F.Y. & Snowberger, E.A. 1987, Induced cytochrome P450 in winter flounder (*Preudopleuronectes americannus*) from coastal massachusetts evaluated by catalytic assay and monoclonal Antibody probes. *Canadian Journal of Fisheries & Aquatic Sciences,* vol. 44, no. 7, pp. 1270-1277.

Street, R., Kulkarni, M., Stirk, W., Southway, C., Abdillahi, H., Chinsamy, M. & Van Staden, J. 2009, "Effect of cadmium uptake and accumulation on growth and antibacterial activity of *Merwilla plumbea*-An extensively used medicinal plant in South Africa", *South African Journal of Botany,* vol. 75, no. 3, pp. 611-616.

Streit, B. 1998, "Bioaccumulation of contaminants in fish", *Experientia-Supplements Only,* vol. 86, pp. 353-388.

Svobodova, Z., Lloyd, R., Machova, J., Vykusova, B. 1993, Water Quality and fish health, *Food Agriculture Organization*, Rome, Italy.

Szymanski, R. & Jamieson, D.N. 1997, "Ion source brightness and nuclear microprobe applications", *Nuclear Instruments & Methods in Physics Research B,* vol. 130, no. 1, pp. 80-85.

Tanaka, A., Tano, S., Chantes, T., Yokota, Y., Shikazono, N. & Watanabe, H. 1997, "A new Arabidopsis mutant induced by ion beams affects flavonoid synthesis with spotted pigmentation in testa.", *Genes & Genetic Systems,* vol. 72, no. 3, pp. 141-148.

Tanaka, A., Watanabe, H., Shimizu, T., Inoue, M., Kikuchi, M., Kobayashi, Y. & Tano, S. 1997, "Penetration controlled irradiation with ion beams for biological study", *Nuclear Instruments & Methods in Physics Research B,* vol. 129, no. 1, pp. 42-48.

Tang, S., Orlic, I., Yu, K., Sanchez, J., Thong, P., Watt, F. & Khoo, H. 1997, "Nuclear microscopy study of fish scales", *Nuclear Instruments & Methods in Physics Research B,* vol. 130, no. 1, pp. 396-401.

Taub, D.R., Miller, B. & Allen, H. 2007, "Effects of elevated CO_2 on the protein concentration of food crops: a meta-analysis", *Global Change Biology,* vol. 14, no. 3, pp. 565-575.

Taylor, M.C., Demayo, A., Taylor, K.W. & Brungs, W.A. 1982, "Effects of zinc on humans, laboratory and farm animals, terrestrial plants, and freshwater aquatic life", *Critical Reviews in Environmental Science & Technology,* vol. 12, no. 2, pp. 113-181.

Terlecka, E. 2005, "Arsenic speciation analysis in water samples: A review of the hyphenated techniques", *Environmental Monitoring & Assessment,* vol. 107, no. 1, pp. 259-284.

Tseng, C.H. 2009, A review on environmental factors regulating arsenic methylation in humans, *Toxicology & Applied Pharmacology*, vol. 235, pp. 338-350.

Tuzen, M., Soylak, M. 2007, "Determination of trace metals in canned fish marketed in Turkey". *Food Chemistry*, vol. 101, pp. 1378-1382.

Tuzen, M. 2009, Toxic and essential trace elemental contents in fish species from the Black Sea, *Food and Chemical Toxicology*, vol. 47, pp. 1785-1790.

UNEP 1992, Global Biodiversity Strategy, World Resources Institute, Washington DC, USA.

United Nations Environment Programme 2006, *Protecting coastal and marine environments from land-based activities: a guide for national action,* United Nations Publications, UNEP/GPA, The Hague, Netherlands.

University of Toronto, 1943, *A method for the calculation of the growth of fishes from scale measurements*, University of Toronto Press. Toronto, Canada.

van Blerk, L. & Ansell, N. 2006, "Imagining migration: placing children's understanding of „moving house' in Malawi and Lesotho", *Geoforum,* vol. 37, no. 2, pp. 256-272.

Van Dam, R., Humphrey, C. & Martin, P. 2002, "Mining in the Alligator Rivers Region, northern Australia: Assessing potential and actual effects on ecosystem and human health", *Toxicology,* vol. 181, pp. 505-515.

Van den Berg, M., Birnbaum, L.S., Denison, M., De Vito, M., Farland, W., Feeley, M., Fiedler, H., Hakansson, H., Hanberg, A. & Haws, L. 2006, "The 2005 World Health Organization reevaluation of human and mammalian toxic equivalency factors for dioxins and dioxin-like compounds", *Toxicological Sciences,* vol. 93, no. 2, pp. 223-241.

van der Oost, R., Beyer, J. & Vermeulen, N.P. 2003, "Fish bioaccumulation and biomarkers in environmental risk assessment: a review", *Environmental Toxicology & Pharmacology,* vol. 13, no. 2, pp. 57-149.

Van der Perk, M. 2006, Soil and water contamination: from molecular to catchment scale, *Taylor & Francis Group*, London, UK.

Van Espen, P., Van't Dack, L., Adams, F. & Van Grieken, R. 1979, "Effective sample weight from scatter peaks in energy-dispersive X-ray fluorescence", *Analytical Chemistry,* vol. 51, no. 7, pp. 961-967.

Vandecasteele, C. & Block, C.B. 1997, *Modern methods for trace element determination,* Wiley, London, UK.

Vander Zwaag, D.L. & Powers, A. 2008, "The protection of the marine environment from land-based pollution and activities: gauging the tides of global and regional

governance", *The International Journal of Marine and Coastal Law,* vol. 23, no. 3, pp. 423-452.

Veiga, M.M., Baker, R.F., Fried, M.B. & Withers, D. 2004, *Protocols for environmental and health assessment of mercury released by artisanal and small-scale gold miners.* United Nations Publication, New York, vol. 9, no.1, pp. 133-141.

Veiga, M.M., Maxson, P.A. & Hylander, L.D. 2006, "Origin and consumption of mercury in small-scale gold mining", *Journal of Cleaner Production,* vol. 14, no. 3, pp. 436-447.

Veiga, M.M., Scoble, M. & McAllister, M.L. 2001, "Mining with communities", *Natural Resources Forum*, vol. 25, no. 3, pp. 191.

Verbeke, W., Sioen, I., Pieniak, Z., Van Camp, J. & De Henauw, S. 2005, "Consumer perception versus scientific evidence about health benefits and safety risks from fish consumption", *Public Health Nutrition,* vol. 8, no. 04, pp. 422-429.

Verbruggen, N., Hermans, C. & Schat, H. 2009, "Mechanisms to cope with arsenic or cadmium excess in plants", *Current Opinion in Plant Biology,* vol. 12, no. 3, pp. 364-372.

Verma, H.R. 2007, *Atomic and nuclear analytical methods: XRF, Mossbauer, XPS, NAA and ion-beam spectroscopic techniques*, Springer Berlin Heidelberg New York, USA

Viarengo, A., Lowe, D., Bolognesi, C., Fabbri, E. & Kohler, A. 2007, "The use of biomarkers in biomonitoring: a 2-tier approach assessing the level of pollutant-induced stress syndrome in sentinel organisms", *Comparative Biochemistry & Physiology Part C: Toxicology & Pharmacology,* vol. 146, no. 3, pp. 281-300.

Vohra, K. & Mishra, U. 1960, "Evaluation of future levels of radioactive fallout", *Il Nuovo Cimento,* vol. 18, no. 6, pp. 1076-1085.

Vos, A. & Cawood, S. 2010, "The impact of water quality on informally-declared heritage sites: a preliminary study", *Water S.A.,* vol. 36, no. 2, pp. 185-192.

Vuori, K.M., Siren, O. & Luotonen, H. 2003, "Metal contamination of streams in relation to catchment silvicultural practices: a comparative study in Finnish and Russian headwaters", *Boreal Environment Research,* vol. 8, no. 1, pp. 61-70.

Walmsley, R. 2000, Perspectives on eutrophication of surface waters: a Review and Discussion Document, *Water Research Commission*, Pretoria, S.A.

Walsh, P. 1990, The use of seabirds as monitors of metals in the marine environment. Heavy metals in the marine environment, *Critical Reviews in Environmental Control Press*, pp. 183-2004.

Wang, J.P., Qi, *et al.*, 2002, "Areview of animal models for the study of arsenic carcinogenesis". *Toxicol Lett*, vol. 133, pp. 17-31.

Wang, M., Webber, M., Finlayson, B. & Barnett, J. 2008, "Rural industries and water pollution in China", *Journal of Environmental Management,* vol. 86, no. 4, pp. 648-659.

Warriner, K., Huber, A., Namvar, A., Fan, W. & Dunfield, K. 2009, "Recent advances in the microbial safety of fresh fruits and vegetables", *Advances in Food & Nutrition Research,* vol. 57, pp. 155-208.

Watt, F., Grime, G., Brook, A., Gadd, G., Perry, C., Pearce, R., Turnau, K. & Watkinson, S. 1991, "Nuclear microscopy of biological specimens", *Nuclear Instruments & Methods in Physics Research B,* vol. 54, no. 1, pp. 123-143.

Watts, N.S.J. & Wandesforde-Smith, G. 2006, "The Law and Policy of Biodiversity Conservation in the Caribbean: Cutting a Gordian Knot", *Journal of International Wildlife Law & Policy,* vol. 9, no. 3, pp. 209-221.

Weatherley, A.H., Gill, H. & Casselman, J.M. 1987, *The biology of fish growth,* Academic Press, London, UK.

Weis, J.S. & Weis, P. 1994, "Effects of contaminants from chromated copper arsenate-treated lumber on benthos", *Archives of Environmental Contamination & Toxicology,* vol. 26, no. 1, pp. 103-109.

Weis, J.S. & Weis, P. 1996, "The effects of using wood treated with chromated copper arsenate in shallow-water environments: A review", *Estuaries & Coasts,* vol. 19, no. 2, pp. 306-310.

Weisskopf, V.F. 1959, "Quality and quantity in quantum physics", *Daedalus,* vol. 88, no. 4, pp. 592-605.

Weller, R.A. 2002, "Medium-Energy Backscattering and Forward-Recoil Spectrometry", *Characterization of Materials,* vol. 2, pp. 1201-1261.

Wheaton, B.R. 1991, *The tiger and the shark: empirical roots of wave-particle dualism*, Cambridge University Press, Cambridge, UK.

Whicker, F.W. & Schultz, V. 1982, "Radioecology: nuclear energy and the environment", *Ecology*, vol. 64, no. 4, pp.440.

WHO 1981, IPCS, *Environmental health criteria 18, Arsenic*. World Health Organization, Geneva.

Willis, R., Walter, R., Shaw, R. & Gutknecht, W. 1977, "Proton-induced X-ray emission analysis of thick and thin targets", *Nuclear Instruments & Methods in Physics Research B,* vol. 142, no. 1, pp. 67-77.

Williams, L.G. 1964, Possible relationships between plankton-diatom species numbers and water-quality estimates, *Ecology*, vo, 45, pp. 809-823.

Wise, S.A., Koster, B.J., Parris, R.M., Schamtz, M.M., Stone, S.F. & Zeisler, R. 1989, Experiences in Environmental Specimen Banking, *International Journal of Environmental Analytical Chemistry*, vol. 37, pp. 91-106.

Wojnar, R. 2011, "Bone and cartilage-its structure and physical properties", *Biomechanics of Hard Tissues,* Wiley-VCH, UK, pp. 7-16.

Wolanski, E., McLusky, D., Heip, C., Middleburg, J. & Philippart, C. 2011, "Functioning of Ecosystems at the Land-Ocean Interface", University Press, Cambridge, UK.

Wuana, R.A. and Okieimen, F.E., Heavy metals in contaminated soils: A review of sources, chemistry, risks and besta available strategies for remediation, *Improvement Science Research Network Ecology*, vol. 2011, pp. 1-20.

Xenophontos, L., Stevens, G. & Przybylowicz, W. 1999, "Micro-PIXE elemental imaging of pyrites from the Bulawayan-Bubi Greenstone Belt, Zimbabwe", *Nuclear Instruments & Methods in Physics Research B,* vol. 150, no. 1, pp. 496-501.

Yamaguchi, M. 1975, "Estimating growth parameters from growth rate data", *Ecologia,* vol. 20, no. 4, pp. 321-332.

Yang, X. 2012, An assessment of landscape characteristics affectiong estuarine nitrogen loading in an urban watershed, *Journal of Environmental Management*, vol. 94, pp. 50-60.

Yearley, S. 1996, Sociology, environmentalism, globalization: Reinventing the globe, *SAGE Publications Limited*, London UK.

Yilmaz, F. 2009, The comparison of heavy metal concentrations (Cd, Cu, Mn, Pb and Zn) in tissues of three economically important fish (*Anguilla anguilla, Mugil cephalus and Oreochromis niloticus*) Inhabiting Koycegiz Lake-Mugla, *Turkish Journal of Science & Technology*, vol.4, pp. 7-15.

Yilmaz, A.B. & Dogan, M. 2008, Heavy metals in water and in tissues of himri (Carasobarbus luteus) from Orontes (Asi) river, *Environmental Monitoring and Assessment,* vol. 144, pp. 437-444.

Yokoo, E.M., Valente, J.G., Grattan, L., Schmidt, S.L., Platt, I. & Silbergeld, E.K. 2003, "Environmental Health: A Global Access Science Source", *Environmental Health: A Global Access Science Source,* vol. 2, pp. 8.

Yu, Y.Y., Chang, S.S., Lee, C.L. & Wang, C.R.C. 1997, "Gold nanorods: electrochemical synthesis and optical properties", *The Journal of Physical Chemistry B,* vol. 101, no. 34, pp. 6661-6664.

Yusuff, R. & Sonibare, J. 2004, "Characterization of textile industries' effluents in Kaduna, Nigeria and pollution implications", *Global Nest: The International Journal,* vol. 6, no. 3, pp. 212-221.

Zhang, C. & Suslick, K.S. 2005, "A colorimetric sensor array for organics in water", *Journal of the American Chemical Society,* vol. 127, no. 33, pp. 11548-11549.

Zhang, H., Feng, X., Larssen, T., Qiu, G. & Vogt, R.D. 2010, "In inland China, rice, rather than fish, is the major pathway for methylmercury exposure", *Environmental Health Perspectives,* vol. 118, no. 9, pp. 1183.

Zhang, X., Xie, P., Wang, W., Li, D., Li, L., Tang, R., Lei, H. & Shi, Z. 2008, "Dose-dependent effects of extracted microcystins on embryonic development, larval growth and histopathological changes of southern catfish *Silurus meridionalis*", *Toxicon,* vol. 51, no. 3, pp. 449-456.

Zhao, Q., Liu, S., Deng, L., Yang, Z., Dong, S., Wang, C. & Zhang, Z. 2012, "Spatio-temporal variation of heavy metals in fresh water after dam construction: a case study of the Manwan Reservoir, Lancang River", *Environmental Monitoring & Assessment,* vol. 184, no. 7, pp. 4253-4266.

Zhu, D., Ortega, C.F., Motamedi, R., Szewciw, L., Vernerey, F. & Barthelat, F. 2012, "Structure and mechanical performance of a "modern" fish scale", *Advanced Engineering Materials,* vol. 14, no. 4, pp.185-194.

Zingde, M. 2005, *Inputs into the oceans from land/rivers and pollution,* University Press, New Delhi, India.

Zowczak, M., Iskra, M., Torlinski, L. & Cofta, S. 2001, "Analysis of serum copper and zinc concentrations in cancer patients", *Biological Trace Element Research,* vol. 82, no. 1, pp. 1-8.

APPENDIX A
LD_{50} TOXIC VALUES OF IONIC COMPOUNDS

Toxicity values of ionic compounds found in natural waters. The values are evaluated in terms of LD_{50} as indicated by the World Health Organization (from WHO, 1997).

Element	Ionic formula	Common values in fresh water/surface water/ground water	WHO guidelines for aquatic ecosystems
Aluminium	Al^{3+}	0.1 ppm at pH=6.5 (average 0.05 mg/l)	0.2 ppm
Antimony	Sb^{4+}	<0.004ppm	0.005 ppm
Arsenic	As^{3+}	<0.005ppm	0.01 ppm
Barium	Ba^{2+}	<0.003 ppm	0.3 ppm
Cadmium	Cd^{2+}	< 0.001 ppm	0.003 ppm
Chromium	Cr^{+3}, Cr^{+6}	< 0.002 ppm	0.05 ppm
Copper	Cu^{2+}	1-10 ppm	2 ppm
Iron	Fe^{2+}, Fe^{3+}	0.5 - 50 ppm	No guideline
Lead	Pb^{2+}	0.003 ppm	0.01 ppm
Manganese	Mn^{2+}	<0.006 ppm	0.5 ppm
Mercury	Hg^{+}	< 0.005 ppm	0.001 ppm
Molybdenum	Mo^{4+}	< 0.01 ppm	0.07 ppm
Nickel	Ni^{2+}	< 0.02 ppm	0.02 ppm
Selenium	Se^{4+}	< 0.01 ppm	0.01 ppm
Sulphate	SO_4^{2-}	<17 ppm	500 ppm
Zinc	Zn^{2+}	>0.05 ppm in areas of naturally acidic waters 50 ppm	2.0 ppm

The concentrations in natural waters for most of these elements are usually considerably less than 1.0 µg/l or ppm and that toxic effects are seen at concentrations that are not much higher.

APPENDIX B
FUNDAMENTAL EQUATIONS OF THE ANALYTICAL TECHNIQUES

Appendix B1: PIXE

Appendix B1A: Fluorescence yield (ω_x)

As the electron from a higher shell drops to fill a vacancy formed at the inner shell, an X-ray photon is emitted from the atom or the energy is transferred to an outer shell electron which is ejected from the atom. This ejected electron is known as a low-energy Auger electron. For higher number Z atoms there is also a probability of shifting between the L sub shells the primary vacancies resulting from the ionization. In this transition known as the Coster-Kronig the difference in binding energy during the vacancies shifting is not radiated but rather carried off by an outer shell electron. The Coster-Kronig transition is however only possible when the difference in binding energies exceeds the ionization energy of an outer electron. There is always competition between the emission of X-rays and the radiation less Auger and Coster-Kronig transitions. The probability that fluorescence X-rays will be emitted is given by the fluorescence yield, ω_k (Campbell, 1989; Chen, 1990).

The fluorescence yield (ω_k) is therefore defined as the ratio of emitted X-rays to the number of primary vacancies created which is the probability that de-excitation will result in emission of fluorescence X-rays (Verma, 2007). The fluorescence yield can be calculated using a semi empirical mathematical formula (Verma, 2007; Campbell, 1985; Campbell, 1988):

$$\left(\frac{\omega_K}{1-\omega_k}\right)^{\frac{1}{4}} = \sum_{i=0}^{3} B_i Z \qquad \text{(B1)}$$

where B_i are parameters determined by the fit to the data Campbell (1988). The ω_k values agree closely with calculations based upon a Dirac-Hartree-Slater treatment of the bound atomic electron wave functions (Campbell, 2003). The uncertainties in the fitted ω_k values are between 3-5% for Z=10 to 20, 1-3% for Z=21 to 30, 0.5-1% for Z=31 to 40 and 0.3-0.5% for Z > 40 (Campbell, 1988; Dietzel, 2000).

Appendix B1B: Measurement of X-ray spectrum

Background

The PIXE spectrum consists of characteristic X-rays peaks superimposed on a bremsstrahlung continuum background. The bremsstrahlung is electromagnetic radiation produced when a charged particle is decelerating after being deflected by another charged particle. This radiation produces a broad spectrum, which would contribute to the continuum background of the X-ray spectrum. This background reduces the sensitivity and worsens the detection limits of the elements. The X-rays spectrum from PIXE see Chapter 3 of the results has an increased background around 2 KeV which falls to being almost zero above 17 KeV.

The bremsstrahlung emitted by decelerating particles is proportional to the square of the acceleration

$$\text{Intensity } \alpha \text{ (acceleration)}^2$$

$$\text{Since acceleration} = \frac{F}{m} \qquad \text{(B2)}$$

Then

$$\text{Intensity } \alpha \left(\frac{F}{m}\right)^2 \qquad \text{(B3)}$$

where F is the electrostatic force between the particles; m is the mass of the decelerating particle. Comparing the masses of electron and proton, it can be seen from equation B4 that X-ray spectrum obtained by electron excitation has much higher bremsstrahlung background than that by proton excitation. That is why PIXE has a lower continuum background compared to other X-ray techniques such as electron induced X-ray emission analysis, thus making it more sensitive. The bremsstrahlung continuum background is angular dependent. It becomes high at 90^0 and reaches a minimum at 180^0 relative to the beam. Hence, the X-ray detector is normally placed at a backward angle of 135^0 relative to the beam to reduce the background. The main contribution to the bremsstrahlung background in PIXE is from: Secondary electron, atomic and projectile bremsstrahlung.

Secondary electron bremsstrahlung (SEB)

When an ion beam bombards a target, electrons are ejected from the atom. These electrons are scattered by the Coulomb field of an atomic nucleus in the sample, thus resulting in the emission of SEB.

The maximum kinetic energy (K_e) that an incident particle could give to the secondary electron is:

$$K_e = \frac{4m_e}{m_p} E_p \qquad \text{(B4)}$$

where m_e is mass of free electron; m_p is mass of proton; E_p energy of proton. SEB is the main contributor to the bremsstrahlung continuum background in PIXE. It is very strong at low radiation energies, but decreases rapidly at energies higher than K_e.

Atomic bremsstrahlung (AB)

Protons could also excite electrons from inner shells and when returning to their original state the electrons will emit a continuum spectrum. This radiation is called the atomic bremsstrahlung.
AB is normally very small compared to SEB however; its contribution from heavy elements in the sample is significant.

Proton (projectile) bremsstrahlung

The emission of proton bremsstrahlung is due to the deceleration experienced by the protons in Coulombic encounters with bound atomic electrons. The velocity of the ions will decrease until it is comparable to the velocity of electrons. The contribution from this emission is minor as the ions in the beam are massive and are deflected and decelerated less. The proton bremsstrahlung contributes mainly to X-ray energies of higher than K_e.

Appendix B1C: Yield calculations

PIXE emits X-ray with characteristic intensities proportional to their concentrations (Criss, 1968; Willis, 1977). The X-ray yield and the concentration of an element in a homogeneous thick sample can be express by the following equation (Johansson, 1975; Johansson, 1976):

The yield (Y) is calculated using the equation C6.

$$Y = nc_i\, \omega_k \varepsilon \int_{E_0}^{0} \sigma_i(E) T_i(E) \left(\frac{-dE}{dx}\right)^{-1} dE \qquad \text{(B5)}$$

Where n is the number of proton; c_i is the concentration of element i in the sample; ω_k is the probability of the emission of X-rays or the fluorescence field; k is the relative intensity line of possible transitions; ε is the detector efficiency; $\sigma_i(E)$ is the ionization cross section for proton energy E; $T_i(E)$ is the transmission of protons from successive depth in the matrix; $-dE/dx$ is the stopping power of the target for the incoming particles and E_0-is the initial energy of protons.

Appendix B1D: Minimum Detection Limit (MDL)

The minimum detection limit (MDL) is defined as the concentration of an element which would yield an X-ray intensity of 2σ of the background. It is the minimum number of counts which can be reported as coming from the sample with a confidence limit of 95%.

$$MDL = 2\sqrt{B} \qquad \text{(B6)}$$

where B-background counts at the photo peak energy of interest. The MDL depends inversely to the spectrum continuum background, which in turn depends on the sample, its matrix components and the specific measuring conditions.

Appendix B2E: Backscattering (BS)

Some of the particles within a beam may backscatter after colliding with atoms in the near surface region of a target. This phenomenon is known as backscattering (BS). BS is a function of mass and depth of the scattering element within a target. The information of the energies before and after scattering can be used to calculate the relative concentrations and the depth profiles of elements.

Isotopes cannot be distinguished because the energy resolution of the detection system is too coarse. Hence the depth resolution of PIXE is very low there is a need for BS. The X-ray detector has a beryllium window to prevent BS particle to damage the detector. X-rays of the light elements can be concentrated in the Beryllium window when performing PIXE analysis. There is therefore there is a need for BS to determine the light elements.

BS spectra collected simultaneously with PIXE spectra can provide information that can be used to quantify PIXE compositional analysis. Moreover, the accurate

measurement of the beam charge might be a problem as different regions of the sample may have different secondary emission properties (Garman, 2005; Grime, 1996). When a proton of mass M_p, moving with constant velocity, collides elastically with a stationary atom of mass M_0, in a target a certain amount of energy is transferred to the recoiling atom, and the scattered proton emerges with an energy that depends on the angle of scatter and the mass of the scattering atom. Using the principle of conservation of energy and momentum both parallel and perpendicular to the direction of incidence are expressed by the system of equations:

$$\frac{1}{2}M_1v_0^2 = \frac{1}{2}M_1v_{1+}^2\frac{1}{2}M_2v_2^2 \qquad \text{(B7)}$$

$$M_1v_0 = M_1v_1\cos\theta + M_2v_2\cos\emptyset \qquad \text{(B8)}$$

$$0 = M_1v_1\sin\theta - M_2v_2\sin\emptyset \qquad \text{(B9)}$$

After elimination of $\emptyset$ and v_2 in this system of equations obtains

$$\frac{v_1}{v_0} = \frac{M_1\cos\theta \pm \left(M_2^2 - M_1^2 sin^2\theta\right)^{1/2}}{M_1+M_2} \qquad \text{(B10)}$$

For $M_1 \leq M_2$ the plus sign holds. Then by applying the principle of conservation of energy and momentum, the kinematic factor (K) can be defined as the ratio of the projectile energy after the elastic collision to the projectile energy before collision and is given by:

$$K \equiv \frac{E_1}{E_0} \qquad \text{(B11)}$$

where E_0 is the proton energy before the collision, E_1 is the scattered proton energy after the collision, M_1 is the mass of moving particle with constant velocity, M_2 is the mass of stationary particle; v_0, v_1, and v_2 is the velocity of the particle before collision and after collision; θ and $\emptyset$ the scattered and recoil angle respectively are defined as positive numbers and all quantities were refer to the laboratory system of coordinates.

The kinematic factor depends only on the ratio of the projectile ion to the target mass and on the scattering angle θ. Therefore heavy atoms will have high scattering energy implying that less energy was transferred to them during collision. If the mass of the projectile ion and energy of the projectile ion and energy of the projectile be-

fore and after scattering are known then from equation (B9) could be used to identify elements present in the sample target.

Scattering cross section (σ)

Quantitative analyses can be performed using a scattering cross section in certain experimental conditions. Once all assumptions are fulfilled, the differential scattering cross section is given by Rutherford's equation (Rutherford, 1911; Wheaton, 1991; Speller, 2001 & Goldstein, 1959).

$$\left(\frac{d\sigma}{d\Omega}\right)_c = \left[\frac{Z_1 Z_2 e^2}{4E_c sin^2\left(\theta_c/_2\right)}\right]^2 \qquad \text{(B12)}$$

Where the subscript c corresponds to the centre-of-mass coordinates

Z_1 is the atomic number of the particle atom with mass M_1

Z_2 is the atomic number of the target atom with mass M_2

e is the elementary positive charge (1.602176487(40) $\times 10^{-19}$ C (Mohr, Taylor & Newell, 2008).

E is the energy of the particle immediately before scattering

The equation (B11) for M_1 ¡¡ M_2 from the center-of-mass to the laboratory frame of reference yields (Knapp, 1992; Knapp, 1994; Jammer, 1999; Spohn, 2004; Mezzaralma, 2008; Weller, 2002; Bartschat, 2009).

$$\frac{d\sigma}{d\Omega} = \frac{\left[cos\theta + \left(1 - \frac{M_1^2}{M_2^2} sin^2\theta\right)^{1/2}\right]^2}{sin^4\theta\left(1 - \frac{M_1^2}{M_2^2} sin^2\theta\right)^{1/2}} \left(\frac{Z_1 Z_2 e^2}{2E}\right)^2 \qquad \text{(B13)}$$

In the equation (B12) the dependence of the cross-section to Z shows that heavier atoms will produce more scattered yield than the light atoms and the yield favors the beam with heavier ions. The BS spectrum contains counts generated by particle scattered by different elements in the target. Each spectrum will have steps or edges, each corresponding to the maximum energy of the particle ions scattered by a particular element in the target. Thus for a given particle ion and incident energy, the measured scattered energy will depend on M_1 and on the amount of energy lost by the ion in its passage through the target material both before and after the nuclear scattering. Therefore the spectrum may give information on the depth profile based on the energy loss of the particle ions in the sample.

Appendix C

GPS COORDINATES OF SAMPLING POINTS

GPS coordinates of the ravine, estuarine and bay areas of investigation. The rivers are the Matolo-, Umbeluzi-, Coque-, Tembe- and the Maputo River, the Espirito Santos estuary, Maputo estuary and Maputo bay. The sampling points are indicated by GPS coordinates (degrees, minutes, and seconds). The fish species sampled are also indicated.

Area	Sampling point			Fish species	Area	Sampling point			Fish species
Matola River	A1	25 59 35	32 27 57		Maputo River	F1	26 08 25	32 40 42	
	A2	25 58 55	32 27 13			F2	26 12 00	32 41 03	*Macolor niger*
	A3	25 58 29	32 26 14	*Pomadasys kaakan*		F3	26 17 00	32 41 50	
	A4	25 56 34	32 26 08			F4	26 20 40	32 40 00	
	A5	25 54 42	32 25 12			F5	26 23 09	32 40 15	
	A6	25 52 37	32 25 03		Maputo Bay	G1	25 58 07	32 37 20	
	A7	25 51 35	32 27 22			G2	25 00 25	32 36 03	
	A8	25 48 33	32 26 07			G3	26 07 43	32 41 19	
Umbeluze River	B1	26 00 18	32 28 40			G4	26 11 59	32 45 33	
	B2	26 00 05	32 28 08			G5	26 14 45	32 50 19	*Psettodes erumei*
	B3	26 01 40	32 26 07			G6	26 08 57	32 52 10	*Cetoscarus bicolor*
	B4	26 01 51	32 25 21			G7	26 01 24	32 51 58	*Scarus atrilunula*
	B5	26 59 49	32 30 10			G8	26 03 27	32 44 39	
Coque River	C1	26 00 33	32 29 11			G9	25 58 07	32 37 20	
	C2	26 00 41	32 28 40			G10	25 56 58	32 41 27	*Scarus Caudofasciatus*
	C3	26 02 05	32 27 50			G11	25 56 41	32 47 13	
Tembe River	D1	25 59 58	32 29 26			G12	25 57 49	32 53 08	*Anyperodon leucogrammicus*
	D2	26 01 43	32 29 38			G13	25 54 07	32 49 52	*Lithoguathus mormyrus*
	D3	26 03 18	32 28 30	*Pinjalo pinjalo*		H	25 48 58	32 43 48	
	D4	26 05 25	32 27 14		Maputo Estuary	H1	26 07 43	32 41 19	
Espirito Santos Estuary	E1	25 59 21	32 34 38			H2	26 03 27	32 44 39	
	E2	26 58 15	32 33 28			H3	25 48 58	32 43 48	*Scolopsis vosmeri*
	E3	26 57 36	32 31 25						
	E4	26 58 00	32 29 46	*Lutjanus gibbus*					
	E5	26 59 18	32 28 46						

APPENDIX D

CONCENTRATIONS OF SELECTED CATIONS AND THE PHYSICAL PARAMETERS OF WATER SAMPLES

Appendix D1 Concentrations of the major cations and photographs of the water samples using Flame Atomic Absorption Spectrometry taken in the Matola River at 15h40 on the 12 July 2008. A1, A2, A3, A4, A5, A6, A7, A8 and PL (Pequenos Libombos), are the sampling points.

				SAMPLING POINTS						
Element	Concentration	A1	A2	A3	A4	A5	A6	A7	A8	PL
Na	ppm	9938	9918	10069	9797	6494	4050	ND	3868	78
Mg	ppm	1688	1347	1498	1627	921	999	ND	1251	23
K	ppm	367	376	377	368	195	64	ND	60	4
Ca	ppm	410	403	405	418	360	812	ND	872	21
Water parameter										
pH		8	8	8	8	8	8	ND	8	8
Conductivity, µS/cm		50	52	53	55	51	22	ND	20	0.8
Salinity (SU)		35	35	35	37	35	14	ND	13	0.5
Temp (°C)		24	24	25	26	23	22	ND	20	25
Density (kg/m^3)		1024	1024	1024	1025	1024	1008	ND	1002	995
Depth (m)		3.4	4.4	4.2	5	2	1	ND	0.4	10
Transparency (m)		2.3	1.9	1.4	0.9	0.8	0.6	ND	0.3	0

Appendix D2. Photograph (to the left) of the Matola River area investigated. The sampling points are shown. The location of an aluminium smelter (sampling point A5) is shown to illustrate the nearness of the smelting plant to the Matola River. The red drawing indicates the proposed location of a cement industry to be established in the foreseeable future. The limestone in red line necessary for this industry will be mined at a location on the Maputo River, about 80 km from Maputo City.

Appendix D3 Photograph and concentrations of the major cations of the water samples taken in the Matola River at 12h00 on the 11 May 2009 using Flame Atomic Absorption Spectrometry. A1, A2, A3, A4, A5, A6, A7 and A8 are the sampling points.

				SAMPLING POINTS					
Element	Concentration	A1	A2	A3	A4	A5	A6	A7	A8
Na	ppm	11447	10536	12392	12871	12301	3759	ND	4335
Mg	ppm	2169	1426	2029	2210	1390	816	ND	1981
K	ppm	454	438	427	434	448	63.4	ND	226
Ca	ppm	278	259	262	271	314	500	ND	472
Mn	ppm	0.06	0.06	0.06	0.06	0.06	0.03	ND	0.04
Fe	ppm	0.24	0.24	0.25	0.28	0.23	0.06	ND	0.15
Cu	ppm	0.07	0.06	0.06	0.07	0.07	0.04	ND	0.05
Zn	ppm	0.33	0.31	0.31	0.32	0.31	0.29	ND	0.3
Water parameters									
pH		7.9	7.9	7.95	8	8.2	8	ND	7.9
Conductivity, µS/cm		50	52	53	55	51	22	ND	46
Salinity (PSU)		35	35	35	37	35	14	ND	24
Temp (℃)		24	24	25	26	23	22	ND	26
Density (kg/m^3)		1024	1024	1024	1025	1024	1008	ND	997
Depth (m)		3.4	4.4	4.2	5	2	1	ND	2.5
Transparency (m)		2.3	1.9	1.4	0.9	0.8	0.6	ND	0.9

Appendix D4. The vegetation typically mangrove channels and settled charcoals, chorals found along the Matola River, in the intercrossing between Matola River and the Maputo-Witbank highway in the sampling point A8.

Appendix D5 Flame Atomic Absorption Spectrometry result and photograph of the water samples taken at 11h30 on the 08 May 2009 in the Umbeluzi River-B1, B2, B3, PL (Pequenos Libombos) and Coque River-C1, C2 & C3 are the sampling points.

		SAMPLING POINTS						
Element	Concentration	B1	B2	B3	PL	C1	C2	C3
Na	ppm	11753	12225	11590	271	13267	13358	13258
Mg	ppm	2394	2105	1752	21	2115	3123	2658
K	ppm	400	393	382	4.3	390	381	379
Ca	ppm	248	274	245	4.79	252	360	362
Mn	ppm	0.06	0.06	0.06	0.01	0.06	0.06	0.06
Fe	ppm	0.26	0.23	0.21	0.22	0.2	0.27	0.28
Cu	ppm	0.06	0.06	0.06	0.01	0.05	0.08	0.07
Zn	ppm	0.31	0.33	0.33	0.06	0.35	0.36	0.34
Water parameters								
pH		7.9	7.9	7.9	8.56	7.9	7.9	7.9
Conductivity, µS/cm		49	49	49	45	48	48	47
Salinity (PSU)		25	25	24	25	24	24	23
Temp (°C)		32	32	33	29	32	32	32
Density (kg/m^3)		1021	1021	1021	1019	1022	1022	1021
Depth (m)		10	6	11	11	11	9	8
Transparency (m)		1.2	2.2	1.6	0.1	1.1	1.2	1

Appendix D6. Photograph (to the left) of the Umbeluzi River, indicating the sampling points B1, B2 and B3. Photographs of the Pequenos Libombos potable water supply to Maputo City, located on the Umbeluzi River, are shown to the right (up and down).

Appendix D7. Photograph of the Coque River. The sampling points for water and sediments, C1, C2 and C3 are indicated. To the left is the Umbeluze River and to the right the Tembe River.

Appendix D8 Flame Atomic Absorption Spectrometry result and photograph of the water samples taken in the Tembe River-D1, D2, D3, D4 and Espirito Santo Estuary-E1, E2, E3, E4 & E5 are the sampling points respectively at 12h30 on the 09 May 2009.

		SAMPLING POINTS								
Element	Concentration	D1	D2	D3	D4	E1	E2	E3	E4	E5
Na	ppm	12225	12183	12777	13526	11519	11284	10638	11051	11366
Mg	ppm	1534	2047	1479	1299	1661	2088	1361	1341	1681
K	ppm	384	370	388	417	286	255	252	245	242
Ca	ppm	250	260	268	289	167	157	164	164	160
Mn	ppm	0.06	0.05	0.05	0.05	0.08	0.07	0.07	0.07	0.06
Fe	ppm	0.24	0.22	0.22	0.22	0.24	0.21	0.21	0.23	0.18
Cu	ppm	0.06	0.05	0.05	0.05	0.07	0.06	0.06	0.06	0.07
Zn	ppm	0.36	0.34	0.35	0.34	0.38	0.37	0.37	0.41	0.36
Water parameters										
pH		7.9	7.9	7.9	7.9	7.9	7.8	8	7.8	7.8
Conductivity, µS/cm		48	48	49	52	47	47	48	48	48
Salinity (PSU)		24	24	32	24	23	23	23	24	24
Temp (℃)		32	32	33	35	32	32	32	32	32
Density (kg/m^3)		1022	1022	1022	1024	1022	1022	1022	1022	1021
Depth (m)		10	11	11	11	21	20	11	11	11
Transparency (m)		1.2	1.4	1.3	1.1	1.5	1.1	1.1	1.2	1.1

Appendix D9. Photograph of the Tembe River. The sampling points for sediments and water are indicated as D1, D2, D3 and D4. Acacia Xanthophloea (to the right), Tembe River (to the left) in Matutuine, Maputo Province.

Appendix D10. Photograph (to the left) of the Espirito Santo estuary. The water and sediment sampling points E1 to E5 are indicated. To the right is shown some of the shipwrecks along the estuary.


Appendix D11. Photographs of the Matola Cement Industry (to the left) and to the right silos for alumina powder. Both the industry and the silo storage facility are located along the banks of the estuary.

Appendix D12 Flame Atomic Absorption Spectrometry result and photograph of the water samples taken in the Maputo River-F1, F2, F3, F4, F5 and Maputo Estuary-H1, H2, & H3 are the sampling points respectively at 10h45 on the 15 May 2009.

		SAMPLING POINTS							
Element	Concentration	F1	F2	F3	F4	F5	H1	H2	H3
Na	ppm	10553	9325	8429	4197	1998	10137	10683	10679
Mg	ppm	2136	1127	1009	944	229	1513	1536	1535
K	ppm	255	210	195	113	45	232	232	232
Ca	ppm	320	295	268	173	44.5	326	318	317
Mn	ppm	0.06	0.05	0.04	0.02	0.01	0.06	0.06	0.06
Fe	ppm	0.22	0.2	0.18	0.1	0.06	0.14	0.33	0.32
Cu	ppm	0.05	0.06	0.05	0.03	0.02	0.06	0.06	0.06
Zn	ppm	0.48	0.26	0.22	0.12	0.02	0.39	0.18	0.17
Water parameters									
pH		7.9	8	8	8	8	7.9	7.9	7.9
Conductivity, µS/cm		47	41	44	30	17	47	47	49
Salinity (PSU)		23	23	23	24	24	22	32	32
Temp (°C)		32	27	23	23	23	32	22	30
Density (kg/m^3)		1022	1018	999	999	999	1022	1022	1022
Depth (m)		23	11	11	11	11	22	11	11
Transparency (m)		1.2	0.5	0.5	0.4	0.3	0.8	2	1.3

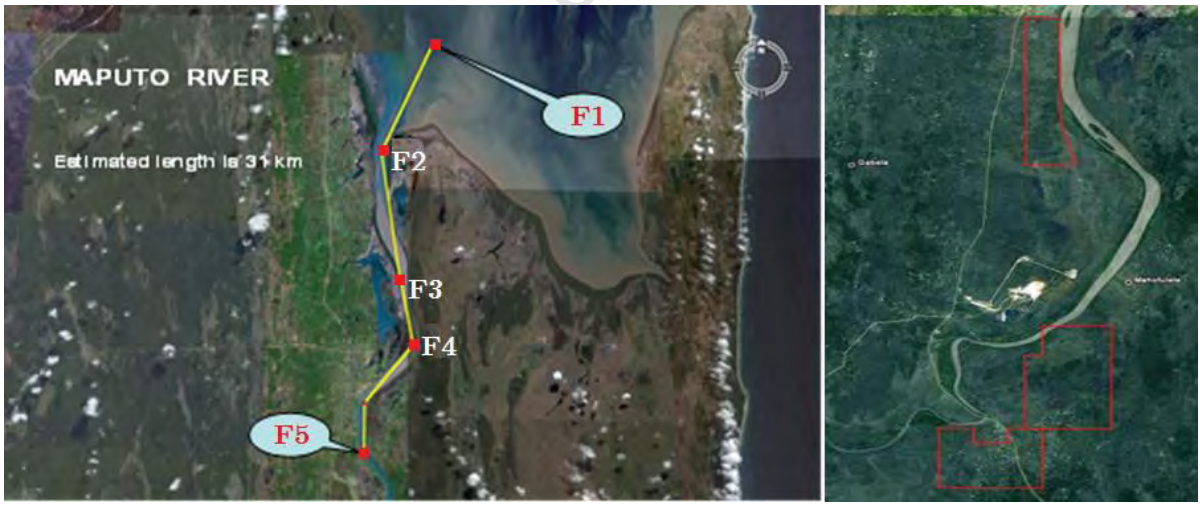

Appendix D13. Photograph of the Maputo River. The sampling points for water and sediment, F1 to F5 are indicated (to the left). The location of the proposed limestone mine (on the right) on the east and west along sampling points F3 and F4 for water and sediments in Maputo River for the proposed Cement plant at the Beluluane Industrial Park, north east of the MOZAL plant and immediately west (adjacent area) of the Matola River.

Appendix D14. The typical vegetation along the Maputo River sampling point F5, Bela Vista (shown on top). The Maputo Estuary (to the bottom) and the Mangrove Forests along the Maputo Estuary.

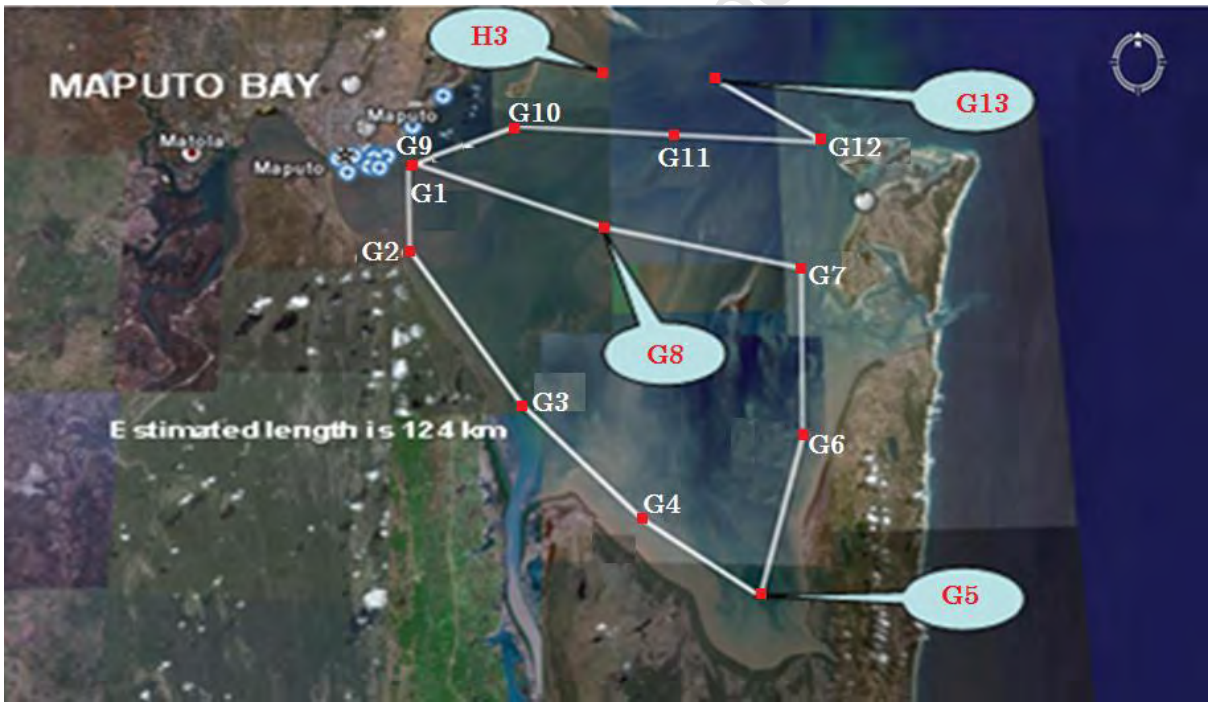

Appendix D15 Photograph of the Maputo Bay. Sediment and water sampling points G1 to G13 and H3 are indicated. The points G3, G8, G11 and H3 lie along the Maputo estuary. Inhaca Island (sampling points of water and sediments G7 and G12) is located to the east of the bay where to the south of Inhaca Island Machangulo Peninsula (samplings points of water and sediments G5 and G6).

Appendix D16 Flame Atomic Absorption Spectrometry result and the photograph of where the water samples were taken at 10h45 on the 15 May 2009 in the Maputo Bay-G1, G2, G3, G4, G5, G6, G7, G8, G9, G10, G11, G12 and G13 are the sampling points respectively.

					SAMPLING POINTS								
Element	Concentration	G1	G2	G3	G4	G5	G6	G7	G8	G9	G10	G11	G12	G13
Na	ppm	9456	9456	10137	11192	11055	10670	ND	10683	9456	9456	10357	10445	9966
Mg	ppm	1343	1343	1513	1450	1314	2323	ND	1536	1343	1612	1660	1386	1700
K	ppm	236	236	232	238	231	229	ND	232	236	370	386	394	384
Ca	ppm	327	327	326	338	328	325	ND	318	327	300	32	298	31
Mn	ppm	0.06	0.06	0.06	0.07	0.06	0.07	ND	0.06	0.06	0.06	0.06	0.06	0.05
Fe	ppm	0.17	0.17	0.14	0.4	0.33	0.33	ND	0.33	0.17	0.24	0.22	0.25	0.2
Cu	ppm	0.06	0.06	0.06	0.07	0.07	0.06	ND	0.06	0.06	0.08	0.07	0.08	0.017
Zn	ppm	0.3	0.3	0.39	0.29	0.13	0.17	ND	0.18	0.3	0.14	0.23	0.12	0.15
Water parameters														
pH		8	7.8	7.9	7.9	7.9	7.9	ND	7.9	7.9	7.9	7.9	7.9	8
Conductivity, µS/cm		47	47	47	48	48	49	ND	47	49	49	49	52	52
Salinity (PSU)		23	22	22	23	32	30	ND	32	27	33	34	35	34
Temp (℃)		32	32	32	32	23	30	ND	22	32	25	24	24	25
Density (kg/m^3)		1021	1022	1022	1022	1022	1022	ND	1022	1021	1023	1023	1024	1024
Depth (m)		11	23	22	11	11	11	ND	11	11	9	10	16	17
Transparency (m)		1.9	1	0.8	0.9	1.3	1.6	ND	2	2	2	2.5	5	1

Appendix D17 Photograph of the Maputo Bay. Maputo River joined with Maputo Bay in the sampling point for water and sediments (G3). Also typical mangroves and coral reefs vegetation extend along the sampling point (G4) for water and sediments respectively. In this photograph can viewed a mouth of the Maputo River (see the arrow) where freshwater is mixing with salt water from the Maputo Bay.

APPENDIX E

CONCENTRATIONS OF SELECTED CATIONS vs ANIONS AND THE PHYSICAL PARAMETERS OF WATER SAMPLES

Appendix E1 Ion Chromatography results for water corresponding sampling points A1, A2, A3, A4, A5, A6 and A8 along Matola River at 11h55 on the 26 May 2007. B1, B2, B3 and PL (Pequenos Libombos) along Umbeluzi River at 12h15 on the 18 June 2007. The concentrations are in ppm except those of pH.

				SAMPLING POINTS							
Element	A1	A2	A3	A4	A5	A6	A8	B1	B2	B3	PL
Na	11760	5823	5329	4585	3500	2435	1778	4852	5422	6792	15
NH_4^+	0	0	0	5000	0	0	0	0	0	0	0
Mg	2560	755	2190	830	1172	870	850	1785	2340	1655	10
K	580	460	440	66	450	100	95	390	68	355	3
Ca	64	320	480	38	190	370	380	405	595	390	3
Cl	23600	10230	13975	16300	8360	5825	5200	12000	14445	14185	21
Br	0	100	25	85	50	28	28	40	70	50	0.3
NO_3^-	2560	55	15	20	18	0	0	35	35	0	0.3
PO_4^{3-}	580	230	0	0	0	40	18	75	115	50	0.1
SO_4^{2-}	640	2100	2460	3800	1522	1510	960	2160	2210	2715	0.2
pH	7.8	7.9	7.9	7.8	7.1	6.7	7.8	7.7	7.9	7.8	6.5

Appendix E2 Ion Chromatography results for water corresponding sampling points D1, D2, D3 and D4 along Tembe River at 10h35 on the 11 June 2007. E1, E2, E3, E4 and E5 along Espirito Santo Estuary at 14h15 on the 11 June 2007. The concentrations are in ppm except those of pH.

			SAMPLING POINTS						
Element	D1	D2	D3	D4	E1	E2	E3	E4	E5
Na	2388	8582	6814	4355	3894	7370	7622	5756	4997
NH_4^+	0	0	0	5365	0	0	0	0	0
Mg	2150	1520	1955	370	1595	1560	1400	1740	2700
K	330	310	390	375	415	405	440	485	505
Ca	910	370	430	145	1595	375	335	425	555
Cl	10235	16695	15605	16755	12280	14920	15040	15035	15318
Br	30	80	55	70	55	60	65	55	85
NO_3^-	10	20	5	15	30	15	25	15	0
PO_4^{3-}	20	20	35	45	60	45	60	15	68
SO_4^{2-}	2095	2425	2180	2415	1935	2565	2210	20	2088
pH	7.7	7.3	7.3	7.2	7.7	7.6	7.4	7.4	7.5

Appendix E3 Ion Chromatography results for water corresponding sampling points F1, F2, F3, F4 and F5 along Maputo River at 13h00 on the 29 May 2007. G1, G2, G3, G4, and G5 along Maputo Bay at 13h45 on the 30 May 2007. The concentrations are in ppm except those of pH.

				SAMPLING POINTS						
Element	F1	F2	F3	F4	F5	G1	G2	G3	G4	G5
Na	7467	7277	4053	3420	244	5147	3234	6113	5858	4152
NH_4^+	0	0	0	0	0	0	0	0	0	0
Mg	1685	1515	1835	830	676	2160	1450	1895	2410	1775
K	400	370	400	258	274	485	505	420	530	385
Ca	320	325	415	323	196	450	425	404	495	400
Cl	15710	15080	11315	7683	2554	13930	9205	14110	14860	11180
Br	70	65	60	30	0	50	35	45	75	35
NO_3^-	5	5	20	8	26	0	25	5	30	50
PO_4^{3-}	30	20	45	13	0	0	0	30	70	40
SO_4^{2-}	2080	1855	1695	1008	454	2000	1560	2490	3230	1795
pH	7.9	7.8	7.9	7.7	7.7	7.7	7.3	7.5	7.3	7.1

Appendix E4 Ion Chromatography results for water corresponding sampling points G6, G7, G8, G9 G10, G11, G12 and G13 along Maputo Bay at 13h45 on the 30 May 2007. H1, H2 and H3 along Maputo Estuary at 15h45 on the 30 May 2007. The concentrations are in ppm except those of pH.

				SAMPLING POIN						
Elemet	G6	G7	G8	G9	G10	G11	G12	G13	H1	H2	H3
Na	3745	5120	5244	5146	5488	3283	4424	4780	6111	5244	6077
NH_4^+	3705	0	0	0	0	0	0	0	0	0	0
Mg	380	2425	2270	2160	2290	1945	1815	1815	1895	2270	1215
K	255	585	555	485	655	410	555	420	420	555	315
Ca	165	565	520	450	570	415	440	465	405	520	370
Cl	12026	14615	14540	13930	15180	10420	11880	12260	14110	14540	12565
Br	35	60	45	50	70	40	55	60	45	45	50
NO_3^-	0	0	0	0	0	10	10	20	5	0	25
PO_4^{3-}	15	70	10	0	30	5	0	45	30	10	0
SO_4^{2-}	3260	2350	2055	2000	1970	1830	1955	2000	2490	2055	1640
pH	7.2	7.7	7.1	7.7	7.6	7.9	7.4	7.8	7.5	7.1	7.5

Appendix E5 The present table shows the relevant information for four fish species used in the present work caught along Matola River, Tembe River, Espirito Santo Estuary and Maputo Bay respectively. The Tide (see Appendix F) was taken in the coordinates: 25^0 58" 05' of latitude and 32^0 34" 02' of longitude along Espirito Santo Estuary in Maputo Mozambique.

				FISHE SPECIES INFORMATION						
Type of Fish	Geographic coordinates		DD	MM	YY	Time of catch	Weight(kg)	Age	Length(cm)	Size of the scale(cm×cm)
1. *Pomadasys kaakan*	25° 58" 29'	32° 26" 14'	26	5	2007	11h00	2.7	12±1	42	1.7 X 1.8
2. *Pinjalo pinjalo*	26° 03" 18'	32° 28" 30'	11	6	2007	15h55	3	12±1	41	1.1 X 1.2
3. *Lutjanus gibbus*	26° 58" 00'	32° 29" 46'	10	9	2007	13h50	2.5	12±1	40	1.4 X 1.6
4. *Lithoguathus mormyrus*	25° 54" 07'	32° 49" 52'	30	5	2007	13h45	2	12±1	39	1.2 X1.3

APPENDIX F
INFORMATION ABOUT TIDES ALONG SAMPLING POINTS

Maputo has a particularly a large tidal range as a result of its location within the large enclosed bay. The tidal from spring high to spring low can varied in excess of 3.4 meters. In comparisons with the tidal range in Cape Town is approximately 2.0 meters.

Appendix F1 The present table shows the relevant information for water and sediments sample. Where DD is the day, MM is the month and YY is the year. A1, A2, A3, A4, A5, A6 and A8 are the sampling points along the Matola River; B1, B2, B3 and PL (Pequenos Libombos) are the sampling points along the Umbeluzi River and C1, C2 and C3 are the sampling points along the Coque River. The Tides were taken in the coordinates: 25^0 58" 05' of latitude and 32^0 34" 02' of longitude along Espirito Santo Estuary in southern of Maputo Mozambique.

					WATER & SEDIMENTS SAMPLE					
Sampling point	Geographic coordinates		Width (m)	Depth (m)	Tide (m)	DD	MM	YY	Time	Bank or Upstream
A1	25° 59" 35'	32° 27" 57'	1800	9.8	2.65	26	5	2007	8h45	1 km upstream from Espirito Santo Estuary
A2	25° 58" 55'	32° 27" 13'	1750	9.5	2.65	26	5	2007	9h50	2 km upstream from Espirito Santo Estuary
A3	25° 58" 29'	32° 26" 14'	1850	9.7	2.65	26	5	2007	11h00	5 km upstream from Espirito Sant. Estuary
A4	25° 56" 34'	32° 26" 08'	1600	8	2.65	26	5	2007	13h20	15 km upstream from Espirito Santo Estuary
A5	25° 54" 42'	32° 25" 12'	120	6	3.09	18	6	2007	12h15	20 km upstream from Espirito Santo Estuary
A6	25° 52" 37'	32° 25" 03'	99	4	3.09	18	6	2007	13h20	25 km upstream from Espirito Santo Estuary
A8	25° 48" 33'	32° 26" 07'	130	3	3.09	18	6	2007	15h30	30 km upstream from Espirito Santo Estuary
B1	26° 00" 18'	32° 28" 40'	2050	9.8	2.65	26	5	2007	15h45	1 km upstream from Espirito Santo Estuary
B2	26° 00" 05'	32° 28" 08'	1750	8.9	2.65	26	5	2007	16h50	7 km upstream from Espirito Santo Estuary
B3	26° 01" 40'	32° 26" 07'	1450	6	2.65	26	5	2007	18h15	13 km upstream from Espirito Santo Estuary
PL	26° 59" 49'	32° 30" 10'	2030	9-33	0.71	10	6	2008	10h30	87 km upstream from Espirito Santo Estuary
C1	26° 00" 33'	32° 29" 11'	199	9.9	2.91	11	6	2007	10h35	7.5 km from Cement Industry
C2	26° 00" 41'	32° 28" 40'	182	8.9	2.91	11	6	2007	11h15	9 km from Cement Industry
C3	26° 02" 05'	32° 27" 50'	175	8.2	2.91	11	6	2007	12h10	11 km from Cement Industry

Appendix F2. The present table shows the relevant information for water and sediments sample. Where DD is the day, MM is the month and YY is the year. D1, D2, D3 and D4 are the sampling points along the Tembe River; E1, E2, E3, E4 and E5 are the sampling points along the Espirito Santo Estuary and F1, F2, F3, F4 and F5 are the sampling points along the Maputo River. The Tides were taken in the coordinates: 25^0 58" **05**' of 176ongitud and 32^0 34" 02' of 176longitude along Espirito Santo Estuary in southern of Maputo Mozambique.

					WATER & SEDIMENTS SAMPLE					
Sampling point	Geographic coordinates		Width (m)	Depth (m)	Tide (m)	DD	MM	YY	Time	Bank or Upstream
D1	25° 59" 58'	32° 29" 26'	2060	10.5	2.91	11	6	2007	23h50	7 km upstream from Cement Industry
D2	26°01" 43'	32° 29" 38'	1970	10.2	2.91	11	6	2007	14h40	14 km upstram
D3	26° 03" 18'	32° 28" 30'	800	9.8	2.91	11	6	2007	15h55	21 km upstream
D4	26° 05" 25'	32° 27" 14'	600	7.8	2.91	11	6	2007	17h05	27 km upstream
E1	25° 59" 21'	32° 34" 38'	5000	9.4	2.91	11	6	2007	17h10	3 km upstream from Maputo Bay
E2	26° 58" 15'	32° 33" 28'	3800	11	2.91	11	6	2007	17h45	6 km upstream
E3	26° 57" 36'	32° 31" 25'	2100	9.5	2.91	11	6	2007	18h50	9 km upstream
E4	26° 58" 00'	32° 29" 46'	1700	10.5	2.91	11	6	2007	19h45	12 km upstream
E5	26° 59" 18'	32° 28" 46'	2100	11.5	2.91	11	6	2007	20h55	15 km upstream
F1	26° 08" 25'	32° 40" 42'	2500	9.4	3.15	29	5	2007	13h15	6.1 km downstream
F2	26° 12" 00'	32° 41" 03'	1800	8.7	3.15	29	5	2007	14h30	12 km downstream
F3	26° 17" 00'	32° 41" 50'	1100	7.5	3.15	29	5	2007	15h50	18 km downstream
F4	26° 20" 40'	32° 40" 00'	1080	6.3	3.15	29	5	2007	17h00	24 km downstream
F5	26° 23" 09'	32° 40" 15'	850	6	3.15	29	5	2007	18h20	30,7 km downstream from Bela vista

Appendix F3 The present table shows the relevant information for water and sediments sample. Where DD is the day, MM is the month and YY is the year. G1, G2, G3, G4, G5, G6, G7, G8, G9, G10, G11, G12 and G13 are the sampling points along the Maputo Bay; H1, H2 and H3 are the sampling points along the Maputo Estuary. The Tides were taken in the coordinates: 25^0 58" 05' of latitude and 32^0 34" 02' of longitude along Espirito Santo Estuary in southern of Maputo Mozambique.

					WATER & SEDIMENT SAMPLE					
Sampling point	Geographic coordinates		Width (m)	Depth (m)	Tide (m)	DD	MM	YY	Time	Bank or Upstream
G1	25° 58" 07'	32° 37" 20'	5000	9.8	3.37	1	6	2007	11h10	12 km upstream from Espirito Santo Estuary
G2	25° 00" 25'	32° 36" 03'	10000	9.6	3.37	1	6	2007	12h15	24 km upstream from Espirito Santo Estuary
G3	26° 07" 43'	32° 41" 19'	15000	9.5	3.37	1	6	2007	13h20	36 km upstream from Espirito Santo Estuary
G4	26° 11" 59'	32° 45" 33'	20000	9.3	3.37	1	6	2007	14h30	48 km upstream from Espirito Santo Estuary
G5	26° 14" 45'	32° 50" 19'	30000	9.2	3.37	1	6	2007	15h45	60 km upstream from Espirito Santo Estuary
G6	26° 08" 57'	32° 52" 10'	35000	9.1	3.37	1	6	2007	16h55	72 km upstream from Espirito Santo Estuary
G7	26° 01" 24'	32° 51" 58'	40000	9.7	2.8	8	6	2007	12h15	84 km upstream from Espirito Santo Estuary
G8	26° 03" 27'	32° 44" 39'	50000	11.4	3.37	1	6	2007	18h30	96 km upstream from Espirito Santo Estuary
G9	25° 58" 07'	32° 37" 20'	55000	9.8	3.27	30	5	2007	18h50	108 km upstream from Espirito Santo Estuary
G10	25° 56" 58'	32° 41" 27'	60000	9.9	3.27	30	5	2007	15h25	120 km upstream from Espirito Santo Estuary
G11	25° 56" 41'	32° 47" 13'	65000	10.7	3.27	30	5	2007	17h30	132 km upstream from Espirito Santo Estuary
G12	25° 57" 49'	32° 53" 08'	70000	9.9	2.8	8	6	2007	15h45	144 km upstream from Espirito Santo Estuary
G13	25° 54" 07'	32° 49" 52'	75000	11.3	3.27	30	5	2007	13h45	156 km upstream from Espirito Santo Estuary
H1	26° 07" 43'	32° 41" 19'	15000	9.5	3.37	1	6	2007	13h20	36 km upstream from Espirito Santo Estuary
H2	26° 03" 27'	32° 44" 39'	50000	11.4	3.37	1	6	2007	18h30	96 km upstream from Espirito Santo Estuary
H3	25° 48" 58'	32° 43" 48'	80000	9.4	3.27	30	5	2007	15h45	168 km upstream from Espirito Santo Estuary

APPENDIX G
RAINFALL INFORMATION

Rainfall for the years 2007-2009 in southern Maputo Province, Mozambique.

Republic of Mozambique

National Institute of Meteorology

The rain season in Maputo is from October to March with an annual average rainfall of approximately 760 mm. The temperatures and humidity somewhat can drop during the drier winter months from April to September. The relative humidity can varied during a month from 58 % during June to 66 % in November.

RAINFALL INFORMATION DURING 2007 TO 2009 IN SOUTHERN MAPUTO PROVINCE, MOZAMBIQUE

YEAR	JAN	FEB	MAR	APR	MAY	JUN	JUL	AUG	SEPT	OCT	NOV	DEC
2007	21.4	47.8	70.7	133.2	0	22.2	15.3	0	0	0	0	0
2008	0	29.9	82.9	64.9	28.4	42.9	11.8	0	0	0	0	0
2009	0	0	55.4	8.7	23.7	16.5	0	0	0	0	0	0

Appendix H
INSTRUMENTATION USED

Instrumentations

Microanalyses were performed on two scales for each species from experimental group using a nuclear microprobe at Material Research Department, National Research Foundation (NRF)-iThemba LABS, South Africa. This microprobe is fundamentally based on 6 MV single ended Van de Graaff accelerator and uses Oxford Microprobe triplet lenses for beam focusing, (Prozesky, 1995 & Churms, 1993).

The 15 m horizontal long flight path of the ions to the sample offers exciting possibilities such as ultimate beam spot sizes obtainable but at the same time makes the Nuclear Microprobe (NMP) more susceptible to beam instabilities which in a vertical accelerator configuration invariably lead to vertical movement of the beam (see AppendixH1).

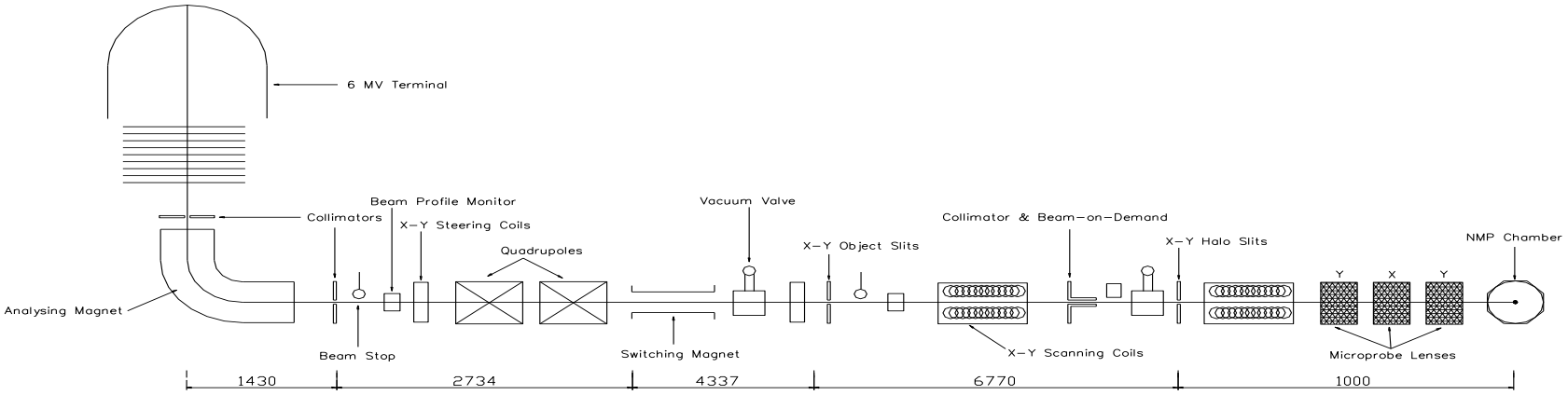

Appendix H1 A schematic of the Van de Graaff accelerator and NMP layout at Material Research Department (MRD), NRF-iThemba LABS. The most important features are shown with distances between key points in mm (not drawn to scale). From top in a vertical position the 6 MV terminals Dom, Collimators and Analyzing Magnet. In a horizontal beam line up Beam Profile Monitor, X-Y Steering Coils, Quadrupoles, Vacuum Valve, X-Y Object Slits, Collimators & Beam-on-Demand and X-Y Hallo Slits. In horizontal at the bottom Beam Stop, Switching Magnet, X-Y Scanning Coils, Microprobe Lenses and at the end NMP Chamber.

After the analyzing magnet the ions travel through the energy stabilization slits situated in front of the main beams top. Ions then pass through a quadrupole duplet for focusing of the beam at the object slits. Before the object slits, the beam passes through a switching magnet with a narrow entrance port in the Y direction (1.2 mm), which is used for the beam lines at an angle to the NMP line. The primary beam allowed to pass through the object slits is defined by a circular water-cooled collimator with a diameter of 1 mm. This protects the slits from beam damage. The 1 μA current in excess are easily transmitted through the collimator and can potentially harm the object slits which seriously affects the ultimate beam size obtainable.

Such variable slits should allow the use of intense beams with small settings of object slits where the aim is to reach the smallest beam spot size as much as possible. In this situation, these slits can be closed down to protect the object slits.
In cases where beam spot size is not critical, the variable slits can be opened to allow more ions to go through the open object slits and impinge on the specimen. The flight path from object slits to the specimen is about more than 7.5 m with the halo slits situated 1 m from the sample.

A schematic Nuclear Microprobe (NMP) chamber at the Material Research Group-NRF-iThemba LABS, is the standard Oxford NMP chamber, Oxford Microbeam, see chapter 2, **figure 2.2**. The chamber has the diameter about 17 cm and 6.5 cm of high is pumped down with a diffusion pump backed by a roughing pump and the time required for pumping down the chamber to better than $6x10^{-6}$ torr in approximately 5 min. This allows for quick sample changing and higher throughput.

The isolated secondary electron suppression ring it is positioned in front of the target with the diameter of 3 mm it is applied a voltage of -1500 V used to collect the charge inside the chamber and after the target it is placed the Faraday cup for collect any particle which pass through the target.

The fish scales were bombarded with different beam energies of 1.5 and 3.0 MeV protons and 2.0 MeV of alpha beam on the surface of the scale and cross sectional. The quality of the specimens for further analyses was inspected using Leo 1430 VP scanning electron microscope from SEM Unit at University of Cape Town.

Proton beam energies of 1.5 MeV and 3.0 MeV protons and 2.0 MeV α-particles beam and current was kept between 100 pA and 150 pA to allow count rates below 3000 c/s. Proton beam was focused to a 3x3 μm^2 spot and its dimensions was not critical and raster scanned over the surface and cross sectional of the twenty two

scales for each group of species. The analyzed structures were always relatively large, of the order of few hundred micrometers.

Proton Induced X-ray emission (PIXE) and Rutherford Backscattering Spectrometry (RBS) measurements were carried out simultaneously. The ladder moving vertical by small motor was used to fix the aluminum stub with the sample stuck on it with the carbon glue used to obtain information on the scale matrix and the accumulated charge received by the scale. External absorbers 25 μm Be and 125 μm Be were placed in between the PIXE Si (Li) and HPGe detectors and the fish scale to attenuate the Ca X-ray intensity hence enhancing the detection sensibility for the higher energy X-rays from the heavier trace elements. However the filters absorbed the X-rays from the lighter elements such as Cl, S, Ca, P, Si, and Mg, which are known to be present in fish scales.

The scan size employed varied from 200 μm x 340 μm to 400 μm x 1760 μm, depending on the size of the specimen being measured. Two Si (Li) X-ray detector were alternatively used a Link Pentameter X-ray detector of 80 mm^2 active area and 8 μm window Be and PGT detector of 30 mm^2. They were both positioned at 135^0 to the incoming beam, about 30 mm from the specimen. Backscattered protons were detected with an annular Si surface barrier (SSB) detector, 100 μm thick placed at 176^0, channeltron electron detector for secondary electron imaging, electron suppression ring in front and behind the specimen and the optical microscope at 45^0 with respect to the normal to the sample surface.

One important device in the present microprobe set-up is beam-on-demand deflection, (Prozesky, 1995). It is applied to minimize the system dead time and by reducing time of exposure to proton beam also reduces the specimen damage. Depending on sizes of the fish scales, beam was scanned over areas from about 450 μm x 450 μm up to 2 mm x 2 mm. The total accumulated charge for the scanned areas varied between 500 nC and 12.5 μC for larger sizes, when the main aim was to obtain elemental maps.

The GeoPIXE programs was the software used for analysis of X-ray spectra Ryan, (1990) and Ryan, (1993). GeoPIXE software, Ryan, (1995) allows the analysis of thin to thick specimen X-ray spectra, with complete thick target corrections for beam stopping, X-ray attenuation and secondary fluorescence. The dynamic analysis (DA) is one of the major advantage of this package hence can perform elemental maps and capability of on-line semi-quantitative analysis of spectra, Ryan, (1993) and Ryan,

(1995). The on-line semi-quantitative analysis capability enhances the location of areas of interest on specimens where localization is difficult using the normal techniques such as the total X-ray map of that area.

Appendix H2 The magnetron sputter coater (Balzers BVC 010, Balzers, Liechtenstein) used to coat the samples with a layer of carbon that is approximately 10 nanometers thick.

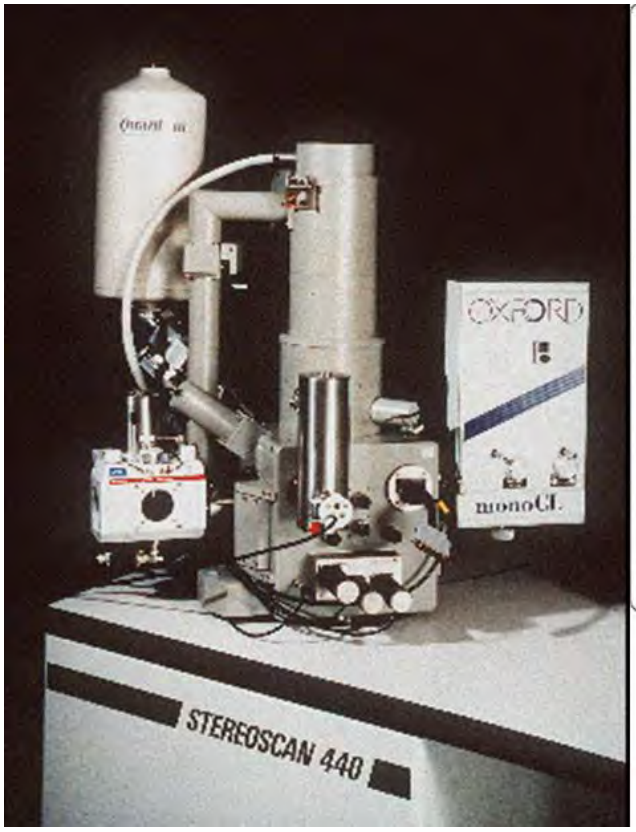

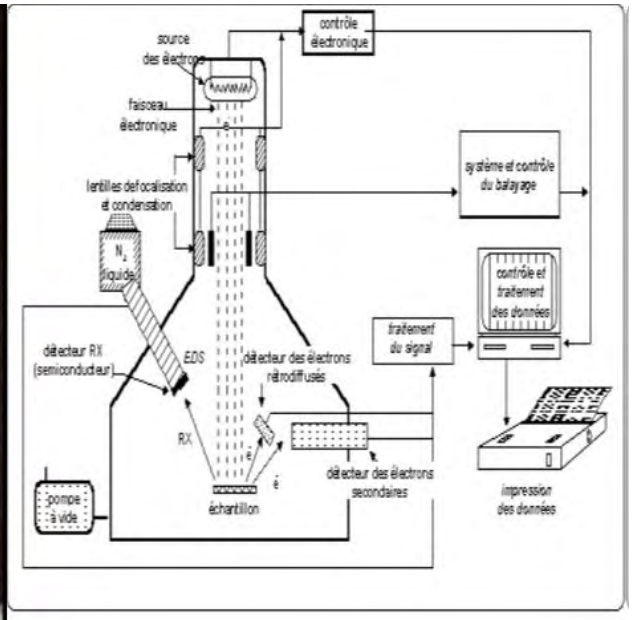

Appendix H3 Leica/LEO-Stereoscan S440 and a schematic for a generic Scanning Electron Microscope Unit at University of Cape Town (UCT), SA

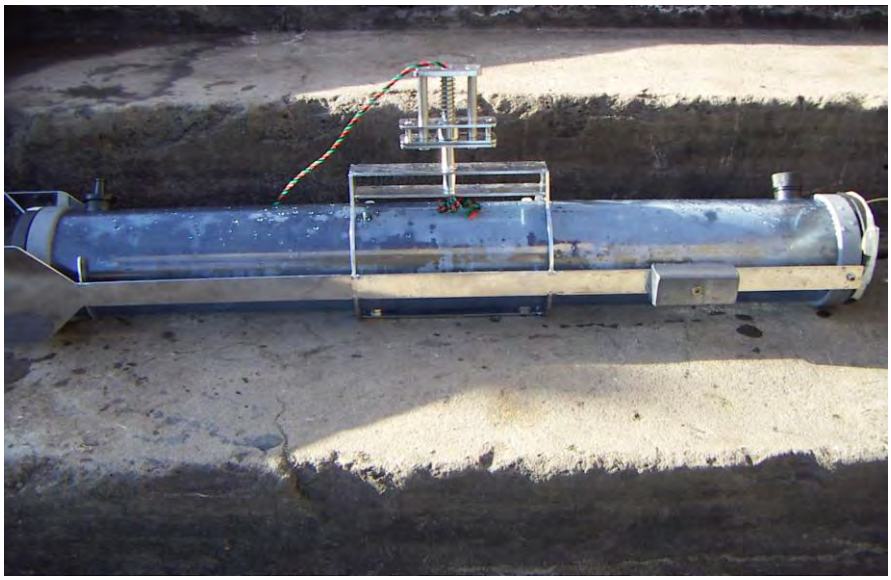

Appendix H4 The Van Dorn water sampling apparatus (Duncan & Associates, Cumbria, United Kingdom) used in this study.

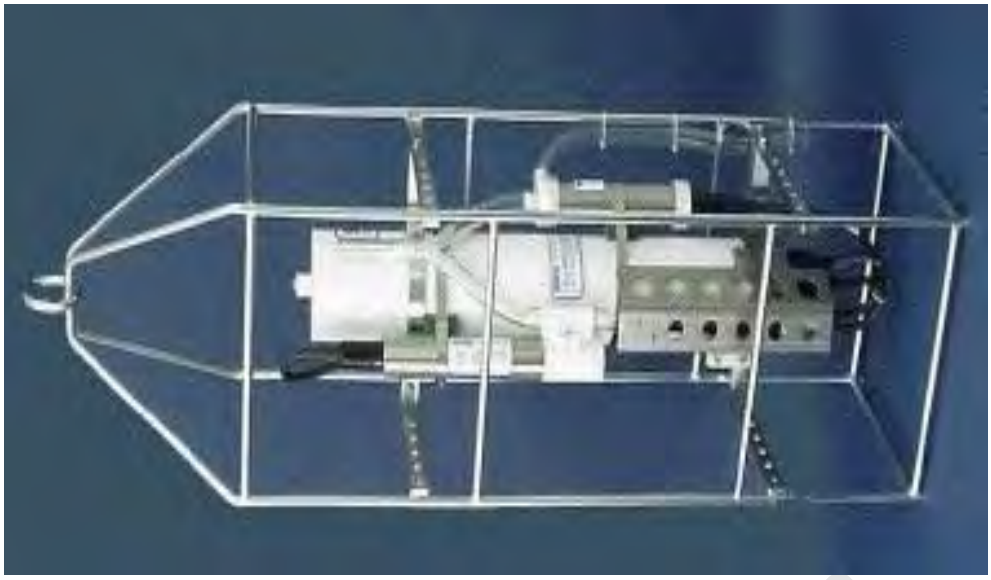

Appendix H5 The CTD probe (engaged in a steel frame) used in the determination of various water parameters such as conductivity, visibility, salinity and temperature.

Appendix H6 The Van Veen grab sampler (Rick Hydrological Co., Columbus, Ohio, USA) used for sediment sampling. A typical sediment sample is also shown.

Appendix H7 Illustrate the fishing net along the sampling points in the rivers, estuary and bay in Maputo-Mozambique during 2007-2009, May.

Appendix I
POLLUTION IN MOZAMBIQUE

Mercury vapours emanating from gold mining and mercury emissions in the Manica district, is indicated in **Appendix** a region in the Manica Province of Mozambique have been established (Rogers *et al.*, 1978; Dondeyne *et al.*, 2009).

Pan African Resources (2012)

The province has an area of 61 661 km^2 but with a population of 1 359 923, (INE, 2006). The district however has a population of 155 731 people. The region borders with the Republic of Zimbabwe in the west, the district of Gondola in the east, the district of Barue to the north through the Pungue River, and the district of Sussundenga in the south, which is bounded by the Revue and Zonue rivers. More than 10 000 individuals of population are directly involved in small-scale artisanal gold mining activities (garimpagem) as this is their main source of livelihood (MICOA & UNIDO, 2005; Dondeyne *et al.*, 2009). Most of artisanal miners (garimpeiros) use mercury to extract gold from the mineral ore (GEF & UNDP, 2005); the amalgation process recovers very little of that mercury, which pollutes the nearby environment (Veiga *et al.*, 2004; Veiga *et al.*, 2006; McDaniels *et al.*, 2010). The majority of the mercury used pollutes local waterways and soil as well as threatening the plant and animal species in the area (Veiga, 2010). Mercury amalgamation results in the discharge of an estimated 1000 tons of mercury per annum, representing about 30 to 40 percent of the world's anthropogenic mercury releases (Veiga, 2010).

It is estimated that over 20 million people work as artisanal miners worldwide (Veiga *et al.*, 2001; UN, 2002; Hentschel *et al.*, 2002; Spiegel & Veiga, 2005). Health impact of mercury, the nervous system is very sensitive to all forms of mercury (Grandjean *et al.*, 1992; Langworth *et al.*, 1997; Mittelmark, 2001; WHO, 2007). Methyl mercury and metallic mercury vapors are more harmful than other forms, because more mercury in these forms reaches the brain (Clarkson, 1997; Boening, 2000; Godman & Shannon, 2001; Davidson *et al.*, 2004). Exposure to high levels of metallic, inorganic or organic mercury can permanently damage the brain, kidneys, and developing fetus (Saleh & Doush, 1997; Chan *et al.*, 2003; Chan & Egenland, 2004; WHO, 2009). Effects on brain functioning may result in irritability, shyness, tumors, changes in vision or hearing, and memory problems (USEPA, 2006; Agrawal *et al.*, 2008; Herbert, 2008; Turkington & Harris, 2009). Short-term exposure to high levels of metallic mercury vapors may cause effects including lung damage, nausea, vomiting, diarrhea, and increases in blood pressure or heart rate, skin rashes (Goyer *et al.*, 1996; Roberts, 1999; UN & WHO, 2001; Risher & Amler, 2005; Martin & Griswold, 2009).

Appendix J
CONFERENCES AND PUBLICATIONS

Guambe, J.F., Mars, J.A. & Day, J. 2012, "Application of PIXE in Pollution Control of the Matola River in Mozambique-analysis of fish scales". *Presented at* 20th International Conference on Ion Beam Analysis, April 10-15, 2011, iTapema, RS-Brasil.

Guambe, J.F., Mars, J.A. & Day, J. 2012, "Application of PIXE in pollution control of the Matola River in Mozambique-analysis of fish scales", *Nuclear Instruments and Methods in Physics Research B,* vol. 273, pp. 171-172.

Guambe, J.F., Mars, J.A. & Day, J. 2012, "Aplication of Particle-Induced X-ray Emission, Scanning Electron Microscopy and Backscattering spectrometry in the Elemental quantification of incremental patterns in scales of the fish *Pomadasys kaakan*: A 2-d study. *Presented at* 7th International Symposium on Bio-PIXE (BIO-PIXE7), 31, October-5, November, 2011, Tohoku University, Sendai-Japan.

Guambe, J.F., Mars, J.A. & Day, J. 2012, "Aplication of Particle-Induced X-ray Emission, Scanning Electron Microscopy and Backscattering spectrometry in the Elemental quantification of incremental patterns in scales of the fish *Pomadasys kaakan*: A 2-d study". *International Journal of PIXE*, vol. 22, pp. 185.

Guambe, J.F., Mars, J.A. & Day, J. 2012, "A 3D Study of the effect of Pollution in Fish scales Using PIXE, SEM and BS". *Presented at* 13th International Conference on Nuclear Microprobe Technology and Application, 22-27, July, 2012, Lisbon-Portugal.

Guambe, J.F., Mars, J.A. & Day, J. 2013, "Application of IBA in the comparative analyses of fish scales used as biomonitors in the Matola River, Mozambique". Not *presented at* 13th International Conference on Particle Induced X-ray Emission, March 3-8, 2013, Gramado, RS-Brasil.

Guambe, J.F., Mars, J.A. & Day, J. 2013, "Application of IBA in the comparative analyses of fish scales as biomonitors of pollution". Not *presented at* 21st International Conference on Ion Beam Analysis, June 23-28, 2013, Marriott Waterfront, Seattle, Washington, USA.

Tylko, G., Guambe, J.F., Borowaska, J., Banach, Z., Pyza, E., Przybylowicz, W. & Mesjasz, J. Distribution and concentration of copper, zinc, cadmium and lead in the housefly's thorax and abdomen. *Microscopy Society of South Africa*, vol., 34, pp. 1-20.